QED final state bremsstrahlung of light fermion pair in Photos Monte Carlo: variants of approximated QED matrix elements and non QED extensions

S. S. Antropov*

The Henryk Niewodniczanski Institute of Nuclear Physics

Polish Academy of Sciences, Krakow, Poland

June 1, 2020

Abstract

I present results for final state emissions of additional leptonic pairs in decays of heavy intermediate states such as Z and W boson. This process constitutes small correction. Presentations of PHOTOS algorithm and short presentations of KORALW, SANC, TAUOLA algorithms are given. Numerical distributions of relevance for LHC and Belle II observables are shown. They are used in discussions of systematic errors in the predictions of pair emissions as implemented in the programs. Testing framework is developed allowing comparison of spectra by PHOTOS with an exact one solutions. Exact matrix element of extra pair emission from the final state of $2f \to Z/\gamma^* \to 2f$ spin summated process has been installed into PHOTOS and tested. Improved PHOTOS prediction for $e^+e^- \to Z \to e^+e^-\mu^+\mu^-$ and $e^+e^- \to Z \to \mu^+\mu^-\mu^+\mu^-$ is higher by respectively 5.4% and 4.6% of their contributions, these contributions are at the level of 10^{-4} if calculated with respect to the $Z \to \ell\ell$. This improvement is localized mostly in the hard part of the additional lepton pair spectrum. Three approximated matrix elements of extra pair emission from the final state of $2f \to Z/\gamma^* \to 2f$ process has been proposed for PHOTOS and has been tested. Numerically these matrix elements are as good as exact one. An improvement in PHOTOS generated spectrum of invariant mass squared of muon pair is reduction of discrepancy (from factor of 4.2 to 7%) with reference spectrum for the hardest extra pair emissions. An improvement in PHOTOS generated spectrum of invariant mass squared of electron pair is reduction of discrepancy (from factor of 2.5 to 17%) with reference spectrum for the hardest extra pair emissions. Basing on a tested approximation, an effective factorization of matrix element of $2f \to Z/\gamma^* \to 4f$ spin summated process is proposed to separate Born level matrix element from the factorized part describing extra pair emission from the final state. Generalization of this factorized part is discussed. Applicability of effective factorization to the matrix element of $2p \to Z/\gamma^* \to 4f$ spin summated process is suggested. Future research in order to verify applicability of obtained factorized part describing final state extra pair emission to other than $2f \to Z/\gamma^* \to 2f$ spin summated processes is suggested.

*E-mail:santrop_2@yahoo.com

Contents

1 Introduction

One of the purposes of LHC experiments is to improve precision of the W boson mass measurement. Precision measurements of the W boson mass rely on a precise reconstruction of momenta for the final state leptons [1] and on comparison of W production and decay with those of Z in LHC and in particular LHC detector conditions. The QED effects of the final state radiation play an important role in such experimental studies [2]. Final state bremsstrahlung is included in all simulation chains and should be studied together with the detector response to leptons. As it is reported [1], systematic error of W boson mass measurement related to final state pair production in the $W \to e\nu$ channel is 3.6 MeV (or 0.8 MeV depending on observable) and the one related to final state pair production in the $W \to \mu\nu$ channel is 4.4 MeV (or 0.8 MeV depending on observable). Moreover, final state pair production affects position and shape of Z peak affecting lepton momentum calibration of Ref. [1]. Systematic error related to muon momentum calibration roughly estimated to be of 10 MeV.

In order to access experimental precision of future circular collider (FCC) the systematic error of W boson mass measurement has to be reduced more than 10 times, down to 0.5 MeV [3] or better. It is true also for the final state pair emission. Moreover, one's of the most important observables of FCC like Z boson mass M_Z, Z boson width Γ_Z, neutrino number N_ν require systematic error reduction related with precise description of pair spectra [3]. Reduction of QED uncertainties in M_Z and Γ_Z below 0.1 MeV is required and there are two main strategies of reduction of systematic error of N_ν discussed in Ref. [3]. First one, is to have Monte-Carlo (MC) generator for Z boson production and decay with QED corrections down to level of $O(\alpha^2)$, which is related, but not directly effected by production of extra pairs. Second one, is based on precise control of muon pairs, that are produced in Z decays [4].

In the manuscript I will concentrate on the effects related to additional pair emissions in decays of heavy bosons, mainly Z. These effects should be included starting from the second order of QED, i.e. from the $\mathcal{O}(\alpha^2)$ corrections. The typical Feynman diagrams for $f_1\overline{f}_1 \to Z/\gamma^* \to f_2\overline{f}_2$ are shown in Fig. 1 and for final state emissions are shown in Fig. 2.

Precise calculations of interesting quantities must include such radiative corrections of precision level of the order of $\sim 0.1\%$, they are usually calculated with a help of MC generators in order to take into account detector acceptance simultaneously. The experimental data are compared to expectations from MC simulation. In the study [1] it is specifically stated that "the dominant source of electroweak corrections to W- and Z- boson production originates from QED final-state radiation, and is simulated with `PHOTOS`" and that "Final-state lepton pair production, through $\gamma^* \to$ lepton pair, constitutes an significant

additional source of energy loss for the W -boson decay products". Present manuscript is focused on improvement of PHOTOS [5–11] algorithm for simulation of the additional pair emissions in decays of γ^* and Z boson Fig. 2.

The basis of PHOTOS application is of the after-burner type. For the previously generated event, with a certain probability, a decay vertex can be replaced with the one featuring additional photons. Similar solution for additional lepton pairs is installed since [11]. The algorithm is based on exact phase space.

In Section 2 of my thesis exact phase-space, as it used by PHOTOS and by KORALW [12], is explained. PHOTOS uses the two-body and four body exact phase space. The best description of its phase-space generation is given in [10].

Before matrix element installation, pre-samplers were introduced and checked as well, respectively for collinear, small virtuality and small energy of virtual photon enhancements. For the case of two chains of singularity structure, two pre-samplers are needed too. In this case phase space parametrization remains exact[1].

As PHOTOS operates an exact phase-space, the room for improvement is in its matrix element. Section 3 explains matrix element. PHOTOS algorithm applies matrix element over the entire phase space [10]. In the published version [11] of the algorithm approximation (formula (1) of Ref. [13]) is used only. This algorithm allows generation of a dominant contribution of an effect of extra pair emission for an any $Z/\gamma^* \to 2f$ decay. The question about quality of spectra by PHOTOS and, thus, a question about room for improvement for PHOTOS will eventually depend on a process under study.

I focus my research on extra pair emission from the final state of $2f \to Z/\gamma^* \to 2f$ process, having in mind generalization of approach for the extra pair emission from the final state of $pp \to Z/\gamma^* \to 2f$ process or for description of any $Z/\gamma^* \to 4f$ decay. Full four fermion end state include contributions from initial state radiation (ISR) and final state radiation (FSR). PHOTOS specialize on generation of FSR and, while ISR contribution is important [14], generation of ISR should be included into simulation chain [15] during generation of a hard process, i.e. before PHOTOS. Feynman diagrams corresponding to $2f \to Z/\gamma^* \to 4f$ process of FSR type are presented in Fig. 2. In Section 4 tests with partially integrated cross sections are presented.

Section 5 collects matrix elements for extra pair emissions. In order to improve PHOTOS, I calculate two fermions to γ/Z to four fermions (FSR only) matrix element (see Chapter 5.1 and corresponding Appendix C). I search for its the most important parts (see Chapter 5.3), having in mind approximation of $2f \to \gamma/Z \to 4f$ matrix element in order to separate extra pair correction from Born level $2f \to \gamma/Z \to 2f$ matrix element.

Section 6 is devoted to discussion of novel kernels for pair emission. The aim is to identify an option to reproduce results of exact matrix element for Z to four fermion decay as close as possible, but to retain the universal form which can be applied to other decays as well.

[1]However, when further particles, such as additionally generated photons appear, parametrization of phase-space ceases to be exact. This is due to the matching of Jacobians for distinct generation branches. This non-exactness appear as in multi-photon's emission or in any other case of more than two body decays in PHOTOS operation. This is for importance of higher order effects.

Section 7 is devoted to study how the new kernel perform for the Tau decay.

Section 8, summary provides conclusions and explanation of obtained improvements.

Appendix A contains formulae and plots that are supplementing Sections 4.1, 4.2. Appendix B collects set of plots, supplementing the ones of Sections 4 and 6. In Appendix C calculation of formulae given in Sections 5 and 6 is provided, it also supplements formulae from Section 3.

2 Phase Space

Element of the two-body phase space reads

$$
\begin{aligned}
&dLips_2\left(P;p_3',p_4'\right)=\int\frac{d^3p_3'}{(2\pi)^3 2(p_3')^0}\frac{d^3p_4'}{(2\pi)^3 2(p_4')^0}(2\pi)^4\delta^4(P-p_3'-p_4')=\\
&=\frac{1}{(2\pi)^2}\int d^4p_3'\delta((p_3')^2-\mu_3^2)\Theta((p_3')^0)d^4p_4'\delta((p_4')^2-\mu_4^2)\Theta((p_4')^0)\delta^4(P-p_3'-p_4')=\\
&=\frac{1}{(2\pi)^2}\int d^4p_3'\delta((p_3')^2-\mu_3^2)\delta((P-p_3')^2-\mu_4^2)\Theta((p_3')^0)\Theta(P^0-(p_3')^0)=\\
&=\frac{1}{(2\pi)^2}\int\frac{d^3p_3'}{2(p_3')^0}\delta((P-p_3')^2-\mu_4^2) \qquad (1)
\end{aligned}
$$

where P^μ is four-momenta of incoming particles[1], $(p_3')^\mu$, $(p_4')^\mu$ are four-momenta of outgoing particles; μ_3 is mass of the particle denoted by momenta $(p_3')^\mu$ and μ_4 is mass of the particle denoted by momenta $(p_4')^\mu$. I choose reference frame of P^μ and parameterize four-momenta p_3' in a spherical coordinates $d^3p_3'=\left|\overline{p}_3'\right|^2 d\left|\overline{p}_3'\right| dcos\theta d\varphi$, where $\left|\overline{p}_3'\right|$ is modulus of spatial part of four-vector $(p_3')^\mu$. I proceed

$$
\begin{aligned}
&dLips_2=\frac{1}{(2\pi)^2}\int d\left|\overline{p}_3'\right| dcos\theta d\varphi\frac{\left|\overline{p}_3'\right|^2}{2\sqrt{\left|\overline{p}_3'\right|^2+\mu_3^2}}\delta(M^2-2M\sqrt{\left|\overline{p}_3'\right|^2+\mu_3^2}+\mu_3^2-\mu_4^2)=\\
&=\frac{1}{(2\pi)^2}dcos\theta d\varphi\frac{1}{8}\frac{\lambda\left(M^2,\mu_3^2,\mu_4^2\right)}{M^2}, \qquad (2)
\end{aligned}
$$

where $M^2=P^2$ and $\lambda\left(M^2,\mu_3^2,\mu_4^2\right)=\sqrt{M^4+\mu_3^4+\mu_4^4-2M^2\mu_3^2-2M^2\mu_4^2-2\mu_3^2\mu_4^2}$. With change of variables

$$
cos\theta=-1+2x_1, \qquad \varphi=2\pi x_2 \qquad (3)
$$

element of two-body phase space finally reads

$$
dLips_2=\frac{1}{2^5\pi^2}\prod_{i=1}^{2}dx_i(4\pi)\frac{\lambda\left(M^2,\mu_3^2,\mu_4^2\right)}{M^2}. \qquad (4)
$$

[1]here I reserve p_1^μ, p_2^μ for four-momenta of incoming fermions $P^\mu=p_1^\mu+p_2^\mu$.

Element of four-body phase space reads

$$dLips_4\left(P;p_3,p_4,p_5,p_6\right)=\int\frac{d^3p_3}{(2\pi)^3 2p_3^0}\frac{d^3p_4}{(2\pi)^3 2p_4^0}\frac{d^3p_5}{(2\pi)^3 2p_5^0}\frac{d^3p_6}{(2\pi)^3 2p_6^0}(2\pi)^4\delta^4(P-p_3-p_4-p_5-p_6)=$$
$$=\frac{1}{(2\pi)^8}\int dM_{34}^2 dM_{56}^2\left[\frac{d^3p_3}{2p_3^0}\frac{d^3p_4}{2p_4^0}\delta^4(k-p_3-p_4)\right]\left[\frac{d^3p_5}{2p_5^0}\frac{d^3p_6}{2p_6^0}\delta^4(q-p_5-p_6)\right]\left[d^4q\delta(q^2-M_{56}^2)\Theta(q^0)\right]\times$$
$$\times\left[d^4k\delta(k^2-M_{34}^2)\Theta(k^0)\right]\delta^4(P-k-q)=\frac{1}{(2\pi)^8}\int dM_{34}^2 dM_{56}^2\left[dcos\theta_1 d\varphi_1\frac{1}{8}\frac{\lambda\left(M_{34}^2,\mu_3^2,\mu_4^2\right)}{M_{34}^2}\right]_{\overline{k}=0}\times$$
$$\times\left[dcos\theta_2 d\varphi_2\frac{1}{8}\frac{\lambda\left(M_{56}^2,\mu_5^2,\mu_6^2\right)}{M_{56}^2}\right]_{\overline{q}=0}\left[\frac{d^3q}{2q^0}\frac{d^3k}{2k^0}\delta^4(P-k-q)\right]=\frac{1}{2^{17}\pi^8}dM_{56}^2 dM_{34}^2\times$$
$$\times dcos\theta_1 d\varphi_1 dcos\theta_2 d\varphi_2 dcos\theta_3 d\varphi_3\frac{\lambda\left(M_{34}^2,\mu_3^2,\mu_4^2\right)}{M_{34}^2}\frac{\lambda\left(M_{56}^2,\mu_5^2,\mu_6^2\right)}{M_{56}^2}\frac{\lambda\left(M^2,M_{34}^2,M_{56}^2\right)}{M^2},\qquad(5)$$

where $M^2=P^2$, $M_{56}^2=\left(p_5+p_6\right)^2$, $M_{34}^2=\left(p_3+p_4\right)^2$; $dcos\theta_1 d\varphi_1$ is the solid-angle element of $\overline{p}_3$ in the rest frame of $(p_3^\mu+p_4^\mu)$; $dcos\theta_2 d\varphi_2$ is the solid-angle element of $\overline{p}_5$ in the rest frame of $(p_5^\mu+p_6^\mu)$; $dcos\theta_3 d\varphi_3$ is the solid-angle element of $(p_3^\mu+p_4^\mu)$ in the rest frame of P^μ. With following change of the variables

$$\begin{aligned}
&cos\theta_1=-1+2x_1, &&\varphi_1=2\pi x_2,\\
&cos\theta_2=-1+2x_3, &&\varphi_2=2\pi x_4,\\
&cos\theta_3=-1+2x_5, &&\varphi_3=2\pi x_6,\\
&M_{56}^2=M_{56,min}^2+(M_{56,max}^2-M_{56,min}^2)x_7,\\
&M_{34}^2=M_{34,min}^2+(M_{34,max}^2-M_{34,min}^2)x_8,
\end{aligned}\qquad(6)$$

the differential form (5) turns into a canonical form

$$dLips_4=\frac{1}{2^{17}\pi^8}\prod_{i=1}^{8}dx_i\frac{\lambda\left(M_{34}^2,\mu_3^2,\mu_4^2\right)}{M_{34}^2}\frac{\lambda\left(M_{56}^2,\mu_5^2,\mu_6^2\right)}{M_{56}^2}\frac{\lambda\left(M^2,M_{34}^2,M_{56}^2\right)}{M^2}\times$$
$$\times(4\pi)^3(M_{56,max}^2-M_{56,min}^2)(M_{34,max}^2-M_{34,min}^2),\qquad(7)$$

where $M_{56,min}=\mu_5+\mu_6$, $M_{56,max}=M$, $M_{34,min}=\mu_3+\mu_4$, $M_{34,max}=M-M_{56}$.

One can relate the two-body and four-body phase space generators as follows: use the the two body events in an inverted sense to obtain the x_1, x_2 random numbers (phase space coordinates first), and later use these numbers in four-body phase space event construction as follows:

$$dLips_4\left(P;p_3,p_4,p_5,p_6\right)=\frac{1}{2^5\pi^2}\prod_{i=1}^{2}dx_i(4\pi)\frac{\lambda\left(M^2,\mu_3^2,\mu_4^2\right)}{M^2}\frac{1}{2^{12}\pi^6}\prod_{i=3}^{8}dx_i\frac{\lambda\left(M_{34}^2,\mu_3^2,\mu_4^2\right)}{M_{34}^2}\times$$
$$\times\frac{\lambda\left(M^2,M_{34}^2,M_{56}^2\right)}{M^2}\frac{\lambda\left(M_{56}^2,\mu_5^2,\mu_6^2\right)}{M_{56}^2}\frac{M^2}{\lambda\left(M^2,\mu_3^2,\mu_4^2\right)}(4\pi)^2(M_{56,max}^2-M_{56,min}^2)\times$$
$$\times(M_{34,max}^2-M_{34,min}^2)=dLips_2\left(P;p_3',p_4'\right)\times\frac{1}{2^{12}\pi^6}\prod_{i=3}^{8}dx_i\frac{\lambda\left(M_{34}^2,\mu_3^2,\mu_4^2\right)}{M_{34}^2}\frac{\lambda\left(M_{56}^2,\mu_5^2,\mu_6^2\right)}{M_{56}^2}\times$$

$$\times \frac{\lambda\left(M^2, M_{34}^2, M_{56}^2\right)}{\lambda\left(M^2, \mu_3^2, \mu_4^2\right)} (4\pi)^2 (M_{56,max}^2 - M_{56,min}^2)(M_{34,max}^2 - M_{34,min}^2). \quad (8)$$

The minimal decay kinematic is transformed into space-time coordinates: angles and invariant masses. Additional variables are generated from crude distributions to complete coordinates necessary to parameterize configurations with new particles added.

Case of pair emission is quite analogous and the kinematical configuration for each decay is first deconvoluted into angular parametrization of two body decay into `emitter` and `spectator`[1]. The corresponding angles, together with extra generated ones, provide parametrization of four body phase space; all necessary phase-space Jacobians are calculated and taken into account. Corresponding algorithm for phase-space is also exact in the case of emission of additional lepton pairs.

In formula (8) ratio of $\lambda\left(M^2, M_{34}^2, M_{56}^2\right) / \lambda\left(M^2, \mu_3^2, \mu_4^2\right)$ compensates for the difference in phase space Jacobians. The formula (8) is used for four body phase space generation with the help of two body events. These two-body events can be generated first by other Monte Carlo. Note also that phase space Jacobian of formula (7) would numerically differ very little between the case of Z decay into electrons or muons, by $(m_\mu^2/M_Z^2) \sim 10^{-6}$ only.

It was checked with samples of 100 million events that once matrix element is set to unity, flat four body phase space generation is achieved. This was checked with default test of `MC-TESTER` [16] and compared with another four-body phase-space generator deduced from `TAUOLA` [17].

3 Pair emission matrix element

By M_{Born} I depict matrix element of Fig. 1, by M_1, M_2, M_3, M_4 I depict matrix elements of Fig. 2. For my purpose only the $Z \to 4f$ part of these amplitudes are needed. Contribution from diagrams $M_1 + M_2$ can be understood as $f_3\overline{f}_3$ extra pair emission from $f_2\overline{f}_2$ final state and for diagrams $M_3 + M_4$ role of the pair interchange. In the following I define four-momenta as they are presented on Feynman diagrams of Figs. 1-2.

`PHOTOS` feature extra pair emission for an any $Z/\gamma^* \to ll$ decay basing on soft factorized matrix element (see Appendix C for more details), which is the soft limit of the the complete pair emission matrix element, of the form which can be used all over the phase space:

$$\sum_{spins} |M_1 + M_2|_{soft}^2 = F_{soft}(p_1, p_2; p_3, p_4, p_5, p_6) \cdot |M(p_1, p_2; p_3', p_4')|_{Born}^2 \,, \quad (9)$$

where p_1, p_2, p_3, p_4, p_5, p_6, q are four-momenta that are described by Fig. 2; p_3', p_4' are four-momenta of two-body phase space (i.e. $p_1^\mu + p_2^\mu = (p_3')^\mu + (p_4')^\mu$), all four-momenta are defined in eqs. (4) and (5) respectively;

$$|M|_{Born}^2 = \frac{\alpha^2 (4\pi)^2}{(p_1 + p_2)^4} Tr\left[(\not{p}_1 + m_1)\gamma_\mu (\not{p}_2 - m_1)\gamma_\nu\right] Tr\left[(\not{p}_3' + m_2)\gamma^\mu (\not{p}_4' - m_2)\gamma^\nu\right] \quad (10)$$

[1]The spectator may represent multiple particles. But as corresponding Jacobians for phase space parametrization do not need to be modified we may omit details from our brief presentation.

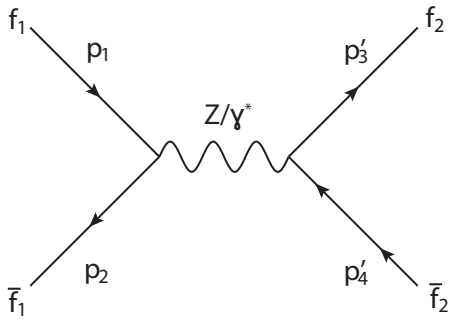

M_{Born}

Figure 1: Feynman diagram corresponding to $f_1(p_1)\overline{f}_1(p_2) \to Z/\gamma^* \to f_2(p_3')\overline{f}_2(p_4')$ Born level process.

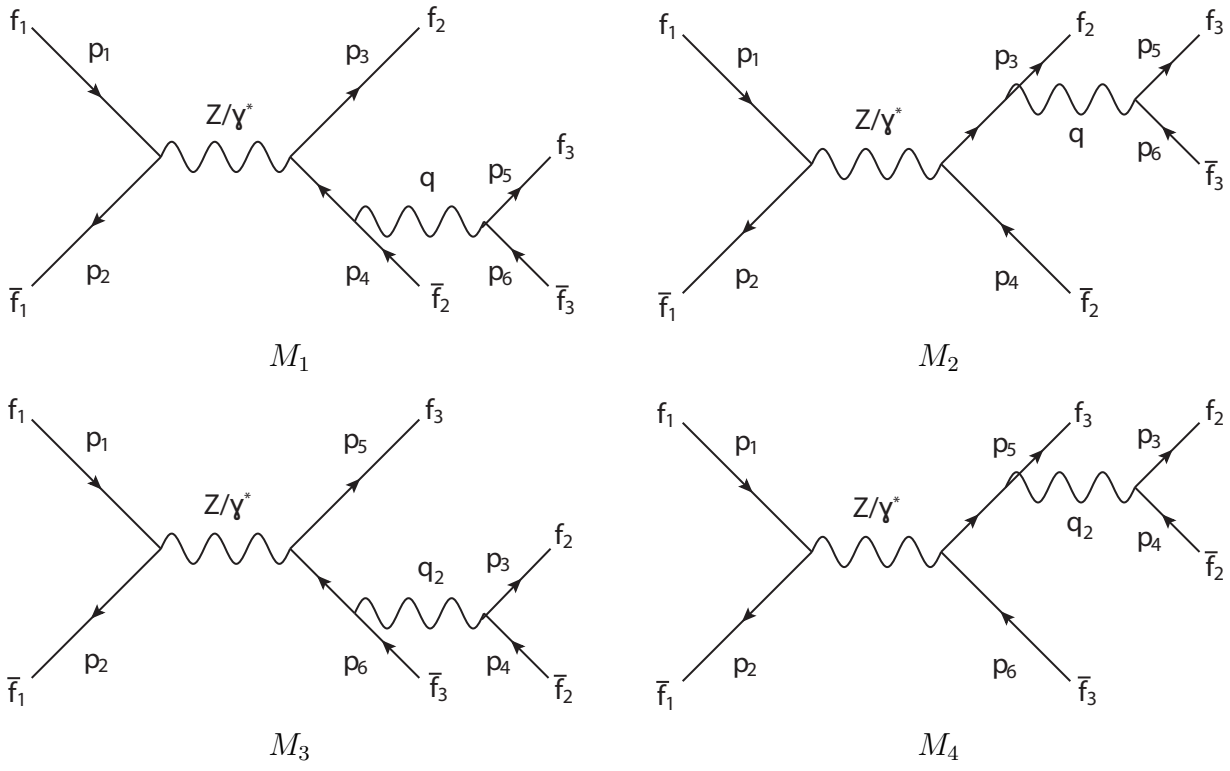

Figure 2: Feynman diagrams corresponding to $f_1(p_1)\overline{f}_1(p_2) \to Z/\gamma^* \to f_2(p_3)\overline{f}_2(p_4)f_3(p_5)\overline{f}_3(p_6)$ process.

is Born level matrix element, m_1 and m_2 are masses of fermions ($p_1^2 = p_2^2 = m_1^2$, $(p_3')^2 = (p_4')^2 = m_2^2$), α is QED constant and

$$F_{soft} = 2\,(4\pi\alpha)^2\,\frac{4p_5^\alpha p_6^\beta - q^2\cdot g^{\alpha\beta}}{q^4}\left(\frac{p_3^\alpha}{p_3 q} - \frac{p_4^\alpha}{p_4 q}\right)\left(\frac{p_3^\beta}{p_3 q} - \frac{p_4^\beta}{p_4 q}\right) \tag{11}$$

is factorized emission part of matrix element. This factorization property of QED is important for PHOTOS design, in particular for construction of its algorithm of pair emission. On its basis universal pair emission algorithm, which can provide reasonable results for any process is established. Born level process $|M|^2_{Born}$ is managed by other than PHOTOS MC generator. Then events of Born level process are modified according to F_{soft} factorized part of matrix element.

4 Testing with inclusive distributions

4.1 Soft integrated cross section

As it is noted before, factorization scheme (9) of matrix element $\sum_{spins}|M_1+M_2|^2_{soft}$ is valid approximation for the case of small energy of the emitted extra pair, but can be used over entire phase space (7). An analytical approach is possible up to some extent: it is possible to split integration of matrix element $\sum_{spins}|M_1+M_2|^2_{soft}$ onto integration of $|M|^2_{Born}$ over two-body phase space (4) and integration of factorized part of matrix element F_{soft} over two-body phase space (4).

Factorized part of matrix element (11) is universal, it is the same for the matrix element describing extra pair emissions for any $Z/\gamma^* \to 2f$ decay. In this case an integral of F_{soft} over phase space, corresponding to an extra pair emitted from incoming fermions, is well known (formula (5) from Ref. [13]). Real soft ISR pair emission factor reads[1]:

$$\begin{aligned}\widetilde{B}_f &= -\frac{2}{3s}(\frac{\alpha}{\pi})^2\int dM_{34}^2\frac{dM_{56}^2}{M_{56}^2}\sqrt{1-\frac{4m_3^2}{M_{56}^2}}\left(1+\frac{2m_3^2}{M_{56}^2}\right)\left(\frac{m_2^2\lambda^{\frac{1}{2}}(s,M_{34}^2,M_{56}^2)}{M_{56}^2 s+\frac{m_2^2}{s}\lambda(s,M_{34}^2,M_{56}^2)}+\right.\\ &+\left.\frac{s-2m_2^2}{\sqrt{1-\frac{4m_2^2}{s}}(s+M_{56}^2-M_{34}^2)}\ln\frac{s+M_{56}^2-M_{34}^2-\sqrt{1-\frac{4m_2^2}{s}}\lambda^{\frac{1}{2}}(s,M_{34}^2,M_{56}^2)}{s+M_{56}^2-M_{34}^2+\sqrt{1-\frac{4m_2^2}{s}}\lambda^{\frac{1}{2}}(s,M_{34}^2,M_{56}^2)}\right)\end{aligned} \tag{12}$$

where m_2 and m_3 are masses of fermions ($p_3^2 = p_4^2 = m_2^2$, $p_5^2 = p_6^2 = m_3^2$), s is center of the mass energy squared of incoming particles $s = E_{CMS}^2 = (p_1+p_2)^2 = (p_3'+p_4')^2$, M_{34}^2 is invariant mass squared of the lepton pair $M_{34}^2 = q_2^2 = (p_3+p_4)^2$, M_{56}^2 is invariant mass squared of the extra lepton pair $M_{56}^2 = q^2 = (p_5+p_6)^2$, and $\lambda(s,M_{34}^2,M_{56}^2) = \sqrt{s^2+M_{34}^4+M_{56}^4-2sM_{34}^2-2sM_{56}^2-2M_{34}^2M_{56}^2}$. Factor $\widetilde{B}_f$ has a meaning of extra pair emission probability. Factor $\widetilde{B}_f$ is introduced in Ref. [13] as an additive analog of YFS [18]

[1]Here I consider parameter a equal zero $a = 0$, since it corresponds to F_{soft} of eq. 11.

soft photon factor; index f refers to sum over all such fermion factors. Factor $\widetilde{B}_f$ is calculated with assumption that emitted pair momenta are small in comparison to those of sources. This is to be taken both in phase space and matrix element ($|M(p_1,p_2;p_3,p_4)|^2_{Born} \approx |M(p_1,p_2;p'_3,p'_4)|^2_{Born}$). On the other hand, in the eq. (12) integration covers all two-body phase space and factor $\widetilde{B}_f$ in the form of eq. (12) is exact. In the Ref. [13] phase space cut is introduced limiting energy of extra pair by Δ. For this case factor $\widetilde{B}_f(\Delta)$ has a meaning of probability of extra pair emission with energy less than Δ. In my tests I calculate $\widetilde{B}_f$ both for full two body phase space and for cutted phase space .

If the energy of the emitted pair E_{56} is smaller than some Δ, which is much smaller than center of the mass energy of incoming particles and is much larger than double the mass of a single extra lepton ($2m_3 \ll \Delta \ll E_{CMS}$), then formula (12) can be used for extra pair emissions from the final state as well [19]. For a harder emissions extra pair emission probability $\widetilde{B}_f$ doesn't cover solution of PHOTOS since $\widetilde{B}_f$ applies to pair emissions from incoming fermions. For technical tests of PHOTOS and for better understanding of its features, I repeat analytical calculation, but for integration of F_{soft} over final state emission phase space. Extra pair emission probability from the final state reads:

$$\begin{aligned} P_{pair} &= -\frac{2}{3s}(\frac{\alpha}{\pi})^2 \int dM^2_{34} \frac{dM^2_{56}}{M^2_{56}} \sqrt{1-\frac{4m_3^2}{M^2_{56}}} \left(1+\frac{2m_3^2}{M^2_{56}}\right) \left(\frac{m_2^2 \sqrt{1-\frac{4m_2^2}{M^2_{34}}} \lambda^{\frac{1}{2}}(s,M^2_{34},M^2_{56})}{M^2_{56}M^2_{34}+\frac{m_2^2}{M^2_{34}}\lambda(s,M^2_{34},M^2_{56})} + \right. \\ &+ \left. \frac{M^2_{34}-2m_2^2}{s-M^2_{56}-M^2_{34}} \ln \frac{s-M^2_{56}-M^2_{34}-\sqrt{1-\frac{4m_2^2}{M^2_{34}}}\lambda^{\frac{1}{2}}(s,M^2_{34},M^2_{56})}{s-M^2_{56}-M^2_{34}+\sqrt{1-\frac{4m_2^2}{M^2_{34}}}\lambda^{\frac{1}{2}}(s,M^2_{34},M^2_{56})} \right). \end{aligned} \tag{13}$$

More details about calculation of formula (13) can be found in the Appendix A. Previous researches in this direction can be found in Ref. [20]. PHOTOS applies factorized matrix element (9) over entire phase space, it means that for a given energy E_{CMS} of incoming particles probability P_{pair} of eq. (13) matches analytically the solution of PHOTOS. If the energy of the extra pair is limited by Δ, then probability of soft extra pair emission from the final state $P_{pair}(\Delta)$ approximates to $\widetilde{B}_f(\Delta)$ from Ref. [13].

4.2 Test with soft integrated cross section

Cross sections σ_{Born} of born level process (see Fig. 1) is given by integral of matrix element $|M|^2_{Born}$ over two-body phase space (4) and cross section σ_{12} of extra pair emission process is given by integral of matrix element $\sum_{spins}|M_1+M_2|^2_{soft}$ over four-body phase space (7). A ratio of differential cross sections $\frac{d\sigma_{Born}}{dM^2_{34}} / \frac{d\sigma_{12}}{dM^2_{34}}$ for center of the mass (CMS) energy of M_Z corresponds to a value of $\widetilde{B_f}(\Delta)$ for a given Δ (and for a given CMS energy).

Values of $\widetilde{B_f}$, that are result of numerical integration of formula (12), are collected in Tab. 1 and are compared with corresponding values of $\frac{d\sigma_{Born}(M_Z)}{dM^2_{34}} / \frac{d\sigma_{12}(M_Z)}{dM^2_{34}}$ obtained by PHOTOS for various values of Δ (Tab. 2). Agreement at the expected level of few percents of

	emitted	$\Delta = 1\ GeV$	$\Delta = 5\ GeV$	$\Delta = 10\ GeV$
$Z_0 \to e^+e^-$	e^+e^-	0.00094772	0.00171442	0.00212938
$Z_0 \to \mu^+\mu^-$	e^+e^-	0.00093813	0.00165131	0.00201747
$Z_0 \to e^+e^-$	$\mu^+\mu^-$	0.00001466	0.00010409	0.00017804
$Z_0 \to \mu^+\mu^-$	$\mu^+\mu^-$	0.00001466	0.00010408	0.00017801

Table 1: Extra pair emission probability $\widetilde{B}_f(\Delta)$ (for pairs with energy less than Δ) as it has been calculated by formula (12).

	emitted	$\Delta = 1\ GeV$	$\Delta = 5\ GeV$	$\Delta = 10\ GeV$
$Z_0 \to e^+e^-$	e^+e^-	0.00093850	0.00167783	0.00205299
$Z_0 \to \mu^+\mu^-$	e^+e^-	0.00093176	0.00162154	0.00194601
$Z_0 \to e^+e^-$	$\mu^+\mu^-$	0.00001507	0.00010231	0.00017137
$Z_0 \to \mu^+\mu^-$	$\mu^+\mu^-$	0.00001480	0.00010191	0.00017026

Table 2: Ratio of differential cross sections $\frac{d\sigma_{Born}}{dM_{34}^2} / \frac{d\sigma_{12}}{dM_{34}^2}$ as it has been calculated by PHOTOS. An error is at level of the last presented digit.

pair effect was found for electrons and muons, and for several choices of maximum energy of emitted lepton pairs. On the other hand, one may expect distorted spectra for the harder generated extra pairs. It is reported [21] that simulations of the $e^+e^- \to Z \to 4l$ decay process with KORALW [12] and with PHOTOS agree better than percent level for the most populated bins of histograms of benchmark distributions. For high energy fermions results from KORALW seems to indicate for somewhat harder spectrum than of PHOTOS.

Here I summarize details of my calculation.

- I monitor again the spectrum of invariant mass for the lepton pair, which is modified by emission of additional pair.
- For results of PHOTOS [11] and for semi-analytical calculation I first generate the sample of events from PYTHIA [22] with initialization summarized in Tab. A.1.
- In order to complete results for PHOTOS, its algorithm is applied on events generated by PYTHIA.
- For calculation with formulae (12-13) I move events, that are generated by PYTHIA, to every possible bin of our test distributions with probabilities obtained from formula (12-13) respectively.

The main difference between formula (12) and (13) is that (13) was obtained by integration over four-body phase space (7), corresponding to FSR pair emission, of matrix element (9). For formula (12) an approximation in phase space was used. Four momenta

that correspond to extra pair emission are treated as soft and as not effecting other four momenta. If energy of the emitted pair is restricted to soft pair emissions limit, the two calculations coincide, as they should.

One can argue that formula (12) is less suitable for tests. This is not necessarily to be the case. For formula (13) a factorization form of matrix element is used, but such approximation is not used for phase space. This is potential source of numerically important mismatches. Even though exact phase space parametrization offer convenient starting point for future work with matrix element, independent tests with calculations based on four fermions final state matrix elements are of importance.

The numerical tests are summarized in Fig. 3 for formula (12) and in Fig. 4 for my new formula (13).

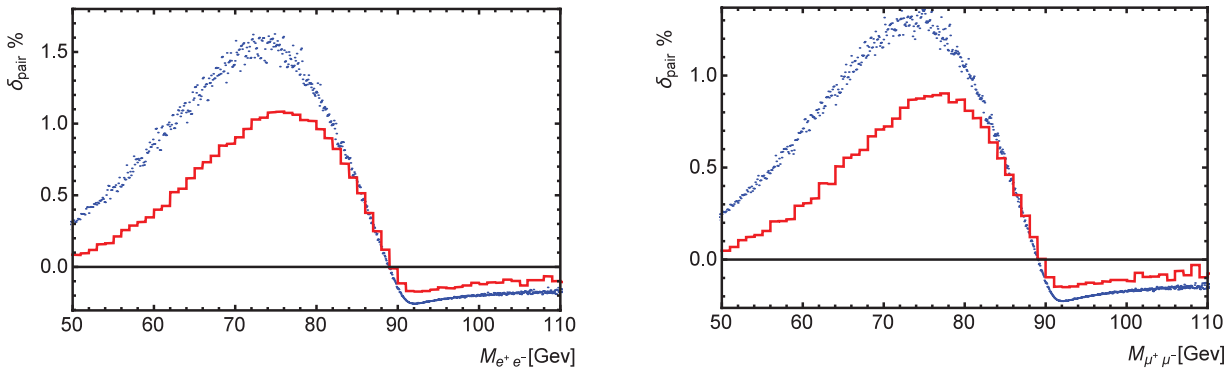

Figure 3: Comparison of PHOTOS simulation and calculations of extra pair emissions, for the processes $pp \to Z \to e^+e^-(e^+e^-)$ (left plot) and $pp \to Z \to \mu^+\mu^-(e^+e^-)$ (right plot) at 14 TeV, with independent semi analytical calculations. Correction to lepton pair invariant mass spectrum of PYTHIA generated sample is given in %. Solid line represents data by PYTHIA×PHOTOS. Points represent results of simulation by PYTHIA, convoluted bin by bin with formula (12) i.e. as of Ref. [13]. PHOTOS generated spectra are not well reproduced by formula (12) for extra pair emissions from incoming fermions.

Analyzing the Figs. 3-4 I conclude, that PHOTOS is well in agreement with analytical calculation (13); agreement is not so good for formula (12). Numerical precision of agreement is better than 5% of the pair effect. Estimation is limited by the numerical calculation and CPU time. It can be improved rather easily. The result is supplemented with Fig. A.1 of Appendix, which is of more technical nature. It includes also plots for $Z \to e^+e^-(\mu^+\mu^-)$ and $Z \to \mu^+\mu^-(\mu^+\mu^-)$.

4.3 PHOTOS-SANC comparison

SANC [23–32] is a computer system for Support of Analytic and Numeric calculations for experiments at Colliders. The PHOTOS and SANC Monte Carlo programs use different approximations for the effect under study. SANC uses formalism of electron structure (frag-

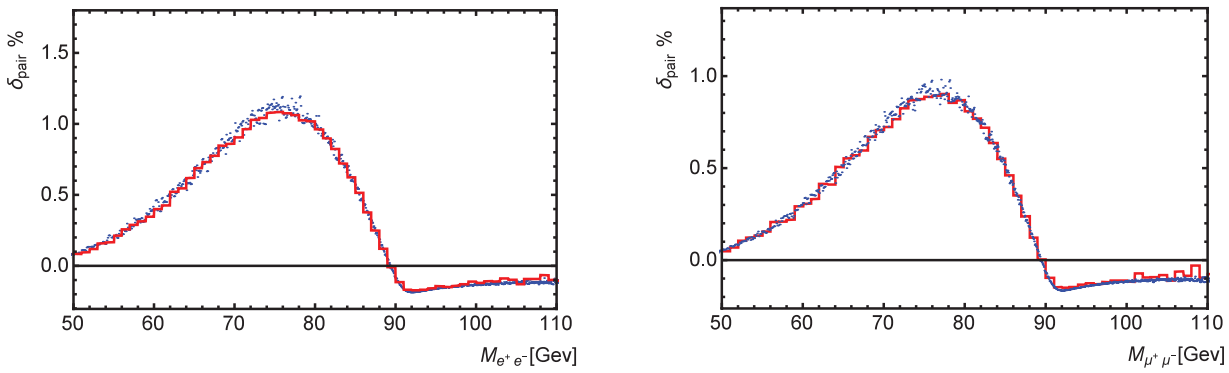

Figure 4: Comparison of PHOTOS simulation and calculations of extra pair emissions, for the processes $pp \to Z \to e^+e^-(e^+e^-)$ (left plot) and $pp \to Z \to \mu^+\mu^-(e^+e^-)$ (right plot) at 14 TeV, with independent semi analytical calculations. Correction to lepton pair invariant mass spectrum of PYTHIA generated sample is given in %. Solid line represents data by PYTHIA×PHOTOS. Points represent results of simulation by PYTHIA, convoluted bin by bin with new formula (13). New formula (13) reproduces well results of PHOTOS.

mentation) functions [31,33,34] which describe radiation in the approximation of collinear kinematics.

In SANC the leading logarithmic approximation (LLA) was applied to take into account the corrections of the orders $\mathcal{O}(\alpha^n L^n)$, $n = 2, 3$, where in case of pair emission big logarithms $L(m_\ell, \mu) = \log(\mu^2/m_\ell^2)$ depends on the lepton mass m_ℓ and on the factorization scale μ. I leave technical details regarding SANC algorithm and its input parameters to the Refs. [20,35]. Here I present results of PHOTOS-SANC comparison.

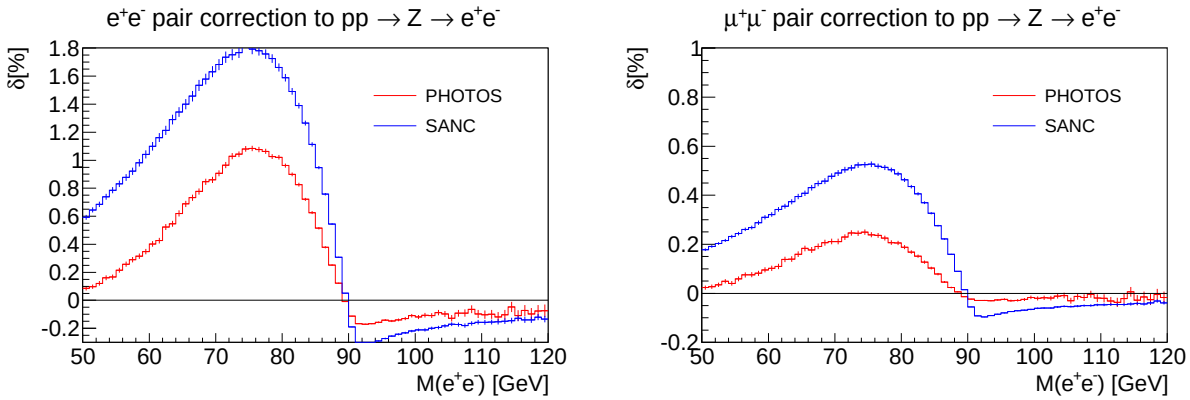

Figure 5: Corrections δ in % for invariant mass $M(e^+e^-)$ distribution in $Z \to e^+e^-$ decay due to extra e^+e^- (left) or $\mu^+\mu^-$ (right) pair emission.

Pair correction is defined as $\delta^{pair} = (\sigma^{pair} - \sigma^{Born})/\sigma^{Born}$. The results for distribution of invariant mass $M(\ell^+\ell^-)$ are presented in Fig. 5 and Fig. 6 for PYTHIA generated sample of

Drell-Yan processes at 14 TeV center of mass energy pp collisions and final state of electron and muon pairs respectively.

An agreement between pair implementation with the help of PHOTOS and SANC seems not to be sufficient, differences are big and dominated, as it is appears later, by non leading terms and of rather hard pair emission. I continue with discussion of results.

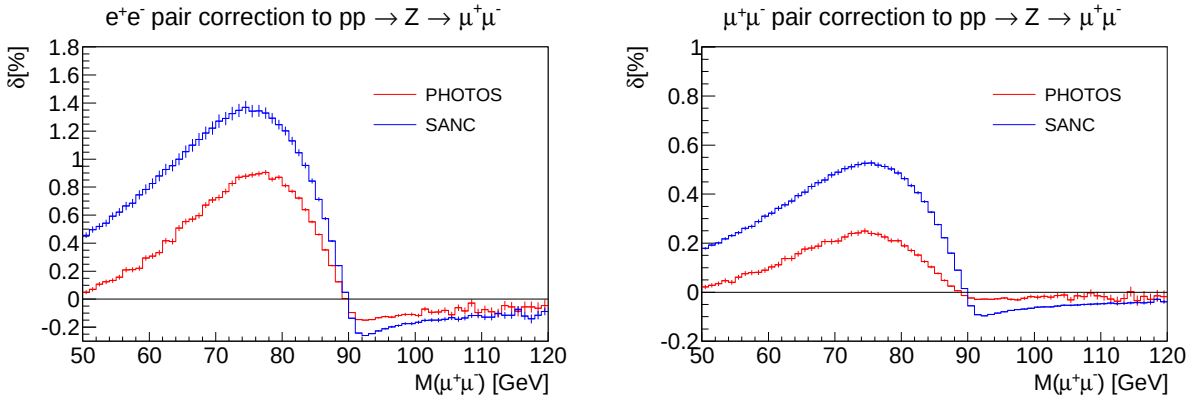

Figure 6: Corrections δ in % for invariant mass $M(\mu^+\mu^-)$ distribution in $Z \to \mu^+\mu^-$ decay due to extra e^+e^- (left) or $\mu^+\mu^-$ (right) pair emission.

The comparison between HORACE [36] and SANC of pair contributions is presented in the Ref. [37]. One can see, that a better agreement was found in this case, but the approximation of pair corrections in HORACE is closer to SANC than to PHOTOS.

The main purpose of SANC is to control dominant, leading logarithm effects of pairs emission for the sake to supplement systematic error evaluation for observables, where pair effects are comparable to systematic errors of other effects. That is why, non leading terms such as $\ln \frac{\mu}{m_\mu} \simeq 6$ may be neglected if they accompany dominant $\ln \frac{\mu}{m_e} \simeq 11$ ones. It may be of interest to implement such non-leading terms into SANC and/or PHOTOS.

The PHOTOS can be used as well to analyze an effect of singlet channel, which is the case of misidentification in the detector of first lepton as secondary one, when lepton pair emit lepton pair of the same kind. In Fig. 7, PHOTOS simulations of singlet channel are presented. Number of events fall down logarithmically with rise of invariant mass of misidentified pair. This perfectly agrees with theory.

In Fig. 8, soft pair corrections are presented. The cutoff $\Delta = 1$ GeV and is applied for energy of the additional lepton pair in the rest frame of colliding partons. This cutoff is chosen both to fulfill the conditions $4m_f^2 \ll \Delta^2 \ll M_Z^2$, which correspond to soft pair emissions, and to simulate an effect of the undetected pairs. Depending on the sensitivity of the detector, part of soft lepton pairs remains undetected causing shift in the $pp \to Z \to l^+l^-$ spectrum.

Both SANC and PHOTOS can generate pair effects simultaneously with emission of photons. Because of rather steep energy spectrum for emitted pairs, the effect of photonic bremsstrahlung on pair emission is not expected to be large. To validate this expectation

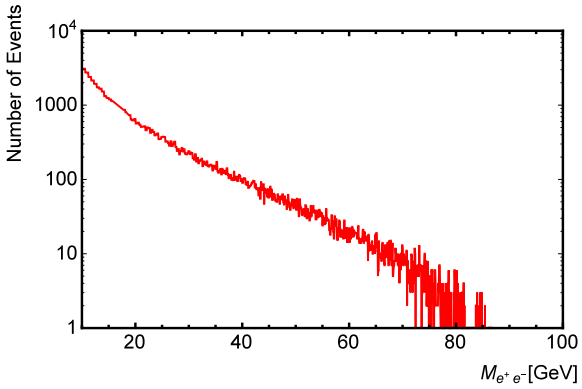

a) $pp \to Z \to e^+e^-(e^+e^-)$; probability for presence of additional pair is $\simeq 3 \cdot 10^{-3}$.

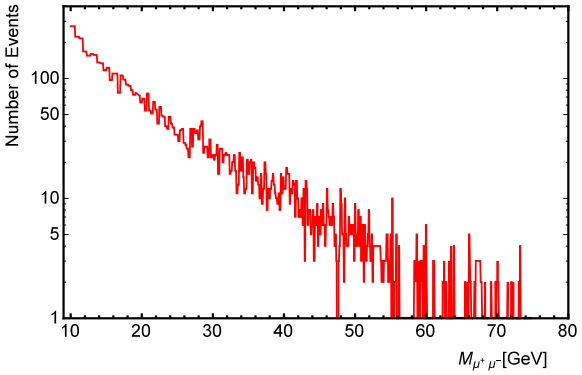

b) $pp \to Z \to \mu^+\mu^-(\mu^+\mu^-)$; probability for presence of additional pair is $\simeq 10^{-4}$.

Figure 7: Invariant mass distribution in the singlet channel, i.e. of pair formed from l^+ of emitting pair and l^- of emitted pair generated by PHOTOS. PYTHIA initialization parameters are presented in Tab. B.1. Generated samples (of $\sim 10^8$ events), were dominated by configurations with $M(l^+l^-) \simeq 10$ GeV.

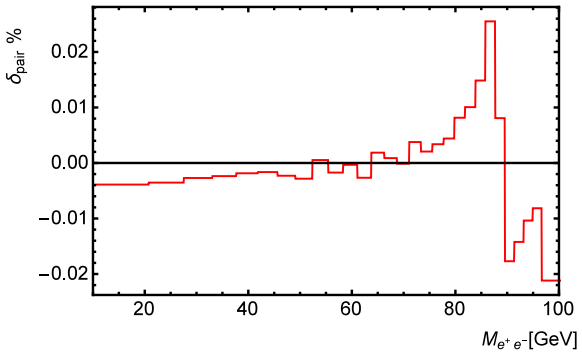

a) $pp \to Z \to e^+e^-(e^+e^-)$.

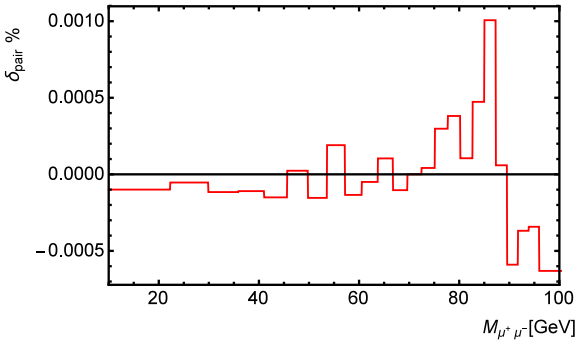

b) $pp \to Z \to \mu^+\mu^-(\mu^+\mu^-)$.

Figure 8: Pair correction to spectrum of lepton pair invariant mass of PYTHIA generated sample is given in %. Original sample is simulated for pp collisions of 14 TeV. Solid line represents data by PYTHIA×PHOTOS. Additional lepton pairs are generated under condition that energy of the additional lepton pair in the rest frame of colliding partons is less than 1 GeV.

we have introduced the following option into PHOTOS; instead of generating in 50 % of cases, pair emission before algorithm for photon emission is involved we have always generated pairs as the last step. Standard tests with the help of MC-TESTER demonstrate about 4 % increase in the number of final states consisting of configurations with added pair and at least one real photon of energy above 1 GeV. Shapes of distributions remained not modified in a noticeable way for the sample of 100 MeV events (see [38]).

This provides not only consistency check, but also confirms that PHOTOS can be used with generator such as KKMC [39] for generation of final state pair emissions. This, of course, require that intermediate Z/γ^* state is present in the event record. Such intermediate state can be obtained from the information of low level generation in KKMC. Even if it is not physically justified to define Z/γ^* intermediate state once initial-final state interference is taken into account, resulting inconsistency is only at the % level, at most, of the pair emission effect which itself is at % level too. It is thus at the 10^{-4} precision level.

Note, that if results from formula (12) are used, see Fig. 3, results of SANC are much closer than of PHOTOS to that variant of semi-analytical calculation. Taking all these results together we can conclude that we understand numerical difference between PHOTOS and SANC.

We can conclude that we control bulk of pair effects, down to 10 % of their size in the regions of phase space of importance for experimental conditions, that is for emitted pairs of rather small energies, or collinear. Rare events featuring hard pairs, could bring larger ambiguities, but are expected also to be outside of experimental acceptance. For this region of phase space taken separately, uncertainty is larger, of order of even 50%, but on the other hand, events of such configurations contribute to the overall Drell-Yan sample at sub-permille level.

The origin of the differences between PHOTOS and SANC results used for the systematic error evaluation is localized and confirmed with semi-analytical calculation. It is due to variant of soft pair approximation used in PHOTOS and SANC (for the details see eq. (A.10). Phase space, as used in PHOTOS algorithm, is explicit and exact, enabling for straightforward improvement of matrix element. Note that PHOTOS usage of approximation in matrix element, but not in phase space, may not be optimal. This is why solution used in SANC, a priori, is not of lower precision than that of PHOTOS. We argue to improve the precision tag from 0.3% to 0.1% for the pair implementation of the two programs and in applications for observables relevant for heavy boson reconstruction. We provide indications for steps necessary to improve beyond 0.1% precision level.

For the estimation of ambiguities size, the comparisons with KORALW, where complete $2 \to 4$ fermion matrix element is available, was instrumental. It may need to be continued in the future, but as hard pairs contribute to the bulk of differences, it may not be of urgency for present day experimental effort. This region of phase-space is expected to remain outside of experimental acceptance.

5 New matrix elements

5.1 PHOTOS with full matrix element

I dedicate this section to description of FSR $2f \to Z \to 4f$ matrix elements, the exact one and approximated ones. For my purpose only the $Z \to 4f$ part of these amplitudes are needed. In the physical gauge, contribution from diagrams $M_1 + M_2$ of Fig. 2 can be understood as $f_3\overline{f}_3$ pair emission from $f_2\overline{f}_2$ final state and for diagrams $M_3 + M_4$ role of the pair interchange. In my calculation I attempt to exploit features of these amplitudes in order to improve emission kernel used in `PHOTOS` and thus its precision. I delegate calculations to Appendix C.

Appendix C contains complete step by step calculation of matrix element for Z boson production and FSR decay into four fermion final state. Part C.2 of this Appendix is devoted to calculation of matrix element of photon production $f_1\overline{f}_1 \to \gamma \to f_2\overline{f}_2$ and decay $\sum_{spins} |M_1 + M_2|^2$ with extra $f_3\overline{f}_3$ pair emission. Using symmetry of description of the four fermion final state with regard to interchange of pairs $f_2\overline{f}_2 \leftrightarrow f_3\overline{f}_3$, part C.2 of the Appendix C corresponds to matrix element $\sum_{spins} |M_3 + M_4|^2$ as well. Part C.3 of the Appendix C completes four fermion FSR matrix element of photon production and decay with interference terms between diagrams $M_1 + M_2$ and $M_3 + M_4$.

Here I present matrix element $\sum_{spins} |M_1 + M_2|^2$ for an extra $f_3\overline{f}_3$ pair emission from the final state of the $f_1\overline{f}_1 \to Z/\gamma^* \to f_2\overline{f}_2$ spin summated process of Fig. 2

$$
\begin{aligned}
&\sum_{spins} |M_1 + M_2|^2 (p_1, p_2; p_3, p_4, m_2, p_5, p_6, m_3) = \sum_{spins} |M_3 + M_4|^2 (p_1, p_2; p_5, p_6, m_3, p_3, p_4, m_2) = \\
&= \sum_{spins} |M_1 + M_2|^2_{soft} + \frac{\alpha^4 (4\pi)^4}{(p_1 + p_2)^4} \frac{1}{q^4} Tr\left[(\not{p}_1 + m_1)\gamma_\mu (\not{p}_2 - m_1)\gamma_\nu\right] \times \\
&\times \left\{ \frac{16}{\left(2(p_3 q) + q^2\right)^2} \left[4g^{\mu\nu} m_2^2 \frac{q^2}{2} \left(\frac{q^2}{2} + m_3^2\right) + Tr\left[\not{p}_3\gamma^\mu \not{p}_4\gamma^\nu\right] \frac{q^2}{2} \cdot p_3 q + \right.\right. \\
&+ Tr\left[\not{p}_4\gamma^\mu (\not{p}_5 - \not{p}_6)\gamma^\nu\right] \frac{q^2}{2} \cdot p_3 (p_5 - p_6) - \\
&\left.\left. - Tr\left[\not{p}_4\gamma^\mu \not{p}_5\gamma^\nu\right] \left(2(p_3 p_6)^2 + m_2^2 \frac{q^2}{2}\right) - Tr\left[\not{p}_4\gamma^\mu \not{p}_6\gamma^\nu\right] \left(2(p_3 p_5)^2 + m_2^2 \frac{q^2}{2}\right) \right] + \right. \\
&+ \frac{16}{\left(2(p_4 q) + q^2\right)^2} \left[4g^{\mu\nu} m_2^2 \frac{q^2}{2} \left(\frac{q^2}{2} + m_3^2\right) + Tr\left[\not{p}_3\gamma^\mu \not{p}_4\gamma^\nu\right] \frac{q^2}{2} \cdot p_4 q + \right. \\
&+ Tr\left[\not{p}_3\gamma^\mu (\not{p}_5 - \not{p}_6)\gamma^\nu\right] \frac{q^2}{2} \cdot p_4 (p_5 - p_6) - \\
&\left. - Tr\left[\not{p}_3\gamma^\mu \not{p}_5\gamma^\nu\right] \left(2(p_4 p_6)^2 + m_2^2 \frac{q^2}{2}\right) - Tr\left[\not{p}_3\gamma^\mu \not{p}_6\gamma^\nu\right] \left(2(p_4 p_5)^2 + m_2^2 \frac{q^2}{2}\right) \right] +
\end{aligned}
$$

$$
+\frac{16}{(2\,(p_3q)+q^2)\,(2\,(p_4q)+q^2)}\Bigg[-\left(Tr\left[\not p_5\gamma^\mu \not p_5\gamma^\nu\right]+Tr\left[\not p_6\gamma^\mu \not p_6\gamma^\nu\right]\right)\left(m_2^2\frac{q^2}{2}+m_3^2\frac{q_2^2}{2}\right)-
$$

$$
-2Tr\left[\not p_5\gamma^\mu \not p_6\gamma^\nu\right]\left(m_2^2m_3^2+p_3p_6\cdot p_4p_5+p_3p_5\cdot p_4p_6-p_3p_4\cdot p_5p_6\right)+
$$

$$
+Tr\left[\not q_2\gamma^\mu \not q\gamma^\nu\right]\left(p_3p_4\frac{q^2}{2}\right)-Tr\left[\not p_3\gamma^\mu \not p_3\gamma^\nu\right]p_4q\frac{q^2}{2}-Tr\left[\not p_4\gamma^\mu \not p_4\gamma^\nu\right]p_3q\frac{q^2}{2}+
$$

$$
+2Tr\left[\left(\not p_3+\not p_4+\not p_6\right)\gamma^\mu \not p_6\gamma^\nu\right](p_3p_5\cdot p_4p_5)+2Tr\left[\left(\not p_3+\not p_4+\not p_5\right)\gamma^\mu \not p_5\gamma^\nu\right](p_3p_6\cdot p_4p_6)+
$$

$$
+4g^{\mu\nu}\Bigg(2m_3^2\left(p_3p_5\cdot p_4p_5+p_3p_6\cdot p_4p_6\right)-2p_5p_6\left(p_3p_6\cdot p_4p_5+p_3p_5\cdot p_4p_6\right)-
$$

$$
-2m_3^2\frac{q^2}{2}\left(\frac{q_2^2}{2}+p_3p_4\right)\Bigg)\Bigg]+16m_3^2\left(\frac{1}{(2\,(p_3q)+q^2)}+\frac{1}{(2\,(p_4q)+q^2)}\right)\times
$$

$$
\times\left(\frac{Tr\left[\not p_3\gamma^\mu \not q\gamma^\nu\right]p_4q}{2p_4q+q^2}+\frac{Tr\left[\not p_4\gamma^\mu \not q\gamma^\nu\right]p_3q}{2p_3q+q^2}-\frac{Tr\left[\not p_3\gamma^\mu \not p_4\gamma^\nu\right]\frac{q^2}{2}}{2\,(p_3q)+q^2}-\frac{Tr\left[\not p_3\gamma^\mu \not p_4\gamma^\nu\right]\frac{q^2}{2}}{2\,(p_4q)+q^2}\right)\Bigg\},\quad(14)
$$

where $\sum_{spins}|M_1+M_2|^2_{soft}$ is defined now by

$$
\sum_{spins}|M_1+M_2|^2_{soft}=F_{soft}(p_1,p_2;p_3,p_4,p_5,p_6)\cdot|M(p_1,p_2,p_3,p_4)|^2_{Born}\,;\qquad(15)
$$

it differs from (9) by replacing four-momenta p_3', p_4' with four-momenta p_3, p_4; factorized part of soft matrix element F_{soft} is defined by formula (11); Born level matrix element $|M(p_1,p_2;p_3,p_4)|^2_{Born}$ is defined by formula (10); four-momenta p_1, p_2, p_3, p_4, p_5, p_6, q, q_2 and masses m_1, m_2, m_3 of particles are defined as they are in the Fig. 2. The analytical form of matrix element used for generation is known and the required corrections (like eq. 11) can be introduced by weight: the ratio of new and old matrix elements squared.

I present matrix element $\sum_{spins}|M_1+M_2|^2$ (14) in a form of contraction of two tensors: tensor of the initial state, describing incoming particles, and tensor of final state. Tensor corresponding to the final state of eq. (14) is exact. If photon is decaying particle, the tensor, describing outgoing particles of eq. (14), can be used together with tensor, describing any possible initial state. If Z boson is decaying particle, tensor, describing outgoing particles of eq. (14), describes unpolarized Z boson decay. Matrix element $\sum_{spins}|M_1+M_2|^2$ (14) is a good basis for calculation of matrix element corresponding to polarized Z boson production and decay. I separate denominators in the tensor, describing outgoing particles of eq. (14), in order to organize terms that may contribute the most to collinear pseudo singularities. Overall factor $\frac{1}{q^4}$ contains soft pseudo singularity. Terms like $\frac{1}{2(p_4q)+q^2}$, $\frac{1}{2(p_3q)+q^2}$ and $\frac{1}{q^4}$ in the matrix element (14) can't be singular since emitted extra pair has a mass, however, states with smallest invariant mass of the extra pair q^2 have the highest probability density.

As it is mentioned, `PHOTOS` uses residual of matrix element to the Born level one. In order to install matrix element (14) into `PHOTOS` the F_{soft} of eq. (11) has to be replaced

with F_{full} of the following form:

$$F_{full} = \frac{\sum_{spins} |M_1 + M_2|^2}{|M(p_1, p_2; p_3', p_4')|^2_{Born}}, \tag{16}$$

where p_1, p_2 are 4-momenta of incoming electron-positron pair; p_3', p_4' are 4-momenta of born level outgoing lepton pair $f_2\overline{f}_2$ (before modification of the event by PHOTOS).

In an obvious way factor (16) requires knowledge about process and about incoming particles. Goal of my research is to find such modification of PHOTOS that both improves spectra generated by PHOTOS (comparing to exact ones) and that can be applied for the widest possible range of processes.

5.2 Gauge invariance

In my calculations I rely on comparisons of numerical results obtained from the gauge invariant calculation of KORALW. When I define my approximations, which I later cross check with these results, I do not need to rely on gauge invariant formulae.

I take

- spinor $u(p_1, s)$ for incoming fermion, $(\not{p}_1 - m_1)u(p_1, s) = 0$, where s is spin;
- spinor $\bar{v}(p_2, s)$ for incoming anti-fermion, $\bar{v}(p_2, s)(\not{p}_2 + m_1) = 0$;
- spinor $\bar{u}(p_3, s)$ for outgoing fermion, $\bar{u}(p_3, s)(\not{p}_3 - m_2) = 0$;
- spinor $v(p_4, s)$ for outgoing anti-fermion, $(\not{p}_4 + m_2)v(p_4, s) = 0$;
- $\frac{i(\not{p}+m)}{p^2-m^2+i\varepsilon}$ for fermion propagator, where $\varepsilon \to 0$;
- $-\frac{ig_{\mu\nu}}{q^2+i\varepsilon}$ for photon propagator, where $\varepsilon \to 0$.

As I am using tree level spin amplitudes of Fig. 2, gauge invariance of calculations from some diagrams taken alone is mathematically assured, because internal photon propagators are attached to outgoing fermion pairs that are on mass shell. Phase of outgoing fermion wave functions are canceling out in calculation of amplitude squares and there are no wave functions of photons in these diagrams.

5.3 Parts of matrix element

I focus on analysis of matrix element (14) and on indication of its tensor components ($H_i^{\mu\nu}$, $i = 1..8$) that are small giving small invariant mass of extra pair with:

$$\sum_{spins} |M_1 + M_2|^2 = \sum_{spins} |M_1 + M_2|^2_{soft} + \frac{\alpha^4 (4\pi)^4}{(p_1 + p_2)^4} \frac{1}{q^4} Tr\left[(\not{p}_1 + m_1)\gamma_\mu (\not{p}_2 - m_1)\gamma_\nu\right] \times \sum_{i=1}^{8} H_i^{\mu\nu}, \tag{17}$$

where

$$H_1^{\mu\nu} = \frac{16}{\left(2\left(p_3q\right)+q^2\right)\left(2\left(p_4q\right)+q^2\right)}\left[Tr\left[\not{q}_2\gamma^\mu\not{q}\gamma^\nu\right]\left(p_3p_4\frac{q^2}{2}\right) - 4g^{\mu\nu}\left(2m_3^2\frac{q^2}{2}2p_3p_4\right)\right] \quad (18)$$

$$H_2^{\mu\nu} = \frac{16}{\left(2\left(p_3q\right)+q^2\right)^2}\left[Tr\left[\not{p}_4\gamma^\mu\left(\not{p}_5-\not{p}_6\right)\gamma^\nu\right]\frac{q^2}{2}\cdot p_3\left(p_5-p_6\right)\right]+$$

$$+\frac{16}{\left(2\left(p_4q\right)+q^2\right)^2}\left[Tr\left[\not{p}_3\gamma^\mu\left(\not{p}_5-\not{p}_6\right)\gamma^\nu\right]\frac{q^2}{2}\cdot p_4\left(p_5-p_6\right)\right], \quad (19)$$

$$H_3^{\mu\nu} = \frac{16}{\left(2\left(p_3q\right)+q^2\right)^2}\left[Tr\left[\not{p}_3\gamma^\mu\not{p}_4\gamma^\nu\right]\frac{q^2}{2}\cdot p_3q\right] - \frac{16}{\left(2\left(p_3q\right)+q^2\right)\left(2\left(p_4q\right)+q^2\right)}\left[Tr\left[\not{p}_3\gamma^\mu\not{p}_3\gamma^\nu\right]p_4q\frac{q^2}{2}\right]+$$

$$+\frac{16}{\left(2\left(p_4q\right)+q^2\right)^2}\left[Tr\left[\not{p}_3\gamma^\mu\not{p}_4\gamma^\nu\right]\frac{q^2}{2}\cdot p_4q\right] - \frac{16}{\left(2\left(p_3q\right)+q^2\right)\left(2\left(p_4q\right)+q^2\right)}\left[Tr\left[\not{p}_4\gamma^\mu\not{p}_4\gamma^\nu\right]p_3q\frac{q^2}{2}\right], \quad (20)$$

$$H_4^{\mu\nu} = \frac{16}{\left(2\left(p_3q\right)+q^2\right)^2}\left[-2Tr\left[\not{p}_4\gamma^\mu\not{p}_5\gamma^\nu\right]\left(p_3p_6\right)^2 - 2Tr\left[\not{p}_4\gamma^\mu\not{p}_6\gamma^\nu\right]\left(p_3p_5\right)^2\right]+$$

$$+\frac{16}{\left(2\left(p_4q\right)+q^2\right)^2}\left[-2Tr\left[\not{p}_3\gamma^\mu\not{p}_5\gamma^\nu\right]\left(p_4p_6\right)^2 - 2Tr\left[\not{p}_3\gamma^\mu\not{p}_6\gamma^\nu\right]\left(p_4p_5\right)^2\right]+$$

$$+\frac{16}{\left(2\left(p_3q\right)+q^2\right)\left(2\left(p_4q\right)+q^2\right)}\Big[2Tr\left[\not{p}_3\gamma^\mu\not{p}_6\gamma^\nu\right]\left(p_3p_5\cdot p_4p_5\right)+2Tr\left[\not{p}_4\gamma^\mu\not{p}_6\gamma^\nu\right]\left(p_3p_5\cdot p_4p_5\right)+$$

$$+2Tr\left[\not{p}_3\gamma^\mu\not{p}_5\gamma^\nu\right]\left(p_3p_6\cdot p_4p_6\right)+2Tr\left[\not{p}_4\gamma^\mu\not{p}_5\gamma^\nu\right]\left(p_3p_6\cdot p_4p_6\right)\Big], \quad (21)$$

$$H_5^{\mu\nu} = \frac{16}{\left(2\left(p_3q\right)+q^2\right)^2}\left[4g^{\mu\nu}m_2^2\frac{q^2}{2}\left(\frac{q^2}{2}+m_3^2\right) - Tr\left[\not{p}_4\gamma^\mu\not{p}_5\gamma^\nu\right]m_2^2\frac{q^2}{2} - Tr\left[\not{p}_4\gamma^\mu\not{p}_6\gamma^\nu\right]m_2^2\frac{q^2}{2}\right]+$$

$$+\frac{16}{\left(2\left(p_4q\right)+q^2\right)^2}\left[4g^{\mu\nu}m_2^2\frac{q^2}{2}\left(\frac{q^2}{2}+m_3^2\right) - Tr\left[\not{p}_3\gamma^\mu\not{p}_5\gamma^\nu\right]m_2^2\frac{q^2}{2} - Tr\left[\not{p}_3\gamma^\mu\not{p}_6\gamma^\nu\right]m_2^2\frac{q^2}{2}\right]+$$

$$+\frac{16}{\left(2\left(p_3q\right)+q^2\right)\left(2\left(p_4q\right)+q^2\right)}\left[-2Tr\left[\not{p}_5\gamma^\mu\not{p}_6\gamma^\nu\right]\left(m_2^2m_3^2\right) - 4g^{\mu\nu}\left(2m_3^2\frac{q^2}{2}m_2^2\right)-\right.$$

$$\left.-\left(Tr\left[\not{p}_5\gamma^\mu\not{p}_5\gamma^\nu\right]+Tr\left[\not{p}_6\gamma^\mu\not{p}_6\gamma^\nu\right]\right)\left(m_2^2\frac{q^2}{2}+m_3^2m_2^2\right), \quad (22)$$

$$H_6^{\mu\nu} = \frac{16}{\left(2\left(p_3q\right)+q^2\right)\left(2\left(p_4q\right)+q^2\right)}\Big[-2Tr\left[\not{p}_5\gamma^\mu\not{p}_6\gamma^\nu\right]\left(p_3p_6\cdot p_4p_5+p_3p_5\cdot p_4p_6\right)+$$

$$+2Tr\left[\not{p}_6\gamma^\mu\not{p}_6\gamma^\nu\right]\left(p_3p_5\cdot p_4p_5\right)+2Tr\left[\not{p}_5\gamma^\mu\not{p}_5\gamma^\nu\right]\left(p_3p_6\cdot p_4p_6\right)+$$

$$+4g^{\mu\nu}\left(2m_3^2\left(p_3p_5\cdot p_4p_5+p_3p_6\cdot p_4p_6\right)-2p_5p_6\left(p_3p_6\cdot p_4p_5+p_3p_5\cdot p_4p_6\right)\right)\Big], \quad (23)$$

$$H_7^{\mu\nu} = \frac{16}{(2(p_3q)+q^2)(2(p_4q)+q^2)}\Bigg[2Tr\left[\not p_5\gamma^\mu \not p_6\gamma^\nu\right] p_3p_4 \cdot p_5p_6 -$$

$$-\left(Tr\left[\not p_5\gamma^\mu \not p_5\gamma^\nu\right] + Tr\left[\not p_6\gamma^\mu \not p_6\gamma^\nu\right]\right) m_3^2 \cdot p_3p_4\Bigg], \tag{24}$$

$$H_8^{\mu\nu} = 16m_3^2\left(\frac{1}{(2(p_3q)+q^2)} + \frac{1}{(2(p_4q)+q^2)}\right)\left(\frac{Tr\left[\not p_3\gamma^\mu \not q\gamma^\nu\right] p_4q}{2p_4q+q^2} + \frac{Tr\left[\not p_4\gamma^\mu \not q\gamma^\nu\right] p_3q}{2p_3q+q^2} -\right.$$

$$\left. - \frac{Tr\left[\not p_3\gamma^\mu \not p_4\gamma^\nu\right]\frac{q^2}{2}}{2(p_3q)+q^2} - \frac{Tr\left[\not p_3\gamma^\mu \not p_4\gamma^\nu\right]\frac{q^2}{2}}{2(p_4q)+q^2}\right). \tag{25}$$

There are multiple ways to organize cancelations in matrix element (14) resulting in different choices of tensors (18-25). I use following criteria for organization of such tensors: tensors should go to zero with invariant mass of extra pair going to zero; tensors should go to zero for collinear p_5 and p_6; tensors should remain the same after applying symmetry operations $p_3 \leftrightarrow p_4$, $p_5 \leftrightarrow p_6$.

I consider tensors $H_1^{\mu\nu} - H_4^{\mu\nu}$ among tensors $H_1^{\mu\nu} - H_8^{\mu\nu}$ bare the most influence on matrix element $\sum_{spins}|M_1+M_2|^2$, while effect of tensors $H_5^{\mu\nu} - H_8^{\mu\nu}$ on matrix element $\sum_{spins}|M_1+M_2|^2$ is small. Here follows arguments illustrating that.

Squared mass of the extra pair q^2 is small. One may expect this, because of pseudo singularity in the overall factor $1/q^4$ in the matrix element $\sum_{spins}|M_1+M_2|^2$. It is verified by many tests (see Section 6). I use this knowledge as a basis of the following analysis.

Tensors $H_1^{\mu\nu} - H_3^{\mu\nu}$ bare q^2 as overall factor. Here I do not go into analysis of cancelations in tensors $H_1^{\mu\nu} - H_3^{\mu\nu}$, so my task is to show that tensors $H_5^{\mu\nu} - H_8^{\mu\nu}$ are of order smaller than q^2.

Tensors $H_8^{\mu\nu}$ contains lepton mass squared as overall factor, so it is smaller than q^2 comparing to other tensors $H_i^{\mu\nu}$. Each term of tensor $H_5^{\mu\nu}$ contains lepton mass cubed or lepton mass squared times q^2, so tensor $H_5^{\mu\nu}$ is smaller than q^4 comparing to tensors $H_1^{\mu\nu} - H_4^{\mu\nu}$.

All of the generated extra pairs are of small invariant mass, that means collinearity of p_5 and p_6. In order to analyze tensors $H_6^{\mu\nu}$ and $H_7^{\mu\nu}$ I introduce new variables

$$n^\mu = \frac{p_5^\mu + p_6^\mu}{2} = \frac{q^\mu}{2}, \tag{26}$$

$$m^\mu = \frac{p_5^\mu - p_6^\mu}{2}, \tag{27}$$

$$p_5^\mu \to \frac{n^\mu + m^\mu}{2}, \tag{28}$$

$$p_6^\mu \to \frac{n^\mu - m^\mu}{2}, \tag{29}$$

$$\tag{30}$$

where, giving q^2 is small, $m^0 \sim \sqrt{q^2}$ and $|\overline{m}| \sim \sqrt{q^2}$ are small. I apply this change of variables for numerators of $H_6^{\mu\nu}$ and $H_7^{\mu\nu}$ only:

$$H_6^{\mu\nu} = \frac{1}{(2p_3q+q^2)\,(2p_4q+q^2)} \Bigg[8Tr\left[\not{m}\gamma^\mu \not{m}\gamma^\nu\right] p_3n\cdot p_4n + 8Tr\left[\not{n}\gamma^\mu \not{n}\gamma^\nu\right] p_3m\cdot p_4m -$$

$$-8Tr\left[\not{n}\gamma^\mu \not{m}\gamma^\nu\right](+p_3n\cdot p_4m + p_3m\cdot p_4n) + 4g^{\mu\nu}\left(8n^2\cdot p_3m\cdot p_4m + 8m^2\cdot p_3n\cdot p_4n\right)\Bigg], \quad (31)$$

$$H_7^{\mu\nu} = \frac{1}{(2p_3q+q^2)\,(2p_4q+q^2)} \Bigg[-4p_3p_4\cdot n^2 4Tr\left[\not{m}\gamma^\mu \not{m}\gamma^\nu\right] - 4\left(Tr\left[\not{n}\gamma^\mu \not{n}\gamma^\nu\right]\right) p_3p_4\cdot\left(m^2\right)\Bigg]. \quad (32)$$

It is seen from the expressions (31,32) that tensors $H_6^{\mu\nu}$ and $H_7^{\mu\nu}$ are of order of m^2, that is smaller than q^2 when comparing to tensors $H_1^{\mu\nu} - H_4^{\mu\nu}$. I should note that in the variables $\{n^\mu, m^\mu\}$, tensor $H_3^{\mu\nu}$ appears of order of m^2. However, tensor $H_3^{\mu\nu}$ contains pseudo singularities of second order $1/(2p_3q+q^2)^2$ and $1/(2p_4q+q^2)^2$, while tensor $H_6^{\mu\nu}$ contains pseudo singularities of first order $1/\left((2p_3q+q^2)(2p_4q+q^2)\right)$. Therefore, it is expected that an effect size of tensor $H_3^{\mu\nu}$ on matrix element (14) is larger than effect size of tensor $H_6^{\mu\nu}$. Further analysis is continued in Section 6.3.

5.4 Fix for $\sum_{spins} |M_1 + M_2|^2_{soft}$ not being soft enough

Soft matrix element (9) of basic PHOTOS [11] is an approximation. It contains Born level momenta $\{p'_3,\, p'_4\}$ and it differs from soft matrix element of formula (15). Leading part of full matrix element (14) is soft matrix element by formula (15). It is interesting to introduce a correction which turns matrix element (9) into matrix element (15). Then it would be possible to put full matrix element (14) into PHOTOS in an additive way.

PHOTOS phase-space algorithm generates a four particle final state $\{p_3,\, p_4,\, p_5,\, p_6\}$ replacing a two particle state $\{p'_3,\, p'_4\}$ and taking care of momentum-energy conservation $(p'_3)^\alpha + (p'_4)^\alpha = p_3^\alpha + p_4^\alpha + p_5^\alpha + p_6^\alpha$. Each four particle state $\{p_3,\, p_4,\, p_5,\, p_6\}$ is not completely independent of their prior two particle state $\{p'_3,\, p'_4\}$, although it is not necessary since $\{p'_3,\, p'_4\}$ state is completely random by itself. As reference frame remains the same (see Section 2) spatial direction of four-vector p_4 is the same as of four-vector p'_4, modulus of spatial part of p_4 is random, however, in practice it doesn't differ much from modulus of spatial part of p'_4. Taking into account that $(p'_4)^2 = p_4^2 = m_2^2 \ll M_Z^2/4 = ((p'_4)^0)^2$ I assume four-vectors p'_4 and p_4 are parallel to each other and $p_4 = (1-\lambda)p'_4$, where λ is small. Rigorously speaking, $\lambda \in [0,1]$ and for values of $\lambda \sim 1$ four-vectors p'_4 and p_4 are not parallel. In practice, while monitoring values of λ for an accepted extra pair emissions, I've encountered values of $\lambda \sim 0$ only.

An effect of replacement of matrix element (9) by matrix element (15) is given by their difference. Taking into account algebraic properties of the traces of expressions (9) and (15), I proceed

$$Tr\left[\left(\not{p}'_3 + m_2\right)\gamma^\mu\left(\not{p}'_4 - m_2\right)\gamma^\nu\right] - Tr\left[\left(\not{p}_3 + m_2\right)\gamma^\mu\left(\not{p}_4 - m_2\right)\gamma^\nu\right] =$$

$$= Tr\left[\not p'_3\gamma^\mu \not p'_4\gamma^\nu\right] - Tr\left[\not p_3\gamma^\mu \not p_4\gamma^\nu\right] = Tr\left[\not p'_3\gamma^\mu (1-\lambda)^{-1}\not p_4\gamma^\nu\right] - Tr\left[\not p_3\gamma^\mu \not p_4\gamma^\nu\right] \approx$$
$$\approx Tr\left[\left(\not p'_3(1+\lambda) - \not p_3\right)\gamma^\mu \not p_4\gamma^\nu\right] \approx Tr\left[\left(\left(\not p_3 + \not q - \lambda \not p_4\right)(1+\lambda) - \not p_3\right)\gamma^\mu \not p_4\gamma^\nu\right] =$$
$$= Tr\left[\not q\gamma^\mu \not p_4\gamma^\nu\right] + O(\lambda).$$

Therefore, a leading part of difference between matrix elements (9) and (15) is described by the following matrix element

$$\sum_{spins} |M_1 + M_2|^2_{corr} = \frac{\alpha^2 (4\pi)^2}{(p_1+p_2)^4} Tr\left[\left(\not p_1 + m_1\right)\gamma_\mu \left(\not p_2 - m_1\right)\gamma_\nu\right] Tr\left[\not q\gamma^\mu \not p_4\gamma^\nu\right] \times$$
$$\times\, 2\,(4\pi\alpha)^2\, \frac{4p_5^\alpha p_6^\beta - q^2\cdot g^{\alpha\beta}}{q^4}\left(\frac{p_3^\alpha}{p_3 q} - \frac{p_4^\alpha}{p_4 q}\right)\left(\frac{p_3^\beta}{p_3 q} - \frac{p_4^\beta}{p_4 q}\right). \tag{33}$$

Subtracting matrix element (33) from matrix element (14), I receive corrected matrix element's residual

$$F_{test1} = F_{soft} + \frac{(4\pi\alpha)^2}{q^4}\cdot \frac{Tr\left[\left(\not p_1 + m_1\right)\gamma_\mu \left(\not p_2 - m_1\right)\gamma_\nu\right] \times \left(H_1^{\mu\nu} + H_2^{\mu\nu} + H_3^{\mu\nu} + H_4^{\mu\nu} + H_5^{\mu\nu} + H_6^{\mu\nu} + H_7^{\mu\nu} + H_8^{\mu\nu} - H_9^{\mu\nu}\right)}{Tr\left[\left(\not p_1 + m_1\right)\gamma^\mu \left(\not p_2 - m_1\right)\gamma^\nu\right] Tr\left[\left(\not p'_3 + m_2\right)\gamma_\mu \left(\not p'_4 - m_2\right)\gamma_\nu\right]}, \tag{34}$$

where tensors $H_1^{\mu\nu}$-$H_8^{\mu\nu}$ are given by formulae (18-25), F_{soft} is given by formula (11) and tensor $H_9^{\mu\nu}$ is given by formula

$$H_9^{\mu\nu} = -\frac{16}{\left(2\left(p_3 q\right) + q^2\right)^2}\left[2Tr\left[\not p_4\gamma^\mu \not q\gamma^\nu\right]\left(p_3 p_5 \cdot p_3 p_6\right)\right] - \frac{16}{\left(2\left(p_4 q\right) + q^2\right)^2}\left[2Tr\left[\not p_4\gamma^\mu \not q\gamma^\nu\right]\left(p_4 p_5 \cdot p_4 p_6\right)\right] +$$
$$+\frac{16}{\left(2\left(p_3 q\right) + q^2\right)\left(2\left(p_4 q\right) + q^2\right)}\left[2Tr\left[\not p_4\gamma^\mu \not q\gamma^\nu\right]\left(p_3 p_5 \cdot p_4 p_6 + p_3 p_6 \cdot p_4 p_5 + p_3 p_4 \cdot \frac{q^2}{2}\right)\right]. \tag{35}$$

I should note that it is mathematically justified way of correction of PHOTOS kernel for the case of the hardest extra pair emissions.

I assume that correction (33) to matrix element (14) describes bulk of an effect of overproduction of hard extra pairs by PHOTOS kernel, it is tested numerically in Section 6.4 and is shown that this assumption is, indeed, valid.

The last statement suggests that, while generating an extra pair with PHOTOS, constituent parts of matrix element (14), like

$$\begin{aligned} &Tr\left[\left(\not p_1 + m_1\right)\gamma^\mu \left(\not p_2 - m_1\right)\gamma^\nu\right] Tr\left[\left(\not p_3 + \not q + m_2\right)\gamma_\mu \left(\not p_4 - m_2\right)\gamma_\nu\right] \approx \\ \approx &Tr\left[\left(\not p_1 + m_1\right)\gamma^\mu \left(\not p_2 - m_1\right)\gamma^\nu\right] Tr\left[\left(\not p'_3 + m_2\right)\gamma_\mu \left(\not p'_4 - m_2\right)\gamma_\nu\right], \end{aligned} \tag{36}$$

can be approximated to Born level matrix element $|M(p_1,p_2;p'_3,p'_4)|^2_{Born}$ times corresponding factor. Such a factor would have a meaning of probability density of extra pair emission. All such factors are to be added into PHOTOS kernel and to be tested.

As it is discussed earlier in Section 5.3, tensors $H_5^{\mu\nu} - H_8^{\mu\nu}$ are supposed to give small contribution to matrix element $F_{test1}\cdot|M(p_1,p_2;p'_3,p'_4)|^2_{Born}$. In order to confirm above statement, following expression for matrix element residual should be tested

$$F_{test2} = F_{soft} + \frac{(4\pi\alpha)^2}{q^4}\cdot \frac{Tr\left[\left(\not p_1 + m_1\right)\gamma_\mu \left(\not p_2 - m_1\right)\gamma_\nu\right] \times \left(H_1^{\mu\nu} + H_2^{\mu\nu} + H_3^{\mu\nu} + H_4^{\mu\nu} - H_9^{\mu\nu}\right)}{Tr\left[\left(\not p_1 + m_1\right)\gamma^\mu \left(\not p_2 - m_1\right)\gamma^\nu\right] Tr\left[\left(\not p'_3 + m_2\right)\gamma_\mu \left(\not p'_4 - m_2\right)\gamma_\nu\right]}, \tag{37}$$

where tensors $H_1^{\mu\nu} - H_4^{\mu\nu}$ are given by formulae (18-21), F_{soft} is given by formula (11) and tensor $H_9^{\mu\nu}$ is given by formula (35).

I remind that presence of the tensor $H_9^{\mu\nu}$ in the matrix element residual F_{test2} is result of approximation (36), that should compensate overproduction of hard pairs by factorized part of matrix element F_{soft} of PHOTOS. In order to reduce denominator in the formula for matrix element residual F_{test2} (37) for as much terms as possible, I rewrite it with help of approximation (36). I write sum of tensors in a following way

$$
\begin{aligned}
H_{10}^{\mu\nu} = H_1^{\mu\nu} + H_2^{\mu\nu} + H_3^{\mu\nu} + H_4^{\mu\nu} - H_9^{\mu\nu} = \frac{16}{\left(2\left(p_3q\right)+q^2\right)^2}\left[Tr\left[\left(\not{p}_3+\not{q}\right)\gamma^\mu\not{p}_4\gamma^\nu\right]\frac{q^2}{2}\cdot p_3q\right]+ \\
+\frac{16}{\left(2\left(p_4q\right)+q^2\right)^2}\left[Tr\left[\left(\not{p}_3-\not{p}_4\right)\gamma^\mu\not{q}\gamma^\nu\right]\left(2p_4p_5\cdot p_4p_6-\frac{q^2}{2}\cdot\frac{q^2}{2}\right)+Tr\left[\left(\not{p}_3+\not{q}\right)\gamma^\mu\not{p}_4\gamma^\nu\right]\frac{q^2}{2}\cdot p_4q\right]+ \\
-\frac{8}{2\left(p_4q\right)+q^2}\left[3Tr\left[\left(\not{p}_3-\not{p}_4\right)\gamma^\mu\not{q}\gamma^\nu\right]\frac{q^2}{2}\right]+\frac{16}{\left(2\left(p_3q\right)+q^2\right)\left(2\left(p_4q\right)+q^2\right)}\left[Tr\left[\left(\not{p}_3-\not{p}_4\right)\gamma^\mu\not{q}\gamma^\nu\right]\left(p_3p_4\frac{q^2}{2}\right)-\right. \\
-4g^{\mu\nu}\left(2m_3^2\frac{q^2}{2}2p_3p_4\right)-2Tr\left[\left(\not{p}_3-\not{p}_4\right)\gamma^\mu\not{p}_6\gamma^\nu\right]p_3p_6\cdot p_4p_5-2Tr\left[\left(\not{p}_3-\not{p}_4\right)\gamma^\mu\not{p}_5\gamma^\nu\right]p_3p_5\cdot p_4p_6- \\
-Tr\left[\not{p}_3\gamma^\mu\not{p}_3\gamma^\nu\right]p_4q\frac{q^2}{2}-Tr\left[\not{p}_4\gamma^\mu\not{p}_4\gamma^\nu\right]p_3q\frac{q^2}{2}-2Tr\left[\not{p}_3\gamma^\mu\not{p}_6\gamma^\nu\right]\frac{q^2}{2}\cdot p_4p_5 \\
\left.-2Tr\left[\not{p}_3\gamma^\mu\not{p}_5\gamma^\nu\right]\frac{q^2}{2}\cdot p_4p_6-2Tr\left[\not{p}_4\gamma^\mu\not{p}_5\gamma^\nu\right]\frac{q^2}{2}\cdot p_3p_6-2Tr\left[\not{p}_4\gamma^\mu\not{p}_6\gamma^\nu\right]\frac{q^2}{2}\cdot p_3p_5\right]. \qquad (38)
\end{aligned}
$$

While recurring symmetries of tensor (38), like $Tr\left[\left(\not{p}_3-\not{p}_4\right)\gamma^\mu\not{q}\gamma^\nu\right]$, are interesting and look esthetic, they can not be factorized. Factorizable tensor of the matrix element (14) is

$$
H_{11}^{\mu\nu} = \frac{16}{\left(2\left(p_3q\right)+q^2\right)^2}\left[Tr\left[\left(\not{p}_3+\not{q}\right)\gamma^\mu\not{p}_4\gamma^\nu\right]\frac{q^2}{2}\cdot p_3q\right]+\frac{16}{\left(2\left(p_4q\right)+q^2\right)^2}\left[Tr\left[\left(\not{p}_3+\not{q}\right)\gamma^\mu\not{p}_4\gamma^\nu\right]\frac{q^2}{2}\cdot p_4q\right]. \qquad (39)
$$

I should note, that tensor $H_8^{\mu\nu}$ (25) contains factorizable parts, but they are not included into consideration, since effect of tensor $H_8^{\mu\nu}$ (25) on extra pair production is small and it is neglected. Following expression for matrix element residual to be tested in PHOTOS kernel

$$
\begin{aligned}
F_{test3} = F_{soft} + \frac{\left(8\pi\alpha\right)^2}{q^2}\left(\frac{1}{2\left(p_3q\right)+q^2}+\frac{1}{2\left(p_4q\right)+q^2}\right)+ \\
+\frac{\left(4\pi\alpha\right)^2}{q^4}\cdot\frac{Tr\left[\left(\not{p}_1+m_1\right)\gamma_\mu\left(\not{p}_2-m_1\right)\gamma_\nu\right]\times\left(H_{10}^{\mu\nu}-H_{11}^{\mu\nu}\right)}{Tr\left[\left(\not{p}_1+m_1\right)\gamma^\mu\left(\not{p}_2-m_1\right)\gamma^\nu\right]Tr\left[\left(\not{p}_3'+m_2\right)\gamma_\mu\left(\not{p}_4'-m_2\right)\gamma_\nu\right]}, \qquad (40)
\end{aligned}
$$

where tensors $H_{10}^{\mu\nu}$ and $H_{11}^{\mu\nu}$ are given by formulae (38-39), F_{soft} is given by formula (11).

Following formula for matrix elements residual to be tested in PHOTOS kernel is a result of fine tuning of kernel F_{test3} (for details see Section 6.4). As it is illustrated in Section 5.3 (and it is shown in Section 6.3), effect of tensors $H_6^{\mu\nu}$ and $H_7^{\mu\nu}$ on matrix element

$\sum_{spins} |M_1 + M_2|^2$ is small. In order to improve precision of extra pair generation by kernel F_{test3} I subtract tensors $H_6^{\mu\nu}$, $H_7^{\mu\nu}$ from the tensors $H_{10}^{\mu\nu} - H_{11}^{\mu\nu}$ of F_{test3}:

$$F_{test4} = F_{soft} + \frac{(8\pi\alpha)^2}{q^2} \cdot \left(\frac{1}{2\,(p_3 q) + q^2} + \frac{1}{2\,(p_4 q) + q^2} \right) + \\ + \frac{(4\pi\alpha)^2}{q^4} \cdot \frac{Tr\left[(\not{p}_1 + m_1)\,\gamma_\mu\,(\not{p}_2 - m_1)\,\gamma_\nu \right] \times (H_{10}^{\mu\nu} - H_{11}^{\mu\nu} - H_6^{\mu\nu} - H_7^{\mu\nu})}{Tr\left[(\not{p}_1 + m_1)\,\gamma^\mu\,(\not{p}_2 - m_1)\,\gamma^\nu \right] Tr\left[\left(\not{p}'_3 + m_2\right)\gamma_\mu\left(\not{p}'_4 - m_2\right)\gamma_\nu \right]}, \qquad (41)$$

where tensors $H_6^{\mu\nu}$, $H_7^{\mu\nu}$, $H_{10}^{\mu\nu}$, $H_{11}^{\mu\nu}$ are given by formulae (23, 24, 38, 39), F_{soft} is given by formula (11).

Following formula for matrix elements residual to be tested in PHOTOS kernel is a result of fine tuning of kernel F_{test1}. In order to improve precision of extra pair generation by kernel F_{test1} I subtract tensors $H_6^{\mu\nu}$, $H_7^{\mu\nu}$ from tensor sum, likewise it in formula for F_{test3}. Next step is to delete tensors $H_1^{\mu\nu}$, $H_9^{\mu\nu}$ from tensor sum of F_{test1}, because tensor $H_1^{\mu\nu}$ includes $Tr\left[\not{q}_2\gamma^\mu\not{q}\gamma^\nu\right]\left(p_3 p_4 \frac{q^2}{2}\right)$ which is similar to $Tr\left[2\not{p}_4\gamma^\mu\not{q}\gamma^\nu\right]\left(p_3 p_4 \frac{q^2}{2}\right)$ of tensor $H_9^{\mu\nu}$. Here is formula for matrix elements residual

$$F_{test5} = F_{soft} + \frac{(4\pi\alpha)^2}{q^4} \cdot \frac{Tr\left[(\not{p}_1 + m_1)\,\gamma_\mu\,(\not{p}_2 - m_1)\,\gamma_\nu \right] \times (H_2^{\mu\nu} + H_3^{\mu\nu} + H_4^{\mu\nu} - H_6^{\mu\nu} - H_7^{\mu\nu} + H_8^{\mu\nu})}{Tr\left[(\not{p}_1 + m_1)\,\gamma^\mu\,(\not{p}_2 - m_1)\,\gamma^\nu \right] Tr\left[\left(\not{p}'_3 + m_2\right)\gamma_\mu\left(\not{p}'_4 - m_2\right)\gamma_\nu \right]}, \qquad (42)$$

where tensors $H_i^{\mu\nu}$ are given by formulae (18-25) and F_{soft} is given by formula (11). Results are presented in Section 6.4.

5.5 Effective factorization of matrix element

As it will be shown in Section 6.4, tests of PHOTOS kernels based on approximations $F_{test3} \cdot |M(p_1, p_2; p'_3, p'_4)|^2_{Born}$ (40), $F_{test4} \cdot |M(p_1, p_2; p'_3, p'_4)|^2_{Born}$ (41) and $F_{test5} \cdot |M(p_1, p_2; p'_3, p'_4)|^2_{Born}$ (42) of matrix element (14) indicate that these approximations are good. However, matrix elements residuals F_{test3}, F_{test4} and F_{test5} bare dependance on Born level matrix $|M(p_1, p_2; p'_3, p'_4)|^2_{Born}$ and are not factorized parts of matrix element (14). Therefore, I ignore most of the complexity of the matrix element (14) to make its factorizable approximation $F_{test6} \cdot |M(p_1, p_2; p'_3, p'_4)|^2_{Born}$, where F_{test6} is given by

$$F_{test6} = F_{soft} + \frac{(8\pi\alpha)^2}{q^2} \cdot \left(\frac{1}{2\,(p_3 q) + q^2} + \frac{1}{2\,(p_4 q) + q^2} \right), \qquad (43)$$

F_{soft} is given by formula (11).

It is expected, and it is shown in Section 6.5, that matrix element $F_{test6} \cdot |M(p_1, p_2; p'_3, p'_4)|^2_{Born}$ overproduces hardest extra pairs comparing to exact matrix element (14). On the other hand, since difference between F_{test6} and F_{soft} is of order of q^2, considering the softest extra pairs production, it is expected (and it is shown in Section 6.5) that matrix element $F_{test6} \cdot |M(p_1, p_2; p'_3, p'_4)|^2_{Born}$ is as good as exact matrix element (14).

I apply a naive correction to factorized part of matrix element F_{test6} (45). This correction is based on linear reduction of probability of extra pair emission depending on invariant mass $(p_3+p_4)^2$:

$$F_{test7} = \left[F_{soft} + \frac{(8\pi\alpha)^2}{q^2} \left(\frac{1}{2\,(p_3 q) + q^2} + \frac{1}{2\,(p_4 q) + q^2} \right) \right] / \left[\left(1 - A \cdot \frac{(p_3+p_4)^2}{(p_1+p_2)^2} \right) + A \right], \quad (44)$$

where F_{soft} is given by formula (11), values of constant A are discussed at Section 6.5. The form of the fitting function used for matrix element is inspired by the functional form of Altarelli-Parisi kernel [40]. I expect, that this could be explained but with the substantial effort only. One would need to expand around spin states to intermediate virtual particles. This ambiguous procedure was not continued. It is also difficult to match with the requirement to define simplified amplitudes, nonetheless valid all over the phase space. In principle, choice for the fitted function inspired by Altarelli-Parisi kernel can be a polynomial of the second order, but restriction to first order linear function seems sufficient, for higher energy fraction where it could play a role distributions fall massively.

6 Tests of new matrix elements

6.1 KORALW-PHOTOS comparison framework

In the following I describe KORALW-PHOTOS comparison in details.

The best test of PHOTOS generated spectra for the process $ee \to Z \to 4l$ is given by KORALW-PHOTOS comparison [12, 21, 41]. This comparison [21, 41] provides source of benchmarks for my tests and is basis for continuation of my studies, all my PHOTOS tests are compared to these data, if it is possible. Both PHOTOS and KORALW have well separated segments for exact phase-space description and matrix element calculations, which is of lowest order exact in KORALW but of approximation in PHOTOS.

An easy way to generate complete 4f end state spectra by PHOTOS is to perform two runs, i.e. $f_1\overline{f}_1 \to Z/\gamma^* \to f_2\overline{f}_2$ and $f_1\overline{f}_1 \to Z/\gamma^* \to f_3\overline{f}_3$. During first run PHOTOS generates extra $f_3\overline{f}_3$ pair for a Born level process $f_1\overline{f}_1 \to Z/\gamma^* \to f_2\overline{f}_2$ (M_1 and M_2 from Fig. 2), during second run PHOTOS generates extra $f_2\overline{f}_2$ pair for a Born level process $f_1\overline{f}_1 \to Z\gamma^* \to f_3\overline{f}_3$ (M_3 and M_4 from Fig. 2). Following this scheme an interference between diagrams M_1, M_2 and diagrams M_3, M_4 is ignored breaking gauge invariance. A numerical effect of this breakdown for the simulation of the processes $e^+e^- \to Z \to e^+e^-\mu^+\mu^-$ and $e^+e^- \to Z \to \mu^+\mu^-\mu^+\mu^-$ is discussed at Section 6.2.

KORALW [12] feature both complete and exact matrix element for Z production and decay to four fermions. While emission of extra pair from the incoming particles (ISR) in KORALW is switched off its matrix element corresponds to four Feynman graphs presented in Fig. 2. For switching off extra pair ISR in KORALW the center of mass energy is set to equal Z boson mass and Z width is set to a very small value. The KORALW Monte Carlo has been used to simulate $e^+e^- \to Z \to e^+e^-\mu^+\mu^-$ and $e^+e^- \to Z \to \mu^+\mu^-\mu^+\mu^-$ channels.

PYTHIA has been used to simulate $e^+e^- \to Z \to e^+e^-$ and $e^+e^- \to Z \to \mu^+\mu^-$ channels providing input data for PHOTOS, PHOTOS has been used to generate $e^+e^- \to Z \to e^+e^-\mu^+\mu^-$ and $e^+e^- \to Z \to \mu^+\mu^-\mu^+\mu^-$ events. PYTHIA setup parameters are presented in Tab. B.1.

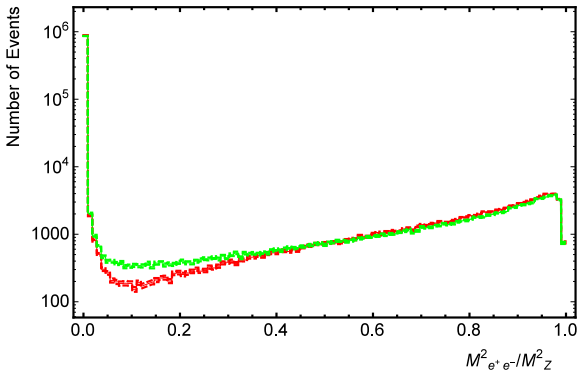

a) Normalized to M_Z^2 spectrum of electron pair mass squared.

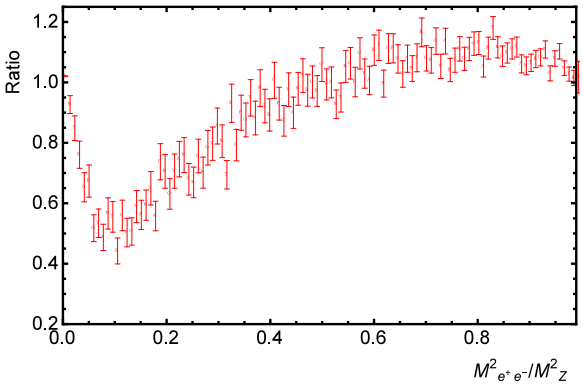

b) Normalized to M_Z^2 ratio of PHOTOS generated spectrum to the one generated by KORALW.

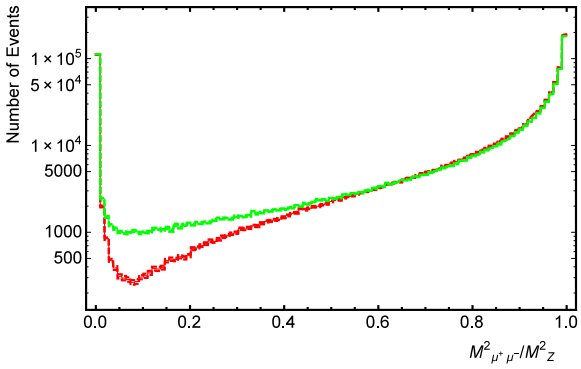

c) Normalized to M_Z^2 spectrum of muon pair mass squared.

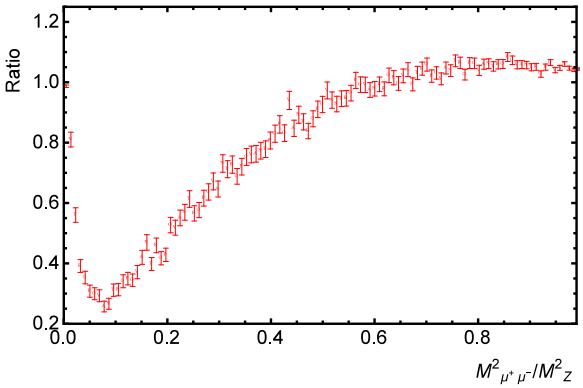

d) Normalized to M_Z^2 ratio of PHOTOS generated spectrum to the one generated by KORALW.

Figure 9: Lepton pair invariant mass spectra in the channel $Z \to \mu^+\mu^-e^+e^-$. Spectra generated by PHOTOS [11] (red (dark grey) error bars) are obtained from samples of equal number of $Z \to e^+e^-$ and $Z \to \mu^+\mu^-$ PYTHIA generated decays. They are compared with spectra by KORALW (green (light grey) error bars) where four fermion final state matrix elements are used.

PHOTOS generated distributions are compared with the one's obtained from KORALW for the $Z \to e^+e^-\mu^+\mu^-$ channel. Fig. 9 presents spectra of squared mass of e^+e^- pair ($M^2_{e^+e^-}$) and of $\mu^+\mu^-$ pair ($M^2_{\mu^+\mu^-}$) and ratios of PHOTOS generated spectra to the corresponding ones by KORALW. These spectra are of the most interest, since pair masses $M_{e^+e^-}$ and $M_{\mu^+\mu^-}$ are experiment observables [1]. Sharp peak of the number of e^+e^- pairs is for pairs with

small invariant mass squared $M^2_{e^+e^-} \sim 0$. Local maximum of the number of e^+e^- pairs is for pairs with invariant mass squared close to beam CMS energy squared $M^2_{e^+e^-} \sim M^2_Z$. The agreement between KORALW generated spectrum and PHOTOS generated spectrum is the best for the most populated bins, that are near these maximums. Minimum of the number of e^+e^- pairs is for pairs with square of invariant mass lying between $0.05 \cdot M^2_Z$ and $0.15 \cdot M^2_Z$. The difference between KORALW generated spectrum and PHOTOS generated spectrum is highest at this minimum and is up to factor of 2.5 for some bins. Sharp peaks of the number of $\mu^+\mu^-$ pairs is both for pairs with small invariant mass squared $M^2_{e^+e^-} \sim 0$ and for pairs with invariant mass squared close to beam CMS energy squared $M^2_{e^+e^-} \sim M^2_Z$. The agreement between KORALW generated spectrum and PHOTOS generated spectrum is the best for the most populated bins, that are near these maximums. Minimum of the number of $\mu^+\mu^-$ pairs is for pairs with square of invariant mass lying between $0.05 \cdot M^2_Z$ and $0.1 \cdot M^2_Z$. The difference between KORALW generated spectrum and PHOTOS generated spectrum is highest at this minimum and is up to factor of 4.2 for some bins.

Other plots, for other than $M^2_{e^+e^-}$ and $M^2_{\mu^+\mu^-}$ observables (Figs. B.1-B.4) and also for $Z \to \mu^+\mu^-\mu^+\mu^-$ channel (Figs. B.5-B.6), are delegated to Appendix B.1.

Each spectrum of Fig. 9 consists of 120 bins. Noise is observable at the right hand side of Fig. 9 for ratios of spectra, it comes from random number generators and effect of this noise is comparable with bin error for each bin. Normalization of spectra in number of events by PHOTOS to the one by KORALW is nontrivial task by itself, since PHOTOS is MC generator of afterburner type and since KORALW manages production-decay processes by its own. The criteria are that the numbers of lepton pairs of each kind of small invariant mass by PHOTOS and by KORALW are the same (it is not always the case for further tests) and that the numbers of lepton pairs of each kind of invariant mass $\sim M_Z$ by PHOTOS and by KORALW are the same. In this test 10^6 events are generated in the $e^+e^-\mu^+\mu^-$ channel and 10^6 events are generated in the $\mu^+\mu^-\mu^+\mu^-$ channel by KORALW. $3.665 * 10^8$ $e^+e^- \to Z \to e^+e^-$ events and $3.665 * 10^8$ $e^+e^- \to Z \to \mu^+\mu^-$ events is generated by PYTHIA at CMS energy of 91.187 GeV, with up and down limits on CMS energy 91.17 GeV and 91.2 GeV respectively – one doesn't have to restrict CMS energy for PYTHIA generation as precise as one does for KORALW. $1.002 * 10^6$ events are generated by PYTHIA-PHOTOS in the $e^+e^-\mu^+\mu^-$ channel and $1.001 * 10^6$ events are generated in the $\mu^+\mu^-\mu^+\mu^-$ channel. Each further PHOTOS test, which is compared with KORALW spectra, has the same setup to the one described above.

6.2 PHOTOS with full matrix element, tests

Particle spectra in numbers of events by itself (see left hand side of Fig. 9) are not very informative for precision tests, during further tests I present ratios of the corresponding spectra only (with some exceptions). For a proper analysis of ratios of lepton pair spectra one should have in mind general features of particles spectra (see Section 6.1, Fig. 9 and Appendix B.1). All of the PYTHIA generated pairs $f_2\overline{f}_2$ have invariant mass of M_Z. Emission of extra pair $f_3\overline{f}_3$ by PHOTOS creates spectrum with invariant mass of $f_2\overline{f}_2$ pair ranging from M_Z to a very small values. The most populated bins ($M^2_{f_2\overline{f}_2} \sim M^2_Z$) correspond to soft extra pair emission, thus given ratio is desired to variate around 1 as close as possible.

All of the generated extra pairs have a small invariant mass ($M^2_{f_3\overline{f}_3} \sim 0$), so a vast majority of them are in the first bin of corresponding spectrum, it doesn't matter whether spectrum consists of 24 bins (see below) or of 120 bins.

I start with an approximation of $2f \to Z \to 4f$ matrix element (with FSR extra pair emission): I neglects interference terms between pairs $\sum_{spins} |M_1 + M_2 + M_3 + M_4|^2 \approx \sum_{spins} |M_1 + M_2|^2 + \sum_{spins} |M_3 + M_4|^2$, there are few reasons of doing that. Matrix elements $\sum_{spins} |M_1 + M_2|^2$ and $\sum_{spins} |M_3 + M_4|^2$ are much simpler than matrix element $\sum_{spins} |M_1 + M_2 + M_3 + M_4|^2$, it means less bugs during tests. Due to PHOTOS algorithm structure matrix element $\sum_{spins} |M_1 + M_2|^2$ is easier to install into PHOTOS kernel and to test. Then all the events (and distributions) are generated independently according to $\sum_{spins} |M_1 + M_2|^2$ matrix element ($f_3\overline{f}_3$ pair emission from $f_2\overline{f}_2$ final state corresponding to M_1 and M_2 from Fig. 2) and according to $\sum_{spins} |M_3 + M_4|^2$ matrix element ($f_2\overline{f}_2$ pair emission from $f_3\overline{f}_3$ final state corresponding to M_3 and M_4 from Fig. 2).

Distributions by PHOTOS with matrix element (14) are presented at Fig. 10 and are compared with distributions by KORALW. These sample requires proper normalization, the numbers of events is 1/1.036 of number of PHOTOS events at Fig. 9. For further tests I stick to this normalization .

Fig. 10 presents ratios of PHOTOS generated spectra of squared mass of e^+e^- pair ($M^2_{e^+e^-}$), of $\mu^+\mu^-$ pair ($M^2_{\mu^+\mu^-}$), of squared mass of $\mu^+e^+e^-$ three ($M^2_{\mu^+e^+e^-}$) and of squared mass of $e^+\mu^+\mu^-$ three ($M^2_{e^+\mu^+\mu^-}$) to the corresponding one's by KORALW. Agreement between PHOTOS with matrix element (14) and KORALW is good. Numbers of PHOTOS test events and KORALW test events for any bin never differ greatly in the ratio more than 20%. Such difference rather vanishes with statistics increase. It is seen, that agreement between PHOTOS and KORALW is reached for the least populated bins $0 < M^2_{e^+e^-}, M^2_{\mu^+\mu^-} < 0.5$ of e^+e^- pair and $\mu^+\mu^-$ pair spectra. It is seen, that PHOTOS with matrix element (14) produces slightly less e^+e^- and $\mu^+\mu^-$ pairs in the most populated parts of the spectra $M^2_{e^+e^-}, M^2_{\mu^+\mu^-} > 0.5$ comparing to unmodified PHOTOS. Spectrum of $e^+\mu^+\mu^-$ three is indistinguishable from spectrum of $e^-\mu^+\mu^-$ three and possesses the same characteristic features, so it is not presented. Spectrum of $\mu^-e^+e^-$ is not presented because of the same reasons.

To illustrate an improvement of PHOTOS I present here results of χ^2 test [42] from ROOT 5.5 [43] for e^+e^- pair and $\mu^+\mu^-$ pair spectra. For spectra of squared mass of e^+e^- pair: comparison between unmodified PHOTOS [11] and KORALW gives χ^2/NDF of 13.1[1], while comparison between PHOTOS with matrix element (14) and KORALW gives χ^2/NDF of 1.3. For spectra of squared mass of $\mu^+\mu^-$ pair: comparison between unmodified PHOTOS [11] and KORALW gives χ^2/NDF of 90.9, while comparison between PHOTOS with matrix element (14) and KORALW gives χ^2/NDF of 2.6. Such big values of χ^2/NDF are related to somewhat naive application of χ^2 test over noisy weighted histograms. I skip from consideration here questions about how change of a random seed number in one/each of generators or rebinding of histograms would effect corresponding values of χ^2/NDF. However, presented values of χ^2/NDF are enough to estimate an improvement of PHOTOS by installation of

[1]Number of degrees of freedom (NDF).

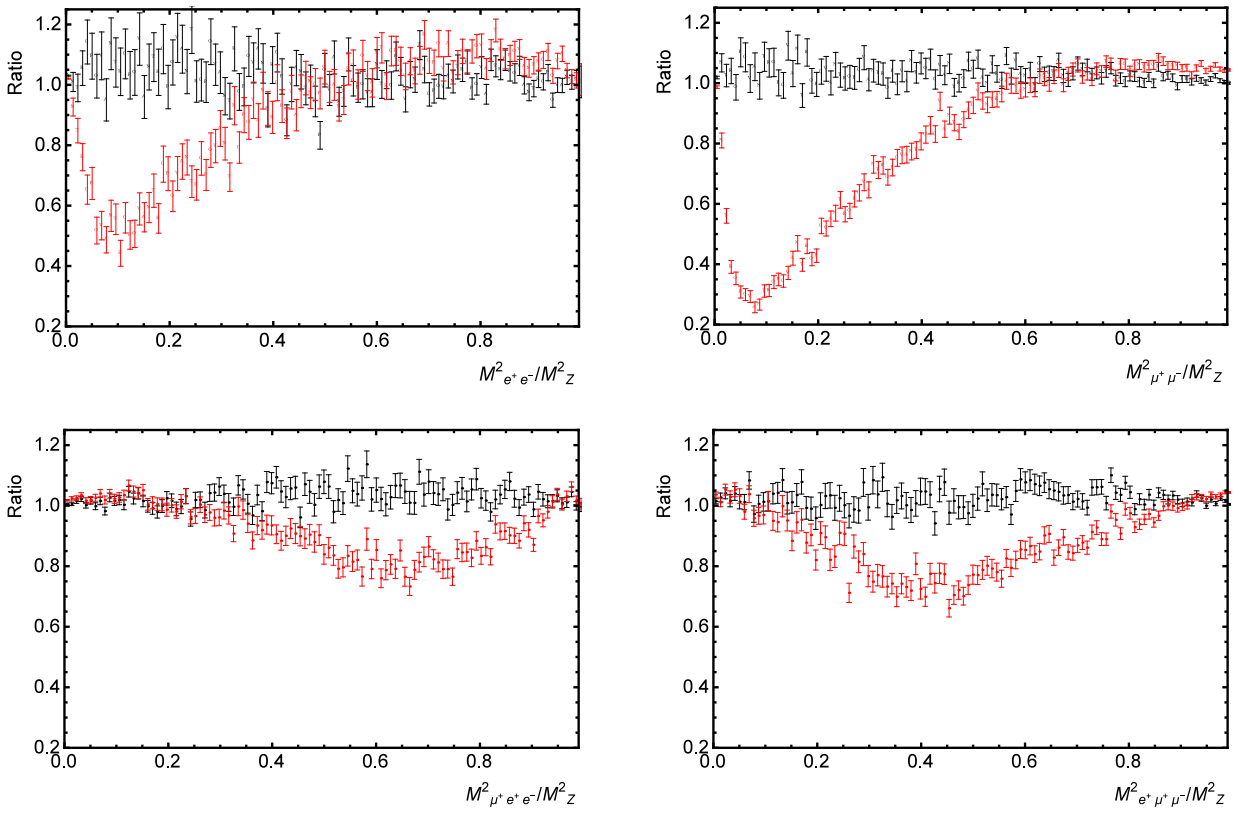

Figure 10: Ratios of PHOTOS generated spectra (of squared mass of e^+e^- pair ($M^2_{e^+e^-}$), of $\mu^+\mu^-$ pair ($M^2_{\mu^+\mu^-}$), of squared mass of $\mu^+e^+e^-$ three ($M^2_{\mu^+e^+e^-}$) and of squared mass of $e^+\mu^+\mu^-$ three ($M^2_{e^+\mu^+\mu^-}$)) in the $Z \to \mu^+\mu^-e^+e^-$ channel to the corresponding one's by KORALW. Spectra generated by PHOTOS are obtained from samples of equal number of PYTHIA generated $Z \to e^+e^-$ and $Z \to \mu^+\mu^-$ decays. Black error bars represent spectra by improved PHOTOS with matrix element (14). Red (dark grey) error bars represent spectra by unmodified PHOTOS [11], they are presented as a reference.

matrix element (14).

Other plots, for other than $M^2_{e^+e^-}$, $M^2_{\mu^+\mu^-}$, $M^2_{\mu^+e^+e^-}$ and $M^2_{e^+\mu^+\mu^-}$ observables (Fig. B.7) and also for $Z \to \mu^+\mu^-\mu^+\mu^-$ channel (Fig. B.8), are delegated to Appendix B.1.

Agreement between PHOTOS with $\sum_{spins} |M_1 + M_2|^2$ matrix element and KORALW is remarkable since interference between diagrams M_1, M_2 and M_3, M_4 is ignored in matrix element $\sum_{spins} |M_1 + M_2|^2$. However, all of the generated by PHOTOS extra pairs are of small invariant mass (it is true for all tested kernels), so an effect of gauge invariance breakdown is negligible. Correspondence of sum of $\sum_{spins} |M_1 + M_2|^2$ and of $\sum_{spins} |M_3 + M_4|^2$ to the exact solution of KORALW is so good that no further need of implementation of matrix element $\sum_{spins} |M_1 + M_2 + M_3 + M_4|^2$ is recognized.

As it is seen in the Fig. 10, ratios of particles spectra, that are presented as error bars, are noisy. Therefore, for the intermediate results I reserve mean value plots since both they are easy to read and they present main features of an introduced changes. In the following I present error bar plots when I talk about precision of an approach.

Installation of new matrix element for pair emissions into PHOTOS

In PHOTOS pair emission simulation starts in void function PHTYPE()[1] by calling void function PHOPAR() at lines 2421, 2422, 2510, 2511. Void function PHOPAR()[2] searches through HEPevents [44] for proper lepton pairs events, then particles data are transmitted to void function trypar()[3]. Four four vectors describing outgoing particles are generated in the function trypar(). At line 599 of PHOTOS/src/photos-C/pairs.cxx all particles four-momenta are generated and the calculation of F_{soft} factorized part of matrix element starts [13]. At this point arrays PAA and PNEUTR store modified four-momenta of the generated by PYTHIA lepton pair, while arrays PP and PE store four-momenta of the additional lepton pair. PHOTOS operates both at the beginning of function trypar() and at the moment of calculation of probability[4] of $f_3\overline{f}_3$ extra pair emission in the same reference frame as PYTHIA; it is easy to verify by printing content of arrays PCHAR, PNEU from the one line before trypar() is called or by printing content of arrays PAA, PNEUTR from the line 598 in PHOTOS/src/photos-C/pairs.cxx.

Factorized part of matrix element F_{soft}, as it is coded in PHOTOS at lines 628-649 in PHOTOS/src/photos-C/pairs.cxx, is $1/(8\pi\alpha)^2$ of the one defined by eq. (11). This factor of $1/(8\pi\alpha)^2$ is cumulative product of all constant factors that affect probability of event generation and that are hardcoded in PHOTOS, like number of attempts to generate emission for particular two particles in cascade or like powers of coupling constant, or like constant factors coming from four-body phase space, etc. Factor of $1/(8\pi\alpha)^2$ is required setup for proper installation of matrix element (14) (or any matrix element) into PHOTOS.

[1] line 2357 in PHOTOS/src/photos-C/photosC.cxx in developers version of PHOTOS.

[2] line 2543 in PHOTOS/src/photos-C/photosC.cxx.

[3] function call is at line 2620 in PHOTOS/src/photos-C/photosC.cxx, function code starts at line 237 in PHOTOS/src/photos-C/pairs.cxx.

[4] variable YOT1 at the line 612 in PHOTOS/src/photos-C/pairs.cxx.

6.3 Parts of matrix element, tests

Setup of the tests (like number of events, number of bins, CMS energy of colliding beams, etc.), that are presented in Fig. 9, is defined by the PHOTOS-KORALW comparison [41]. Since there are technical complications for running new KORALW tests, it leads to necessity of usage of existing KORALW data. As it is in Fig. 9, improved PHOTOS with matrix element (14) is in good agreement with KORALW, therefore, I use spectra by improved PHOTOS with matrix element (14) for the cases when comparison with KORALW spectra is hard or not possible[1]. At this point I am free to chose setup parameters. In order to speed up simulation, I set number of bins to be 24, multiply emission probability of extra pair by factor of 10, reduce number of PYTHIA generated events by factor of 250 simultaneously attempting to generate emission by PHOTOS for each event 100 times more. I use listed above setup for the most of tests that are compared to spectra by improved PHOTOS with matrix element (14) installed into it.

In order to estimate an effect of each tensor $H_i^{\mu\nu}$ on the extra pair emission I perform simulations by PHOTOS with matrix element (14) missing one of the tensor $H_i^{\mu\nu}$.

Fig. 11 presents ratios of PHOTOS generated spectra of squared mass of e^+e^- pair ($M^2_{e^+e^-}$) and of $\mu^+\mu^-$ pair ($M^2_{\mu^+\mu^-}$) to the corresponding one's by KORALW in the $e^+e^-\mu^+\mu^-$ channel. I have selected to present specifically these two particle spectra since they are the most sensitive to the changes in matrix element. From Fig. 11 it is seen that tensors $H_1^{\mu,\nu} - H_4^{\mu,\nu}$ are of most importance for precision spectra generation, while tensors $H_5^{\mu,\nu} - H_8^{\mu,\nu}$ can be easily dropped off from matrix element (14). All PHOTOS tests are performed out of PYTHIA generated samples of equal size[2], this automatically manages normalization of spectra. Contraction of sum of tensors $H_1^{\mu,\nu} - H_4^{\mu,\nu}$ with the tensor describing incoming particles completes matrix elements residual (16). It is desirable to interpret each one of these contraction as probability density in four particle phase space, which is not rigorous. e^+e^- and $\mu^+\mu^-$ pair spectra clearly indicates rise in number of events at most populated parts of the spectra when tensor (21) is missing in the matrix elements residual. Following that logic means, that contraction involving tensor (21) has to have meaning of negative probability density at some parts of the spectra. The same problem is true for $\mu^+\mu^-$ pair spectra and tensor (22). Other thing to notice is that for all the test the number of pairs with invariant mass close to collision energy ($M^2_{e^+e^-} \sim M_Z^2$, $M^2_{\mu^+\mu^-} \sim M_Z^2$) matches the one from the corresponding etalon spectra. That is not the case for some tests for the numbers of pairs with smallest invariant mass ($M^2_{e^+e^-} \sim 0$, $M^2_{\mu^+\mu^-} \sim 0$). Therefore, normalization of spectra for the further test comparisons with KORALW can not uphold on the number of lightest pairs. For the 24 bins spectra, I interpret the number of e^+e^- pairs with smallest invariant mass (the number of pairs in the first bin) as a total number of generated extra pairs thus as general performance of emission algorithm; for the 120 bins spectra, the number of e^+e^- pairs in the first bin is approx. 88% of total number of generated extra pairs. For the $\mu^+\mu^-$ pair spectra, the number of $\mu^+\mu^-$ pairs in the first bin is approx. 10%

[1]The most of such examples are delegated to the Appendix B.

[2]I remind here that for 120 bin spectra one PYTHIA generated sample is of $3.665 * 10^8$ events, for 24 bin spectra one PYTHIA generated sample is of $1.5 * 10^6$ events.

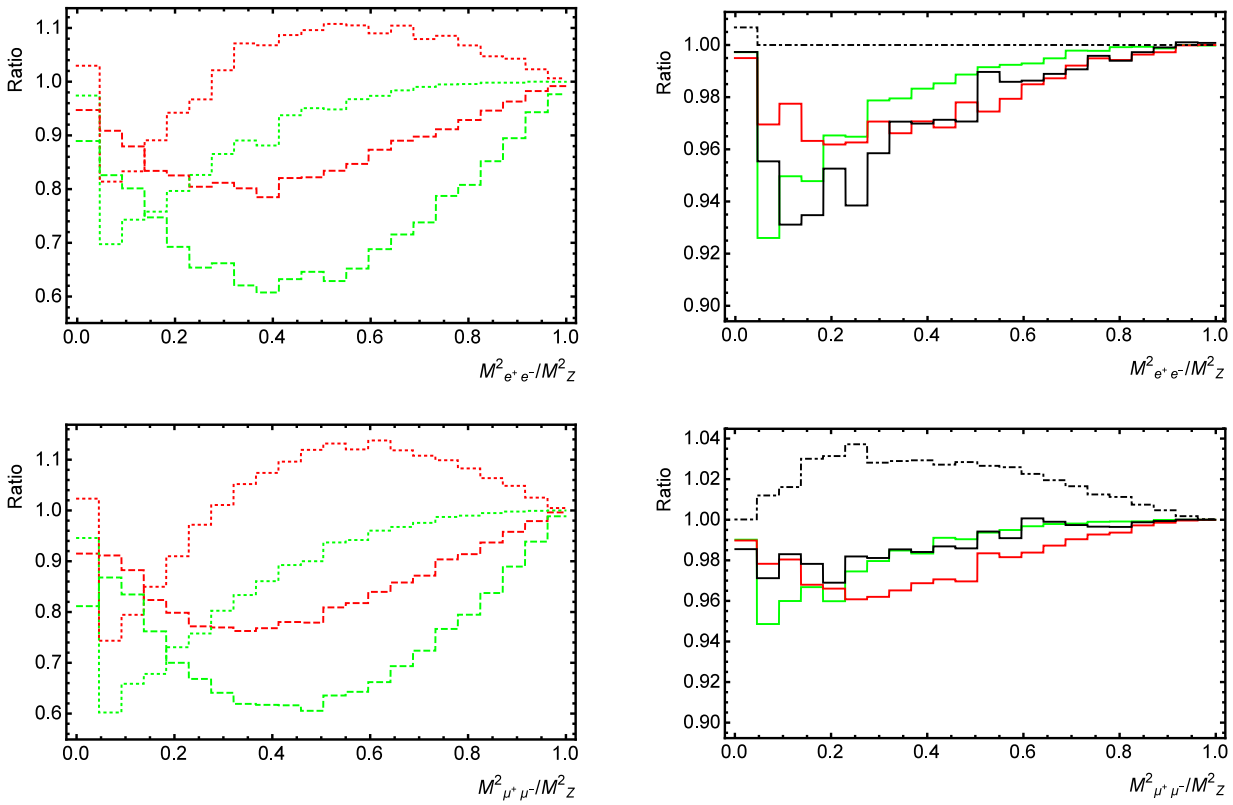

Figure 11: Normalized to M_Z^2 ratio of PHOTOS generated spectra in the channel $Z \to \mu^+\mu^- e^+ e^-$ to the ones, that are generated by PHOTOS with kernel by eq. (16). Spectra generated by PHOTOS are obtained from samples of equal number of $Z \to e^+e^-$ and $Z \to \mu^+\mu^-$ PYTHIA generated decays. Green (light grey) dashed line represents data corresponding to absence of the tensor $H_1^{\mu,\nu}$ in the kernel by eq. (16); green (light grey) dotted line – tensor $H_2^{\mu,\nu}$, red (dark grey) dashed line – tensor $H_3^{\mu,\nu}$, red (light grey) dotted line – tensor $H_4^{\mu,\nu}$, black dash-dotted line – tensor $H_5^{\mu,\nu}$, green (light grey) solid line – tensor $H_6^{\mu,\nu}$, red (dark grey) solid line – tensor $H_7^{\mu,\nu}$, black solid – tensor $H_8^{\mu,\nu}$.

of total number of generated extra pairs.

6.4 Fix for $\sum_{spins} |M_1 + M_2|^2_{soft}$ not being soft enough, tests

Spectra by PHOTOS with kernel F_{test1} (34) are presented in Figs. 12.

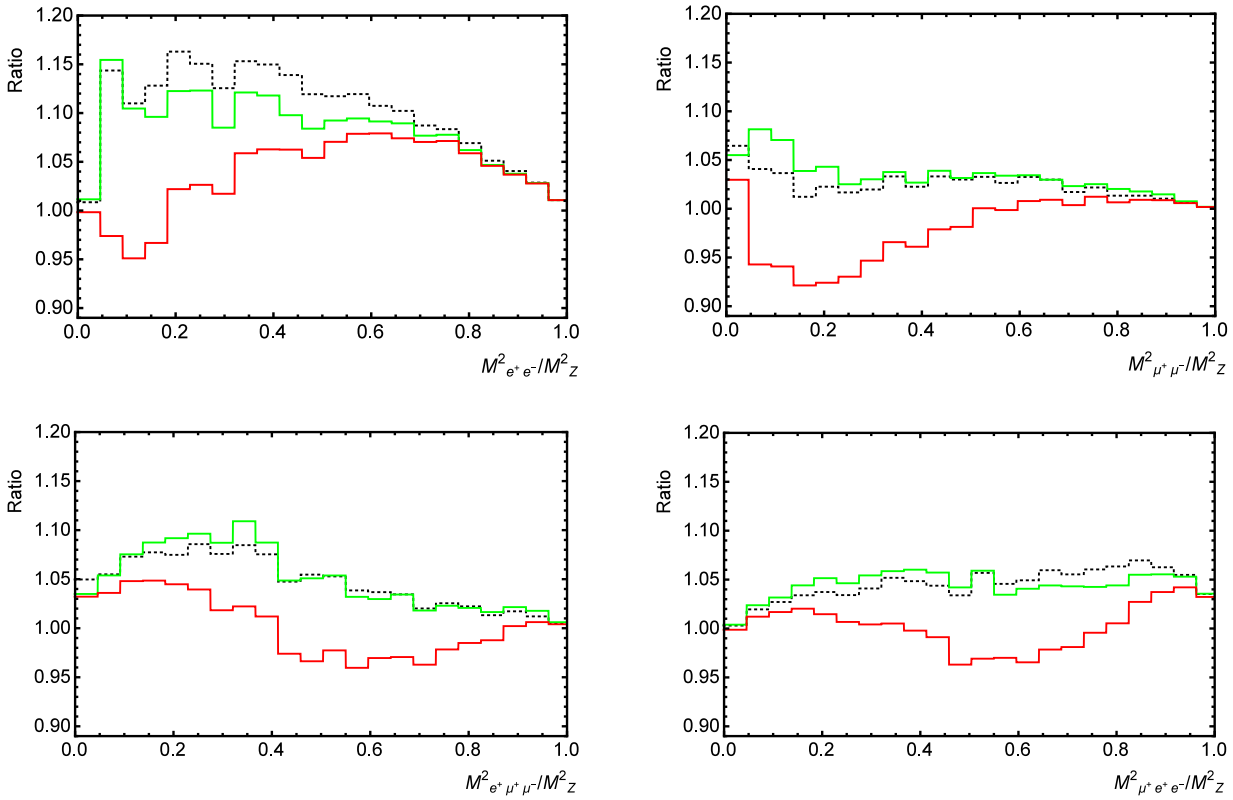

Figure 12: Normalized to M_Z^2 ratios of PHOTOS generated spectra in the channel $Z \to \mu^+\mu^- e^+ e^-$ to the ones, that are generated by PHOTOS with matrix element (14) installed into it. Spectra generated by PHOTOS are obtained from samples of equal number of $Z \to e^+e^-$ and $Z \to \mu^+\mu^-$ PYTHIA generated decays. Black dotted line represents spectra by PHOTOS with kernel of extra pair emission given by the formula (34). Solid red line (solid dark grey in greyscale) represents spectra by PHOTOS with kernel of extra pair emission given by the formula (37). Green solid line (solid light grey in greyscale) represents spectra by PHOTOS with kernel of extra pair emission given by the formula (40).

Fig. 12 presents ratios of PHOTOS generated spectra of squared mass of e^+e^- pair ($M^2_{e^+e^-}$), of $\mu^+\mu^-$ pair ($M^2_{\mu^+\mu^-}$), of squared mass of $\mu^+e^+e^-$ three ($M^2_{\mu^+e^+e^-}$) and of squared mass of $e^+\mu^+\mu^-$ three ($M^2_{e^+\mu^+\mu^-}$) to the corresponding one's by improved PHOTOS with matrix element (14). Agreement between PHOTOS with kernel F_{test1} (34) and PHOTOS with matrix element (14) is good. PHOTOS with kernel F_{test1} (34) tends to slightly overproduce e^+e^- pairs in the least populated part of the spectrum (up to 15% not taking error into

account) causing overproduction of $\mu^+\mu^-$ pairs (up to 7%) in the first bin. Numbers of $\mu^+\mu^-$ pairs never deviate more than 4% from corresponding numbers of etalon spectra. Numbers of e^+e^- and $\mu^+\mu^-$ pairs with invariant mass close to beam CMS energy coincide with corresponding numbers of etalon spectra.

Other plots, for other than $E_{CMS} = M_Z$ collision energies (Figs. B.10, B.12) and also for $Z \to e^+e^-e^+e^-$ and $Z \to \mu^+\mu^-\mu^+\mu^-$ channels (Figs. B.9, B.11, B.13), are delegated to Appendix B.3.

Matrix element residual F_{test2} (37) differs from matrix element residual F_{test1} (34) by lack of tensors $H_5^{\mu\nu} - H_8^{\mu\nu}$. Numerical effect of that is expected to be small, but that requires verification.

Spectra by PHOTOS with kernel F_{test2} (37) are presented in Fig. 12. Other plots, for other than $E_{CMS} = M_Z$ collision energies (Figs. B.10, B.12) and also for $Z \to e^+e^-e^+e^-$ and $Z \to \mu^+\mu^-\mu^+\mu^-$ channels (Figs. B.9, B.11, B.13), are delegated to Appendix B.3.

Agreement between PHOTOS with kernel F_{test2} (37) and PHOTOS with matrix element (14) is good. Numbers of $\mu^+\mu^-$ and e^+e^- pairs in any channel never deviate more than 7% from corresponding numbers of etalon spectra. Numbers of e^+e^- and $\mu^+\mu^-$ pairs with invariant mass close to beam CMS energy coincide with corresponding numbers of etalon spectra.

Agreement between PHOTOS with kernel F_{test2} (37) and PHOTOS with kernel F_{test1} (34) is good. However, numbers of $\mu^+\mu^-$ and e^+e^- pairs by PHOTOS with kernel F_{test1} (34) in any channel are larger than corresponding numbers of spectra by PHOTOS with kernel F_{test2} (37). Difference between PHOTOS with kernel F_{test2} (37) and PHOTOS with kernel F_{test1} (34) is the most for minimums of pair spectra. This difference is up to 17% for e^+e^- pair spectra in the $Z \to e^+e^-\mu^+\mu^-$ channel and for $\mu^+\mu^-$ pair spectra in the $Z \to \mu^+\mu^-\mu^+\mu^-$ channel. This difference is up to 12% for $\mu^+\mu^-$ pair spectra in the $Z \to e^+e^-\mu^+\mu^-$ channel and for e^+e^- pair spectra in the $Z \to e^+e^-e^+e^-$ channel. Numbers of e^+e^- and $\mu^+\mu^-$ pairs with invariant mass close to beam CMS energy from spectra by PHOTOS with kernel F_{test2} (37) coincide with corresponding numbers from spectra by PHOTOS with kernel F_{test1} (34).

Spectra by PHOTOS with kernel F_{test3} (40) are presented in Fig. 12. Other plots, for other than $E_{CMS} = M_Z$ collision energies (Figs. B.10, B.12) and also for $Z \to e^+e^-e^+e^-$ and $Z \to \mu^+\mu^-\mu^+\mu^-$ channels (Figs. B.9, B.11, B.13), are delegated to Appendix B.3.

Agreement between PHOTOS with kernel F_{test3} (40) and PHOTOS with matrix element (14) is good. Considering $Z \to e^+e^-\mu^+\mu^-$ channel: PHOTOS with kernel F_{test3} (40) tends to slightly overproduce e^+e^- pairs in the least populated part of the spectrum (up to 15% not taking error into account) causing overproduction of $\mu^+\mu^-$ pairs (up to 6%) in the first bin; numbers of $\mu^+\mu^-$ pairs never deviate more than 10% from corresponding numbers of etalon spectra. Considering $Z \to \mu^+\mu^-\mu^+\mu^-$ channel: PHOTOS with kernel F_{test3} (40) tends to slightly overproduce $\mu^+\mu^-$ pairs in the least populated part of the spectrum (up to 15% not taking error into account) causing overproduction of $\mu^+\mu^-$ pairs (up to 6%) in the first bin. Considering $Z \to e^+e^-e^+e^-$ channel: numbers of e^+e^- pairs never deviate more than 5% from corresponding numbers of etalon spectra. For each channel numbers of e^+e^- and $\mu^+\mu^-$ pairs with invariant mass close to beam CMS energy coincide with corresponding numbers from etalon spectra. For each channel and for each bin the number of e^+e^- or $\mu^+\mu^-$ pairs generated by PHOTOS with kernel F_{test3} (40) is larger than corresponding

number from samples by PHOTOS with kernel F_{test2} (37), their difference is small.

Comparing last two numerical tests (F_{test2} (37) and F_{test3} (40)) I conclude that tensor $H_{11}^{\mu\nu}$ (39), which is part of matrix element (14), can be approximated in a way it is presented by formula (40); tensor $H_{11}^{\mu\nu}$ (39) should be placed in the PHOTOS kernel.

Spectra by PHOTOS with kernel F_{test4} (41) are presented in Fig. 13.

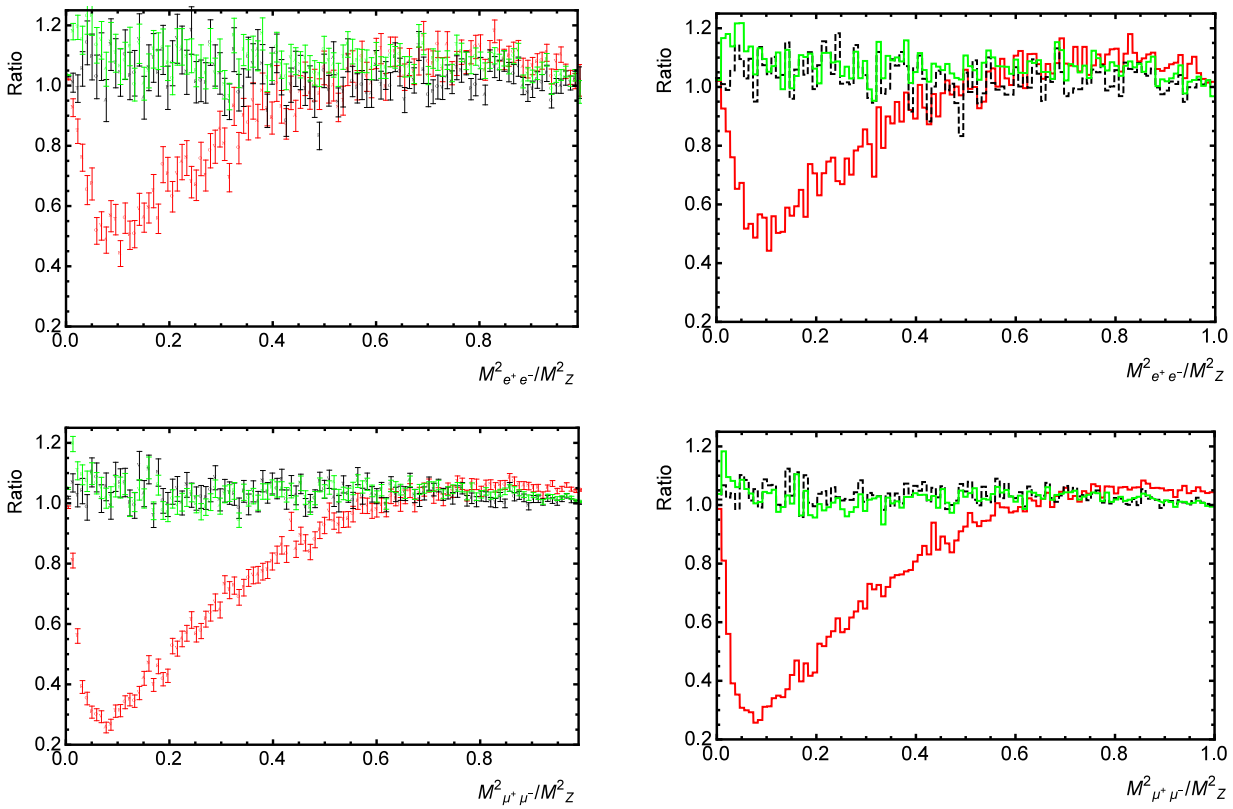

Figure 13: Ratios of PHOTOS generated spectra (of squared mass of e^+e^- pair ($M^2_{e^+e^-}$), of $\mu^+\mu^-$ pair ($M^2_{\mu^+\mu^-}$)) in $Z \to e^+e^-\mu^+\mu^-$ channel to the corresponding one's by KORALW. Spectra generated by PHOTOS are obtained from samples of equal number of $Z \to e^+e^-$ and $Z \to \mu^+\mu^-$ PYTHIA generated decays. Red (dark grey in greyscale) solid line and red (dark grey) error bars represent spectra by unmodified PHOTOS [11]. Black dashed line and black error bars represent spectra by improved PHOTOS with matrix element (14) installed into it. Green (light grey in greyscale) solid line and green (light grey) error bars represent spectra by improved PHOTOS with kernel of extra pair emission given by the formula (41).

Fig. 13 presents ratios of PHOTOS generated spectra of squared mass of e^+e^- pair ($M^2_{e^+e^-}$) and of $\mu^+\mu^-$ pair ($M^2_{\mu^+\mu^-}$) to the corresponding one's by KORALW. Left hand side of Fig. 13 presents data in form of error bars. Right hand side of Fig. 13 presents mean values of corresponding spectra, that should improve readability of the plots. Agreement between PHOTOS with kernel F_{test4} (41) and both KORALW and PHOTOS with matrix element (14) is good. Numbers of PHOTOS test events and KORALW test events for any bin never differ

greatly in the ratio more than 24%. Such difference rather vanishes with statistics increase. It is seen, that desired agreement between PHOTOS and KORALW for the least populated bins $0 < M^2_{e^+e^-}, M^2_{\mu^+\mu^-} < 0.5 \cdot M^2_Z$ of e^+e^- pair and $\mu^+\mu^-$ pair spectra is reached. It is seen, that PHOTOS with kernel F_{test4} (41) produces slightly less e^+e^- and $\mu^+\mu^-$ pairs in the most populated parts of the spectra $M^2_{e^+e^-}, M^2_{\mu^+\mu^-} > 0.5 \cdot M^2_Z$ comparing to unmodified PHOTOS [11]. χ^2 test for e^+e^- pair spectra by PHOTOS with kernel F_{test4} (41) and by KORALW gives χ^2/NDF of 2.9[1]. χ^2 test for $\mu^+\mu^-$ pair spectra by PHOTOS with kernel F_{test4} (41) and by KORALW gives χ^2/NDF of 6.1[2].

Other plots, for other than $M^2_{e^+e^-}$ and $M^2_{\mu^+\mu^-}$ observables (Fig. B.14), for other than $E_{CMS} = M_Z$ collision energies (Figs. B.17, B.19) and also for $Z \to e^+e^-e^+e^-$ and $Z \to \mu^+\mu^-\mu^+\mu^-$ channels (Figs. B.16, B.18, B.20), are delegated to Appendix B.3.

I should note that agreement between PHOTOS with kernel F_{test4} (41) and KORALW is quite remarkable and numerically stable.

Spectra by PHOTOS with kernel F_{test5} (42) are presented in Fig. 14.

Fig. 14 presents ratios of PHOTOS generated spectra of squared mass of e^+e^- pair ($M^2_{e^+e^-}$) and of $\mu^+\mu^-$ pair ($M^2_{\mu^+\mu^-}$) to the corresponding one's by KORALW. Left hand side of Fig. 14 presents simulation sample in form of error bars. Right hand side of Fig. 14 presents simulation sample in form of mean values, that should improve readability of the plots. Agreement between PHOTOS with kernel F_{test5} (42) and KORALW is good. Agreement between PHOTOS with kernel F_{test5} (42) and PHOTOS with matrix element (14) is good. Numbers of PHOTOS test events and KORALW test events for any bin never differ greatly in the ratio more than 22%. Such difference rather vanishes with statistics increase. It is seen, that desired agreement between PHOTOS and KORALW for the least populated bins $0 < M^2_{e^+e^-}, M^2_{\mu^+\mu^-} < 0.5 \cdot M^2_Z$ of e^+e^- pair and $\mu^+\mu^-$ pair spectra is reached. It is seen, that PHOTOS with kernel F_{test5} (42) produces slightly less e^+e^- and $\mu^+\mu^-$ pairs in the most populated parts of the spectra $M^2_{e^+e^-}, M^2_{\mu^+\mu^-} > 0.5 \cdot M^2_Z$ comparing to unmodified PHOTOS [11]. χ^2 test for e^+e^- pair spectra by PHOTOS with kernel F_{test5} (42) and by KORALW gives χ^2/NDF of 2.6. χ^2 test for $\mu^+\mu^-$ pair spectra by PHOTOS with kernel F_{test5} (42) and by KORALW gives χ^2/NDF of 6.

Other plots, for other than $M^2_{e^+e^-}$ and $M^2_{\mu^+\mu^-}$ observables (Fig. B.21), for other than $E_{CMS} = M_Z$ collision energies (Figs. B.25-B.28) and also for $Z \to e^+e^-e^+e^-$ and $Z \to \mu^+\mu^-\mu^+\mu^-$ channels (Figs. B.22, B.24, B.26, B.28), are delegated to Appendix B.3.

I should note that agreement between PHOTOS with kernel F_{test5} (42) and KORALW is quite remarkable (Figs. 14) and numerically stable.

6.5 Effective factorization of matrix element, tests

Kernel F_{test6} ignores most of the complexity of the matrix element (14), but this approximation leads to factorization of matrix element $F_{test6} \cdot |M(p_1, p_2; p'_3, p'_4)|^2_{Born}$. Spectra by PHOTOS with kernel F_{test6} (43) are presented in Fig. 15.

[1] Corresponding χ^2/NDF, but for unmodified PHOTOS [11], is 13.1.

[2] Corresponding χ^2/NDF, but for unmodified PHOTOS [11], is 90.9.

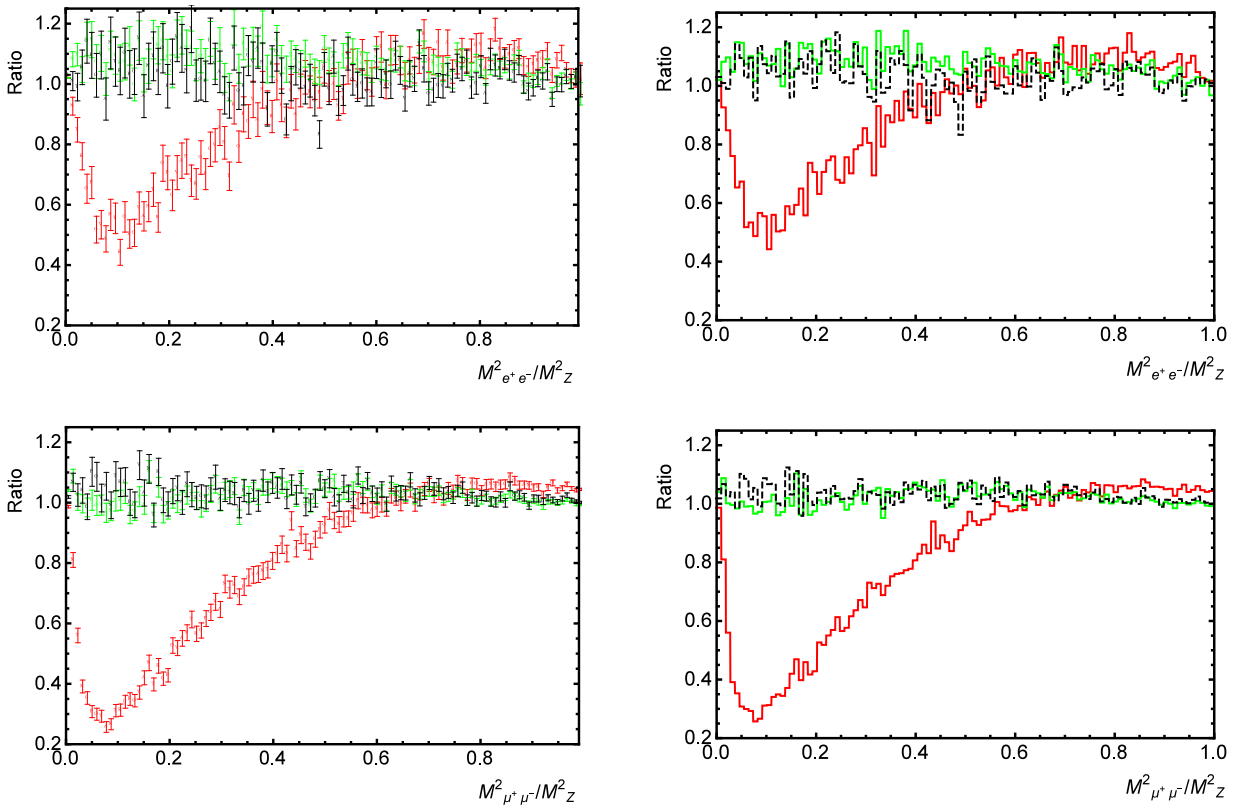

Figure 14: Ratios of PHOTOS generated spectra (of squared mass of e^+e^- pair ($M^2_{e^+e^-}$), of $\mu^+\mu^-$ pair ($M^2_{\mu^+\mu^-}$)) in $Z \to e^+e^-\mu^+\mu^-$ channel to the corresponding one's by KORALW. Spectra generated by PHOTOS are obtained from samples of equal number of $Z \to e^+e^-$ and $Z \to \mu^+\mu^-$ PYTHIA generated decays. Red (dark grey in greyscale) solid line and red (dark grey) error bars represent spectra by unmodified PHOTOS [11]. Black dashed line and black error bars represent spectra by improved PHOTOS with matrix element (14) installed into it. Green (light grey in greyscale) solid line and green (light grey) error bars represent spectra by improved PHOTOS with kernel of extra pair emission given by the formula (42).

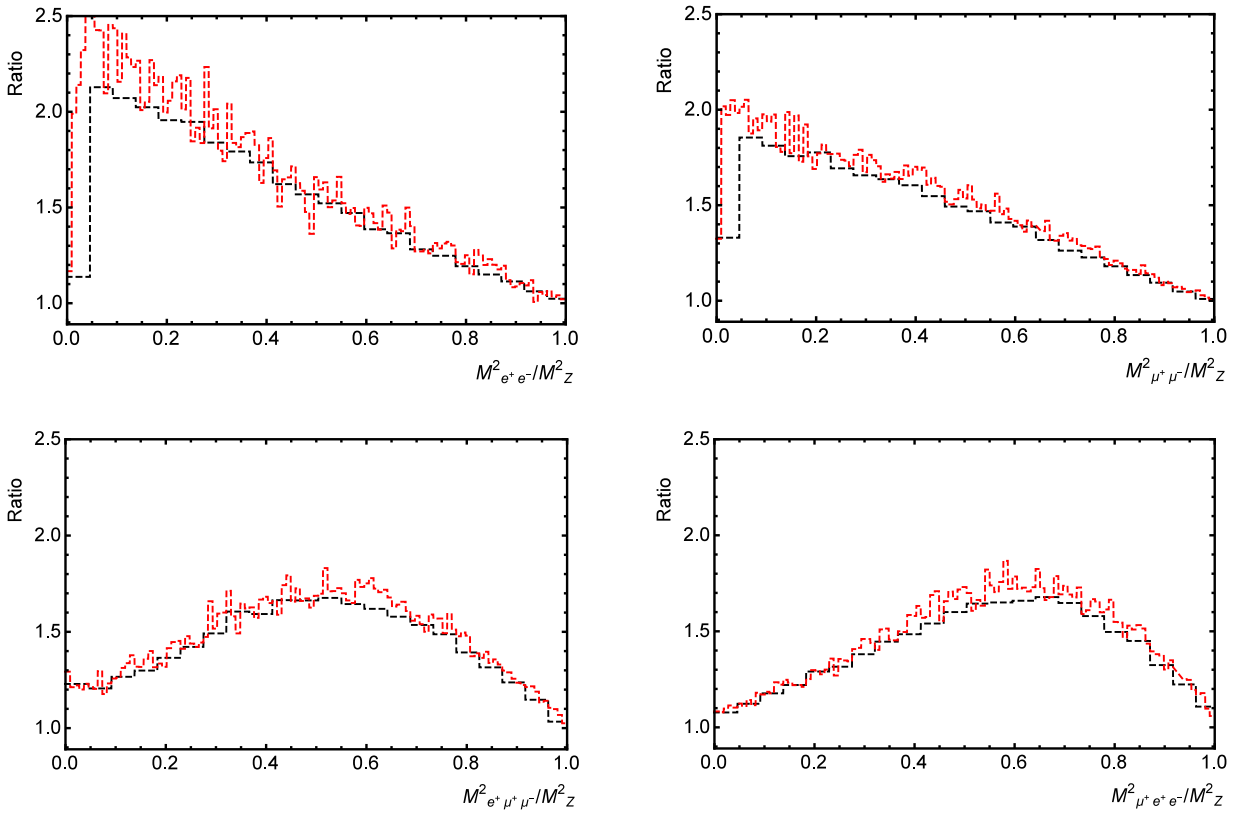

Figure 15: Ratios of PHOTOS generated spectra (of squared mass of e^+e^- pair ($M^2_{e^+e^-}$), of $\mu^+\mu^-$ pair ($M^2_{\mu^+\mu^-}$), of squared mass of $\mu^+e^+e^-$ three ($M^2_{\mu^+e^+e^-}$) and of squared mass of $e^+\mu^+\mu^-$ three ($M^2_{e^+\mu^+\mu^-}$)) in $Z \to e^+e^-\mu^+\mu^-$ channel to the corresponding one's, that are generated by KORALW, and to the corresponding one's, that are generated by improved PHOTOS with matrix element (14) installed into it. Spectra generated by PHOTOS are obtained from samples of equal number of $Z \to e^+e^-$ and $Z \to \mu^+\mu^-$ PYTHIA generated decays. Red (dark grey) dashed line represents ratios of spectra by PHOTOS with kernel of extra pair emission given by the formula (43) to the one's by KORALW. Dark dashed line represents ratios of spectra by PHOTOS with kernel of extra pair emission given by the formula (43) to the one's, that are generated by improved PHOTOS with matrix element (14) installed into it.

Fig. 15 presents ratios of PHOTOS generated spectra of squared mass of e^+e^- pair ($M^2_{e^+e^-}$), of $\mu^+\mu^-$ pair ($M^2_{\mu^+\mu^-}$), of squared mass of $\mu^+e^+e^-$ three ($M^2_{\mu^+e^+e^-}$) and of squared mass of $e^+\mu^+\mu^-$ three ($M^2_{e^+\mu^+\mu^-}$) to the corresponding one's by PHOTOS with matrix element (14).

Other plots, for other than $E_{CMS} = M_Z$ collision energies (Figs. B.30, B.32) and also for $Z \to e^+e^-e^+e^-$ and $Z \to \mu^+\mu^-\mu^+\mu^-$ channels (Figs. B.29, B.31, B.20), are delegated to Appendix B.4.

Results of this test are unsatisfying. In each channel disagreement between e^+e^- (or $\mu^+\mu^-$) pair spectrum by PHOTOS with kernel F_{test6} (43) and by PHOTOS with matrix element (14) is up to 150% for some parts of the spectra. However, considered pair spectra ratios for each tested CMS beam energy ($E_{CMS} = 0.6 \cdot M_Z,\ 0.8 \cdot M_Z,\ M_Z$) and in the each channel ($e^+e^-\mu^+\mu^-$, $\mu^+\mu^-\mu^+\mu^-$ and $e^+e^-e^+e^-$) have some remarkable similarities. First, presented in this test, pair spectra ratios fluctuate around 1 for the one's of the most populated and the most important bins of the spectra, that are $M_{pair} \sim E_{CMS}$. Second, derivative of presented pair spectra ratios seems to be constant. All these constants (one for each pair spectra ratio) are the same number for each kind of an extra pair. Last one hypothesis suggests that complexity of cancelations between neglected tensors $H^{\mu\nu}_{10} - H^{\mu\nu}_{11}$ of matrix element residual (16) can be effectively reproduced by a linear correction of matrix element residual F_{test6}:

$$F_{test8} = \left[F_{soft} + \frac{(8\pi\alpha)^2}{q^2} \left(\frac{1}{2\,(p_3 q) + q^2} + \frac{1}{2\,(p_4 q) + q^2} \right) \right] / \left[A - B \cdot \frac{(p_3 + p_4)^2}{(p_1 + p_2)^2} \right], \quad (45)$$

where A and B are some constant parameters that can be extracted by the fitting procedure. In order to obtain A and B I do linear fit with weights that are given by numbers of events in corresponding bins. As it is stated above, the first bin $M_{pair} \sim 0$ of each pair spectra contains the biggest number of events and indicates an overall performance of generation of extra pair emission, which can be far from ideal. I exclude the first bin of each pair spectra from the fitting procedure, causing that the most weighted bins are for pairs of the highest invariant mass $M_{pair} \sim E_{CMS}$. Fitting results are presented in the Tab. 3.

All presented values of adjusted R^2 are close to 1 indicating success of fitting procedure. From the Tab. 3 it is seen that all the fitted lines go thought point $\{1, 1\}$[1]. This is desirable result. It verifies, that pair emission kernel F_{test8} of eq. (45) can be written in form of eq. (44).

Correction, likewise it is in formula (44), is a task for one parameter fit; such fitting procedure should reduce error of parameter A comparing to the one's from the Tab. 3. However, the presented level of precision for parameter A is enough. It is seen from the Tab. 3, that for each channel and each beam CMS energy E_{CMS} the values of parameter A corresponding to emission of extra e^+e^- pair match down to 3-rd digit, the same is true for $\mu^+\mu^-$ pair. It seems that parameter A increases with decrease of the beam CMS

[1]It is observed for each tested CMS energy.

Channel	E_{CMS}	Extra pair	Parameter A	Parameter B	Input	Adj. R^2
$e^+e^-\mu^+\mu^-$	M_Z	$\mu^+\mu^-$	2.18 ± 0.02	1.21 ± 0.02	Fig. 15	0.992
$e^+e^-\mu^+\mu^-$	M_Z	$\mu^+\mu^-$	2.32 ± 0.02	1.35 ± 0.03	Fig. 15	0.949
$e^+e^-\mu^+\mu^-$	$0.8 \cdot M_Z$	$\mu^+\mu^-$	2.21 ± 0.02	1.24 ± 0.03	Fig. B.30	0.991
$e^+e^-\mu^+\mu^-$	$0.6 \cdot M_Z$	$\mu^+\mu^-$	2.25 ± 0.02	1.29 ± 0.03	Fig. B.32	0.987
$e^+e^-\mu^+\mu^-$	M_Z	e^+e^-	1.951 ± 0.008	0.957 ± 0.009	Fig. 15	0.998
$e^+e^-\mu^+\mu^-$	M_Z	e^+e^-	2.05 ± 0.01	1.05 ± 0.0113	Fig. 15	0.988
$e^+e^-\mu^+\mu^-$	$0.8 \cdot M_Z$	e^+e^-	1.962 ± 0.007	0.969 ± 0.008	Fig. B.30	0.998
$e^+e^-\mu^+\mu^-$	$0.6 \cdot M_Z$	e^+e^-	1.977 ± 0.005	0.985 ± 0.006	Fig. B.32	0.999
$e^+e^-e^+e^-$	M_Z	e^+e^-	1.935 ± 0.009	0.94 ± 0.01	Fig. B.29	0.998
$e^+e^-e^+e^-$	$0.8 \cdot M_Z$	e^+e^-	1.942 ± 0.008	0.947 ± 0.009	Fig. B.31	0.998
$e^+e^-e^+e^-$	$0.6 \cdot M_Z$	e^+e^-	1.943 ± 0.009	0.95 ± 0.01	Fig. B.33	0.997
$\mu^+\mu^-\mu^+\mu^-$	M_Z	$\mu^+\mu^-$	2.20 ± 0.02	1.23 ± 0.02	Fig. B.29	0.992
$\mu^+\mu^-\mu^+\mu^-$	$0.8 \cdot M_Z$	$\mu^+\mu^-$	2.23 ± 0.02	1.27 ± 0.03	Fig. B.31	0.989
$\mu^+\mu^-\mu^+\mu^-$	$0.6 \cdot M_Z$	$\mu^+\mu^-$	2.26 ± 0.02	1.30 ± 0.03	Fig. B.33	0.989

Table 3: Results of linear fitting of ratio of e^+e^- pair (or $\mu^+\mu^-$ pair) spectrum by PHOTOS with kernel F_{test6} (43) to the corresponding reference spectrum by PHOTOS with matrix element (14). Line two and line five represent results, but for KORALW generated spectra used as reference.

energy E_{CMS}. However, this effect is small, it is in 3-rd digit. It is smaller than the effect of changing of the reference spectra from the PHOTOS generated ones (PHOTOS with matrix element (14), see Fig. B.15) to the KORALW generated ones. The values of parameter A corresponding to extra e^+e^- pair emission differ from the ones corresponding to extra $\mu^+\mu^-$ pair emission, the difference is in 2-nd digit, corresponding errors exclude overlap.

For the following test I put parameter $B \equiv 1$, the kernel F_{test7} can be written now in form of eq. (44). I choose parameter $A_{\mu\mu} = 2.2$ for the generation of extra $\mu^+\mu^-$ pair and parameter $A_{ee} = 1.95$ for the generation of extra e^+e^- pair. Basing on given in Tab. 3 precision choice of parameter $A_{\mu\mu} = 2.2$ seems to be optimal, however, for comparisons in $Z \to e^+e^-\mu^+\mu^-$ channel with KORALW data one may expect slight overproduction of high energy extra $\mu^+\mu^-$ pairs, which should be related to some overproduction of low virtuality e^+e^- pairs.

Spectra by PHOTOS with kernel F_{test7} (44) are presented in Figs. 16, 17.

Fig. 16 presents ratios of KORALW generated spectra of squared mass of e^+e^- pair ($M^2_{e^+e^-}$), of $\mu^+\mu^-$ pair ($M^2_{\mu^+\mu^-}$) to the corresponding one's by PHOTOS; and presents ratios of PHOTOS generated spectra of squared mass of e^+e^- pair ($M^2_{e^+e^-}$), of $\mu^+\mu^-$ pair ($M^2_{\mu^+\mu^-}$), of squared mass of $\mu^+e^+e^-$ three ($M^2_{\mu^+e^+e^-}$) and of squared mass of $e^+\mu^+\mu^-$ three ($M^2_{e^+\mu^+\mu^-}$) to the corresponding one's by KORALW. Fig. 17 presents low virtuality parts of spectra of squared mass of e^+e^- pair ($M^2_{e^+e^-}$) and of $\mu^+\mu^-$ pair ($M^2_{\mu^+\mu^-}$)) and their ratios to the corresponding one's by KORALW.

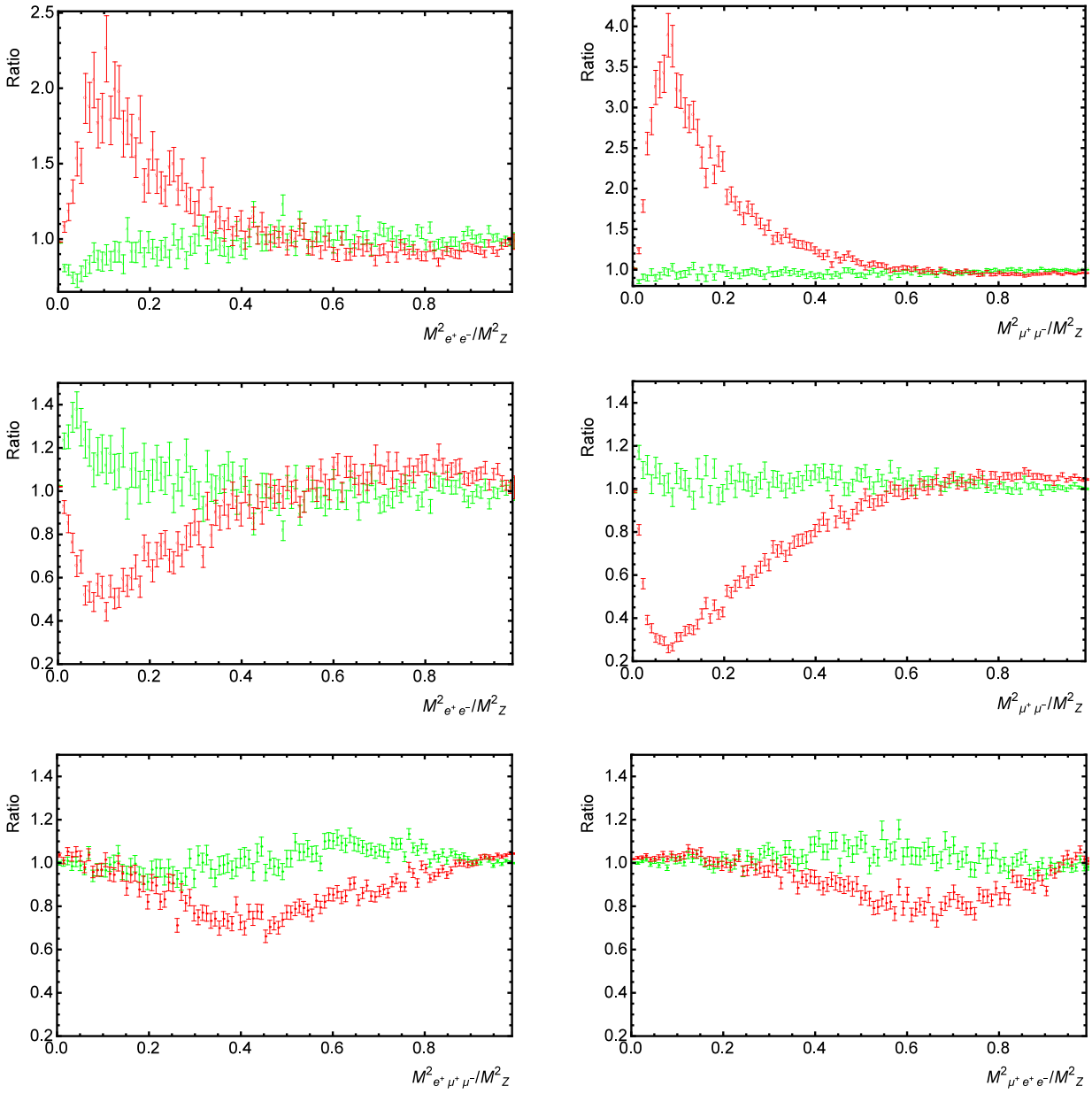

Figure 16: Ratios of KORALW generated spectra (of squared mass of e^+e^- pair ($M^2_{e^+e^-}$), of $\mu^+\mu^-$ pair ($M^2_{\mu^+\mu^-}$)) in the $Z \to \mu^+\mu^-e^+e^-$ channel to the corresponding one's by PHOTOS; ratios of PHOTOS generated spectra (of squared mass of e^+e^- pair ($M^2_{e^+e^-}$), of $\mu^+\mu^-$ pair ($M^2_{\mu^+\mu^-}$), of squared mass of $\mu^+e^+e^-$ three ($M^2_{\mu^+e^+e^-}$) and of squared mass of $e^+\mu^+\mu^-$ three ($M^2_{e^+\mu^+\mu^-}$)) in the $Z \to \mu^+\mu^-e^+e^-$ channel to the corresponding one's by KORALW. Spectra generated by PHOTOS are obtained from samples of equal number of $Z \to e^+e^-$ and $Z \to \mu^+\mu^-$ PYTHIA generated decays. Red (dark grey) error bars represent spectra by unmodified PHOTOS [11]. Green (light grey) error bars represent spectra by improved PHOTOS with kernel of extra pair emission given by the formula (44).

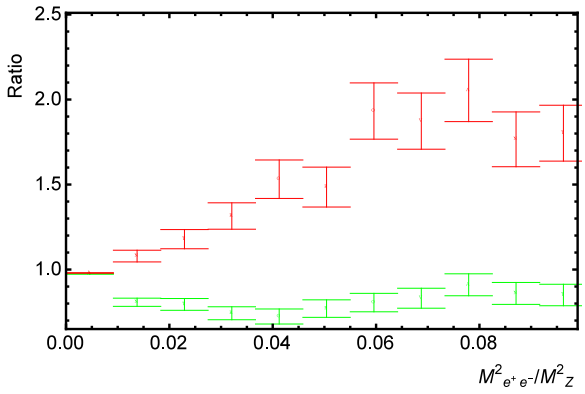

a) Ratio of KORALW generated spectrum to the one generated by PHOTOS.

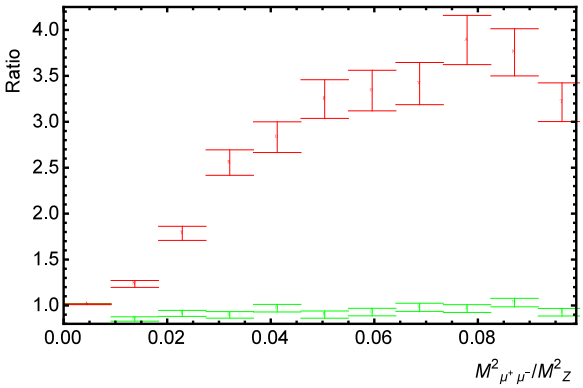

b) Ratio of KORALW generated spectrum to the one generated by PHOTOS.

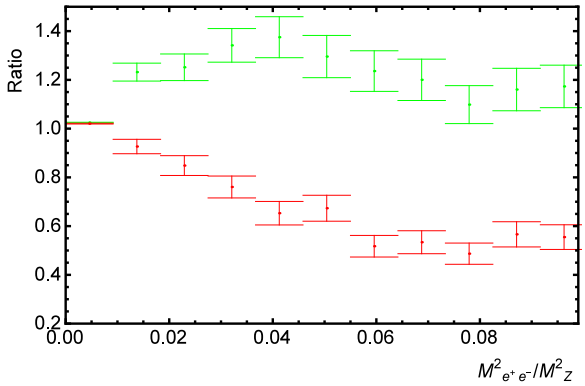

c) Ratio of PHOTOS generated spectrum to the one generated by KORALW.

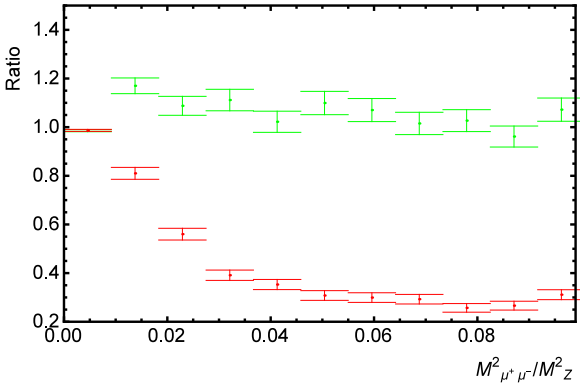

d) Ratio of PHOTOS generated spectrum to the one generated by KORALW.

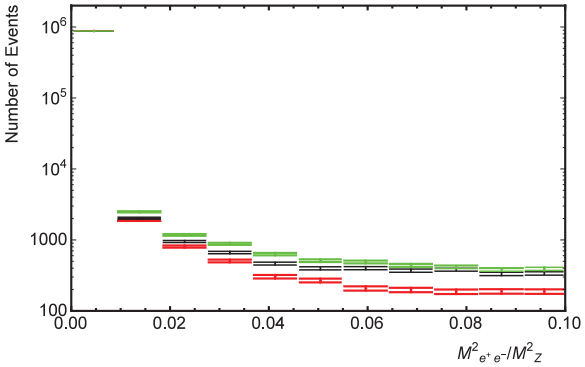

e) Spectrum of electron pair mass squared.

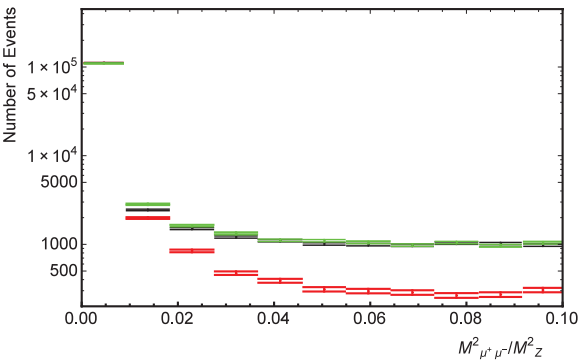

f) Spectrum of muon pair mass squared.

Figure 17: Low virtuality ends of spectra of squared mass of e^+e^- pair ($M^2_{e^+e^-}$) and of $\mu^+\mu^-$ pair ($M^2_{\mu^+\mu^-}$)) and their ratios to the corresponding one's by KORALW. This Figure supplements Fig. 16. There are $1.006\cdot10^6$ events in the $Z\to\mu^+\mu^-e^+e^-$ channel. The very first bin of of e^+e^- pair spectra by improved PHOTOS contains $885\cdot10^3$ events, the second bin contains $2.5\cdot10^3$ events, the third bin contains $1.2\cdot10^3$ events, the fourth bin contains $0.9\cdot10^3$ events. Given numbers illustrate insignificance of discrepancy in e^+e^- pair spectrum by KORALW and by improved PHOTOS with kernel of extra pair emission given by the formula (44) also in region of low virtuality of e^+e^- pair.

Agreement between PHOTOS with kernel F_{test7} (44) and KORALW is at least factor of four better than agreement between unmodified PHOTOS [11] and KORALW. The ratio of numbers of e^+e^- pairs by PHOTOS and by KORALW never differs from 1. more than 25% for most of the bins $M^2_{e^+e^-} > 0.1 \cdot M^2_Z$, ratio error decreases for the most populated bins $M^2_{e^+e^-} > 0.6 \cdot M^2_Z$. The ratio of numbers of $\mu^+\mu^-$ pairs by PHOTOS and by KORALW never differs from 1. more than 15% for most of the bins $M^2_{\mu^+\mu^-} > 0.1 \cdot M^2_Z$, ratio error decreases for the most populated bins $M^2_{\mu^+\mu^-} > 0.6 \cdot M^2_Z$. Such a difference vanishes for most of the bins with statistics increase. It is distinct overproduction (up to factor of 1.4) of e^+e^- pairs of a small invariant mass and of the least populated part of spectrum. Overproduction specifically in this part of the spectrum indicates both overproduction of soft extra e^+e^- pairs and overproduction of the hard extra $\mu^+\mu^-$ pairs. This overproduction can be neglected since it is for few bins only and these bins are near minimum of the spectrum. Slight overproduction (up to 20%) of soft $\mu^+\mu^-$ pairs is observed. χ^2 test for e^+e^- pair spectra by PHOTOS with kernel F_{test7} (44) and by KORALW gives χ^2/NDF of 3[1]. χ^2 test for $\mu^+\mu^-$ pair spectra by PHOTOS with kernel F_{test7} (44) and by KORALW gives χ^2/NDF of 3.4[2].

Other plots, for $Z \to e^+e^-e^+e^-$ and $Z \to \mu^+\mu^-\mu^+\mu^-$ channels (Figs. B.34, B.36, B.38, B.40) and also for other than $E_{CMS} = M_Z$ collision energies (Figs. B.37, B.39, B.38, B.40), are delegated to Appendix B.3.

An effect size of both an overproduction of e^+e^- pairs and an overproduction of $\mu^+\mu^-$ pairs is slightly larger when ratios of spectra to ones by KORALW are discussed. This is expectable since Tab. 3 collects slightly larger values of correction constants $A_{\mu\mu}$ and A_{ee} in the case of comparison with KORALW data. Last one suggests further verification of the effective factorization $F_{test7} \cdot |M(p_1, p_2; p'_3, p'_4)|^2_{Born}$ (44) of matrix element (14) by comparison of spectra by improved PHOTOS to the rigorously generated spectra in the $e^+e^-\mu^+\mu^-$, $e^+e^-e^+e^-$, $\mu^+\mu^-\mu^+\mu^-$ channels at collision energies ranging between few GeV up to $0.6 \cdot M_Z$.

PHOTOS with kernel given by the formula (44) together with constants $A_{\mu\mu} = 2.2$ and $A_{ee} = 1.95$ generates particle spectra in the $e^+e^-\mu^+\mu^-$, $e^+e^-e^+e^-$ and $\mu^+\mu^-\mu^+\mu^-$ channels remarkably close to the ones that are generated as result of exact solution. Considering comparison of PHOTOS generated spectra to the one's by exact solution of KORALW: reduction of χ^2/NDF of factor 4.4 is reach for e^+e^- pair spectrum by PHOTOS with kernel given by the formula (44) comparing to spectrum by unmodified PHOTOS [11]; reduction of χ^2/NDF of factor 26.4 is reach for $\mu^+\mu^-$ pair spectrum by PHOTOS with kernel given by the formula (44) comparing to spectrum by unmodified PHOTOS [11]. Imprecision of PHOTOS with kernel given by the formula (44) stays for the least populated part of the two particle spectra. It is significant, since formula (44) is result of effective factorization of matrix element (14), it describes extra pair emission for collisions of any fermion pair (giving fermion mass can be neglected comparing to energy of colliding pair). Therefore, I expect effective factorization (44) to work for simulation of $pp \to Z/\gamma^* \to 4f$ spin summated process as extra pair emission from the final state of $pp \to Z/\gamma^* \to 2f$ spin summated process. Formula (44) requires verification for collision energies less than $E_{CMS} = 0.6 \cdot M_Z$ and

[1] Corresponding χ^2/NDF, but for unmodified PHOTOS [11], is 13.1.

[2] Corresponding χ^2/NDF, but for unmodified PHOTOS [11], is 90.9.

down to some small value of E_{CMS}.

7 Pair emissions for the τ decay. Phase space parametrization

In this Section I collect the formulae that numerical algorithm of TAUOLA [17, 45] relies on. They also provide platform to perform tests. I focus on a pair of channels $\tau^- \to \bar{\nu}_\mu \mu^- \nu_\tau$ and $\tau^- \to \bar{\nu}_\mu \mu^- e^- e^+ \nu_\tau$, but obtained formulae are of use for $\tau^- \to \bar{\nu}_e e^- \nu_\tau$ and $\tau^- \to \bar{\nu}_e e^- e^- e^+ \nu_\tau$ channels as well. The second channel in each pair differs from the first one by the presence of a $e^- e^+$ pair and can be understood as a contribution to bremsstrahlung correction. The dominant contribution is due to $e^- e^+$ pair of small virtuality (originating from the decay of nearly real photon). In calculations I use in general notation of [46]. I shorten: $\bar{\nu}$ mean $\bar{\nu}_\ell$, where ℓ, either electron or muon, and ν means ν_τ.

3 body decay

An integral of matrix element squared $|M|^2 \equiv |M(p_\tau, p_\nu, p_{\overline{\nu}}, p_\mu)|^2$ over 3-body phase space $dLips_3(p_\tau, p_\nu, p_{\overline{\nu}}, p_\mu)$ reads:

$$\int |M|^2 \, dLips_3(p_\tau, p_\nu, p_{\overline{\nu}}, p_\mu) = \int |M|^2 \, \frac{d^3p_\nu}{(2\pi)^3 2p_\nu^0} \frac{d^3p_{\overline{\nu}}}{(2\pi)^3 2p_{\overline{\nu}}^0} \frac{d^3p_\mu}{(2\pi)^3 2p_\mu^0} (2\pi)^4 \delta^4(p_\tau - p_\nu - p_{\overline{\nu}} - p_\mu) =$$

$$= \frac{1}{2^{11}\pi^5} \int\limits_{m_\mu^2}^{(m_\tau - m_\mu)^2} dM_{\bar{\nu}\mu}^2 \int\limits_{-1}^{1} dcos\theta_\nu \int\limits_0^{2\pi} d\varphi_\nu \left(1 - \frac{M_{\bar{\nu}\mu}^2}{m_\tau^2}\right) \int\limits_{-1}^{1} dcos\theta_{\overline{\nu}} \int\limits_0^{2\pi} d\varphi_{\overline{\nu}} \left(1 - \frac{m_\mu^2}{M_{\bar{\nu}\mu}^2}\right) |M|^2, \tag{46}$$

where p_τ, p_ν, $p_{\overline{\nu}}$, p_μ are four-momenta of τ^-, ν, $\overline{\nu}_\mu$, μ^- correspondingly; $dcos\theta_\nu d\varphi_\nu$ is the solid angle element of p_ν in the rest frame of τ^-, $dcos\theta_{\overline{\nu}} d\varphi_{\overline{\nu}}$ is the solid angle element of $p_{\overline{\nu}}$ in the rest frame of $(p_{\overline{\nu}} + p_\mu)$; $M_{\bar{\nu}\mu}^2 = (p_{\overline{\nu}} + p_\mu)^2$; m_μ is mass of μ^- and m_τ is mass of τ^-.

5 body decay

I proceed with writing a cross section for the 5-body decay $\tau^- \to \bar{\nu}_\mu \mu^- e^- e^+ \nu_\tau$ assuming the matrix element $|M|^2 \equiv |M(p_\tau, p_{e-}, p_{e+}, p_\nu, p_{\overline{\nu}}, p_\mu)|^2$ can be factorized. I focus on a soft pair emissions:

$$|M|^2 = |M(p_\tau, p_\nu, p_{\overline{\nu}}, p_\mu)|^2 \times |M_F(p_{e-}, p_{e+})|^2 . \tag{47}$$

Therefore:

$$\int |M|^2 \, dLips_5(p_\tau, p_{e-}, p_{e+}, p_\nu, p_{\overline{\nu}}, p_\mu) =$$

$$= \int |M_F|^2 \, \frac{d^3p_{e-}}{(2\pi)^3 2p_{e-}^0} \frac{d^3p_{e+}}{(2\pi)^3 2p_{e+}^0} \, d^4R \, \delta^4(R - p_\tau + p_{e-} + p_{e+}) \times$$

$$\times \int |M(p_\tau, p_\nu, p_{\overline{\nu}}, p_\mu)|^2 \, \frac{d^3p_\nu}{(2\pi)^3 2p_\nu^0} \frac{d^3p_{\overline{\nu}}}{(2\pi)^3 2p_{\overline{\nu}}^0} \frac{d^3p_\mu}{(2\pi)^3 2p_\mu^0} (2\pi)^4 \delta^4(R - p_\nu - p_{\overline{\nu}} - p_\mu), \tag{48}$$

where p_τ, p_{e-}, p_{e+}, p_ν, $p_{\overline{\nu}}$, p_μ are four-momenta of τ^-, e^-, e^+, ν, $\overline{\nu}_\mu$, μ^- correspondingly. At first and for a test, I put $|M_F|^2 \equiv 1$. Since the factorized part of matrix element squared $|M_F|^2$ does not depend on p_{e-}, p_{e+} anymore, for a soft pair emission we can drop e^+ and e^- from the conditions of momentum-energy conservation. Thus the technical integral element $d^4R\ \delta^4(R - p_\tau + p_{e-} + p_{e+})$ reduces to $R = p_\tau$ and

$$\begin{aligned}
&\int |M|^2\, dLips_5\left(p_\tau, p_{e-}, p_{e+}, p_\nu, p_{\overline{\nu}}, p_\mu\right) \approx \\
&= \int \frac{d^3p_{e-}}{(2\pi)^3 2p^0_{e-}} \frac{d^3p_{e+}}{(2\pi)^3 2p^0_{e+}} \int |M|^2\, dLips_3\left(p_\tau, p_\nu, p_{\overline{\nu}}, p_\mu\right) = \\
&= \frac{1}{2^8\pi^6} \int \left[dcos\theta_{e-} d\varphi_{e-} \frac{|\overline{p}_{e-}|^2 d|\overline{p}_{e-}|}{\sqrt{|\overline{p}_{e-}|^2 + m_e^2}} \right]_{\overline{p}_\tau = 0} \left[dcos\theta_{e+} d\varphi_{e+} \frac{|\overline{p}_{e+}|^2 d|\overline{p}_{e+}|}{\sqrt{|\overline{p}_{e+}|^2 + m_e^2}} \right]_{\overline{p}_\tau = 0} \times \\
&\times \int \left| M\left(p_\tau, p_\nu, p_{\overline{\nu}}, p_\mu\right) \right|^2 dLips_3(p_\tau, p_\nu, p_{\overline{\nu}}, p_\mu),
\end{aligned} \tag{49}$$

where $\overline{p}_{e-}$, $\overline{p}_{e+}$ are three-momenta of e^-, e^+ correspondingly; subscript $\overline{p}_\tau = 0$ or $\overline{p}_{\overline{\nu}} + \overline{p}_\mu = 0$ means that the variables into square brackets are in τ^- rest frame; $dcos\theta_{e-} d\varphi_{e-}$ is the solid angle element of p_{e^-}, $dcos\theta_{e+} d\varphi_{e+}$ is the solid angle element of p_{e^+}.

Formula 49 is valid for soft e^+e^- only, that is why I can work only with a part of the phase space. I introduce a cutoff parameter Δ_1: $p^0_{e+} < \Delta_1$, $p^0_{e^-} < \Delta_1$. Such a conditions match the limitation introduced for the `TAUOLA` generation. I obtain:

$$\int |M|^2\, dLips_5\left(p_\tau, p_{e-}, p_{e+}, p_\nu, p_{\overline{\nu}}, p_\mu\right) \approx \frac{\Delta_1^4}{2^6\pi^4} \int |M|^2\, dLips_3\left(p_\tau, p_\nu, p_{\overline{\nu}}, p_\mu\right) \tag{50}$$

and soft pair emission probability of the test reads:

$$P_{test1}(\Delta_1) \approx \frac{\Delta_1^4}{2^6\pi^4}. \tag{51}$$

Alternatively, the second test with $|M_F|^2 \equiv 1$ is through writing cross section for the 5-body decay in terms of invariant mass variables:

$$\int |M|^2\, dLips_5(p_\tau) = \frac{1}{2^{11}\pi^5} \int dM^2_{\overline{\nu}\mu ee} \int d\Omega_\nu \left(1 - \frac{M^2_{\overline{\nu}\mu ee}}{m^2_\tau}\right) \int d\Omega_{\overline{\nu}} \left(1 - \frac{M^2_{\mu ee}}{M^2_{\overline{\nu}\mu ee}}\right) \left| M\left(p_\tau, p_\nu, p_{\overline{\nu}}, p_\mu\right) \right|^2 \times \tag{52}$$

$$\times \frac{1}{2^{12}\pi^6} \int d\Omega_\mu \int d\Omega_e \int dM^2_{ee} \left|M_F\right|^2 \sqrt{1 - \frac{4m_e^2}{M^2_{ee}}} \int dM^2_{\mu ee} \frac{\sqrt{\left(M^2_{\mu ee} - M^2_{ee} - m^2_\mu\right)^2 - 4M^2_{ee} m^2_\mu}}{M^2_{\mu ee}}, \tag{53}$$

where $M^2_{\overline{\nu}\mu ee} = \left(p_{\overline{\nu}} + p_\mu + p_{e-} + p_{e+}\right)^2$, $M^2_{\mu ee} = \left(p_\mu + p_{e-} + p_{e+}\right)^2$, $M^2_{ee} = \left(p_{e-} + p_{e+}\right)^2$; $d\Omega_\nu$ is the solid angle element of p_ν in the rest frame of τ^-, $d\Omega_{\overline{\nu}}$ is the solid angle element of $p_{\overline{\nu}}$ in

the rest frame of $(p_{e-}+p_{e+}+p_{\overline{\nu}}+p_\mu)$, $d\Omega_\mu$ is the solid angle element of p_μ in the rest frame of $(p_{e-}+p_{e+}+p_\mu)$, $d\Omega_e$ is the solid angle element of p_{e-} in the rest frame of $(p_{e-}+p_{e+})$. Considering pair emission is soft, I can approximate $M^2_{\overline{\nu}\mu ee} \approx M^2_{\overline{\nu}\mu}$, $M^2_{\mu ee} = m^2_\mu$, thus first part of cross section (52) coincide with cross section (46) for 3-body decay $\tau^- \to \bar{\nu}_\mu \mu^- \nu_\tau$. Soft pair emission probability reads:

$$P_{test2}(\Delta_2) = \frac{1}{2^8\pi^4} \int\limits_{4m_e^2}^{\Delta_2^2} dM^2_{ee} \sqrt{1-\frac{4m_e^2}{M^2_{ee}}} \int\limits_{(m_\mu+M_{ee})^2}^{(m_\mu+\Delta_2)^2} dM^2_{\mu ee} \frac{\sqrt{\left(M^2_{\mu ee}-M^2_{ee}-m^2_\mu\right)^2 - 4M^2_{ee}m^2_\mu}}{M^2_{\mu ee}}. \quad (54)$$

Here cutoff Δ_2 limits invariant mass of the e^+e^- pair, therefore cutoff could be invoked in TAUOLA easily. Double integral of soft pair emission probability Eq. (54) doesn't have a simple analytical solution. On the other hand, numerical solution works perfectly for testing purposes.

The P_{test2} of Eq. (54) as function of Δ_2 can be easily translated into Δ_2 dependent partial widths simply multiplying partial width of $\tau^- \to \bar{\nu}_\mu \mu^- \nu_\tau$ decay by $P_{test2}(\Delta_2)$. Results obtained that way and those from Monte Carlo simulation are collected in Tab. 4. They provide also a test of approach used in Eq. (47) - tests with simplified matrix element.

Δ_2 [GeV]	Partial width [GeV]	
	$P_{test2}(\Delta_2) \times \Gamma(\tau \to \bar{\nu}\mu\nu)$	Monte Carlo
0.00125	$0.42866 \cdot 10^{-30}$	$0.42729 \cdot 10^{-30}$
0.0025	$0.16289 \cdot 10^{-27}$	$0.15965 \cdot 10^{-27}$
0.005	$0.48627 \cdot 10^{-26}$	$0.46480 \cdot 10^{-26}$
0.01	$0.92486 \cdot 10^{-23}$	$0.84837 \cdot 10^{-23}$
0.02	$0.15208 \cdot 10^{-22}$	$0.12664 \cdot 10^{-22}$

Table 4: Partial width obtained for different cutoff Δ_2 from Monte Carlo run and numerically from P_{test2} of Eq.(54). Note, that with increasing cutoff Δ_2, pairs are allowed to be somewhat harder, therefore assumption $\Gamma(\tau \to \bar{\nu}\mu ee\nu) \approx P_{test2} * \Gamma(\tau \to \bar{\nu}\mu\nu)$ works worse. Uncertainty of MC results is at the level of 1%.

Similar tests with $|M_F|^2$ closer to a physical model are performed next. I choose factorized part of matrix element squared to be: $|M_F|^2 = \frac{(4\pi\alpha)^2}{(p_{e+}+p_{e-})^2}$. Such a choice should represent numerical effects of a singular behavior during simulation of soft pair emission. Soft pair emission probability in this case reads:

$$P_{test3} = \int |M_F|^2 \frac{d^3p_{e-}}{(2\pi)^3 2p^0_{e-}} \frac{d^3p_{e+}}{(2\pi)^3 2p^0_{e+}} d^4R\delta^4(R-p_\tau+p_{e-}+p_{e+}) =$$
$$= \frac{1}{(2\pi)^6} \int \frac{(4\pi\alpha)^2}{q^2} \frac{d^3p_{e-}}{2p^0_{e-}} \frac{d^3p_{e+}}{2p^0_{e+}} d^4q dM^2_{ee} \delta(q^2-M^2_{ee}) \Theta(q^0) \times$$

$$\times\delta^4(q-p_{e+}-p_{e-})d^4RdM^2_{\mu\nu\overline{\nu}}\delta(R^2-M^2_{\mu\nu\overline{\nu}})\Theta(R^0)\delta^4(R-p_\tau+q), \quad (55)$$

where I've introduced $q=p_{e-}+p_{e+}$; $R=p_\nu+p_{\overline{\nu}}+p_\mu$, which represents 4-momentum of rest of the particles system after pair emission takes place, and invariant mass squares $M^2_{ee}=(p_{e+}+p_{e-})^2$ and $M^2_{\mu\nu\overline{\nu}}=(p_\nu+p_{\overline{\nu}}+p_\mu)^2$. With help of formulae

$$\begin{aligned}
&\int\frac{d^3p_{e-}}{2p^0_{e-}}\frac{d^3p_{e+}}{2p^0_{e+}}d^4q\delta^4(q-p_{e+}-p_{e-})=\int d^4qdcos\theta_1d\varphi_1\frac{1}{8}\sqrt{1-\frac{4m_e^2}{q^2}},\\
&\int d^4qdM^2_{ee}\delta(q^2-M^2_{ee})\Theta(q^0)=\int\frac{d^3q}{2q^0},\\
&\int d^4RdM^2_{\mu\nu\overline{\nu}}\delta(R^2-M^2_{\mu\nu\overline{\nu}})\Theta(R^0)=\int\frac{d^3R}{2R^0}
\end{aligned} \quad (56)$$

P_{test3} reads:

$$P_{test3}=\frac{\alpha^2}{2^3\pi^3}\int\frac{dM^2_{ee}}{M^4_{ee}}\sqrt{1-\frac{4m_e^2}{M^2_{ee}}}dM^2_{\mu\nu\overline{\nu}}dcos\theta_2d\varphi_2\frac{\lambda^{1/2}(m^2_\tau,M^2_{ee},M^2_{\mu\nu\overline{\nu}})}{8m^2_\tau}, \quad (57)$$

where $\lambda^{1/2}(m^2_\tau,M^2_{ee},M^2_{\mu\nu\overline{\nu}})=\sqrt{\left(m^2_\tau+M^2_{ee}-M^2_{\mu\nu\overline{\nu}}\right)^2-4m^2_\tau M^2_{\mu\nu\overline{\nu}}}$.

Integration over angular variables performs trivially. An easy way to proceed with integration is to integrate over energy $E_{ee}=\frac{m^2_\tau+M^2_{ee}-M^2_{\mu\nu\overline{\nu}}}{2m_\tau}$ of the pair in the rest frame of τ^-. For the condition $dM^2_{ee}=0$, differential of the energy of the pair reads $dE_{ee}=-\frac{dM^2_{\mu\nu\overline{\nu}}}{2m_\tau}$ leading to $\lambda^{1/2}(m^2_\tau,M^2_{ee},M^2_{\mu\nu\overline{\nu}})=2m_\tau\sqrt{E^2_{ee}-M^2_{ee}}$.

Soft pair emission probability reads:

$$\begin{aligned}
&P_{test3}=\frac{\alpha^2}{2^2\pi^2}\int\limits_{4m_e^2}^{\Delta_3^2}\frac{dM^2_{ee}}{M^2_{ee}}\sqrt{1-\frac{4m_e^2}{M^2_{ee}}}\int\limits_{M_{ee}}^{\Delta_3}dE_{ee}\sqrt{E^2_{ee}-M^2_{ee}}=\\
&=\frac{\alpha^2}{2^3\pi^2}\int\limits_{4m_e^2}^{\Delta_3^2}\frac{dM^2_{ee}}{M^2_{ee}}\sqrt{1-\frac{4m_e^2}{M^2_{ee}}}\left(\Delta_3\sqrt{\Delta_3^2-M^2_{ee}}+M^2_{ee}\ln\frac{M_{ee}}{\Delta_3+\sqrt{\Delta_3^2-M^2_{ee}}}\right),
\end{aligned} \quad (58)$$

where Δ_3, maximal energy of the pair in the τ^- rest frame, determines the maximal $M^2_{ee}\leq\Delta^2_3$. Analytical expression for $P_{test3}(\Delta_3)$ for this choice of $|M_F|^2$ is long and is not instructive. Partial widths obtained using this new $P_{test3}(\Delta_3)$ and those from Monte Carlo simulation are collected in Tab. 5.

In the following test I finally use physical factorized part of matrix element squared

$$|M_F|^2=2e^4\frac{4p^\alpha_{e-}p^\beta_{e+}-q^2g^{\alpha\beta}}{q^4}\left(\frac{p_\mu}{qp_\mu}-\frac{p_\tau}{qp_\tau}\right)_\alpha\left(\frac{p_\mu}{qp_\mu}-\frac{p_\tau}{qp_\tau}\right)_\beta, \quad (59)$$

Δ_3 [GeV]	Partial width [GeV]	
	$P_{test3}(\Delta_3) \times \Gamma(\tau \to \bar{\nu}\mu\nu)$	Monte Carlo
0.0025	$0.59970 \cdot 10^{-24}$	$0.59826 \cdot 10^{-24}$
0.005	$0.82769 \cdot 10^{-23}$	$0.81803 \cdot 10^{-23}$
0.01	$0.64485 \cdot 10^{-22}$	$0.64446 \cdot 10^{-22}$
0.02	$0.39679 \cdot 10^{-21}$	$0.38269 \cdot 10^{-21}$

Table 5: Partial width obtained for different cutoff Δ_3 from Monte Carlo run and numerically from P_{test3} of Eq.(58). Note, that with increasing cutoff Δ_3, pairs are allowed to be somewhat harder therefore assumption $\Gamma(\tau \to \bar{\nu}\mu ee\nu) \approx P_{test3} * \Gamma(\tau \to \bar{\nu}\mu\nu)$ works worse. Uncertainty of MC results is at the level of 1%. Those results, together with the ones collected in Tab. 4, provide a confirmation that approach of Eq. (47) is justified as well as provide technical test for the phase space generation in `TAUOLA`.

it represents soft pair emission from τ and from the outgoing charged particle. Soft pair emission probability in this case essentially depend on four-momentum of muon p_μ (without loose of generality it could be electron). This dependence reduces usability of soft pair emission probability, since this probability should be included into formula for three particles decay, which has been considered as fully independent:

$$\int |M|^2 \, dLips_5 \left(p_\tau, p_{e-}, p_{e+}, p_\nu, p_{\overline{\nu}}, p_\mu\right) \approx \int |M|^2 \, dLips_3 \left(p_\tau, p_\nu, p_{\overline{\nu}}, p_\mu\right) P_\tau(p_4).$$

Following calculations are very similar to the ones, that are discussed in work [13]. Soft pair emission probability writes

$$\begin{aligned}
&P_\tau(p_4) = \int |M_F|^2 \frac{d^3p_{e-}}{(2\pi)^3 2p^0_{e-}} \frac{d^3p_{e+}}{(2\pi)^3 2p^0_{e+}} d^4R \delta^4(R - p_\tau + p_{e-} + p_{e+}) = \\
&= \frac{2\left(4\pi\alpha\right)^2}{(2\pi)^6} \int \frac{4p^\alpha_{e-}p^\beta_{e+} - q^2 g^{\alpha\beta}}{q^4} \left(\frac{p_\mu}{qp_\mu} - \frac{p_\tau}{qp_\tau}\right)_\alpha \left(\frac{p_\mu}{qp_\mu} - \frac{p_\tau}{qp_\tau}\right)_\beta \frac{d^3p_{e-}}{2p^0_{e-}} \frac{d^3p_{e+}}{2p^0_{e+}} d^4q dM^2_{ee} \times \\
&\times \delta(q^2 - M^2_{ee}) \Theta(q^0) \delta^4(q - p_{e+} - p_{e-}) d^4R dM^2_{\mu\nu\overline{\nu}} \delta(R^2 - M^2_{\mu\nu\overline{\nu}}) \Theta(R^0) \delta^4 \delta^4(R - p_\tau + q).
\end{aligned}$$

In order to perform following integration I work temporarily in $(p_{e+} + p_{e-})$ at rest frame

$$\begin{aligned}
&\frac{d^3p_{e-}}{2p^0_{e-}} \frac{d^3p_{e+}}{2p^0_{e+}} d^4q \delta^4(q - p_{e+} - p_{e-}) = \int d^4q dcos\theta_1 d\varphi_1 \frac{1}{8} \sqrt{1 - \frac{4m_e^2}{q^2}}, \\
&\int d^4q dcos\theta_1 d\varphi_1 \frac{4p^\alpha_{e-}p^\beta_{e+} - q^2 g^{\alpha\beta}}{q^4} \left(\frac{p_\mu}{qp_\mu} - \frac{p_\tau}{qp_\tau}\right)_\alpha \left(\frac{p_\mu}{qp_\mu} - \frac{p_\tau}{qp_\tau}\right)_\beta = \\
&= -\frac{8\pi}{3} \int \frac{d^4q}{q^2} \left(1 + \frac{2m_e^2}{q^2}\right) \left(\frac{p_\mu}{qp_\mu} - \frac{p_\tau}{qp_\tau}\right)^2.
\end{aligned}$$

Note that at this point of calculation Lorentz-invariance of integrand is restored and I am free to choose any suitable rest frame. Having integration of delta-functions performed

$$\int d^4q dM^2_{ee}\delta(q^2-M^2_{ee})\Theta(q^0)=\int\frac{d^3q}{2q^0},$$
$$\int d^4R dM^2_{\mu\nu\overline{\nu}}\delta(R^2-M^2_{\mu\nu\overline{\nu}})\Theta(R^0)=\int\frac{d^3R}{2R^0}$$

I continue calculation

$$B_f(p_4)=-\frac{\alpha^2}{2\pi^4}\frac{8\pi}{3\cdot 8}\int\frac{dM^2_{ee}}{M^2_{ee}}\sqrt{1-\frac{4m_e^2}{M^2_{ee}}}\left(1+\frac{2m_e^2}{M^2_{ee}}\right)\left(\frac{p_\mu}{qp_\mu}-\frac{p_\tau}{qp_\tau}\right)^2\frac{d^3q}{2q^0}\frac{d^3R}{2R^0}dM^2_{\mu\nu\overline{\nu}}\delta^4(R-p_1+q)=$$
$$=-\frac{\alpha^2}{6\pi^3}\int\frac{dM^2_{ee}}{M^2_{ee}}\sqrt{1-\frac{4m_e^2}{M^2_{ee}}}\left(1+\frac{2m_e^2}{M^2_{ee}}\right)\left(\frac{p_\mu}{qp_\mu}-\frac{p_\tau}{qp_\tau}\right)^2 dM^2_{\mu\nu\overline{\nu}}\frac{d^3q}{2q^0}\delta(M^2_{\mu\nu\overline{\nu}}-(p_1-q)^2)=$$
$$=-\frac{\alpha^2}{6\pi^3}\int\frac{dM^2_{ee}}{M^2_{ee}}\sqrt{1-\frac{4m_e^2}{M^2_{ee}}}\left(1+\frac{2m_e^2}{M^2_{ee}}\right)\left(\frac{p_\mu}{qp_\mu}-\frac{p_\tau}{qp_\tau}\right)^2 dM^2_{\mu\nu\overline{\nu}}dcos\theta_2 d\varphi_2\frac{\lambda^{1/2}(m_\tau^2,M^2_{ee},M^2_{\mu\nu\overline{\nu}})}{8m_\tau^2},$$

where $dcos\theta_2 d\varphi_2$ is solid angle of momentum of the pair $p_{e-}+p_{e+}$ in the rest frame of τ^-. Next step of calculation is to write four-momenta p_μ and p_τ in rest frame of τ^-. For my choice of variables four-momentum of muon is not fully independent variable. Space orientation of three momentum of pair $\overline{q}$ (specifically angle θ_2) for given invariant mass $M_{\mu\overline{\nu}\nu}$ affects momentum of muon p_μ. Assuming soft pair emission I ignore this dependence, so expression $\left(\frac{p_\mu}{qp_\mu}-\frac{p_\tau}{qp_\tau}\right)^2$ can be integrated

$$\left(\frac{p_\mu}{qp_\mu}-\frac{p_\tau}{qp_\tau}\right)^2=\frac{p_\mu^2}{(qp_\mu)^2}+\frac{p_\tau^2}{(qp_\tau)^2}-\frac{2p_\mu p_\tau}{qp_\mu\cdot qp_\tau}=$$
$$=\frac{m_\mu^2}{\left(p_\mu^0q^0-|\overline{p}_\mu||\overline{q}|cos\theta_2\right)^2}+\frac{m_\tau^2}{(m_\tau q^0)^2}-\frac{2m_\tau p_\mu^0}{\left(p_\mu^0q^0-|\overline{p}_\mu||\overline{q}|cos\theta_2\right)\cdot m_\tau q^0},$$
$$\int\limits_{-1}^{+1}\left(\frac{p_\mu}{qp_\mu}-\frac{p_\tau}{qp_\tau}\right)^2 dcos\theta_2=\frac{2m_\mu^2}{\left(p_\mu^0q^0\right)^2-\left(|\overline{p}_\mu||\overline{q}|\right)^2}+\frac{2}{(q^0)^2}+\frac{2p_\mu^0}{q^0\left(|\overline{p}_\mu||\overline{q}|\right)}\ln\frac{p_\mu^0q^0-|\overline{p}_\mu||\overline{q}|}{p_\mu^0q^0+|\overline{p}_\mu||\overline{q}|},$$

leading to

$$P_\tau(p_4)=-\frac{\alpha^2}{6\pi^3}\frac{2\pi\cdot 2}{8m_\tau^2}\int\frac{dM^2_{ee}}{M^2_{ee}}\sqrt{1-\frac{4m_e^2}{M^2_{ee}}}\left(1+\frac{2m_e^2}{M^2_{ee}}\right)dM^2_{\mu\nu\overline{\nu}}\times$$
$$\times\left(\frac{m_\mu^2}{\left(p_\mu^0q^0\right)^2-\left(|\overline{p}_\mu||\overline{q}|\right)^2}+\frac{1}{(q^0)^2}+\frac{p_\mu^0}{q^0\left(|\overline{p}_\mu||\overline{q}|\right)}\ln\frac{p_\mu^0q^0-|\overline{p}_\mu||\overline{q}|}{p_\mu^0q^0+|\overline{p}_\mu||\overline{q}|}\right)\lambda^{1/2}. \qquad (60)$$

I change here integration variable from square of invariant mass $M^2_{\mu\nu\overline{\nu}}$ to energy of the pair E_{ee} at rest frame of

$$E_{ee} = q^0 = \frac{m_\tau^2 + M_{ee}^2 - M_{\mu\nu\overline{\nu}}^2}{2m_\tau},$$
$$dE_{ee} = -\frac{dM_{\mu\nu\overline{\nu}}^2}{2m_\tau},$$
$$\lambda^{1/2}(m_\tau^2, M_{ee}^2, M_{\mu\nu\overline{\nu}}^2) = 2m_\tau\sqrt{E_{ee}^2 - M_{ee}^2}.$$

Next one important thing to make analytical integration possible is to assume $p_\mu^0 \equiv E_\mu \approx |\overline{p}_\mu|$. It is weak assumption since muon mass is not something small to neglect. This assumption works much better when muon is replaced by electron. Soft pair emission probability writes

$$P_\tau(E_\mu, \Delta) = \frac{\alpha^2}{3\pi^2}\frac{(2m_\tau)^2}{4m_\tau^2}\int\limits_{4m_e^2}^{\Delta}\frac{dM_{ee}^2}{M_{ee}^2}\sqrt{1-\frac{4m_e^2}{M_{ee}^2}}\left(1+\frac{2m_e^2}{M_{ee}^2}\right)\times$$
$$\times\int\limits_{M_{ee}}^{\Delta} dE_{ee}\left(\frac{m_\mu^2\sqrt{E_{ee}^2-M_{ee}^2}}{E_\mu^2 M_{ee}^2}+\frac{\sqrt{E_{ee}^2-M_{ee}^2}}{E_{ee}^2}+\left[\frac{1}{E_{ee}}\ln\frac{E_{ee}-\sqrt{E_{ee}^2-M_{ee}^2}}{E_{ee}+\sqrt{E_{ee}^2-M_{ee}^2}}\right]\right). \quad (61)$$

Part of the integrand, which is in square brackets, coincides with the one from formula (8) in Ref. [13]. For this part integration goes the same way like in the Ref. [13], so I jump to a well known expression:

$$I_1(\Delta) = \frac{\alpha^2}{3\pi^2}\int\limits_{4m_e^2}^{\Delta}\frac{dM_{ee}^2}{M_{ee}^2}\sqrt{1-\frac{4m_e^2}{M_{ee}^2}}\left(1+\frac{2m_e^2}{M_{ee}^2}\right)\int\limits_{M_{ee}}^{\Delta} dE_{ee}\frac{1}{E_{ee}}\ln\frac{E_{ee}-\sqrt{E_{ee}^2-M_{ee}^2}}{E_{ee}+\sqrt{E_{ee}^2-M_{ee}^2}} =$$
$$= \frac{\alpha^2}{3\pi^2}\left(\frac{1}{3}\ln^3\frac{2\Delta}{m_e}+\frac{5}{6}\ln^2\frac{2\Delta}{m_e}+\left(\frac{14}{9}-\frac{\pi^2}{6}\right)\ln\frac{2\Delta}{m_e}+\zeta(3)+\frac{5}{6}\pi^2-\frac{41}{27}\right), \quad (62)$$

where $\zeta(z)$ is Riemann zeta function. Part $I_1(\Delta)$ of the soft pair emission probability $P_\tau(E_\mu, \Delta)$ is 1/2 of the real soft fermion pair factor $\tilde{B}_f(\Delta)$ of eq. (11) from Ref. [13]. One may expect such similarity of the two expressions, since $\tilde{B}_f$ describes soft pair emission from the two incoming fermions, while $P_\tau(E_\mu)$ from the one incoming fermion (τ).

I continue calculation of the rest of expression of $P_\tau(p_4)$

$$P_\tau(E_\mu, \Delta) - I_1(\Delta) = \frac{\alpha^2}{3\pi^2}\int\limits_{4m_e^2}^{\Delta}\frac{dM_{ee}^2}{M_{ee}^2}\sqrt{1-\frac{4m_e^2}{M_{ee}^2}}\left(1+\frac{2m_e^2}{M_{ee}^2}\right)\left(\left(\frac{m_\mu^2\Delta^2}{2E_\mu^2 M_{ee}^2}-1\right)\sqrt{1-\frac{M_{ee}^2}{\Delta^2}}+\right.$$
$$\left.+\ln\frac{\Delta+\sqrt{\Delta^2-M_{ee}^2}}{M_{ee}}\right). \quad (63)$$

Here I split integrand on parts and proceed with integration of eq. (61) independently:

$$I_2(\Delta) = -\frac{\alpha^2}{3\pi^2}\int\limits_{4m_e^2}^{\Delta}\frac{dM_{ee}^2}{M_{ee}^2}\sqrt{1-\frac{4m_e^2}{M_{ee}^2}}\left(1+\frac{2m_e^2}{M_{ee}^2}\right)\sqrt{1-\frac{M_{ee}^2}{\Delta^2}} =$$

$$= -\frac{\alpha^2}{9\pi^2}\left(\left(4\left(\frac{2m_e}{\Delta}\right)^2+6\right)K\left(1-\left(\frac{2m_e}{\Delta}\right)^2\right)+\left(\left(\frac{2m_e}{\Delta}\right)^2-11\right)E\left(1-\left(\frac{2m_e}{\Delta}\right)^2\right)\right), \quad (64)$$

where $K(x)$ is the complete elliptic integral of the first kind

$$K\left(x\right) = \int\limits_0^{\pi/2}\frac{dy}{\sqrt{1-x\cdot sin^2 y}} \quad (65)$$

and $E(x)$ is the complete elliptic integral of the second kind

$$E\left(x\right) = \int\limits_0^{\pi/2} dy\sqrt{1-x\cdot sin^2 y}. \quad (66)$$

I stress here, that expression (64) is exact. My most interest is in case of $2m_e \ll \Delta$, thus an approximated expression fore $I_2(\Delta)$ can be more convenient:

$$I_2(\Delta) \approx -\frac{\alpha^2}{3\pi^2}\left(2\ln\frac{2\Delta}{m_e}-\frac{11}{3}\right). \quad (67)$$

I proceed with calculation of $P_\tau(p_4)$

$$I_3(\Delta) = \frac{\alpha^2}{6\pi^2}\frac{m_\mu^2}{E_\mu^2}\int\limits_{4m_e^2}^{\Delta}\frac{\Delta^2 dM_{ee}^2}{M_{ee}^4}\sqrt{1-\frac{4m_e^2}{M_{ee}^2}}\left(1+\frac{2m_e^2}{M_{ee}^2}\right)\sqrt{1-\frac{M_{ee}^2}{\Delta^2}} =$$

$$= \frac{\alpha^2}{45\pi^2}\frac{m_\mu^2}{E_\mu^2}\left(\left(\left(\frac{2m_e}{\Delta}\right)^3+\frac{8m_e}{\Delta}+\frac{3\Delta}{m_e}\right)E\left(1-\left(\frac{\Delta}{2m_e}\right)^2\right)-\left(\frac{2m_e}{\Delta}+\frac{21\Delta}{2m_e}\right)K\left(1-\left(\frac{\Delta}{2m_e}\right)^2\right)\right), \quad (68)$$

where approximation for the case of $2m_e \ll \Delta$ is

$$I_3(\Delta) \approx \frac{\alpha^2}{6\pi^2}\frac{m_\mu^2}{E_\mu^2}\left(\frac{1}{5}\left(\frac{\Delta}{m_e}\right)^2-\ln\left(\frac{2\Delta}{m_e}\right)+\frac{1}{3}\right). \quad (69)$$

In order to manage integration of the one remaining part of integrand from eq. (61) I use trick that is introduced in Ref. [13], I split range of integration into two and then approximate integrand function for the each integration range independently:

$$I_4(\Delta) \approx \frac{\alpha^2}{6\pi^2}\int\limits_{4m_e^2}^{2\Delta m_e}\frac{dM_{ee}^2}{M_{ee}^2}\sqrt{1-\frac{4m_e^2}{M_{ee}^2}}\left(1+\frac{2m_e^2}{M_{ee}^2}\right)\ln\frac{4\Delta^2}{M_{ee}^2} \approx$$

$$\approx \frac{\alpha^2}{3\pi^2}\left(\frac{3}{4}\ln^2\frac{2\Delta}{m_e}+\frac{14}{9}-\frac{\pi^2}{12}-\frac{5}{3}\ln\frac{2\Delta}{m_e}\right), \tag{70}$$

$$I_5(\Delta)\approx\frac{\alpha^2}{3\pi^2}\int\limits_{2\Delta m_e}^{\Delta^2}\frac{dM_{ee}^2}{M_{ee}^2}\left(\ln\left(1+\sqrt{1-\frac{M_{ee}^2}{\Delta^2}}\right)-\frac{1}{2}\ln\frac{M_{ee}^2}{\Delta^2}\right)\approx$$
$$\approx\frac{\alpha^2}{3\pi^2}\left(\frac{1}{4}\ln^2\frac{2\Delta}{m_e}-\frac{\pi^2}{12}\right). \tag{71}$$

Since I have identified that I_1 is direct consequence of the pair emission from the τ, I relate sum $I_2+I_3+I_4+I_5$ with pair emission from outgoing muon (it can be electron as well):

$$I_2+I_3+I_4+I_5=\frac{\alpha^2}{3\pi^2}\Bigg(\ln^2\frac{2\Delta}{m_e}-\frac{11}{3}\ln\frac{2\Delta}{m_e}+\frac{47}{9}-\frac{\pi^2}{6}+$$
$$+\frac{m_\mu^2}{2E_\mu^2}\left[\frac{1}{5}\left(\frac{\Delta}{m_e}\right)^2-\ln\left(\frac{2\Delta}{m_e}\right)+\frac{1}{3}\right]\Bigg). \tag{72}$$

Soft pair emission probability reads

$$P_\tau(E_\mu,\Delta)=\frac{\alpha^2}{3\pi^2}\left(\frac{1}{3}\ln^3\frac{2\Delta}{m_e}+\frac{11}{6}\ln^2\frac{2\Delta}{m_e}+\left(\frac{19}{9}-\frac{\pi^2}{6}\right)\ln\frac{2\Delta}{m_e}+\zeta(3)+\frac{100}{27}+\frac{2}{3}\pi^2+\right.$$
$$\left.+\frac{m_\mu^2}{2E_\mu^2}\left[\frac{1}{5}\left(\frac{\Delta}{m_e}\right)^2-\ln\left(\frac{2\Delta}{m_e}\right)+\frac{1}{3}\right]\right)\left(1+O\left(\frac{\Delta}{m_\tau},\frac{m_e}{\Delta}\right)\right). \tag{73}$$

I note here, that all line of calculations for formula (73) is valid under condition $\Delta\ll E_\mu$, it restricts region of phase space where formula (73) can be used. Uncertainty related to this condition for the case $\Delta\sim E_\mu$ is not estimated analytically since analytical solution of integrals in eq. (60) is not known. Extra pair emission probability (73) is integrated factorized part of matrix element for soft lepton extra pair emission (59). Formula (59) and formula (73), with its precondition of $E_l\ll m_l$ being ignored, have been added to `TAUOLA` and have been crosschecked in the $\tau^-\to\bar{\nu}_\mu\mu^-e^-e^+\nu_\tau$ and $\tau^-\to\bar{\nu}_e e^-e^-e^+\nu_\tau$ channels: total cross sections for $\tau^-\to\bar{\nu}_\mu\mu^-e^-e^+\nu_\tau$ process agree at level of 98%, total cross sections for $\tau^-\to\bar{\nu}_e e^-e^-e^+\nu_\tau$ process agree at level of 90%.

8 Summary

- In ATLAS measurement of W boson mass [1] a systematic error due to FSR extra pair emissions is roughly 5 MeV (not including error due to muon momentum calibration), it is not simulated, but only is evaluated using `PHOTOS` and `SANC`. Estimation of extra

pair effect by SANC is roughly 2 times as the one by PHOTOS [21]. Size of this effect is used to evaluate systematic ambiguity [1]. I report full agreement between PHOTOS and my new calculations, thus I report factor of 2 reduction of systematic error of W boson mass measurement due to FSR extra pair emissions, because origin of SANC-PHOTOS differences now is understood.

- Later I have improved PHOTOS kernel for extra pair emissions from the final state of $2f \to Z \to 2f$ spin summated amplitudes. For $2f \to Z \to 4f$ process I have reached agreement between PYTHIA + improved PHOTOS and exact complete solution of KORALW for all test distributions (see Figs. 16 and 17, more plots are collected in Appendix B) in the $e^+e^-\mu^+\mu^-$ and in the $\mu^+\mu^-\mu^+\mu^-$ channels. As it seen from Fig. 16, in the $e^+e^-\mu^+\mu^-$ channel an improvement of PHOTOS with kernel of eq. (44) comparing to basic version [11] is: factor of 4.4 reduction of χ^2/NDF (from 13.1 to 3) for χ^2 test of PYTHIA+PHOTOS generated and of KORALW generated e^+e^- pair spectrum; reduction of deviation (from factor of 2.5 to 17%) between reference distribution and PYTHIA+PHOTOS generated e^+e^- pair spectrum for pairs with virtuality of approx. $22 - 36$ GeV, which corresponds to increase in numbers of the hardest emitted $\mu^+\mu^-$ pairs; factor of 26.4 reduction of χ^2/NDF (from 90.9 to 3.4) for χ^2 test of PYTHIA+PHOTOS generated and of KORALW generated $\mu^+\mu^-$ pair spectrum; reduction of deviation (from factor of 4.2 to 7%) between reference distribution and PYTHIA+PHOTOS generated $\mu^+\mu^-$ pairs spectrum for pairs with virtuality of approx. $20 - 34$ GeV, which corresponds to increase in numbers of the hardest emitted e^+e^- pairs. Together with discussed above factor of 2, muon pair precision improves roughly up to factor of 8 (down to 0.6 MeV), which is close to FCC requirements for theoretical precision of W mass measurements [3]. Of course, a theoretical precision evaluation of an experiment requires simulations with experiment observables with cuts and detector response simulations, that may change my estimation of precision.

- To achieve this results I have analytically reproduced soft fermion pairs emission coefficient [13]. I have semi-analytically reproduced extra pair emission probability matching solution of PHOTOS. Extra pair emission probability is based on new integral formula (13), it describes soft (FSR) extra pair emission. This semi-analytic formula is used together with PYTHIA generated spectra $\frac{d\sigma(pp\to Z\to ll)}{dM_{ll}^2}$ as an integer valued piecewise function. Numerical integration is taken over squares of invariant masses of fermion pairs. Comparison (see Tabs. 1-2 and Fig. 4) of semi-analytic formula (13) and PHOTOS indicates full agreement. That verifies PHOTOS algorithm together with pair emission matrix element (11). As it is expected, if energy of extra pair is small, formula of extra pair emission probability (13) matches the one of emission factor of real soft fermion pair from Ref. [13].

- Complete matrix element is complex. Improvement of PHOTOS is based on an approximation of matrix element $\sum_{spins} |M_1 + M_2 + M_3 + M_4|^2$ for FSR $2f \to Z \to 4f$ spin summated process of Fig. 2 (I calculate it in the Appendix C.3). Approximation

consists in $\sum_{spins} |M_1 + M_2 + M_3 + M_4|^2 \approx \sum_{spins} |M_1 + M_2|^2 + \sum_{spins} |M_3 + M_4|^2$ and neglects interference terms, but is easier to install into PHOTOS kernel. For $\sum_{spins} |M_1 + M_2|^2$ matrix element $f_3\overline{f}_3$ pair is secondary and $f_2\overline{f}_2$ pair represents emitter. For $\sum_{spins} |M_3 + M_4|^2$ matrix element $f_2\overline{f}_2$ pair is secondary and $f_3\overline{f}_3$ pair represents emitter. I have reached agreement between PYTHIA + improved PHOTOS with matrix element (14) and exact complete solution of KORALW (see Fig. 10) for $2f \to Z \to 4f$ process at $E_{CMS} = M_Z$ with FSR extra pair emission in the $e^+e^-\mu^+\mu^-$ and $\mu^+\mu^-\mu^+\mu^-$ channels; ISR by KORALW has been effectively switched off for that simulations. Agreement in each channel for the most populated bins of each distribution is better than 3% (see Fig. 10, more plots are collected in Appendix B). Ratios between PYTHIA+PHOTOS generated spectra and corresponding KORALW generated spectra fluctuate around 1. For the most important observables, such as e^+e^- pair and $\mu^+\mu^-$ pair spectra, standard deviation for each bin of each ratio is not exceed 0.07; error bars of most of the bins of each ratio include 1. Values of χ^2/NDF from χ^2 test of KORALW generated spectrum and of PYTHIA + PHOTOS (with matrix element (14)) generated spectrum are 1.3 for the case of e^+e^- pair spectrum (corresponding value for unmodified PHOTOS [11] is 13.1) and 2.6 for the case of $\mu^+\mu^-$ pair spectrum (corresponding value for unmodified PHOTOS [11] is 90.9). By reaching agreement between KORALW and PYTHIA + PHOTOS with matrix element (14) I have shown that interference terms between $M_1 + M_2$ and $M_3 + M_4$ in the matrix element $\sum_{spins} |M_1 + M_2 + M_3 + M_4|^2$ are negligible for the given conditions $\sum_{spins} |M_1 + M_2 + M_3 + M_4|^2 \approx \sum_{spins} |M_1 + M_2|^2 + \sum_{spins} |M_3 + M_4|^2$.

- As for my purpose only the $Z \to 4f$ part of matrix elements is needed, I present matrix element (14) as Lorentz contraction of tensor, describing incoming particles, and tensor, describing outgoing particles. Feature properties of matrix element (14) with regard to four-body final state are analyzed and discussed (see Section 5). I propose three approximations of matrix element (14) (see formula (41), formula (42) and formula (44)), each one is analytically simpler than previous one. They are as good for simulation of extra pair emission as exact matrix element (14) (see Fig. 13, Fig. 14 and Fig. 16 correspondingly).

- Approximation (44) of matrix element (14) is the best of all mentioned approximations. It leads to factorization of matrix element describing extra pair emission from the final state of $2f \to Z \to 2f$ spin summated process, where the factored part can be integrated independently from Born level matrix element. Therefore, factored part of matrix element (44) describing extra pair emission from the final state of $q\bar{q} \to Z \to 2f$ process are compatible with MC simulation of $2p \to Z \to 2f$ process in order to obtain precise $Z \to 4f$ spectra.

- Number of events by improved PHOTOS (comparing to basic version of PHOTOS [11]) for a given number of events in the Born level PYTHIA generated sample in the $e^+e^- \to Z \to e^+e^-\mu^+\mu^-$ channel at the energy $E_{CMS} = M_Z$ has increased by 5.4%, in the

$e^+e^- \to Z \to \mu^+\mu^-\mu^+\mu^-$ channel at the energy $E_{CMS} = M_Z$ has increased by 4.6%; these corrections are at the level of 10^{-4} if calculated with respect to the $Z \to \ell\ell$. This improvement in an any $4f$ channel goes for emission of hardest low virtuality extra pairs, that goes together with production of corresponding soft pairs. Proper soft pair counting is important for estimation of missing energy, while proper hardest extra pair counting is important for reducing of effect of singlet channel [1].

- Exact matrix element (14) of extra pair emission from the final state of $2f \to Z \to 2f$ process is good as a reference, I propose to use it for tests. Factorized part of effective matrix element (44) for extra pair emission from the final state of $2f \to Z \to 2f$ process is expected to be compatible with simulation of $2p \to Z \to 2f$ process in order to obtain precise $Z \to 4f$ spectra, I propose to install factorized part of effective matrix element (44) into `PHOTOS` library as well.

- Matrix element (14) suits for simulation of τ decays as well, since its tensor, describing outgoing particles, is exact and contribution from charged extra lepton, comparing to τ decay, can be switched off by zeroing corresponding four-momentum and propagators.

- I have calculated factorized part of matrix element (59) for soft lepton extra pair (from τ and an outgoing charged lepton) emission in the τ decay. Matrix element for $\tau \to \nu\overline{\nu}l + L\bar{L}$ process is added to `TAUOLA` (see Section 7).

- I have calculated soft (ISR and FSR) extra pair emission probability (63) for decay of τ lepton. This function (63) depends on cutoff parameter Δ for energy of extra pair and energy of outgoing charged lepton E_l in the rest frame of decaying τ. Conditions for approximation are that cutoff parameter Δ is much less than both mass of decaying particle and energy of outgoing charged lepton E_l, and that energy E_l is much larger than mass m_l of this outgoing particle. Therefore, conditions of applicability of extra pair emission probability (63) imply phase space restrictions during simulations of $\tau^- \to \bar{\nu}_l l^- e^- e^+ \nu_\tau$ decays. Extra pair emission probability (73) is integrated factorized part of matrix element for soft lepton extra pair emission (59). Formula (59) and formula (73), with its precondition of $E_l \ll m_l$ being ignored, have been added to `TAUOLA` and have been crosschecked in the $\tau^- \to \bar{\nu}_\mu \mu^- e^- e^+ \nu_\tau$ and $\tau^- \to \bar{\nu}_e e^- e^- e^+ \nu_\tau$ channels: total cross sections for $\tau^- \to \bar{\nu}_\mu \mu^- e^- e^+ \nu_\tau$ process agree at level of 98%, total cross sections for $\tau^- \to \bar{\nu}_e e^- e^- e^+ \nu_\tau$ process agree at level of 90% (see Section 7).

Acknowledgments.

This work was partially supported by the funds of Polish National Science Center under decisions UMO-2014/15/B/ST2/00049, DEC-2017/27/B/ST2/01391, grant 2016/23/B /ST2/03927 and the CERN FCC Design Study Programme. Useful discussions with Maciej Skrzypek and also his help with `KORALW` installation are appreciated. The work is supported in part by the Programme of the French-Polish Cooperation between IN2P3 and COPIN within the collaborations Nos. 10-138 and 11-142.

I now have the pleasure to express my gratitude to my supervisor Prof. Dr Hab. Zbigniew Was, noting his soft but powerful Will, without which this Result would have been impossible.

References

[1] ATLAS Collaboration, M. Aaboud *et al.*, *Eur. Phys. J.* **C78** (2018), no. 2 110, [Erratum: Eur. Phys. J.C78,no.11,898(2018)], 1701.07240.

[2] C. M. Carloni Calame, M. Chiesa, H. Martinez, G. Montagna, O. Nicrosini, F. Piccinini, and A. Vicini, *Phys. Rev.* **D96** (2017), no. 9 093005, 1612.02841.

[3] S. Jadach and M. Skrzypek, *Eur. Phys. J. C* **79** (2019), no. 9 756, 1903.09895.

[4] A. Blondel and S. Jadach, *QED corrections to high precision measurement of the Z invisible width at electron-positron collide, In preparation.*

[5] E. Barberio, B. van Eijk, and Z. Was, *Comput.Phys.Commun.* **66** (1991) 115–128.

[6] E. Barberio and Z. Was, *Comput.Phys.Commun.* **79** (1994) 291–308.

[7] P. Golonka and Z. Was, *Eur.Phys.J.* **C45** (2006) 97–107, hep-ph/0506026.

[8] G. Nanava and Z. Was, *Eur.Phys.J.* **C51** (2007) 569–583, hep-ph/0607019.

[9] P. Golonka and Z. Was, *Eur.Phys.J.* **C50** (2007) 53–62, hep-ph/0604232.

[10] G. Nanava, Q. Xu, and Z. Was, *Eur.Phys.J.* **C70** (2010) 673–688, 0906.4052.

[11] N. Davidson, T. Przedzinski, and Z. Was, *Comput. Phys. Commun.* **199** (2016) 86–101, 1011.0937.

[12] S. Jadach, W. Placzek, M. Skrzypek, B. Ward, and Z. Was, *Comput.Phys.Commun.* **119** (1999) 272–311, hep-ph/9906277.

[13] S. Jadach, M. Skrzypek, and B. Ward, *Phys.Rev.* **D49** (1994) 1178–1182.

[14] A. Vicini, *CERN* (2018) https://indico.cern.ch/event/766590/contributions/3189736.

[15] R. Corke and T. Sjostrand, *JHEP* **03** (2011) 032, 1011.1759.

[16] N. Davidson, P. Golonka, T. Przedzinski, and Z. Was, *Comput.Phys.Commun.* **182** (2011) 779–789, 0812.3215.

[17] S. Jadach, Z. Was, R. Decker, and J. H. Kuhn, *Comput. Phys. Commun.* **76** (1993) 361–380.

[18] D. Yennie, S. C. Frautschi, and H. Suura, *Annals Phys.* **13** (1961) 379–452.

[19] Z. Was, *W Boson Mass Workshop* (2017) https://indico.cern.ch/event/595512/contributions/2467336.

[20] S. Antropov, *Acta Phys. Polon. B* **48** (2017) 891, 1704.06203.

[21] S. Antropov, A. Arbuzov, R. Sadykov, and Z. Was, *Acta Phys. Polon.* **B48** (2017) 1469, 1706.05571.

[22] T. Sjostrand, S. Mrenna, and P. Z. Skands, *Comput. Phys. Commun.* **178** (2008) 852–867, 0710.3820.

[23] A. Andonov, A. Arbuzov, D. Bardin, S. Bondarenko, P. Christova, *et al.*, *Comput.Phys.Commun.* **174** (2006) 481–517, hep-ph/0411186.

[24] A. Arbuzov, D. Bardin, S. Bondarenko, P. Christova, L. Kalinovskaya, *et al.*, *Eur.Phys.J.* **C46** (2006) 407–412, hep-ph/0506110.

[25] A. Arbuzov, D. Bardin, S. Bondarenko, P. Christova, L. Kalinovskaya, *et al.*, *Eur.Phys.J.* **C54** (2008) 451–460, 0711.0625.

[26] A. Arbuzov and R. Sadykov, *J.Exp.Theor.Phys.* **106** (2008) 488–494, 0707.0423.

[27] A. Andonov, A. Arbuzov, S. Bondarenko, P. Christova, V. Kolesnikov, *et al.*, *Phys.Part.Nucl.Lett.* **4** (2007) 451–460.

[28] A. Andonov, A. Arbuzov, D. Bardin, S. Bondarenko, P. Christova, *et al.*, *Comput.Phys.Commun.* **181** (2010) 305–312, 0812.4207.

[29] A. Andonov, A. Arbuzov, S. Bondarenko, P. Christova, V. Kolesnikov, *et al.*, *Phys.Atom.Nucl.* **73** (2010) 1761–1769, 0901.2785.

[30] D. Bardin, S. Bondarenko, P. Christova, L. Kalinovskaya, L. Rumyantsev, *et al.*, *JETP Lett.* **96** (2012) 285–289, 1207.4400.

[31] A. Arbuzov, *Phys.Lett.* **B470** (1999) 252–258, hep-ph/9908361.

[32] A. Arbuzov, *JHEP* **0107** (2001) 043.

[33] E. Kuraev and V. S. Fadin, *Sov. J. Nucl. Phys.* **41** (1985) 466–472.

[34] M. Skrzypek, "Leading logarithmic calculations of QED corrections at LEP", other thesis, 1992.

[35] A. Arbuzov, R. Sadykov, and Z. Was, *Eur.Phys.J.* **C73** (2013), no. 11 2625, 1212.6783.

[36] C. M. Carloni Calame, G. Montagna, O. Nicrosini, and M. Treccani, *Phys. Rev.* **D69** (2004) 037301, hep-ph/0303102.

[37] S. Alioli *et al.*, *Eur. Phys. J.* **C77** (2017), no. 11 280, 1606.02330.

[38] Further numerical results are added here,
http://annapurna.ifj.edu.pl/∼wasm/phNLO.htm.

[39] S. Jadach, B. Ward, and Z. Was, *Comput.Phys.Commun.* **130** (2000) 260–325, hep-ph/9912214.

[40] G. Altarelli and G. Parisi, *Nucl. Phys. B* **126** (1977) 298–318.

[41] Comparison of extra lepton pair emission by PHOTOS and by KORALW,
http://annapurna.ifj.edu.pl/%7Ewasm/eemumu.pdf,
http://annapurna.ifj.edu.pl/%7Ewasm/mumumumu.pdf.

[42] N. Gagunashvili, *Nucl. Instrum. Meth. A* **614** (2010) 287–296, 0905.4221.

[43] R. Brun and F. Rademakers, *Nucl. Instrum. Meth.* **A389** (1997) 81–86.

[44] M. Dobbs and J. B. Hansen, *Comput. Phys. Commun.* **134** (2001) 41–46.

[45] S. Antropov, S. Banerjee, Z. Was, and J. Zaremba, 1912.11376.

[46] Z. Was, "Radiative corrections", in *1993 European School of High-Energy Physics, Zakopane, Poland, 12-25 Sep 1993: Proceedings*, pp. 307–338, 1994.

[47] J. C. Ward, *Phys. Rev.* **78** (1950) 182.

A Integration of soft matrix element

Here I collect formulae of my calculation used to understand details of analytic calculation of Ref. [13]. I have prepared variant of analytic calculation matching solution used in PHOTOS. I start from the phase-space parametrization and integration of matrix element follows.

A.1 Parametrization of the phase space

$$\begin{aligned}\Omega = & \int \frac{d^3q_1}{2(q_1)_0(2\pi)^3}\cdot\frac{d^3q_2}{2(q_2)_0(2\pi)^3}\cdot\frac{d^3p}{2p_0(2\pi)^3}\cdot\frac{d^3p'}{2p'_0(2\pi)^3}(2\pi)^4\delta^4(R-p-p'-q_1-q_2) = \\ = & \int d^4qd^4Q\frac{d^3q_1}{2(q_1)_0(2\pi)^3}\cdot\frac{d^3q_2}{2(q_2)_0(2\pi)^3}\cdot\frac{d^3p}{2p_0(2\pi)^3}\cdot\frac{d^3p'}{2p'_0(2\pi)^3}(2\pi)^4\times \\ \times & \ \delta^4(R-p-p'-q_1-q_2)\delta^4(q-q_1-q_2)\delta^4(Q-p-p') \end{aligned} \tag{A.1}$$

$$\int \frac{d^3q_1}{2(q_1)^0}\frac{d^3q_2}{2(q_2)^0}\delta^4(q-q_1-q_2) = \int \frac{|\overline{q_1}|d\cos\theta_{q_1}d\phi_{q_1}}{4\sqrt{q^2}}, \tag{A.2}$$

where θ_{q_1},ϕ_{q_1} are direction of q_1 in the rest frame of q, $|\overline{q_1}| = |\overline{q_2}| = \sqrt{\frac{q^2}{4}-\mu^2}$.

$$\int \frac{d^3p}{2(p)^0}\frac{d^3p'}{2(p')^0}\delta^4(Q-p-p') = \int \frac{|\overline{p}|d\cos\theta_{p}d\phi_{p}}{4\sqrt{p^2}}, \tag{A.3}$$

where θ_p,ϕ_p are direction of p in the rest frame of Q, $|\overline{p}| = |\overline{p'}| = \sqrt{\frac{Q^2}{4}-m^2}$.

$$\int d^4qd^4Q\delta^4(R-Q-q) = \int (d\cos\theta_q d\phi_q)dM_Q^2dM_q^2\frac{\sqrt{\lambda}}{8s} \tag{A.4}$$

where θ_q,ϕ_q are direction of q in the rest frame of R.

$$\Omega = \frac{1}{(2\pi)^8}\int dM_q^2dM_Q^2dcos\theta_{q_1}d\phi_{q_1}dcos\theta_pd\phi_pdcos\theta_qd\phi_q\frac{1}{8}\sqrt{1-\frac{4\mu^2}{q^2}}\frac{1}{8}\sqrt{1-\frac{4m^2}{Q^2}}\frac{\sqrt{\lambda(s,M_Q^2,M_q^2)}}{8s}. \tag{A.5}$$

I choose that:

1. θ_p,ϕ_p define orientation of p (in the rest frame of Q) with respect to z axis along direction of q (as seen in this frame);
2. θ_{q_1},ϕ_{q_1} define orientation of q_1 (in the rest frame of q) with respect to z axis along boost from this frame to the rest frame of Q;
3. θ_q,ϕ_q define orientation of p with respect to laboratory directions (in the rest frame of R).

A.2 Preparation of the Matrix Element

Let me now turn attention to matrix element. Factorized term obtained from pair emission matrix element and used in Ref. [13] formula (1) as integrand reads:

$$F(p,p',q,q_1,q_2,a) = (\tfrac{\alpha}{\pi})^2 \tfrac{1}{\pi^2} \left(\tfrac{2p-aq}{aq^2-2pq} - \tfrac{2p'-aq}{aq^2-2p'q} \right)_\mu \left(\tfrac{2p-aq}{aq^2-2pq} - \tfrac{2p'-aq}{aq^2-2p'q} \right)_\nu \tfrac{4q_1^\mu q_2^\nu - q^2 g^{\mu\nu}}{2q^4} \quad \text{(A.6)}$$

Note that it includes factor $\frac{1}{(2\pi)^6}$ of the phase-space integration volume. We need to recall that at the end of calculation.

Now I can express all four vectors necessary for formula (A.6) with the help of previously specified angles. Four vectors p, p', q, q_1, q_2 in the rest frame of Q read:

$$\begin{aligned} p &= (E_p, p\cos\phi_p \sin\theta_p, p \sin\phi_p \sin\theta_p, p\cos\theta_p), \\ p' &= (E_p, -p\cos\phi_p \sin\theta_p, -p \sin\phi_p \sin\theta_p, -p\cos\theta_p), \\ q &= (E_q, 0, 0, q), \end{aligned} \quad \text{(A.7)}$$

where

$$\begin{aligned} E_p &= \frac{1}{2} M_Q, \\ p &= \sqrt{\frac{M_Q^2}{4} - m^2}, \\ E_q &= \frac{s - M_Q^2 - M_q^2}{2M_Q}, \\ q &= \frac{\sqrt{(s - M_Q^2 - M_q^2)^2 - 4M_Q^2 M_q^2}}{2M_Q}. \end{aligned} \quad \text{(A.8)}$$

To obtain expressions for E_q and q formulae for p and p' and $s = (p + p' + q)^2$ are needed.

I first define q_1 and q_2 in the the rest frame of q:

$$\begin{aligned} q_1 &= (\frac{M_q}{2}, v\cos\phi_{q_1} \sin\theta_{q_1}, v \sin\phi_{q_1} \sin\theta_{q_1}, v\cos\theta_{q_1}), \\ q_2 &= (\frac{M_q}{2}, -v\cos\phi_{q_1} \sin\theta_{q_1}, -v \sin\phi_{q_1} \sin\theta_{q_1}, -v\cos\theta_{q_1}), \end{aligned}$$

where

$$v = \sqrt{\frac{M_q^2}{4} - \mu^2}. \quad \text{(A.9)}$$

A.3 Integration of matrix element

I have to calculate

$$\sigma = \int d\Omega F |M_B|^2, \quad \text{(A.10)}$$

where F is given by formula (A.6) and $d\Omega$ by (A.5). $|M_B|^2$ is not important as it will be seen.

Question is how to do it in most convenient way without loosing symmetry properties of (A.6).

Observation:

1. F depends on all variables except θ_q, ϕ_q;
2. $|M_B|^2$ depends only on θ_q, ϕ_q;
3. θ_{q_1}, ϕ_{q_1} are present only in $\frac{4q_1^\mu q_2^\nu - q^2 g^{\mu\nu}}{2q^4}$.

It is convenient to integrate $\frac{4q_1^\mu q_2^\nu - q^2 g^{\mu\nu}}{2q^4}$ over θ_{q_1}, ϕ_{q_1} in the rest frame of q. Because of Lorentz invariance we have

$$\int d\theta_q d\phi_q d\frac{4q_1^\mu q_2^\nu - q^2 g^{\mu\nu}}{2q^4} = X g^{\mu\nu} + Y q^\mu q^\nu. \tag{A.11}$$

Thus

$$\begin{aligned}
&\int d\theta_q d\phi_q d\frac{4q_1^\mu q_2^\nu - q^2 g^{\mu\nu}}{2q^4} = \\
&= \frac{16\pi}{2M_q^4}\begin{pmatrix} \frac{M_q^2}{4} & 0 & 0 & 0 \\ 0 & -\frac{1}{3}\left(\frac{M_q^2}{4} - \mu^2\right) & 0 & 0 \\ 0 & 0 & -\frac{1}{3}\left(\frac{M_q^2}{4} - \mu^2\right) & 0 \\ 0 & 0 & 0 & -\frac{1}{3}\left(\frac{M_q^2}{4} - \mu^2\right) \end{pmatrix} - \frac{4\pi M_q^2}{2M_q^4}\begin{pmatrix} 1 & 0 & 0 & 0 \\ 0 & -1 & 0 & 0 \\ 0 & 0 & -1 & 0 \\ 0 & 0 & 0 & -1 \end{pmatrix} = \\
&= \frac{1}{M_q^2}\begin{pmatrix} 0 & 0 & 0 & 0 \\ 0 & \frac{4\pi}{3}\left(1 + \frac{2\mu^2}{M_q^2}\right) & 0 & 0 \\ 0 & 0 & \frac{4\pi}{3}\left(1 + \frac{2\mu^2}{M_q^2}\right) & 0 \\ 0 & 0 & 0 & \frac{4\pi}{3}\left(1 + \frac{2\mu^2}{M_q^2}\right) \end{pmatrix} = \\
&= -\frac{1}{M_q^2}\cdot\frac{4\pi}{3}\left(1 + \frac{2\mu^2}{M_q^2}\right)\begin{pmatrix} 1 & 0 & 0 & 0 \\ 0 & -1 & 0 & 0 \\ 0 & 0 & -1 & 0 \\ 0 & 0 & 0 & -1 \end{pmatrix} + \frac{1}{M_q^2}\cdot\frac{4\pi}{3}\left(1 + \frac{2\mu^2}{M_q^2}\right)\begin{pmatrix} 1 & 0 & 0 & 0 \\ 0 & 0 & 0 & 0 \\ 0 & 0 & 0 & 0 \\ 0 & 0 & 0 & 0 \end{pmatrix} = \\
&= -\frac{1}{M_q^2}\cdot\frac{4\pi}{3}\left(1 + \frac{2\mu^2}{M_q^2}\right) g^{\mu\nu} + \frac{1}{M_q^2}\cdot\frac{4\pi}{3}\left(1 + \frac{2\mu^2}{M_q^2}\right)\frac{q^\mu q^\nu}{M_q^2}.
\end{aligned} \tag{A.12}$$

It is easy to verify, that

$$\left(\frac{2p - aq}{aq^2 - 2pq} - \frac{2p' - aq}{aq^2 - 2p'q}\right)_\mu \left(\frac{2p - aq}{aq^2 - 2pq} - \frac{2p' - aq}{aq^2 - 2p'q}\right)_\nu q^\mu q^\nu \tag{A.13}$$

equals zero, and second part of (A.12) does not contribute. This is a consequence of property resulting from Ward identity of QED [47].

Products of four-vectors can be expressed with the help of invariants and masses used in phase-space parametrization

$$\begin{aligned} p\cdot p' &= \frac{M_Q^2}{2}-m^2; \\ p\cdot q &= \frac{s-M_Q^2-M_q^2}{4}-\sqrt{\frac{M_Q^2}{4}-m^2}\frac{\lambda^{\frac{1}{2}}(s,M_Q^2,M_q^2)}{2M_Q}\cos\theta_p; \\ p'\cdot q &= \frac{s-M_Q^2-M_q^2}{4}+\sqrt{\frac{M_Q^2}{4}-m^2}\frac{\lambda^{\frac{1}{2}}(s,M_Q^2,M_q^2)}{2M_Q}\cos\theta_p. \end{aligned} \tag{A.14}$$

In case of $a=0$ calculation is particularly simple:

$$\begin{aligned} &\left(\frac{2p-aq}{aq^2-2pq}-\frac{2p'-aq}{aq^2-2p'q}\right)^2 = \\ &= \frac{4m^2}{\left(\frac{s-M_Q^2-M_q^2}{2}-\sqrt{\frac{M_Q^2}{4}-m^2}\frac{\lambda^{\frac{1}{2}}(s,M_Q^2,M_q^2)}{M_Q}\cos\theta_p\right)^2}+ \\ &+ \frac{4m^2}{\left(\frac{s-M_Q^2-M_q^2}{2}+\sqrt{\frac{M_Q^2}{4}-m^2}\frac{\lambda^{\frac{1}{2}}(s,M_Q^2,M_q^2)}{M_Q}\cos\theta_p\right)^2}- \\ &- 2\frac{2M_Q^2-4m^2}{\frac{(s-M_Q^2-M_q^2)^2}{4}-\left(\frac{M_Q^2}{4}-m^2\right)\frac{\lambda(s,M_Q^2,M_q^2)}{M_Q^2}\cos^2\theta_p}. \end{aligned} \tag{A.15}$$

In general case, thanks to (A.7), I obtain

$$\begin{aligned} &\left(\frac{2p-aq}{aq^2-2pq}-\frac{2p'-aq}{aq^2-2p'q}\right)^2 = \left(\frac{4p^\mu p_\mu+a^2q^\mu q_\mu-4ap_\mu q^\mu}{(aq^\mu q_\mu-2E_pE_q+2pq\cos\theta_p)^2}+\frac{4p^\mu p_\mu+a^2q^\mu q_\mu-4ap'_\mu q^\mu}{(aq^\mu q_\mu-2E_pE_q-2pq\cos\theta_p)^2}\right. \\ &\left.-2\frac{4p^\mu p'_\mu-2aq_\mu(p+p')^\mu+a^2q^\mu q_\mu}{(aq^\mu q_\mu-2E_pE_q+2pq\cos\theta_p)(aq^\mu q_\mu-2E_pE_q-2pq\cos\theta_p)}\right) \\ &= \left(\frac{4m^2+aM_q^2-4aE_pE_q+4apq\cos\theta_p}{(aM_q^2-2E_pE_q+2pq\cos\theta_p)^2}\right. \\ &\left.+\frac{4m^2+aM_q^2-4aE_pE_q-4apq\cos\theta_p}{(aM_q^2-2E_pE_q-2pq\cos\theta_p)^2}-2\frac{4(m^2+2p^2)-4aE_qE_p+a^2M_q^2}{(aM_q^2-2E_pE_q)^2-4p^2q^2\cos^2\theta_p}\right). \end{aligned} \tag{A.16}$$

In order to integrate expression (A.16) over $\cos\theta_p$ I separate it into three parts corresponding to distinct polynomials in $\cos\theta_p$. Integrals read:

$$C_1 = \int_1^{-1} d\cos\theta_p\left(\frac{4m^2+aM_q^2-4aE_pE_q}{(aM_q^2-2E_pE_q+2pq\cos\theta_p)^2}+\frac{4m^2+aM_q^2-4aE_pE_q}{(aM_q^2-2E_pE_q-2pq\cos\theta_p)^2}\right);$$

$$C_2 = \int\limits_1^{-1} d\cos\theta_p \left(\frac{4apq\cos\theta_p}{(aM_q^2 - 2E_pE_q + 2pq\cos\theta_p)^2} - \frac{4apq\cos\theta_p}{(aM_q^2 - 2E_pE_q - 2pq\cos\theta_p)^2} \right);$$

$$C_3 = \int\limits_1^{-1} d\cos\theta_p \frac{4(m^2+2p^2) - 4aE_qE_p + a^2M_q^2}{(aM_q^2 - 2E_pE_q)^2 - 4p^2q^2\cos^2\theta_p}. \quad (A.17)$$

Let me now return to main eq. (A.10). I get

$$\sigma = \frac{1}{(2\pi)^8}\frac{1}{\pi^2}\int |M_B|^2 dM_q^2 dM_Q^2 dcos\theta_p d\phi_p dcos\theta_q d\phi_q \frac{1}{8}\sqrt{1-\frac{4\mu^2}{q^2}}\frac{1}{8}\sqrt{1-\frac{4m^2}{Q^2}}\frac{\sqrt{\lambda(s,M_Q^2,M_q^2)}}{8s}\times$$
$$\times \ (\frac{\alpha}{\pi})^2 \left(\frac{2p-aq}{aq^2-2pq} - \frac{2p'-aq}{aq^2-2p'q}\right)_\mu \left(\frac{2p-aq}{aq^2-2pq} - \frac{2p'-aq}{aq^2-2p'q}\right)^\mu \frac{1}{M_q^2}\cdot\frac{(-4\pi)}{3}\left(1+\frac{2\mu^2}{M_q^2}\right) \quad (A.18)$$

or after re-ordering of terms

$$\sigma = -\frac{1}{3\cdot 2^{15}\pi^9 s}(\frac{\alpha}{\pi})^2 \int \left[|M_B|^2 dcos\theta_q d\phi_q\right] dM_Q^2 \frac{dM_q^2}{M_q^2} dcos\theta_p d\phi_p \sqrt{1-\frac{4\mu^2}{M_q^2}}\left(1+\frac{2\mu^2}{M_q^2}\right)\sqrt{1-\frac{4m^2}{M_Q^2}}\times$$
$$\times \ \lambda^{\frac{1}{2}}(s,M_Q^2,M_q^2)\left(\frac{2p-aq}{aq^2-2pq} - \frac{2p'-aq}{aq^2-2p'q}\right)_\mu \left(\frac{2p-aq}{aq^2-2pq} - \frac{2p'-aq}{aq^2-2p'q}\right)^\mu \quad (A.19)$$

I simplify integral (A.19) with the help of (A.15). Expression (A.14) or(A.16) does not depend on ϕ_p, integration over ϕ_p is trivial and gives an overall factor 2π. One also notice that integrals over $\cos\theta_p$ of first and second part of (A.15) are equal. I obtain

$$\sigma = -\frac{1}{3\cdot 2^{15}\pi^9 s}(\frac{\alpha}{\pi})^2 \int \left[|M_B|^2 dcos\theta_q d\phi_q\right] dM_Q^2 \frac{dM_q^2}{M_q^2} 2\pi \sqrt{1-\frac{4\mu^2}{M_q^2}}\left(1+\frac{2\mu^2}{M_q^2}\right)\sqrt{1-\frac{4m^2}{M_Q^2}}\times$$
$$\times \ \lambda^{\frac{1}{2}}(s,M_Q^2,M_q^2)\int\limits_1^{-1} dcos\theta_p \left[\frac{8m^2}{\left(\frac{s-M_Q^2-M_q^2}{2} - \sqrt{\frac{M_Q^2}{4}-m^2}\frac{\lambda^{\frac{1}{2}}(s,M_Q^2,M_q^2)}{M_Q}\cos\theta_p\right)^2} - \right.$$
$$\left. - \ 2\frac{2M_Q^2-4m^2}{\frac{(s-M_Q^2-M_q^2)^2}{4} - \left(\frac{M_Q^2}{4}-m^2\right)\frac{\lambda(s,M_Q^2,M_q^2)}{M_Q^2}\cos^2\theta_p}\right]. \quad (A.20)$$

Now I need to integrate over $\cos\theta_p$. The following formulas are helpful

$$\int\limits_{-1}^{1} \frac{dx}{(A-Bx)^2} = \frac{2}{A^2-B^2}$$

and

$$\int\limits_{-1}^{1} \frac{dx}{A^2-B^2x^2} = -\frac{1}{AB}\ln\frac{A-B}{A+B}.$$

With help of these, I get:

$$\begin{aligned}
\sigma &= -\frac{1}{3\cdot 2^{15}\pi^9 s}(\frac{\alpha}{\pi})^2 \int \left[|M_B|^2 dcos\theta_q d\phi_q\right] dM_Q^2 \frac{dM_q^2}{M_q^2} 2\pi \sqrt{1-\frac{4\mu^2}{M_q^2}}\left(1+\frac{2\mu^2}{M_q^2}\right)\sqrt{1-\frac{4m^2}{M_Q^2}}\times \\
&\times \lambda^{\frac{1}{2}}(s,M_Q^2,M_q^2)\left[\frac{16m^2}{\frac{(s-M_Q^2-M_q^2)^2}{4}-\left(\frac{M_Q^2}{4}-m^2\right)\frac{\lambda(s,M_Q^2,M_q^2)}{M_Q^2}}+\right. \\
&+ \left. 2\frac{2M_Q^2-4m^2}{\frac{s-M_Q^2-M_q^2}{2}\sqrt{\frac{M_Q^2}{4}-m^2}\frac{\lambda^{\frac{1}{2}}(s,M_Q^2,M_q^2)}{M_Q}}\ln\frac{\frac{s-M_Q^2-M_q^2}{2}-\sqrt{\frac{M_Q^2}{4}-m^2}\frac{\lambda^{\frac{1}{2}}(s,M_Q^2,M_q^2)}{M_Q}}{\frac{s-M_Q^2-M_q^2}{2}+\sqrt{\frac{M_Q^2}{4}-m^2}\frac{\lambda^{\frac{1}{2}}(s,M_Q^2,M_q^2)}{M_Q}}\right] \qquad \text{(A.21)}
\end{aligned}$$

Some ordering of terms gives

$$\begin{aligned}
\sigma &= -\frac{1}{3\cdot 2^{10}\pi^8 s}(\frac{\alpha}{\pi})^2 \int \left[|M_B|^2 dcos\theta_q d\phi_q\right] dM_Q^2 \frac{dM_q^2}{M_q^2} \sqrt{1-\frac{4\mu^2}{M_q^2}}\left(1+\frac{2\mu^2}{M_q^2}\right)\sqrt{1-\frac{4m^2}{M_Q^2}}\times \\
&\times \lambda^{\frac{1}{2}}(s,M_Q^2,M_q^2)\left[\frac{m^2}{M_q^2M_Q^2+\frac{m^2}{M_Q^2}\lambda(s,M_Q^2,M_q^2)}+\right. \\
&+ \left. \frac{M_Q^2-2m^2}{(s-M_Q^2-M_q^2)\sqrt{1-\frac{4m^2}{M_Q^2}}\lambda^{\frac{1}{2}}(s,M_Q^2,M_q^2)}\ln\frac{s-M_Q^2-M_q^2-\sqrt{1-\frac{4m^2}{M_Q^2}}\lambda^{\frac{1}{2}}(s,M_Q^2,M_q^2)}{s-M_Q^2-M_q^2+\sqrt{1-\frac{4m^2}{M_Q^2}}\lambda^{\frac{1}{2}}(s,M_Q^2,M_q^2)}\right], \qquad \text{(A.22)}
\end{aligned}$$

or with explicit expression of Born separated (two body phase space is taken from formula (36) of Ref. [46]):

$$\begin{aligned}
\sigma &= \frac{1}{(2\pi)^6}\int\left[\frac{1}{(2\pi)^2}\cdot\frac{\lambda^{\frac{1}{2}}(1,\frac{m^2}{s},\frac{m^2}{s})}{8}|M_B|^2 dcos\theta_q d\phi_q\right]\times\ \lambda^{-\frac{1}{2}}(1,\frac{m^2}{s},\frac{m^2}{s}) \\
&\times \frac{(-2)}{3s}(\frac{\alpha}{\pi})^2\int dM_Q^2\frac{dM_q^2}{M_q^2}\sqrt{1-\frac{4\mu^2}{M_q^2}}\left(1+\frac{2\mu^2}{M_q^2}\right)\times\left[\frac{m^2\sqrt{1-\frac{4m^2}{M_Q^2}}\lambda^{\frac{1}{2}}(s,M_Q^2,M_q^2)}{M_q^2M_Q^2+\frac{m^2}{M_Q^2}\lambda(s,M_Q^2,M_q^2)}\right. \\
&+ \left.\frac{M_Q^2-2m^2}{s-M_q^2-M_Q^2}\ln\frac{s-M_q^2-M_Q^2-\sqrt{1-\frac{4m^2}{M_Q^2}}\lambda^{\frac{1}{2}}(s,M_Q^2,M_q^2)}{s-M_q^2-M_Q^2+\sqrt{1-\frac{4m^2}{M_Q^2}}\lambda^{\frac{1}{2}}(s,M_Q^2,M_q^2)}\right]. \qquad \text{(A.23)}
\end{aligned}$$

A.4 Result

From (A.23) I obtain analog of formula (5) of Ref. [13]:

$$P_{pair} = -\frac{2}{3s}(\frac{\alpha}{\pi})^2\int dM_Q^2\frac{dM_q^2}{M_q^2}\sqrt{1-\frac{4\mu^2}{M_q^2}}\left(1+\frac{2\mu^2}{M_q^2}\right)\left(\frac{m^2\sqrt{1-\frac{4m^2}{M_Q^2}}\lambda^{\frac{1}{2}}(s,M_Q^2,M_q^2)}{M_q^2M_Q^2+\frac{m^2}{M_Q^2}\lambda(s,M_Q^2,M_q^2)}+\right.$$

```
WeakSingleBoson:ffbar2gmZ = on
23:onMode = off
23:onIfAny = 11
23:mMin    = 10.0
23:mMax    = 200.0
HadronLevel:Hadronize = off
SpaceShower:QEDshowerByL = off
SpaceShower:QEDshowerByQ = off
PartonLevel:ISR = off
PartonLevel:FSR = off
Beams:idA =   2212
Beams:idB =   2212
Beams:eCM =  14000.0
```

a) $pp \to Z \to e^+e^-(e^+e^-, \mu^+\mu^-)$

```
WeakSingleBoson:ffbar2gmZ = on
23:onMode = off
23:onIfAny = 13
23:mMin    = 10.0
23:mMax    = 200.0
HadronLevel:Hadronize = off
SpaceShower:QEDshowerByL = off
SpaceShower:QEDshowerByQ = off
PartonLevel:ISR = off
PartonLevel:FSR = off
Beams:idA =   2212
Beams:idB =   2212
Beams:eCM =  14000.0
```

b) $pp \to Z \to \mu^+\mu^-(e^+e^-, \mu^+\mu^-)$

Table A.1: Initialization parameters for PYTHIA.

$$+ \quad \frac{M_Q^2 - 2m^2}{s - M_q^2 - M_Q^2} \ln \frac{s - M_q^2 - M_Q^2 - \sqrt{1 - \frac{4m^2}{M_Q^2}}\lambda^{\frac{1}{2}}(s, M_Q^2, M_q^2)}{s - M_q^2 - M_Q^2 + \sqrt{1 - \frac{4m^2}{M_Q^2}}\lambda^{\frac{1}{2}}(s, M_Q^2, M_q^2)}\Bigg) \tag{A.24}$$

Note that the factor $\frac{1}{(2\pi)^6}$ had to be dropped out to avoid double counting. This factor of phase space parametrization was already incorporated into the formula (A.6).

In order to make comparison with an older calculations, I recall formula (5) of Ref. [13]; case of $a = 0$, which is exact for the emission of extra lepton pair from initial state.

$$\begin{aligned}\widetilde{B_f} &= -\frac{2}{3s}(\frac{\alpha}{\pi})^2 \int dM_Q^2 \frac{dM_q^2}{M_q^2} \sqrt{1 - \frac{4\mu^2}{M_q^2}} \left(1 + \frac{2\mu^2}{M_q^2}\right) \left(\frac{m^2 \lambda^{\frac{1}{2}}(s, M_Q^2, M_q^2)}{M_q^2 s + \frac{m^2}{s}\lambda(s, M_Q^2, M_q^2)} + \right. \\ &+ \left. \frac{s - 2m^2}{\sqrt{1 - \frac{4m^2}{s}}(s + M_q^2 - M_Q^2)} \ln \frac{s + M_q^2 - M_Q^2 - \sqrt{1 - \frac{4m^2}{s}}\lambda^{\frac{1}{2}}(s, M_Q^2, M_q^2)}{s + M_q^2 - M_Q^2 + \sqrt{1 - \frac{4m^2}{s}}\lambda^{\frac{1}{2}}(s, M_Q^2, M_q^2)} \right).\end{aligned} \tag{A.25}$$

I have now collected all formulae necessary for numerical results.

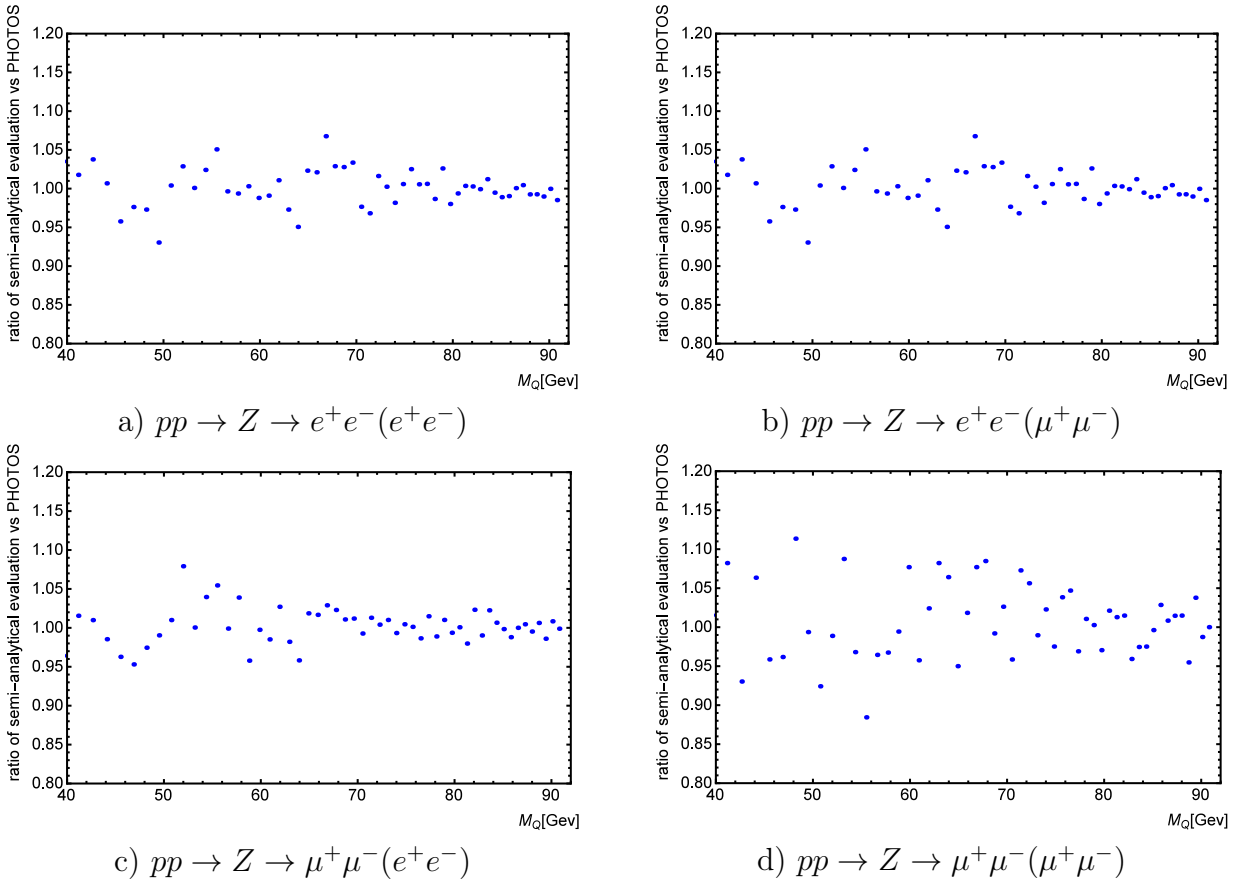

a) $pp \to Z \to e^+e^-(e^+e^-)$

b) $pp \to Z \to e^+e^-(\mu^+\mu^-)$

c) $pp \to Z \to \mu^+\mu^-(e^+e^-)$

d) $pp \to Z \to \mu^+\mu^-(\mu^+\mu^-)$

Figure A.1: Number of events from `PYTHIA` multiplied by a factor resulting from formula (A.24) divided by number of events from `PYTHIA`×`PHOTOS`. For these particular plots there is difference in `PYTHIA` initialization parameters; energy range of leptonic system is limited to $[91.183, 91.252]$ GeV window.

```
WeakSingleBoson:ffbar2gmZ = on
23:onMode  = off
23:onIfAny = 11
23:mWidth  = 0
23:m0      = 91.187
23:mMin    = 91.17
23:mMax    = 91.2
HadronLevel:Hadronize = off
SpaceShower:QEDshowerByL = off
SpaceShower:QEDshowerByQ = off
PartonLevel:ISR = off
PartonLevel:FSR = off
Beams:idA =   11
Beams:idB =  -11
Beams:eCM =  91.187
```

a) $e^+e^- \to Z \to e^+e^-(e^+e^-, \mu^+\mu^-)$

```
WeakSingleBoson:ffbar2gmZ = on
23:onMode = off
23:onIfAny = 13
23:mWidth  = 0
23:m0      = 91.187
23:mMin    = 91.17
23:mMax    = 91.2
HadronLevel:Hadronize = off
SpaceShower:QEDshowerByL = off
SpaceShower:QEDshowerByQ = off
PartonLevel:ISR = off
PartonLevel:FSR = off
Beams:idA =   11
Beams:idB =  -11
Beams:eCM =  91.187
```

b) $e^+e^- \to Z \to \mu^+\mu^-(e^+e^-, \mu^+\mu^-)$

Table B.1: Initialization parameters for PYTHIA.

B Plots

B.1 KORALW-PHOTOS comparison framework, plots

Fig. B.1 presents spectra of squared mass of $\mu^+e^+e^-$ three ($M^2_{\mu^+e^+e^-}$) and of $\mu^-e^+e^-$ three ($M^2_{\mu^-e^+e^-}$) and ratios of PHOTOS generated spectra to the corresponding ones by KORALW. Sharp peaks of the number of $\mu^+e^+e^-$ three correspond to both small values of invariant mass squared $M^2_{\mu^+e^+e^-} \sim 0$ and values of invariant mass squared close to beam CMS energy squared $M^2_{\mu^+e^+e^-} \sim M^2_Z$; agreement between KORALW generated spectrum and PHOTOS generated spectrum is the best for the most populated bins, including these maximums. Minimum of the number of $\mu^+e^+e^-$ three corresponds to square of invariant mass of the three lying between $0.25 \cdot M^2_Z$ and $0.4 \cdot M^2_Z$; difference between KORALW generated spectrum and PHOTOS generated spectrum is highest at this minimum and is up to factor of 1.4 for some bins. Spectrum of $\mu^+e^+e^-$ three is indistinguishable from spectrum of $\mu^-e^+e^-$ three and possesses the same characteristic features.

Fig. B.2 presents spectra of squared mass of $e^+\mu^+\mu^-$ three ($M^2_{e^+\mu^+\mu^-}$) and of $e^-\mu^+\mu^-$ three ($M^2_{e^-\mu^+\mu^-}$) and ratios of PHOTOS generated spectra to the corresponding ones by KORALW. Sharp peaks of the number of $e^+\mu^+\mu^-$ three correspond to both small values of invariant mass squared $M^2_{e^+\mu^+\mu^-} \sim 0$ and values of invariant mass squared close to beam CMS energy squared $M^2_{e^+\mu^+\mu^-} \sim M^2_Z$; agreement between KORALW generated spectrum and PHOTOS generated spectrum is the best for the most populated bins, including these maximums. Minimum of the number of $e^+\mu^+\mu^-$ three corresponds to square of invariant mass of the three lying between $0.55 \cdot M^2_Z$ and $0.7 \cdot M^2_Z$; difference between KORALW generated spectrum and PHOTOS generated spectrum is highest at this minimum and is up to factor of 1.5 for some bins. Spectrum of $e^+\mu^+\mu^-$ three is indistinguishable from spectrum of $e^-\mu^+\mu^-$ three and possesses the same characteristic features.

Figs. B.3-B.4 present spectra of squared mass of $e^+\mu^+$ pair ($M^2_{e^+\mu^+}$), of $e^-\mu^-$ pair

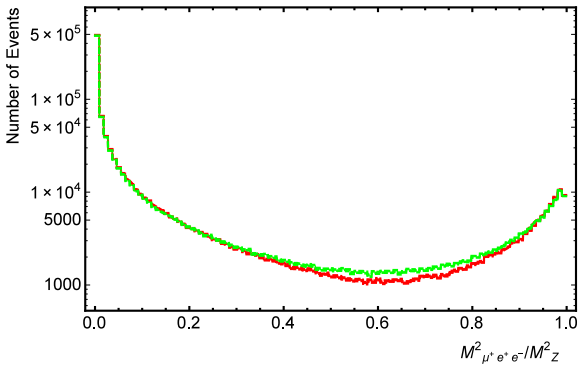

a) Normalized to M_Z^2 spectrum of $\mu^+e^+e^-$ mass squared.

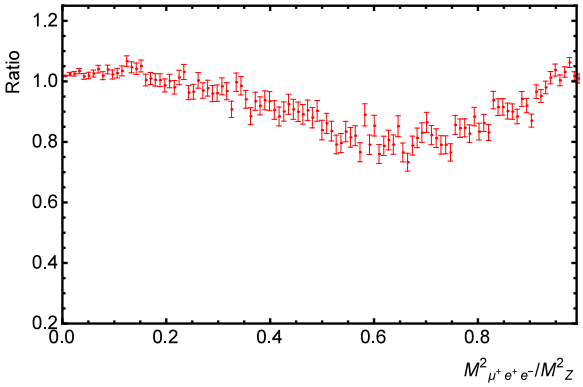

b) Normalized to M_Z^2 ratio of PHOTOS generated spectrum to the one generated by KORALW.

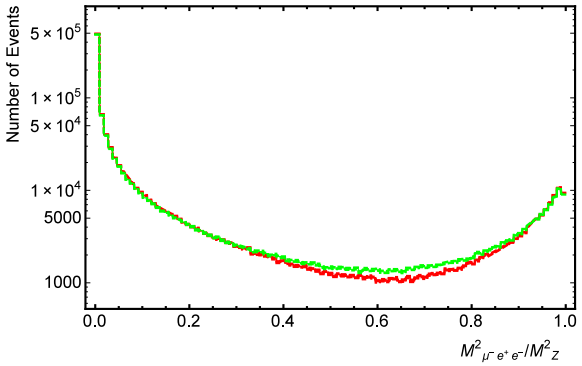

c) Normalized to M_Z^2 spectrum of $\mu^-e^+e^-$ mass squared.

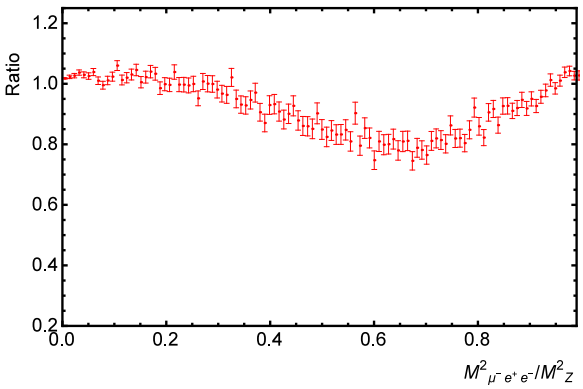

d) Normalized to M_Z^2 ratio of PHOTOS generated spectrum to the one generated by KORALW.

Figure B.1: Three particles invariant mass spectra in the channel $Z \to \mu^+\mu^-e^+e^-$. Spectra generated by PHOTOS (red (dark grey) error bars) are obtained from samples of equal number of $Z \to e^+e^-$ and $Z \to \mu^+\mu^-$ PYTHIA generated decays. They are compared with spectra by KORALW (green (light grey) error bars) where four fermion final state matrix elements are used.

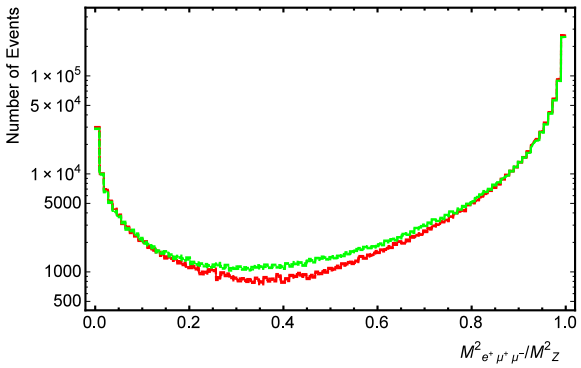

a) Normalized to M_Z^2 spectrum of $e^+\mu^+\mu^-$ mass squared.

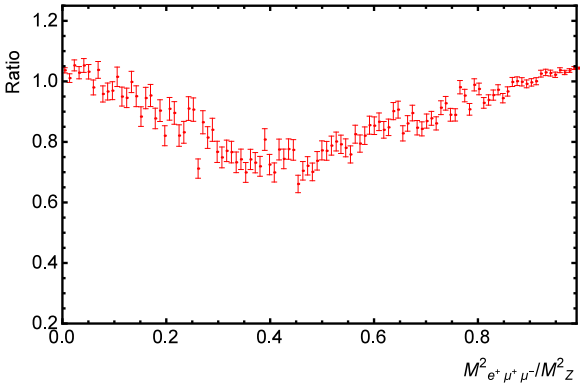

b) Normalized to M_Z^2 ratios of PHOTOS generated spectrums to the one generated by KORALW.

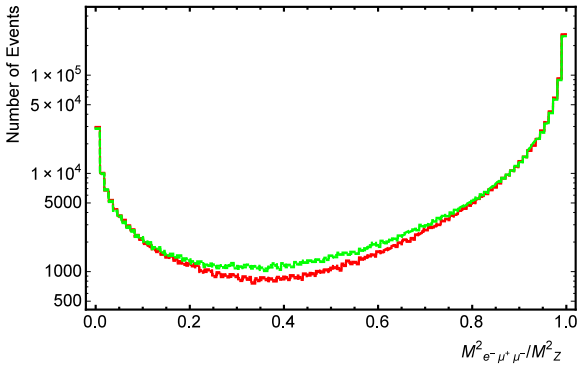

c) Normalized to M_Z^2 spectrum of $e^-\mu^+\mu^-$ mass squared.

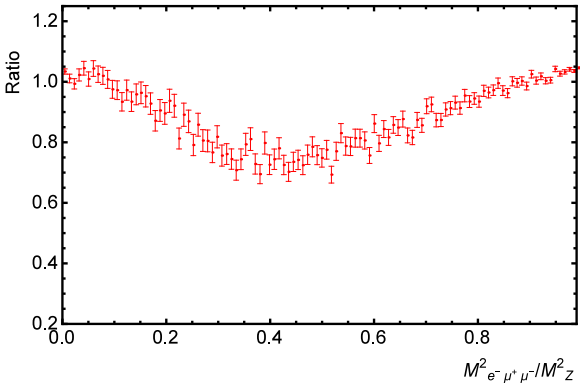

d) Normalized to M_Z^2 ratios of PHOTOS generated spectrums to the one generated by KORALW.

Figure B.2: Three particles invariant mass spectra in the channel $Z \to \mu^+\mu^- e^+ e^-$. Spectra generated by PHOTOS (red (dark grey) error bars) are obtained from samples of equal number of $Z \to e^+e^-$ and $Z \to \mu^+\mu^-$ PYTHIA generated decays. They are compared with spectra by KORALW (green (light grey) error bars) where four fermion final state matrix elements are used.

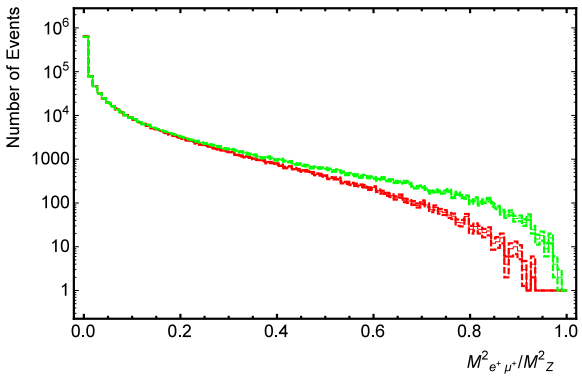

a) Normalized to M_Z^2 spectrum of $e^+\mu^+$ mass squared.

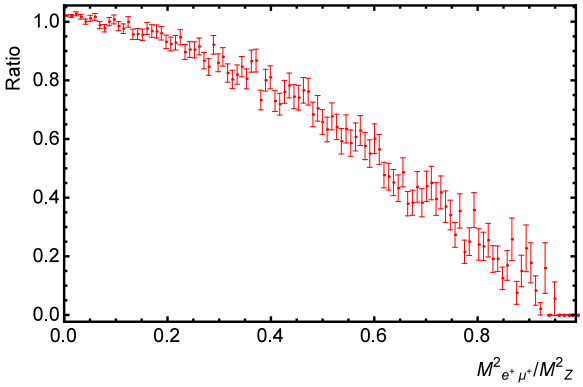

b) Normalized to M_Z^2 ratios of PHOTOS generated spectrums to the one generated by KORALW.

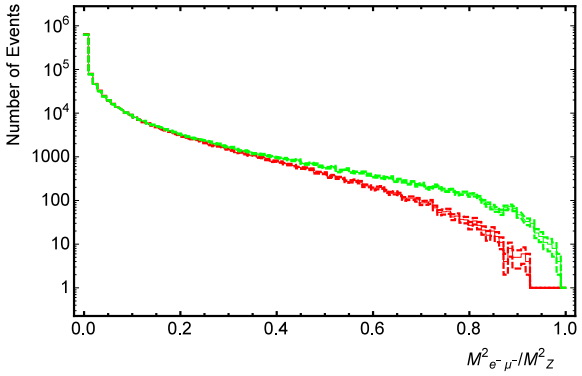

c) Normalized to M_Z^2 spectrum of $e^-\mu^-$ mass squared.

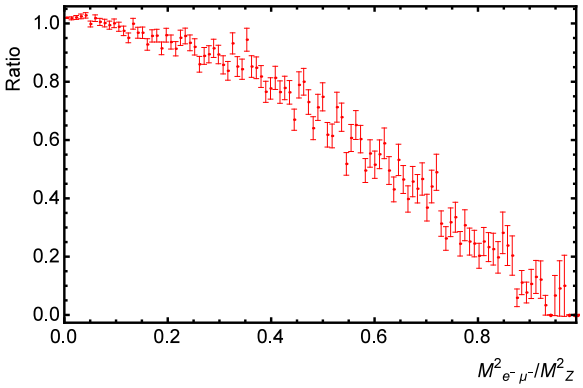

d) Normalized to M_Z^2 ratios of PHOTOS generated spectrums to the one generated by KORALW.

Figure B.3: Pair invariant mass spectra in the channel $Z \to \mu^+\mu^- e^+ e^-$. Spectra generated by PHOTOS (red (dark grey) error bars) are obtained from samples of equal number of $Z \to e^+e^-$ and $Z \to \mu^+\mu^-$ PYTHIA generated decays. They are compared with spectra by KORALW (green (light grey) error bars) where four fermion final state matrix elements are used.

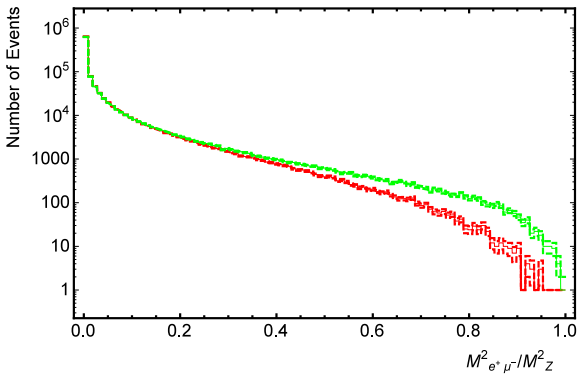

a) Normalized to M_Z^2 spectrum of $e^+\mu^-$ mass squared.

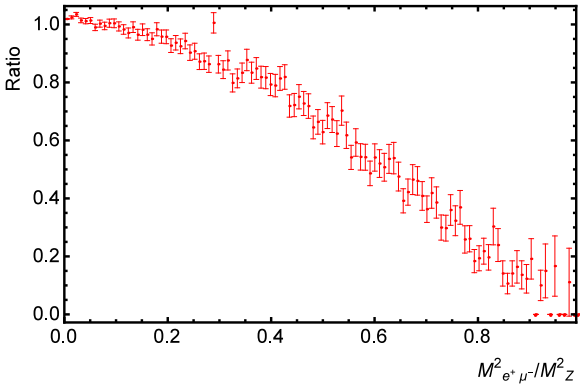

b) Normalized to M_Z^2 ratios of PHOTOS generated spectrums to the one generated by KORALW.

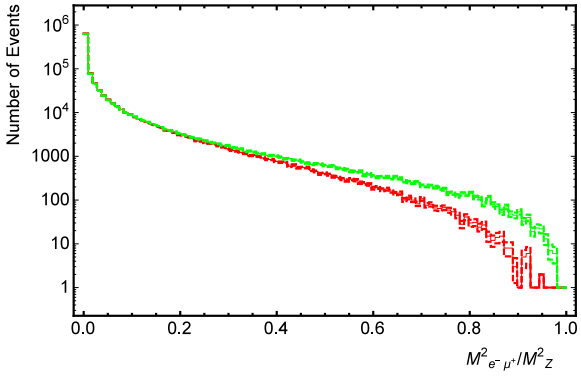

c) Normalized to M_Z^2 spectrum of $e^-\mu^+$ mass squared.

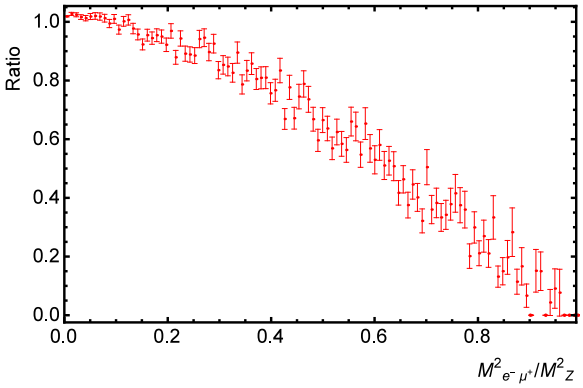

d) Normalized to M_Z^2 ratios of PHOTOS generated spectrums to the one generated by KORALW.

Figure B.4: Pair invariant mass spectra in the channel $Z \to \mu^+\mu^- e^+ e^-$. Spectra generated by PHOTOS (red (dark grey) error bars) are obtained from samples of equal number of $Z \to e^+e^-$ and $Z \to \mu^+\mu^-$ PYTHIA generated decays. They are compared with spectra by KORALW (green (light grey) error bars) where four fermion final state matrix elements are used.

($M^2_{e^-\mu^-}$), of $e^+\mu^-$ pair ($M^2_{e^+\mu^-}$), of $e^-\mu^+$ pair ($M^2_{e^-\mu^+}$) and ratios of PHOTOS generated spectra to the corresponding ones by KORALW. Sharp peak of the number of $e^+\mu^+$ pairs corresponds to small values of invariant mass squared $M^2_{e^+\mu^+} \sim 0$; agreement between KORALW generated spectrum and PHOTOS generated spectrum is the best for the most populated bins, including this maximum. The number of $e^+\mu^+$ pairs decreases not slower than exponentially with $M^2_{e^+\mu^+}$ increase; its minimum is at $M^2_{e^+\mu^+} \sim M^2_Z$. Spectrum of $e^-\mu^-$ pair, spectrum of $e^+\mu^-$ pair and spectrum of $e^-\mu^+$ pair are indistinguishable from spectrum of $e^+\mu^+$ pair and possess the same characteristic features, no charge asymmetry is observed.

Fig. B.5 presents summated spectra of squared mass of $\mu^+\mu^-$ pair ($M^2_{\mu^+\mu^-}$), of squared mass of $\mu^+\mu^+\mu^-$ three ($\mu^+\mu^+\mu^-$), of squared mass of $\mu^+\mu^-\mu^-$ three ($M^2_{\mu^+\mu^-\mu^-}$) and ratios of PHOTOS generated spectra to the corresponding ones by KORALW. For event selection during the tests [41] MC-TESTER [16] has been used. For each four particle event generated by KORALW MC-TESTER has to analyze this event, has to form all possible two and three particle groups out of this event and has to count this groups properly. In case of $e^+e^-\mu^+\mu^-$ channel all particles are different and grouping of them is a trivial task. In case of $\mu^+\mu^-\mu^+\mu^-$ there are two possible ways of defining two $\mu^+\mu^-$ pairs out of $\mu^+\mu^-\mu^+\mu^-$ event, so existing ".root" files [43] by KORALW contain missselected events. It is a way around to use KORALW generated data in the $\mu^+\mu^-\mu^+\mu^-$ channel for comparison: one has to add together all $\mu^+\mu^-$ spectra both in the KORALW and PHOTOS data and then to compare resulting spectra. Such summation is necessary for three particle groups $\mu^+\mu^+\mu^-$, $\mu^+\mu^-\mu^-$ too. All further comparisons with KORALW data in the $\mu^+\mu^-\mu^+\mu^-$ channel are for summated $\mu^+\mu^-$, $\mu^+\mu^+\mu^-$, $\mu^+\mu^-\mu^-$ spectra. Summation averages discrepancy between summated spectra by KORALW and by PHOTOS and thus complicates analysis of corresponding matrix element by PHOTOS. In the following I use these summated spectra as additional reference points ($\mu^+\mu^-\mu^+\mu^-$ channel) and I do not involve these spectra in precision tests. Sharp peak of the number of $\mu^+\mu^-$ pairs corresponds to small values of invariant mass squared $M^2_{\mu^+\mu^-} \sim 0$; agreement between KORALW generated spectrum and PHOTOS generated spectrum is the best for the most populated bins near this peak. Local maximum of the number of $\mu^+\mu^-$ pairs corresponds to values of invariant mass squared close to beam CMS energy squared $M^2_{\mu^+\mu^-} \sim M^2_Z$; comparing to KORALW data, PHOTOS overproduces events near this maximum. Minimum of the number of $\mu^+\mu^-$ pairs corresponds to square of invariant mass of the pair lying between $0.35 \cdot M^2_Z$ and $0.5 \cdot M^2_Z$; difference between KORALW generated spectrum and PHOTOS generated spectrum is highest at this minimum and is up to factor of 1.2 for some bins. Sharp peaks of the number of $\mu^+\mu^+\mu^-$ three correspond to both small values of invariant mass squared $M^2_{\mu^+\mu^+\mu^-} \sim 0$ and values of invariant mass squared close to beam CMS energy squared $M^2_{\mu^+\mu^+\mu^-} \sim M^2_Z$; agreement between KORALW generated spectrum and PHOTOS generated spectrum is the best for the most populated bins, including these maximums. Minimum of the number of $\mu^+\mu^+\mu^-$ three corresponds to square of invariant mass of the three lying between $0.45 \cdot M^2_Z$ and $0.6 \cdot M^2_Z$; difference between KORALW generated spectrum and PHOTOS generated spectrum is highest at this minimum and is up to factor of 1.25 for some bins. Spectrum of $\mu^+\mu^-\mu^-$ three is indistinguishable from spectrum of $\mu^+\mu^-\mu^-$ three and possesses the same characteristic features.

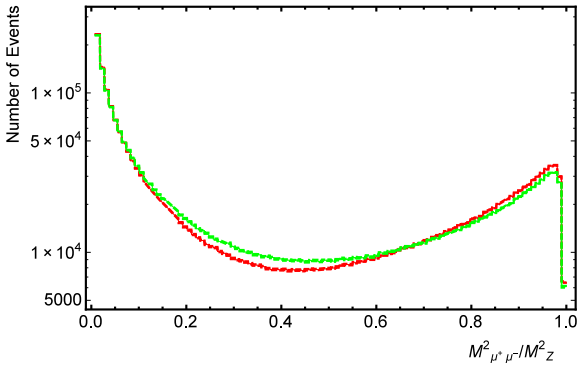

a) Normalized to M_Z^2 sum of spectra of muon pair mass squared.

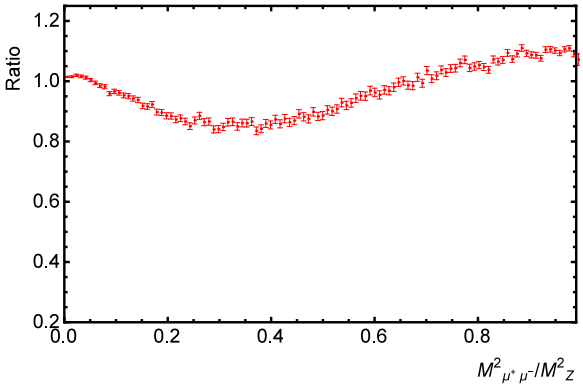

b) Ratio of PHOTOS generated spectrum to the one generated by KORALW.

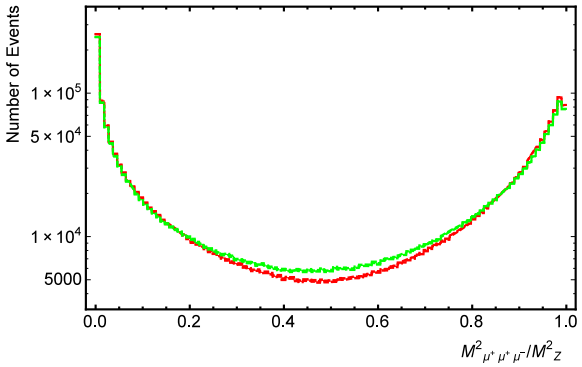

c) Normalized to M_Z^2 sum of spectra of $\mu^+\mu^+\mu^-$ mass squared.

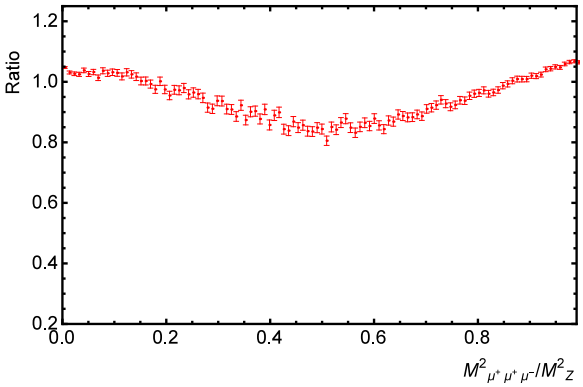

d) Ratio of PHOTOS generated spectrum to the one generated by KORALW.

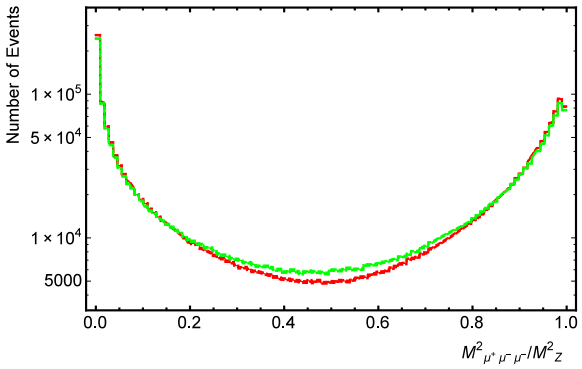

e) Normalized to M_Z^2 sum of spectra of $\mu^+\mu^+\mu^-$ mass squared.

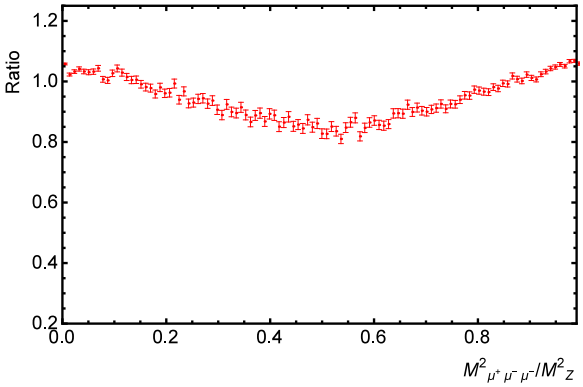

f) Ratio of PHOTOS generated spectrum to the one generated by KORALW.

Figure B.5: Sum of two and sum of three particles invariant mass spectra in the channel $Z \to \mu^+\mu^-\mu^+\mu^-$. Spectra generated by PHOTOS (red (dark grey) error bars) are obtained from sample of $Z \to \mu^+\mu^-$ PYTHIA generated decays. They are compared with spectra by KORALW (green (light grey) error bars) where four fermion final state matrix elements are used.

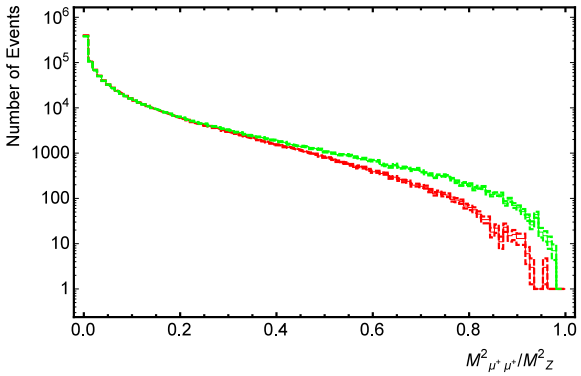

a) Normalized to M_Z^2 sum of spectra of $\mu^+\mu^+$ mass squared.

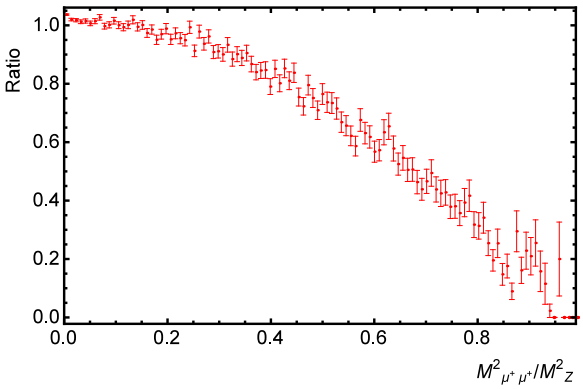

b) Normalized to M_Z^2 ratio of PHOTOS generated spectrum to the one generated by KORALW.

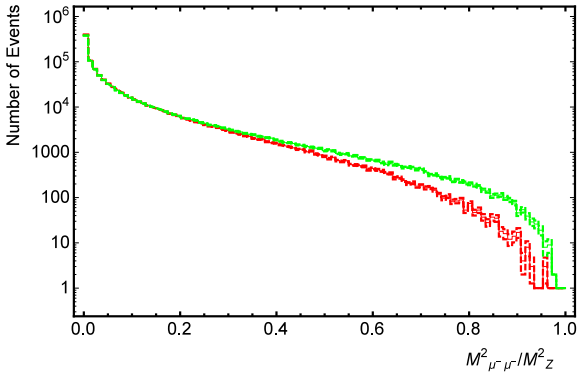

c) Normalized to M_Z^2 sum of spectra of $\mu^-\mu^-$ mass squared.

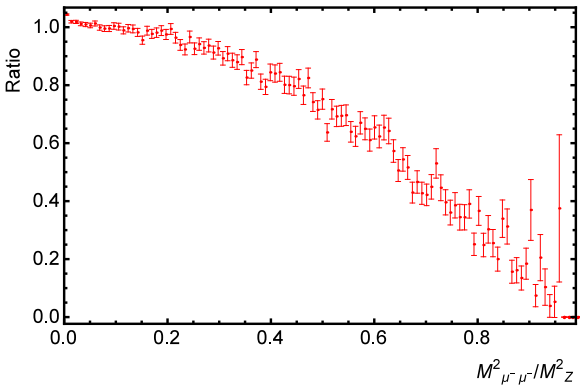

d) Normalized to M_Z^2 ratio of PHOTOS generated spectrum to the one generated by KORALW.

Figure B.6: Pair invariant mass spectra in the channel $Z \to \mu^+\mu^-\mu^+\mu^-$. Spectra generated by PHOTOS [11] (red (dark grey) error bars) are obtained from sample of $Z \to \mu^+\mu^-$ PYTHIA generated decays. They are compared with spectra by KORALW (green (light grey) error bars) where four fermion final state matrix elements are used.

Fig. B.6 presents spectra of squared mass of $\mu^+\mu^+$ pair ($M^2_{\mu^+\mu^+}$), of $\mu^-\mu^-$ pair ($M^2_{\mu^-\mu^-}$) and ratios of PHOTOS generated spectra to the corresponding ones by KORALW. Sharp peak of the number of $\mu^+\mu^+$ pairs corresponds to small values of invariant mass squared $M^2_{\mu^+\mu^+} \sim 0$; agreement between KORALW generated spectrum and PHOTOS generated spectrum is the best for the most populated bins, including this maximum. The number of $\mu^+\mu^+$ pairs decreases not slower than exponentially with $M^2_{\mu^+\mu^+}$ increase; its minimum is at $M^2_{\mu^+\mu^+} \sim M^2_Z$. Spectrum of $\mu^-\mu^-$ pair is indistinguishable from spectrum of $\mu^-\mu^-$ pair and possess the same characteristic features. On the one hand, spectra of $\mu^+\mu^+$ pair and of $\mu^-\mu^-$ pair are least attractive observable in the $\mu^+\mu^-\mu^+\mu^-$ channel for precision tests: hardest emissions are of the most interest and hardest emissions correspond to the most fluctuating and the least populated bins. On the other hand, spectra of $\mu^+\mu^+$ pair and of $\mu^-\mu^-$ pair are not summated leading to clear correspondence between data and matrix element. I keep using these KORALW generated spectra for crosschecks in the $\mu^+\mu^-\mu^+\mu^-$ channel.

B.2 PHOTOS with full matrix element, plots

Fig. B.7 present spectra of squared mass of $e^+\mu^+$ pair ($M^2_{e^+\mu^+}$), of $e^-\mu^+$ pair ($M^2_{e^-\mu^+}$) and ratios of PHOTOS generated spectra to the corresponding ones by KORALW. Agreement between PHOTOS with matrix element (14) and KORALW is good. This agreement is remarkable since it covers difference of 6 powers of magnitude in numbers of events of the presented spectra. Maximum deviation of PHOTOS generated spectra from etalon one is 2.5 times and is for the one of the least populated bins which contains ~ 10 events only. For the most populated bins (number of events between $6 \cdot 10^5$ and 300) this deviation is less than 20%. Spectrum of $e^+\mu^+$ pair is indistinguishable from spectrum of $e^-\mu^+$ pair and possess the same characteristic features, no charge asymmetry is observed. Therefore, spectrum of $e^-\mu^-$ pair and spectrum of $e^+\mu^+$ pair are not presented at all.

Fig. B.8 presents ratios of PHOTOS generated summated spectra of squared mass of $\mu^+\mu^-$ pair ($M^2_{\mu^+\mu^-}$) and of squared mass of $\mu^+\mu^+\mu^-$ three ($\mu^+\mu^+\mu^-$), spectra of squared mass of $\mu^+\mu^+$ pair ($M^2_{\mu^+\mu^+}$), and of $\mu^-\mu^-$ pair ($M^2_{\mu^-\mu^-}$) to the corresponding one's by KORALW. Agreement between PHOTOS with matrix element (14) and KORALW is good. The most clear indicators are spectrum of $\mu^+\mu^+$ pair and spectrum of $\mu^-\mu^-$ pair since these spectra are not summated. $\mu^+\mu^+$ pair and $\mu^-\mu^-$ pair spectra posses characteristic features similar to the one's of $e^+\mu^+$ pair and $e^-\mu^+$ pair spectra (Fig. B.7).

While Figs. 9,B.1-B.6 present full list of spectra, it is not necessary to present all possible spectra during further tests. As it is noticed before, squared mass of e^+e^- pair ($M^2_{e^+e^-}$) and squared mass of $\mu^+\mu^-$ pair ($M^2_{\mu^+\mu^-}$) are experiment observables [1] and their spectra are of most interest. Approximations in matrix elements residual (16) should lead to improvements in terms of MC generation and should not lead significant distortions in particle spectra. e^+e^- pair and $\mu^+\mu^-$ pair spectra are not enough to cover description of four particle end state. Therefore, spectrum of squared mass of $\mu^+e^+e^-$ three ($M^2_{\mu^+e^+e^-}$) and spectrum of squared mass of $e^+\mu^+\mu^-$ three ($M^2_{e^+\mu^+\mu^-}$) are chosen to be presented during further tests. Matrix element (14) do not have resonances for invariant mass of

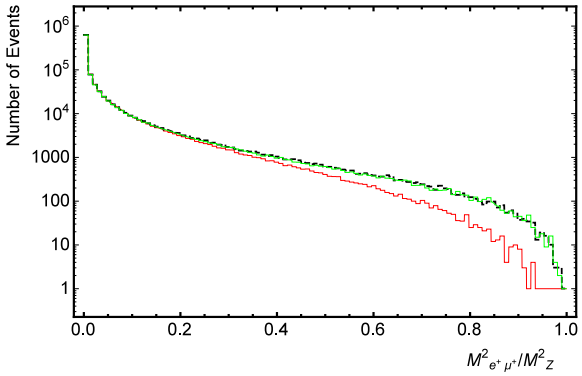

a) Normalized to M_Z^2 spectrum of $e^+\mu^+$ mass squared.

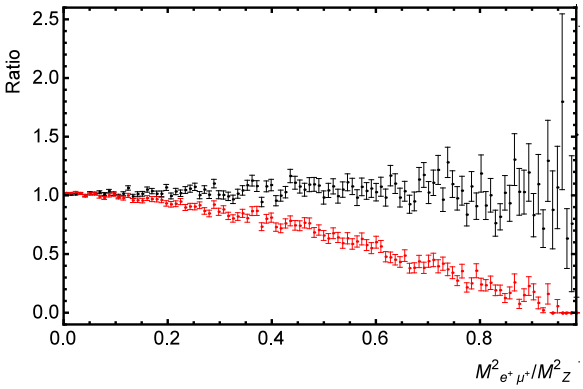

b) Normalized to M_Z^2 ratio of PHOTOS generated spectrum to the one generated by KORALW.

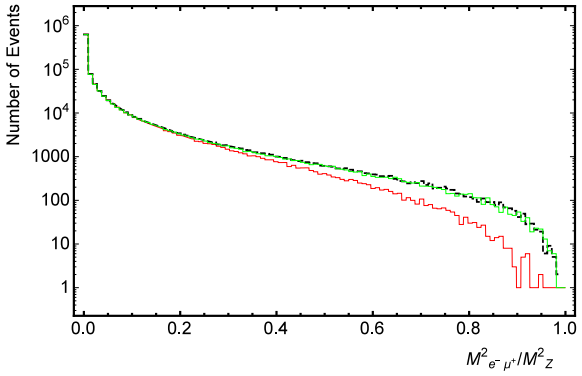

c) Normalized to M_Z^2 spectrum of $e^-\mu^+$ mass squared.

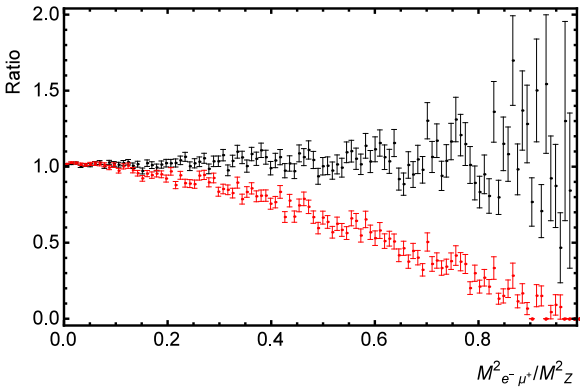

d) Normalized to M_Z^2 ratio of PHOTOS generated spectrum to the one generated by KORALW.

Figure B.7: PHOTOS generated spectra (of squared mass of $e^+\mu^+$ pair ($M^2_{e^+\mu^+}$), of $e^-\mu^+$ pair ($M^2_{e^-\mu^+}$)) in the $Z \to \mu^+\mu^-e^+e^-$ channel. Spectra generated by PHOTOS are obtained from samples of equal number of PYTHIA generated $Z \to e^+e^-$ and $Z \to \mu^+\mu^-$ decays. Red (dark grey) error bars represent spectra by unmodified PHOTOS [11]. Black error bars and black dashed line represent spectra by improved PHOTOS with matrix element (14). They are compared with spectra by KORALW (green (light grey) error bars) where four fermion final state matrix elements are used.

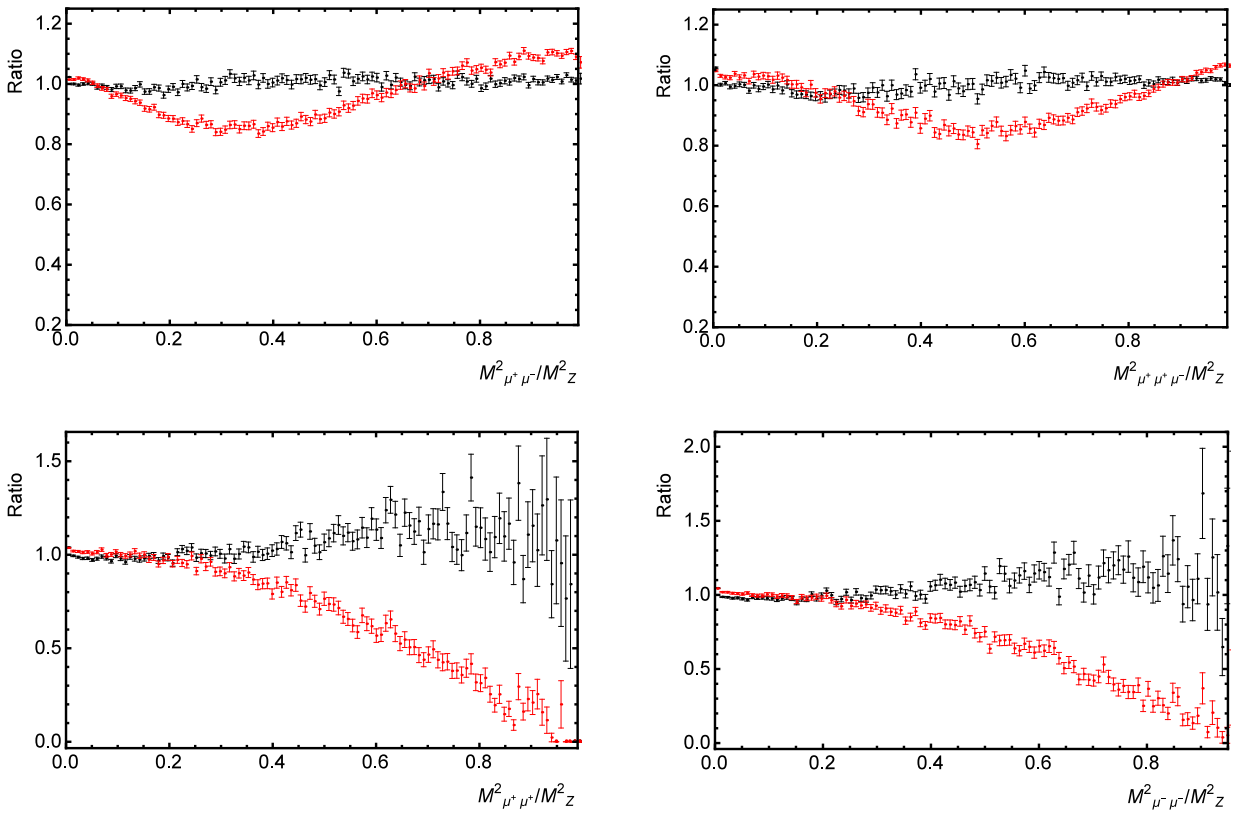

Figure B.8: Ratios of PHOTOS generated spectra (of squared mass of $\mu^+\mu^+\mu^-$ three ($M^2_{\mu^+\mu^+\mu^-}$), of $\mu^+\mu^+$ pair ($M^2_{\mu^+\mu^+}$), of $\mu^-\mu^-$ pair ($M^2_{\mu^-\mu^-}$) and sum of $\mu^+\mu^-$ pair ($M^2_{\mu^+\mu^-}$) spectra) in $Z \to \mu^+\mu^-\mu^+\mu^-$ channel to the corresponding one's by KORALW. Spectra generated by PHOTOS are obtained from sample of $Z \to \mu^+\mu^-$ PYTHIA generated decays. Red (dark grey) error bars represent spectra by unmodified PHOTOS [11]. Black error bars represent spectra by improved PHOTOS with matrix element (14) installed into it.

$e^+\mu^+$ pair, or $e^+\mu^-$ pair, or $e^-\mu^+$, or $e^-\mu^-$ pair going to zero. Additionally, spectra of squared mass of $e^+\mu^+$ pair ($M^2_{e^+\mu^+}$) and of $e^-\mu^+$ pair ($M^2_{e^-\mu^+}$) are noisy. Therefore, I avoid presenting these spectra. Considering $\mu^+\mu^-\mu^+\mu^-$ channel. Due to features of existing KORALW data for the $\mu^+\mu^-\mu^+\mu^-$ channel, all $\mu^+\mu^-$ pair spectra should be summed and all $\mu^+\mu^+\mu^-$ three spectra should be summed. On the other hand, $\mu^+\mu^+$ pair spectrum and $\mu^-\mu^-$ pair spectrum are remaining two not summed observables, making them valuable "reference point" for PHOTOS-KORALW tests in the $\mu^+\mu^-\mu^+\mu^-$ channel.

B.3 Fix for $\sum_{spins} |M_1 + M_2|^2_{soft}$ not being soft enough, plots

Figs. B.9, B.11, B.13 present data in $Z \to e^+e^-e^+e^-$ and $Z \to \mu^+\mu^-\mu^+\mu^-$ channels for beam CMS energies of $E_{CMS} = M_Z, 0.8\cdot M_Z, 0.6\cdot M_Z$ correspondingly. Figs. B.9, B.11, B.13 present ratios of PHOTOS generated spectra of squared mass of e^+e^- pair ($M^2_{e^+e^-}$), of $\mu^+\mu^-$ pair ($M^2_{\mu^+\mu^-}$), of squared mass of $e^+e^+e^-$ three ($M^2_{e^+e^+e^-}$) and of squared mass of $\mu^+\mu^+\mu^-$ three ($M^2_{\mu^+\mu^+\mu^-}$) to the corresponding one's by PHOTOS with matrix element (14). Agreement between PHOTOS with kernel F_{test1} (34) and PHOTOS with matrix element (14) is good. PHOTOS with kernel F_{test1} (34) tends to slightly overproduce $\mu^+\mu^-$ pairs in the least populated part of the spectrum (up to 16% not taking error into account) causing overproduction of $\mu^+\mu^-$ pairs (up to 6%) in the first bin. Numbers of e^+e^- pairs never deviate more than 7% from corresponding numbers of etalon spectra. Numbers of e^+e^- and $\mu^+\mu^-$ pairs with invariant mass close to beam CMS energy coincide with corresponding numbers of etalon spectra.

Figs. B.10, B.12 present data in $Z \to e^+e^-\mu^+\mu^-$ channel for beam CMS energies of $0.8\cdot M_Z$, $0.6\cdot M_Z$ correspondingly. Figs. B.10, B.12 present ratios of PHOTOS generated spectra of squared mass of e^+e^- pair ($M^2_{e^+e^-}$), of $\mu^+\mu^-$ pair ($M^2_{\mu^+\mu^-}$), of squared mass of $\mu^+e^+e^-$ three ($M^2_{\mu^+e^+e^-}$) and of squared mass of $e^+\mu^+\mu^-$ three ($M^2_{e^+\mu^+\mu^-}$) to the corresponding one's by PHOTOS with matrix element (14). Agreement between PHOTOS with kernel F_{test1} (34) and PHOTOS with matrix element (14) is good. PHOTOS with kernel F_{test1} (34) tends to slightly overproduce e^+e^- pairs in the least populated part of the spectrum (up to 15% not taking error into account) causing overproduction of $\mu^+\mu^-$ pairs (up to 7%) in the first bin. Numbers of $\mu^+\mu^-$ pairs never deviate more than 4% from corresponding numbers of etalon spectra. Numbers of e^+e^- and $\mu^+\mu^-$ pairs with invariant mass close to beam CMS energy coincide with corresponding numbers of etalon spectra.

Spectra by PHOTOS with kernel F_{test2} (37) are presented in Figs. B.9-B.13. Agreement between PHOTOS with kernel F_{test2} (37) and PHOTOS with matrix element (14) is good.

Spectra by PHOTOS with kernel F_{test3} (40) are presented in Figs. B.9-B.13.

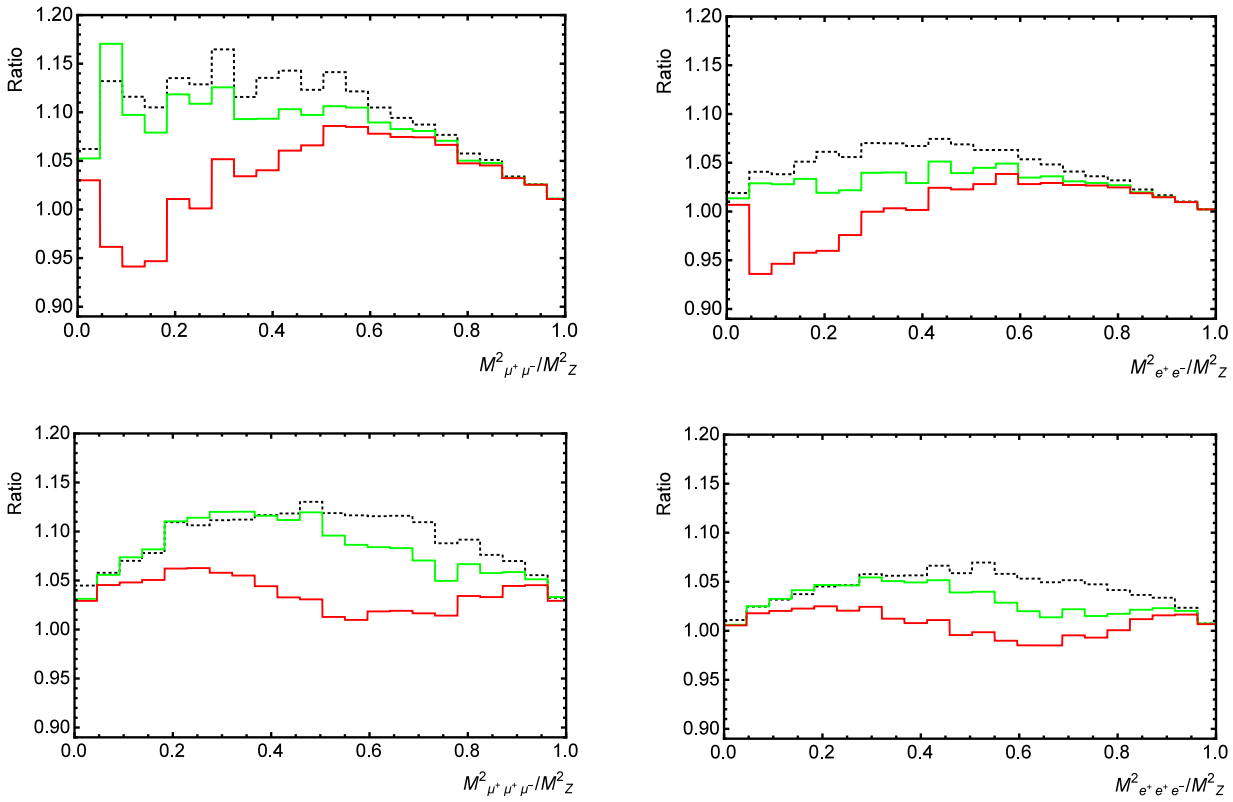

Figure B.9: Ratios of PHOTOS generated spectra (of squared mass of e^+e^- pair ($M^2_{e^+e^-}$), of $\mu^+\mu^-$ pair ($M^2_{\mu^+\mu^-}$), of squared mass of $\mu^+\mu^+\mu^-$ three ($M^2_{\mu^+\mu^+\mu^-}$) and of squared mass of $e^+e^+e^-$ three ($M^2_{e^+e^+e^-}$)) at CMS energy of $E_{CMS} = M_Z$ in $Z \to \mu^+\mu^-\mu^+\mu^-$ and $Z \to e^+e^-e^+e^-$ channels to the corresponding one's by improved PHOTOS with matrix element (14). Spectra generated by PHOTOS are obtained from samples of $Z \to e^+e^-$ and $Z \to \mu^+\mu^-$ PYTHIA generated decays. Black dotted line represents spectra by PHOTOS with kernel of extra pair emission given by the formula (34). Solid red line (solid dark grey in greyscale) represents spectra by PHOTOS with kernel of extra pair emission given by the formula (37). Green solid line (solid light grey in greyscale) represents spectra by PHOTOS with kernel of extra pair emission given by the formula (40).

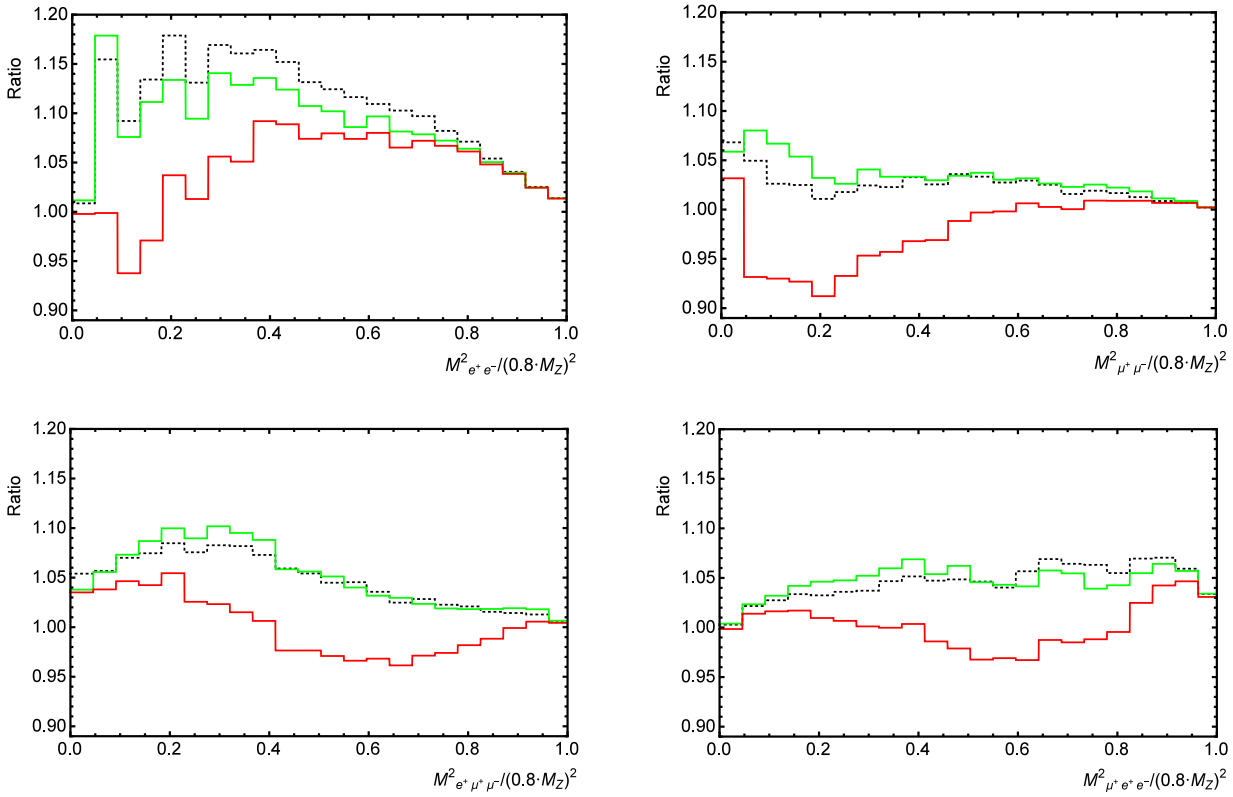

Figure B.10: Ratios of PHOTOS generated spectra (of squared mass of e^+e^- pair ($M^2_{e^+e^-}$), of $\mu^+\mu^-$ pair ($M^2_{\mu^+\mu^-}$), of squared mass of $\mu^+e^+e^-$ three ($M^2_{\mu^+e^+e^-}$) and of squared mass of $e^+\mu^+\mu^-$ three ($M^2_{e^+\mu^+\mu^-}$)) at CMS energy of $E_{CMS} = 0.8 \cdot M_Z$ in $Z \to e^+e^-\mu^+\mu^-$ channel to the corresponding one's by improved PHOTOS with matrix element (14). Spectra generated by PHOTOS are obtained from samples of equal number of $Z \to e^+e^-$ and $Z \to \mu^+\mu^-$ PYTHIA generated decays. Black dotted line represents spectra by PHOTOS with kernel of extra pair emission given by the formula (34). Solid red line (solid dark grey in greyscale) represents spectra by PHOTOS with kernel of extra pair emission given by the formula (37). Green solid line (solid light grey in greyscale) represents spectra by PHOTOS with kernel of extra pair emission given by the formula (40).

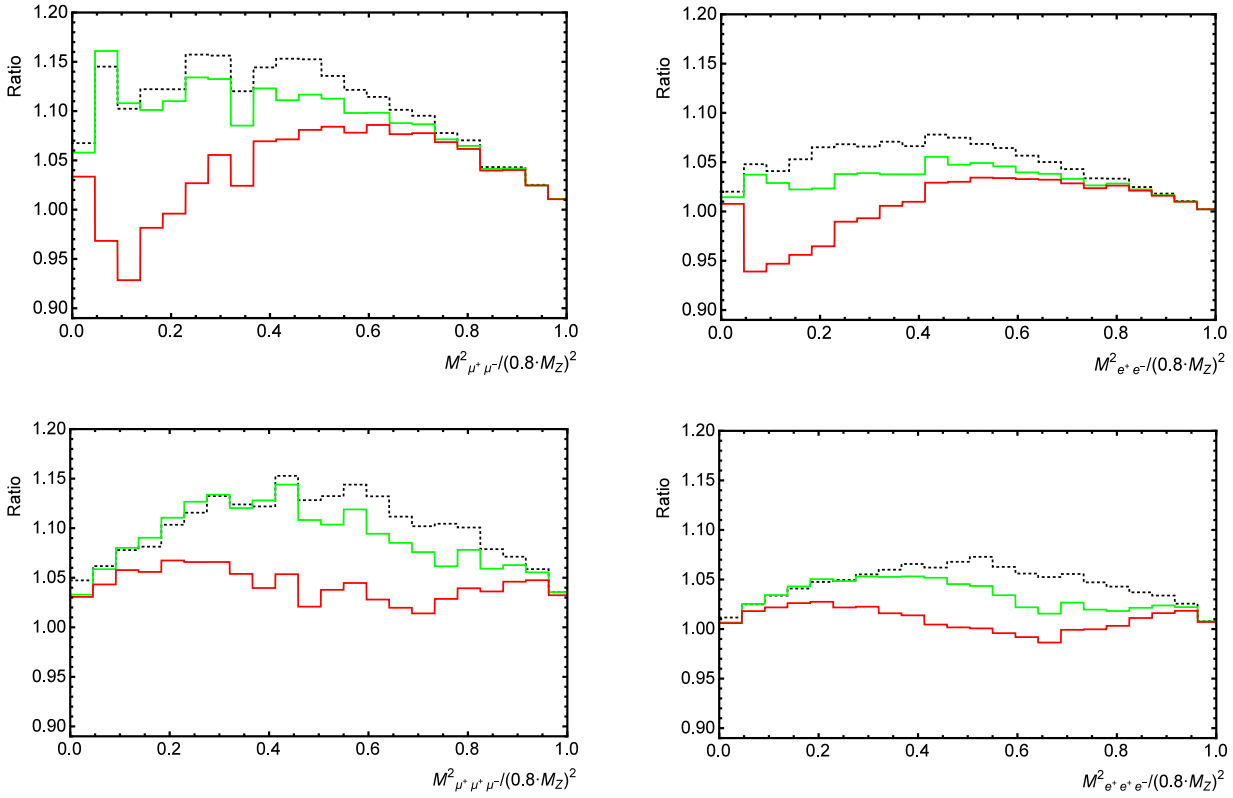

Figure B.11: Ratios of PHOTOS generated spectra (of squared mass of e^+e^- pair ($M^2_{e^+e^-}$), of $\mu^+\mu^-$ pair ($M^2_{\mu^+\mu^-}$), of squared mass of $\mu^+\mu^+\mu^-$ three ($M^2_{\mu^+\mu^+\mu^-}$) and of squared mass of $e^+e^+e^-$ three ($M^2_{e^+e^+e^-}$)) at CMS energy of $E_{CMS} = 0.8\cdot M_Z$ in $Z \to \mu^+\mu^-\mu^+\mu^-$ and $Z \to e^+e^-e^+e^-$ channels to the corresponding one's by improved PHOTOS with matrix element (14). Spectra generated by PHOTOS are obtained from samples of $Z \to e^+e^-$ and $Z \to \mu^+\mu^-$ PYTHIA generated decays. Black dotted line represents spectra by PHOTOS with kernel of extra pair emission given by the formula (34). Solid red line (solid dark grey in greyscale) represents spectra by PHOTOS with kernel of extra pair emission given by the formula (37). Green solid line (solid light grey in greyscale) represents spectra by PHOTOS with kernel of extra pair emission given by the formula (40).

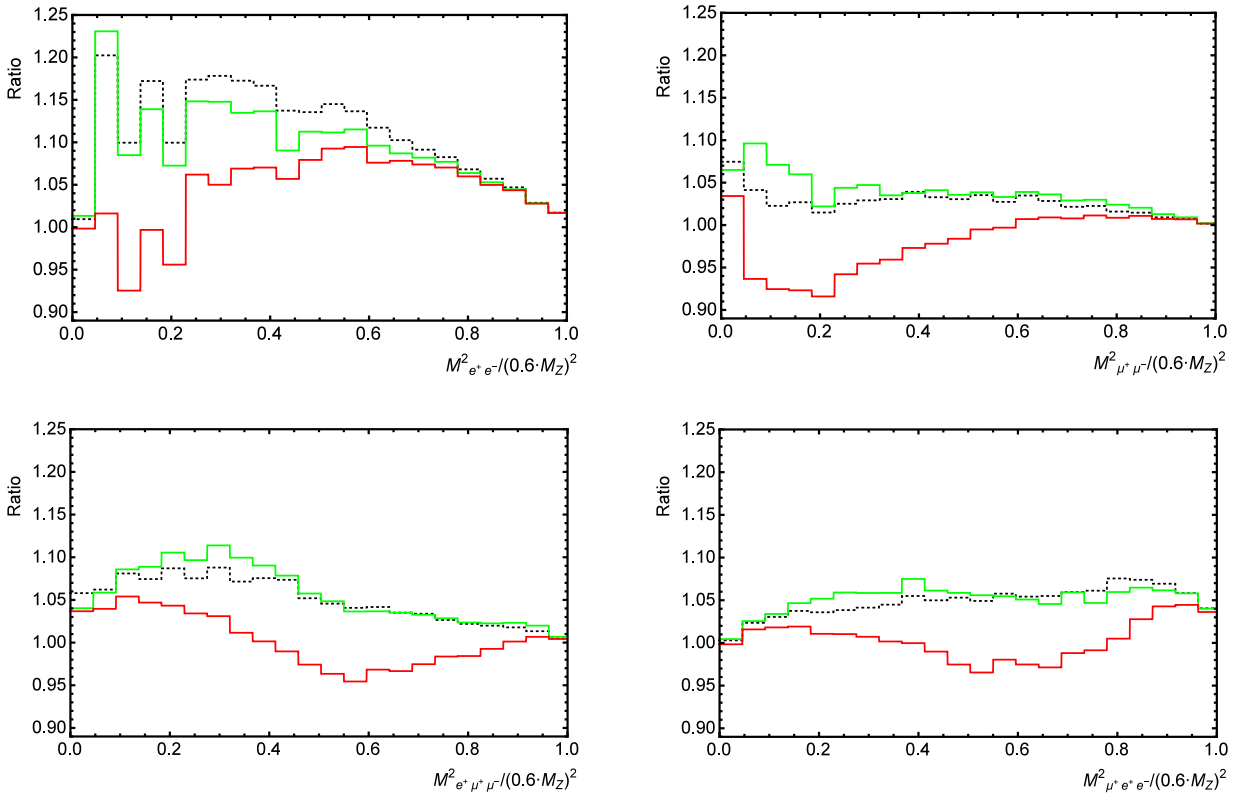

Figure B.12: Ratios of PHOTOS generated spectra (of squared mass of e^+e^- pair ($M^2_{e^+e^-}$), of $\mu^+\mu^-$ pair ($M^2_{\mu^+\mu^-}$), of squared mass of $\mu^+e^+e^-$ three ($M^2_{\mu^+e^+e^-}$) and of squared mass of $e^+\mu^+\mu^-$ three ($M^2_{e^+\mu^+\mu^-}$)) at CMS energy of $E_{CMS} = 0.6 \cdot M_Z$ in $Z \to e^+e^-\mu^+\mu^-$ channel to the corresponding one's by improved PHOTOS with matrix element (14). Spectra generated by PHOTOS are obtained from samples of equal number of $Z \to e^+e^-$ and $Z \to \mu^+\mu^-$ PYTHIA generated decays. Black dotted line represents spectra by PHOTOS with kernel of extra pair emission given by the formula (34). Solid red line (solid dark grey in greyscale) represents spectra by PHOTOS with kernel of extra pair emission given by the formula (37). Green solid line (solid light grey in greyscale) represents spectra by PHOTOS with kernel of extra pair emission given by the formula (40).

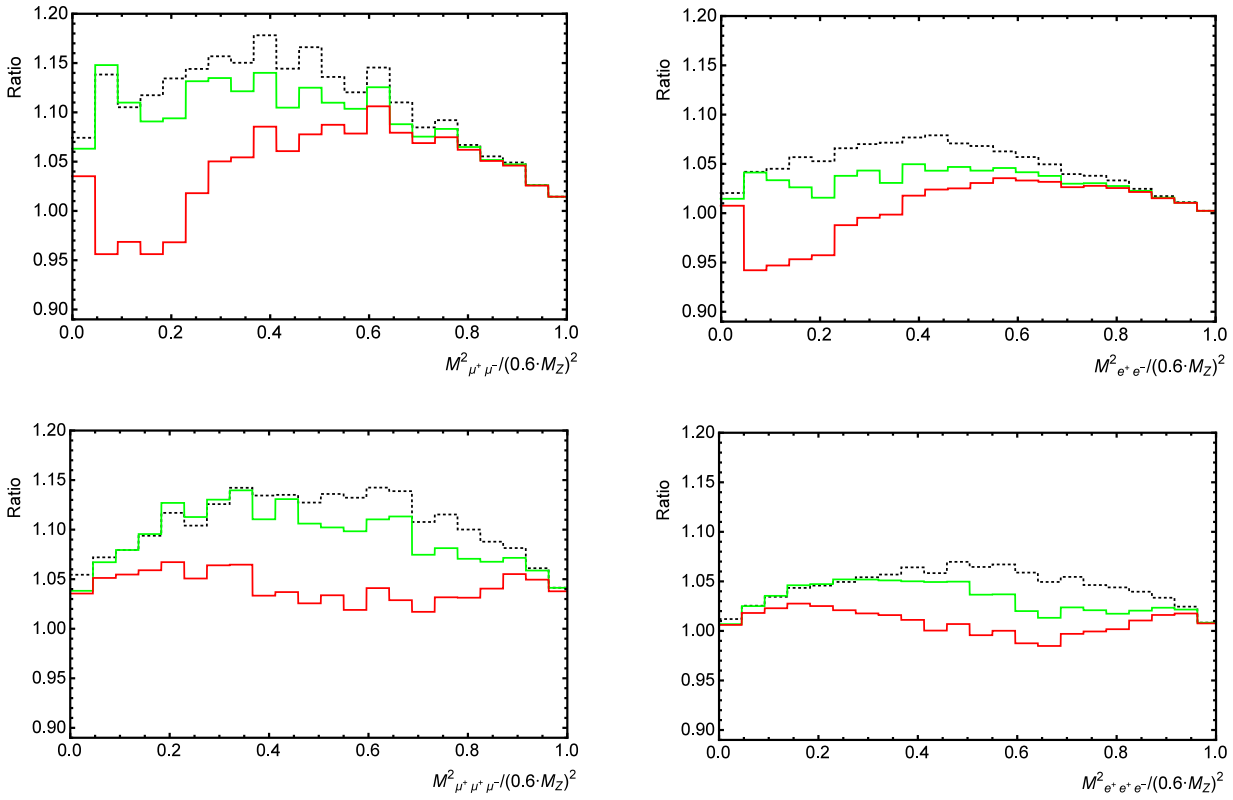

Figure B.13: Ratios of PHOTOS generated spectra (of squared mass of e^+e^- pair ($M^2_{e^+e^-}$), of $\mu^+\mu^-$ pair ($M^2_{\mu^+\mu^-}$), of squared mass of $\mu^+\mu^+\mu^-$ three ($M^2_{\mu^+\mu^+\mu^-}$) and of squared mass of $e^+e^+e^-$ three ($M^2_{e^+e^+e^-}$)) at CMS energy of $E_{CMS} = 0.6 \cdot M_Z$ in $Z \to \mu^+\mu^-\mu^+\mu^-$ and $Z \to e^+e^-e^+e^-$ channels to the corresponding one's by improved PHOTOS with matrix element (14). Spectra generated by PHOTOS are obtained from samples of $Z \to e^+e^-$ and $Z \to \mu^+\mu^-$ PYTHIA generated decays. Black dotted line represents spectra by PHOTOS with kernel of extra pair emission given by the formula (34). Solid red line (solid dark grey in greyscale) represents spectra by PHOTOS with kernel of extra pair emission given by the formula (37). Green solid line (solid light grey in greyscale) represents spectra by PHOTOS with kernel of extra pair emission given by the formula (40).

Considering $Z \to \mu^+\mu^-\mu^+\mu^-$ channel: PHOTOS with kernel F_{test3} (40) tends to slightly overproduce $\mu^+\mu^-$ pairs in the least populated part of the spectrum (up to 15% not taking error into account) causing overproduction of $\mu^+\mu^-$ pairs (up to 6%) in the first bin. Considering $Z \to e^+e^-e^+e^-$ channel: numbers of e^+e^- pairs never deviate more than 5% from corresponding numbers of etalon spectra. For each channel numbers of e^+e^- and $\mu^+\mu^-$ pairs with invariant mass close to beam CMS energy coincide with corresponding numbers from etalon spectra. For each channel and for each bin the number of e^+e^- or $\mu^+\mu^-$ pairs generated by PHOTOS with kernel F_{test3} (40) is larger than corresponding number from data by PHOTOS with kernel F_{test2} (37), their difference is small.

Spectra by PHOTOS with kernel F_{test4} (41) are presented in Figs. B.14-B.20.

Fig. B.14 presents data in $Z \to e^+e^-\mu^+\mu^-$ channel. Fig. B.14 presents ratios of PHOTOS generated spectra of squared mass of $\mu^+e^+e^-$ three ($M^2_{\mu^+e^+e^-}$) and of squared mass of $e^+\mu^+\mu^-$ three ($M^2_{e^+\mu^+\mu^-}$) to the corresponding one's by KORALW. Left hand side of Fig. B.14 presents simulation sample in form of error bars. Right hand side of Fig. B.14 presents simulation sample in form of mean values, that should improve readability of the plots. Agreement between PHOTOS with kernel F_{test4} (41) and KORALW is good. Agreement between PHOTOS with kernel F_{test4} (41) and PHOTOS with matrix element (14) is good. Numbers of PHOTOS test events and KORALW test events for any bin never differ greatly in the ratio more than 22%. Such difference rather vanishes with statistics increase.

Figs. B.15, B.17, B.19 present data in $Z \to e^+e^-\mu^+\mu^-$ channel for beam CMS energies of M_Z, $0.8 \cdot M_Z$, $0.6 \cdot M_Z$ correspondingly. Figs. B.17, B.19 present ratios of PHOTOS generated spectra of squared mass of e^+e^- pair ($M^2_{e^+e^-}$), of $\mu^+\mu^-$ pair ($M^2_{\mu^+\mu^-}$), of squared mass of $\mu^+e^+e^-$ three ($M^2_{\mu^+e^+e^-}$) and of squared mass of $e^+\mu^+\mu^-$ three ($M^2_{e^+\mu^+\mu^-}$) to the corresponding one's by PHOTOS with matrix element (14).

Figs. B.16, B.18, B.20 present data in $Z \to e^+e^-e^+e^-$ and $Z \to \mu^+\mu^-\mu^+\mu^-$ channels for beam CMS energies of $E_{CMS} = M_Z$, $0.8 \cdot M_Z$, $0.6 \cdot M_Z$ correspondingly. Figs. B.16, B.18, B.20 present ratios of PHOTOS generated spectra of squared mass of e^+e^- pair ($M^2_{e^+e^-}$), of $\mu^+\mu^-$ pair ($M^2_{\mu^+\mu^-}$), of squared mass of $e^+e^+e^-$ three ($M^2_{e^+e^+e^-}$) and of squared mass of $\mu^+\mu^+\mu^-$ three ($M^2_{\mu^+\mu^+\mu^-}$) to the corresponding one's by PHOTOS with matrix element (14).

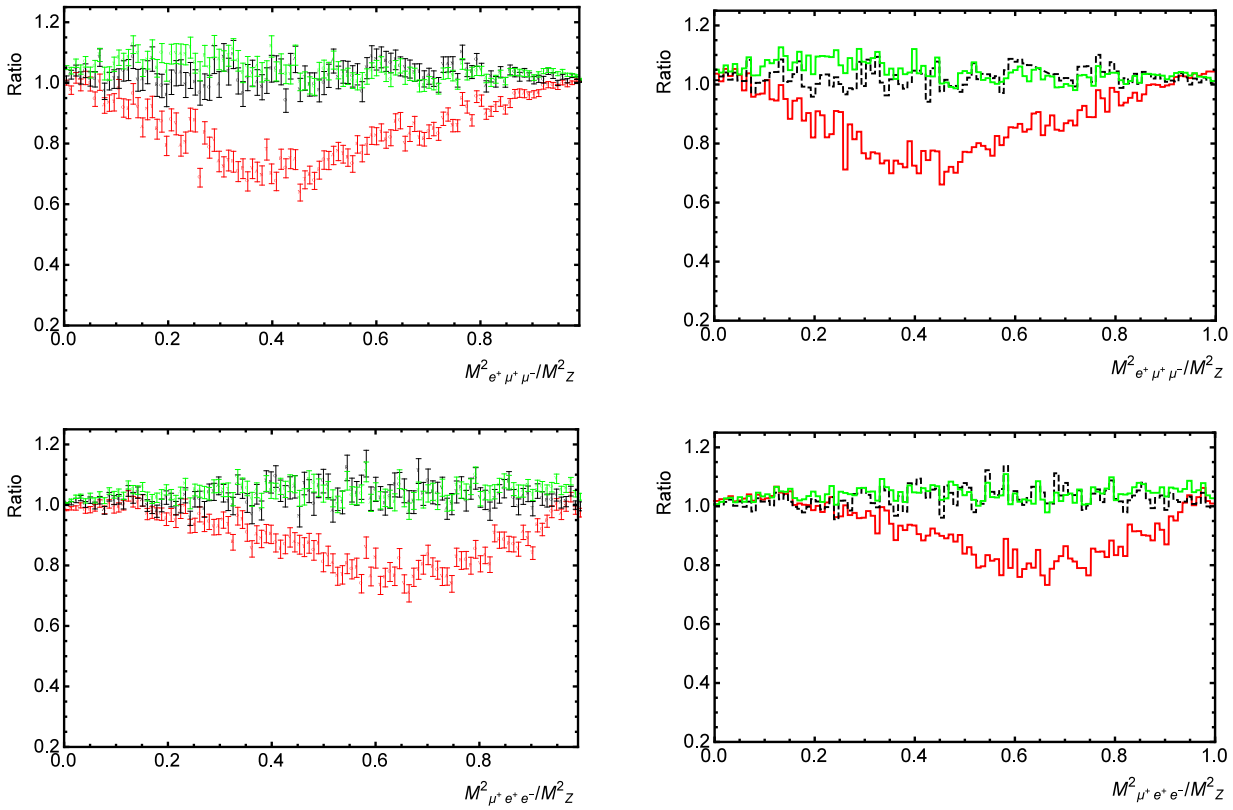

Figure B.14: Ratios of PHOTOS generated spectra (of squared mass of $\mu^+e^+e^-$ three ($M^2_{\mu^+e^+e^-}$) and of squared mass of $e^+\mu^+\mu^-$ three ($M^2_{e^+\mu^+\mu^-}$)) at CMS energy of $E_{CMS} = M_Z$ in $Z \to e^+e^-\mu^+\mu^-$ channel to the corresponding one's by KORALW. Spectra generated by PHOTOS are obtained from samples of equal number of $Z \to e^+e^-$ and $Z \to \mu^+\mu^-$ PYTHIA generated decays. Red (dark grey in greyscale) solid line and red (dark grey) error bars represent spectra by unmodified PHOTOS [11]. Black dashed line and black error bars represent spectra by improved PHOTOS with matrix element (14) installed into it. Green (light grey in greyscale) solid line and green (light grey) error bars represent spectra by improved PHOTOS with kernel of extra pair emission given by the formula (41).

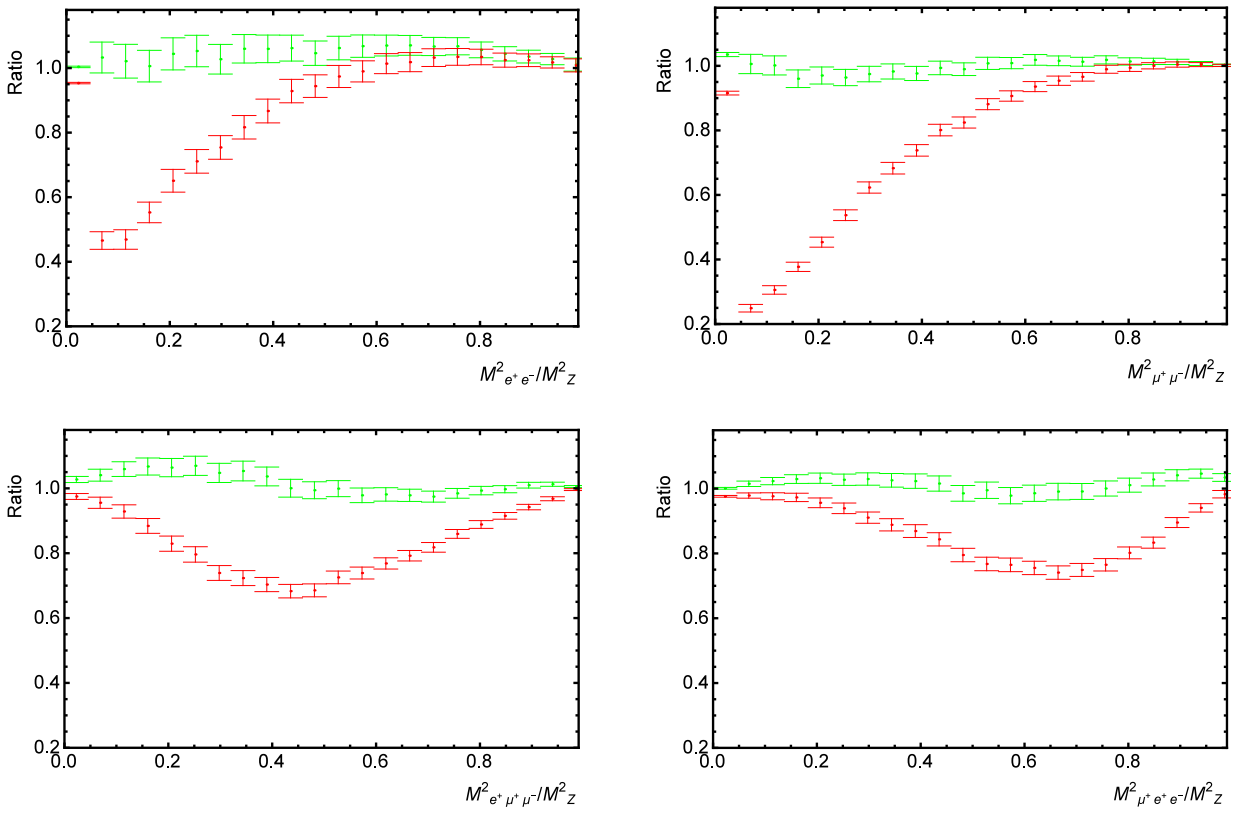

Figure B.15: Ratios of PHOTOS generated spectra (of squared mass of e^+e^- pair ($M^2_{e^+e^-}$), of $\mu^+\mu^-$ pair ($M^2_{\mu^+\mu^-}$), of squared mass of $\mu^+e^+e^-$ three ($M^2_{\mu^+e^+e^-}$) and of squared mass of $e^+\mu^+\mu^-$ three ($M^2_{e^+\mu^+\mu^-}$)) in $Z \to e^+e^-\mu^+\mu^-$ channel to the corresponding one's by improved PHOTOS with matrix element (14). Spectra generated by PHOTOS are obtained from samples of equal number of $Z \to e^+e^-$ and $Z \to \mu^+\mu^-$ PYTHIA generated decays. Red (dark grey) error bars represent spectra by unmodified PHOTOS [11]. Green (light grey) error bars represent spectra by PHOTOS with kernel of extra pair emission given by the formula (41).

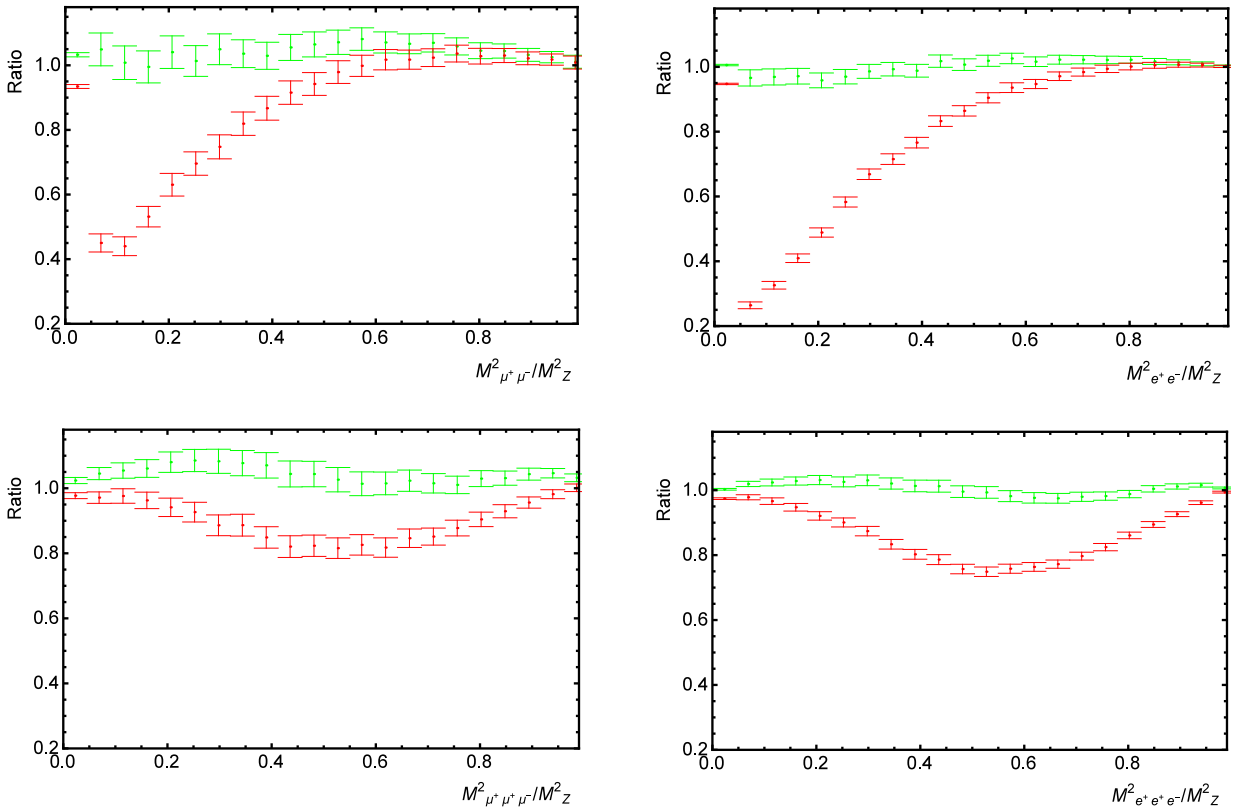

Figure B.16: Ratios of PHOTOS generated spectra (of squared mass of e^+e^- pair ($M^2_{e^+e^-}$), of $\mu^+\mu^-$ pair ($M^2_{\mu^+\mu^-}$), of squared mass of $\mu^+\mu^+\mu^-$ three ($M^2_{\mu^+\mu^+\mu^-}$) and of squared mass of $e^+e^+e^-$ three ($M^2_{e^+e^+e^-}$)) at CMS energy of $E_{CMS} = M_Z$ in $Z \to \mu^+\mu^-\mu^+\mu^-$ and $Z \to e^+e^-e^+e^-$ channels to the corresponding one's by improved PHOTOS with matrix element (14). Spectra generated by PHOTOS are obtained from samples of $Z \to e^+e^-$ and $Z \to \mu^+\mu^-$ PYTHIA generated decays. Red (dark grey) error bars represent spectra by unmodified PHOTOS [11]. Green (light grey) error bars represent spectra by PHOTOS with kernel of extra pair emission given by the formula (41).

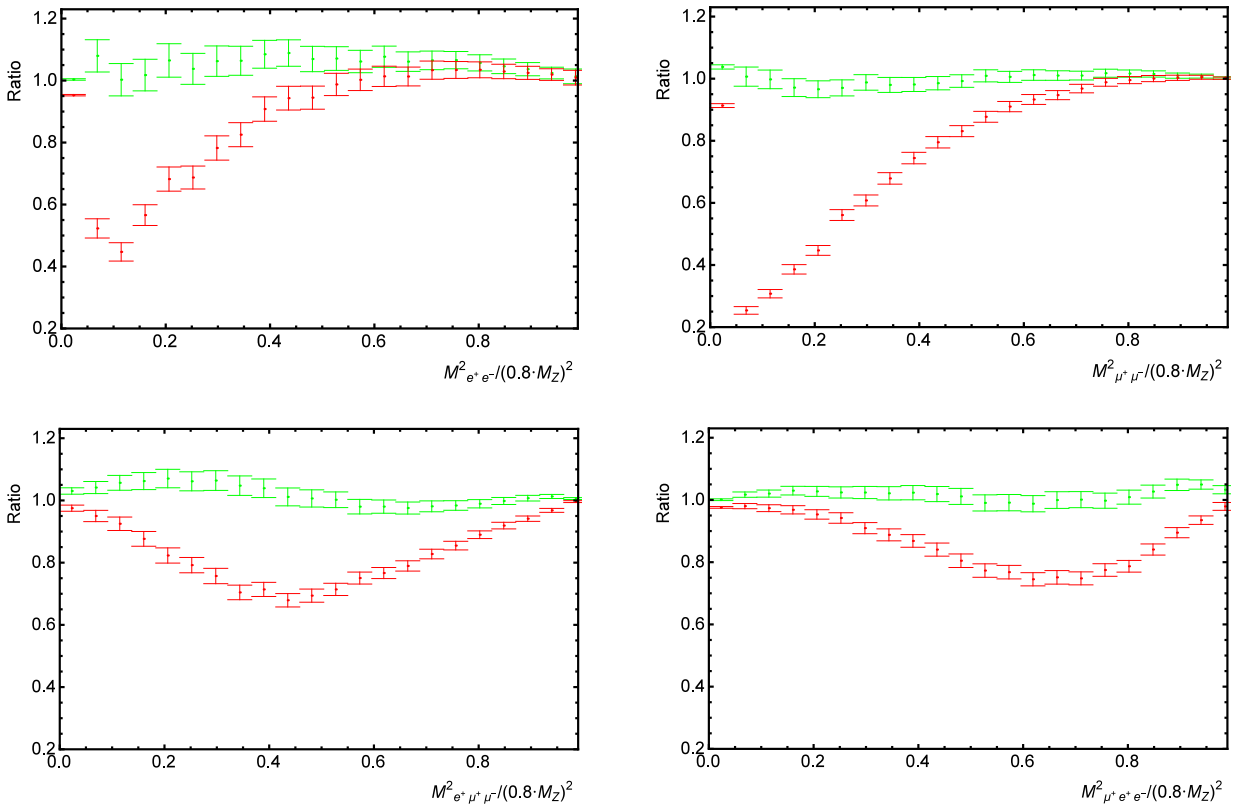

Figure B.17: Ratios of PHOTOS generated spectra (of squared mass of e^+e^- pair ($M^2_{e^+e^-}$), of $\mu^+\mu^-$ pair ($M^2_{\mu^+\mu^-}$), of squared mass of $\mu^+e^+e^-$ three ($M^2_{\mu^+e^+e^-}$) and of squared mass of $e^+\mu^+\mu^-$ three ($M^2_{e^+\mu^+\mu^-}$)) at CMS energy of $E_{CMS} = 0.8 \cdot M_Z$ in $Z \to e^+e^-\mu^+\mu^-$ channel to the corresponding one's by improved PHOTOS with matrix element (14). Spectra generated by PHOTOS are obtained from samples of equal number of $Z \to e^+e^-$ and $Z \to \mu^+\mu^-$ PYTHIA generated decays. Red (dark grey) error bars represent spectra by unmodified PHOTOS [11]. Green (light grey) error bars represent spectra by PHOTOS with kernel of extra pair emission given by the formula (41).

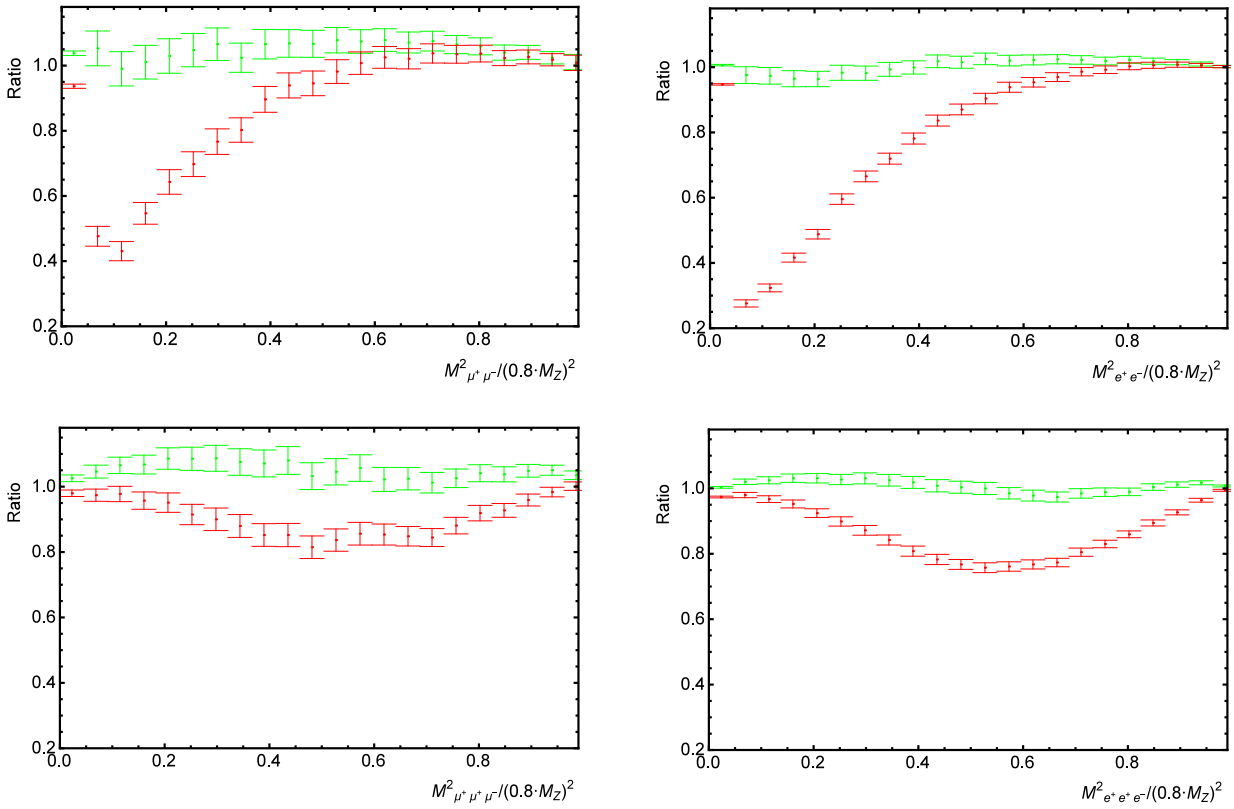

Figure B.18: Ratios of PHOTOS generated spectra (of squared mass of e^+e^- pair ($M^2_{e^+e^-}$), of $\mu^+\mu^-$ pair ($M^2_{\mu^+\mu^-}$), of squared mass of $\mu^+\mu^+\mu^-$ three ($M^2_{\mu^+\mu^+\mu^-}$) and of squared mass of $e^+e^+e^-$ three ($M^2_{e^+e^+e^-}$)) at CMS energy of $E_{CMS} = 0.8 \cdot M_Z$ in $Z \to \mu^+\mu^-\mu^+\mu^-$ and $Z \to e^+e^-e^+e^-$ channels to the corresponding one's by improved PHOTOS with matrix element (14). Spectra generated by PHOTOS are obtained from samples of $Z \to e^+e^-$ and $Z \to \mu^+\mu^-$ PYTHIA generated decays. Red (dark grey) error bars represent spectra by unmodified PHOTOS [11]. Green (light grey) error bars represent spectra by PHOTOS with kernel of extra pair emission given by the formula (41).

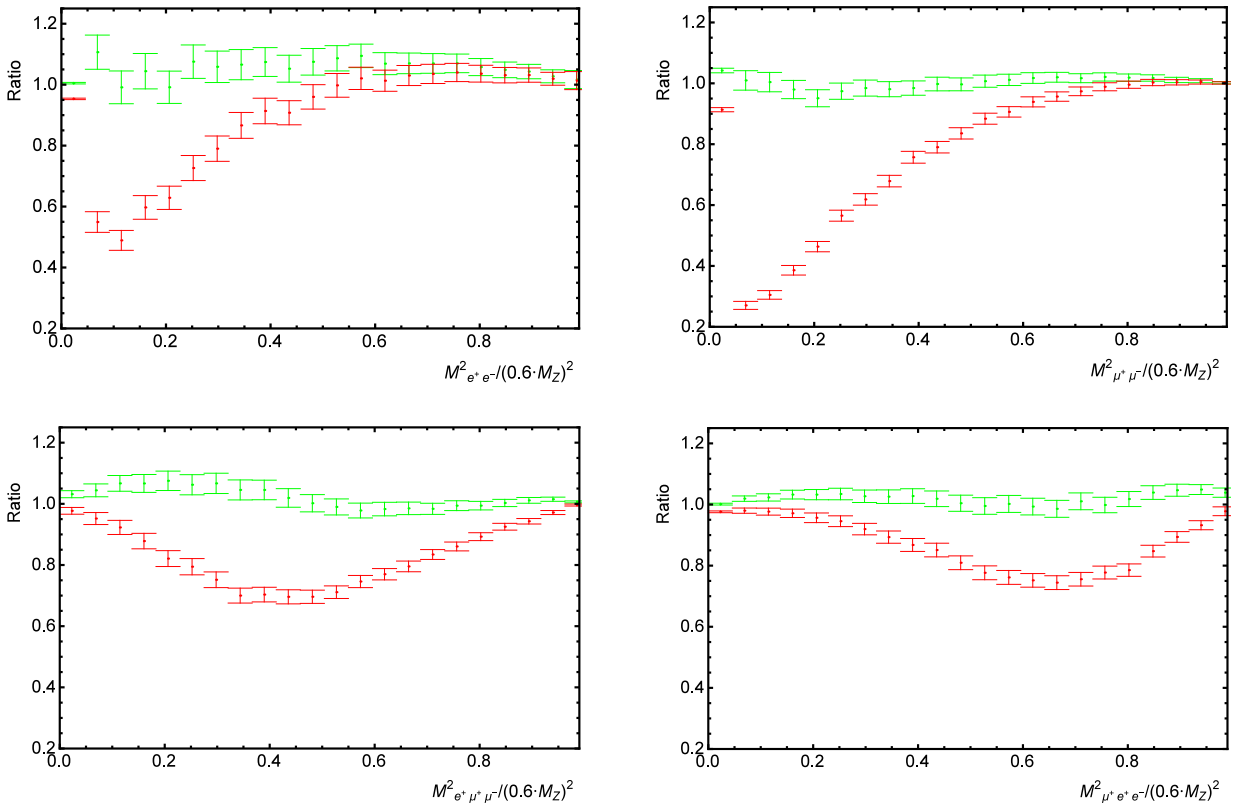

Figure B.19: Ratios of PHOTOS generated spectra (of squared mass of e^+e^- pair ($M^2_{e^+e^-}$), of $\mu^+\mu^-$ pair ($M^2_{\mu^+\mu^-}$), of squared mass of $\mu^+e^+e^-$ three ($M^2_{\mu^+e^+e^-}$) and of squared mass of $e^+\mu^+\mu^-$ three ($M^2_{e^+\mu^+\mu^-}$)) at CMS energy of $E_{CMS} = 0.6 \cdot M_Z$ in $Z \to e^+e^-\mu^+\mu^-$ channel to the corresponding one's by improved PHOTOS with matrix element (14). Spectra generated by PHOTOS are obtained from samples of equal number of $Z \to e^+e^-$ and $Z \to \mu^+\mu^-$ PYTHIA generated decays. Red (dark grey) error bars represent spectra by unmodified PHOTOS [11]. Green (light grey) error bars represent spectra by PHOTOS with kernel of extra pair emission given by the formula (41).

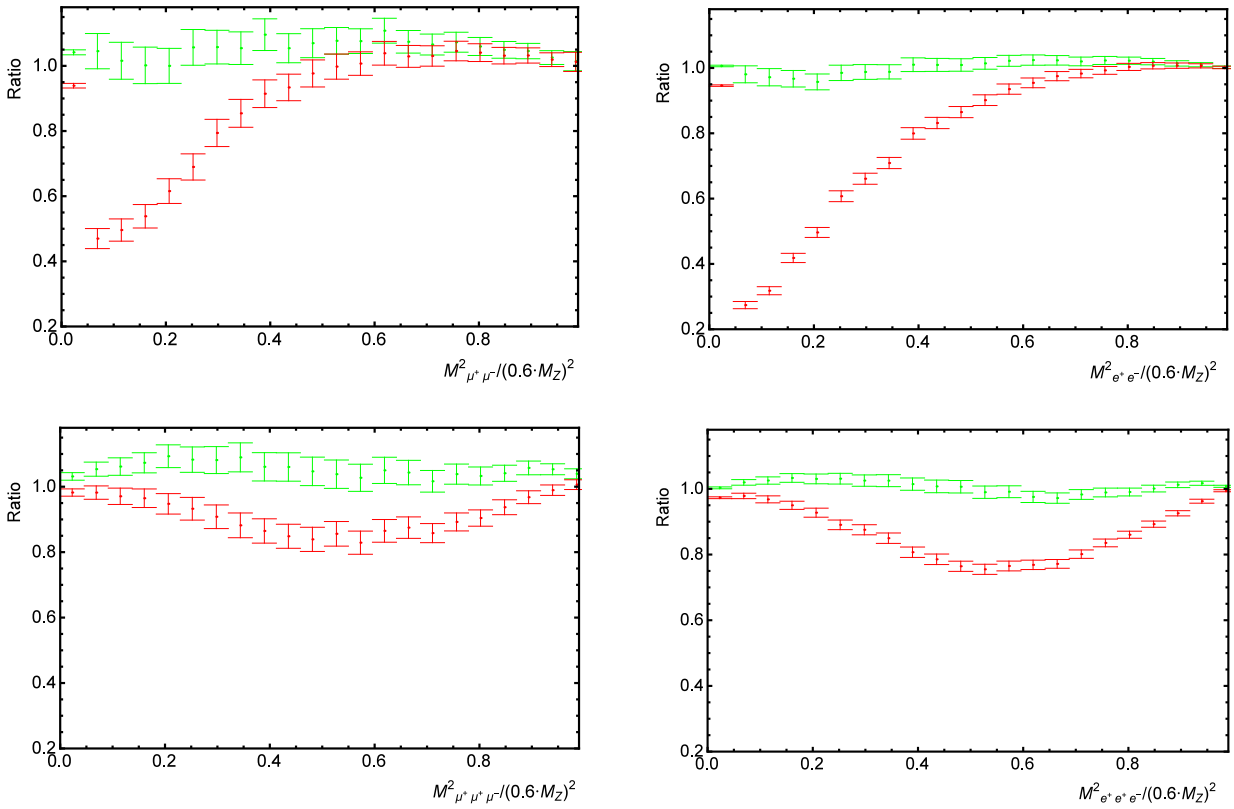

Figure B.20: Ratios of PHOTOS generated spectra (of squared mass of e^+e^- pair ($M^2_{e^+e^-}$), of $\mu^+\mu^-$ pair ($M^2_{\mu^+\mu^-}$), of squared mass of $\mu^+\mu^+\mu^-$ three ($M^2_{\mu^+\mu^+\mu^-}$) and of squared mass of $e^+e^+e^-$ three ($M^2_{e^+e^+e^-}$)) at CMS energy of $E_{CMS} = 0.6 \cdot M_Z$ in $Z \to \mu^+\mu^-\mu^+\mu^-$ and $Z \to e^+e^-e^+e^-$ channels to the corresponding one's by improved PHOTOS with matrix element (14). Spectra generated by PHOTOS are obtained from samples of $Z \to e^+e^-$ and $Z \to \mu^+\mu^-$ PYTHIA generated decays. Red (dark grey) error bars represent spectra by unmodified PHOTOS [11]. Green (light grey) error bars represent spectra by PHOTOS with kernel of extra pair emission given by the formula (41).

Agreement between PHOTOS with kernel F_{test4} (41) and PHOTOS with matrix element (14) is good. Numbers of e^+e^- pairs never deviate more than 10% from corresponding numbers of etalon spectra. Numbers of $\mu^+\mu^-$ pairs never deviate more than 5% from corresponding numbers of etalon spectra. Numbers of e^+e^- and $\mu^+\mu^-$ pairs with invariant mass close to beam CMS energy coincide with corresponding numbers of etalon spectra.

I should note that agreement between PHOTOS with kernel F_{test4} (41) and PHOTOS with matrix element (14) is quite remarkable and numerically stable.

Spectra by PHOTOS with kernel F_{test5} (42) are presented in Figs. B.21-B.28.

Fig. B.21 presents data in $Z \to e^+e^-\mu^+\mu^-$ channel. Fig. B.21 presents ratios of PHOTOS generated spectra of squared mass of $\mu^+e^+e^-$ three ($M^2_{\mu^+e^+e^-}$) and of squared mass of $e^+\mu^+\mu^-$ three ($M^2_{e^+\mu^+\mu^-}$) to the corresponding one's by KORALW. Left hand side of Fig. B.21 presents simulation sample in form of error bars. Right hand side of Fig. B.21 presents simulation sample in form of mean values, that should improve readability of the plots. Agreement between PHOTOS with kernel F_{test5} (42) and KORALW is good. Agreement between PHOTOS with kernel F_{test5} (42) and PHOTOS with matrix element (14) is good. Numbers of PHOTOS test events and KORALW test events for any bin never differ greatly in the ratio more than 22%. Such difference rather vanishes with statistics increase.

Fig. B.22 presents data in $Z \to \mu^+\mu^-\mu^+\mu^-$ channel. Fig. B.22 presents ratios of PHOTOS generated summated spectra of squared mass of $\mu^+\mu^-$ pair ($M^2_{\mu^+\mu^-}$) and of squared mass of $\mu^+\mu^+\mu^-$ three ($\mu^+\mu^+\mu^-$), spectra of squared mass of $\mu^+\mu^+$ pair ($M^2_{\mu^+\mu^+}$), and of $\mu^-\mu^-$ pair ($M^2_{\mu^-\mu^-}$) to the corresponding one's by KORALW. Agreement between PHOTOS with kernel F_{test5} (42) and KORALW is good. Agreement between PHOTOS with kernel F_{test5} (42) and PHOTOS with matrix element (14) is good.

Matrix elements residual F_{test5} (42) is a patchwork made of parts of matrix elements residual F_{full}. Shown agreement between PHOTOS with kernel F_{test5} (42) and KORALW in the $Z \to e^+e^-\mu^+\mu^-$ and $Z \to \mu^+\mu^-\mu^+\mu^-$ channels can be accidental for a given initial conditions. While matrix element (14) is exact and while its tests show good agreement with KORALW tests, it is essential to use PHOTOS with matrix element (14) for generation of etalon spectra for beam CMS energies less than M_Z.

Figs. B.23, B.25, B.27 present data in $Z \to e^+e^-\mu^+\mu^-$ channel for beam CMS energies of $E_{CMS} = M_Z$, $0.8 \cdot M_Z$, $0.6 \cdot M_Z$ correspondingly. Figs. B.23, B.25, B.27 present ratios of PHOTOS generated spectra of squared mass of e^+e^- pair ($M^2_{e^+e^-}$), of $\mu^+\mu^-$ pair ($M^2_{\mu^+\mu^-}$), of squared mass of $\mu^+e^+e^-$ three ($M^2_{\mu^+e^+e^-}$) and of squared mass of $e^+\mu^+\mu^-$ three ($M^2_{e^+\mu^+\mu^-}$) to the corresponding one's by PHOTOS with matrix element (14). Agreement between PHOTOS with kernel F_{test5} (42) and PHOTOS with matrix element (14) is good. The ratio between numbers of events for any bin never differs from 1. more than 10%. It looks that PHOTOS with kernel F_{test5} (42) tends to slightly overproduce e^+e^- pairs in the least populated part of the spectrum causing overproduction of $\mu^+\mu^-$ pairs (up to 5%) in the first bin.

Figs. B.24, B.26, B.28 present data in $Z \to e^+e^-e^+e^-$ and $Z \to \mu^+\mu^-\mu^+\mu^-$ channels for beam CMS energies of $E_{CMS} = M_Z$, $0.8 \cdot M_Z$, $0.6 \cdot M_Z$ correspondingly. Figs. B.24, B.26, B.28 present ratios of PHOTOS generated spectra of squared mass of e^+e^- pair ($M^2_{e^+e^-}$), of $\mu^+\mu^-$ pair ($M^2_{\mu^+\mu^-}$), of squared mass of $e^+e^+e^-$ three ($M^2_{e^+e^+e^-}$) and of squared mass of $\mu^+\mu^+\mu^-$ three ($M^2_{\mu^+\mu^+\mu^-}$) to the corresponding one's by PHOTOS with matrix element (14). Agreement between PHOTOS with kernel F_{test5} (42) and PHOTOS with matrix element (14) is good. The ratio between numbers of events for any bin of e^+e^- pair spectrum never differs from 1. more than 5%. The ratio between numbers of events for any bin of $\mu^+\mu^-$ pair spectrum never differs from 1. more than 8%. It looks that PHOTOS with kernel F_{test5} (42) tends to slightly overproduce $\mu^+\mu^-$ pairs in the least populated part of the spectrum.

I should note that numerical agreement between PHOTOS with kernel F_{test5} (42) and KORALW is quite remarkable (Figs. 14,B.21,B.22) and numerically stable (Figs. B.23-B.28).

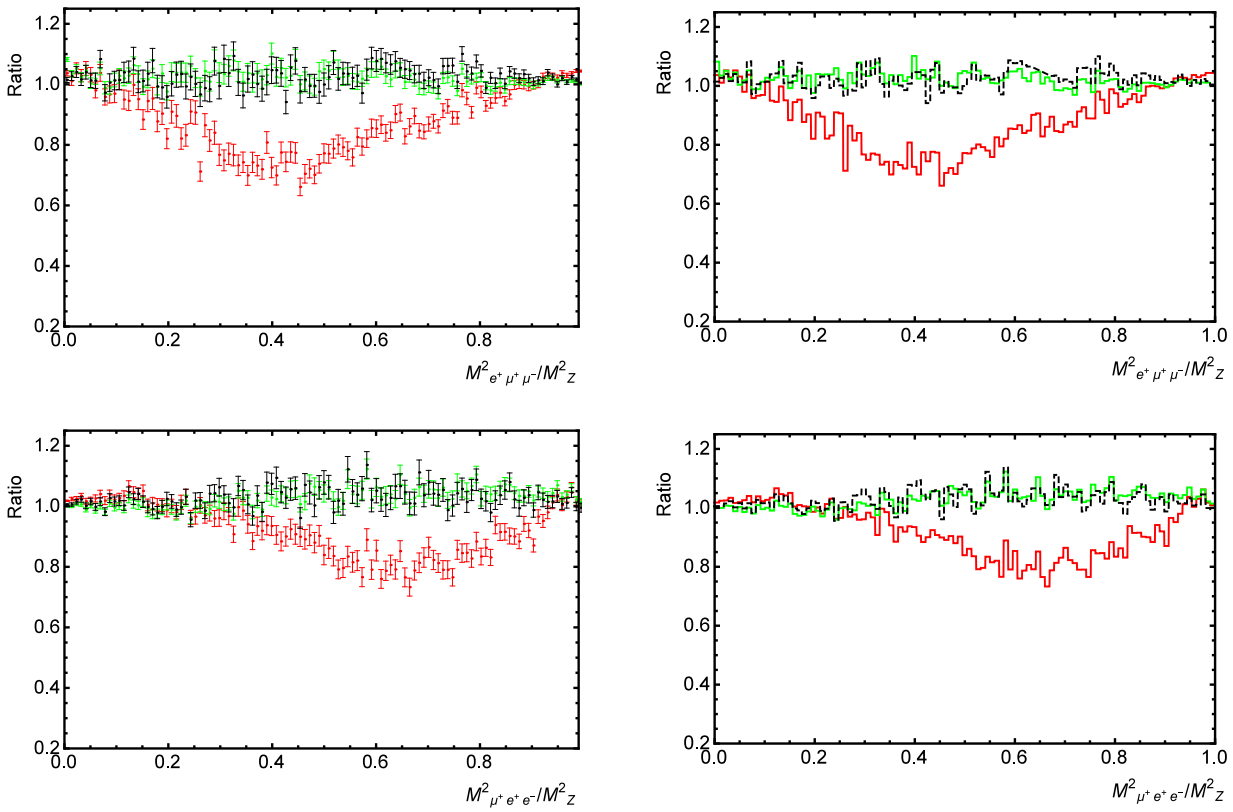

Figure B.21: Ratios of PHOTOS generated spectra (of squared mass of $\mu^+e^+e^-$ three ($M^2_{\mu^+e^+e^-}$) and of squared mass of $e^+\mu^+\mu^-$ three ($M^2_{e^+\mu^+\mu^-}$)) at CMS energy of $E_{CMS} = M_Z$ in $Z \to e^+e^-\mu^+\mu^-$ channel to the corresponding one's by KORALW. Spectra generated by PHOTOS are obtained from samples of equal number of $Z \to e^+e^-$ and $Z \to \mu^+\mu^-$ PYTHIA generated decays. Red (dark grey in greyscale) solid line and red (dark grey) error bars represent spectra by unmodified PHOTOS [11]. Black dashed line and black error bars represent spectra by improved PHOTOS with matrix element (14) installed into it. Green (light grey in greyscale) solid line and green (light grey) error bars represent spectra by improved PHOTOS with kernel of extra pair emission given by the formula (42).

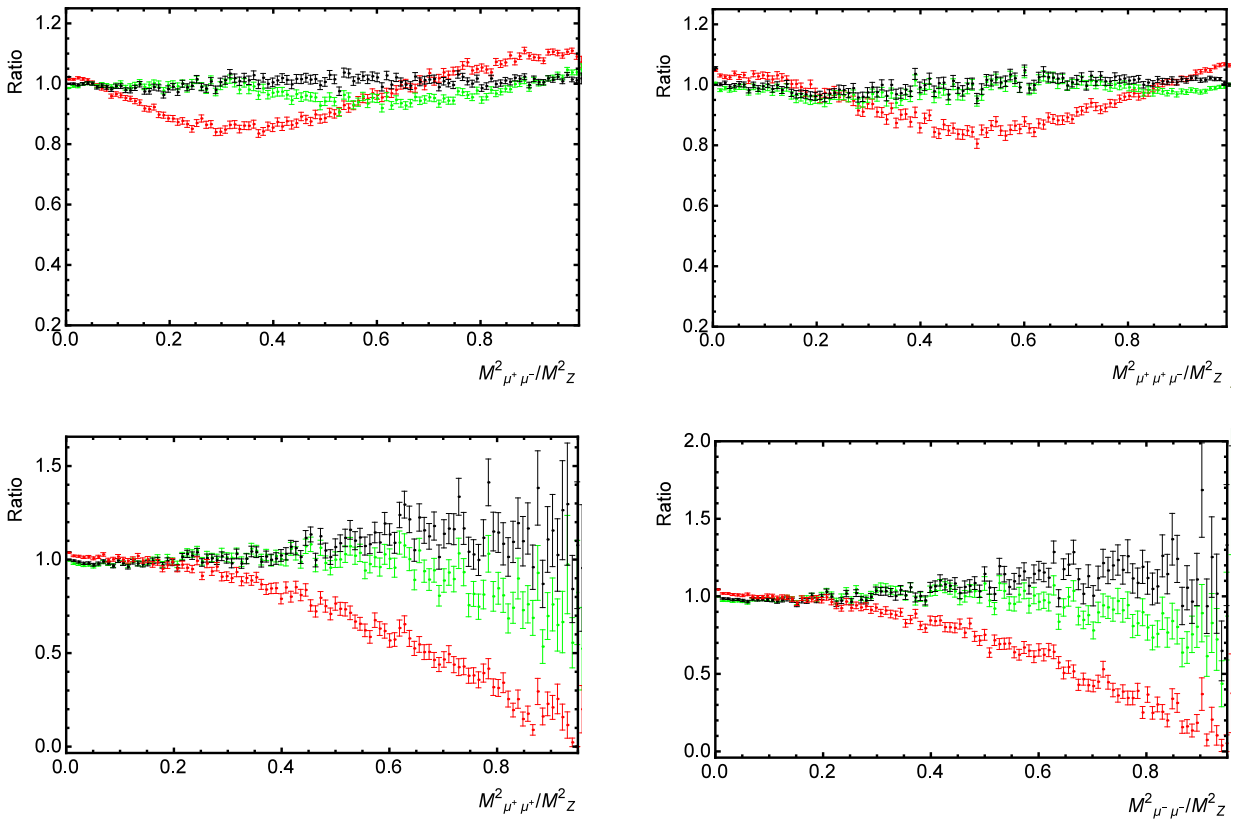

Figure B.22: Ratios of PHOTOS generated spectra (of squared mass of $\mu^+\mu^+\mu^-$ three ($M^2_{\mu^+\mu^+\mu^-}$), of $\mu^+\mu^+$ pair ($M^2_{\mu^+\mu^+}$), of $\mu^-\mu^-$ pair ($M^2_{\mu^-\mu^-}$) and sum of $\mu^+\mu^-$ pair ($M^2_{\mu^+\mu^-}$) spectra) at CMS energy of $E_{CMS} = M_Z$ in $Z \to \mu^+\mu^-\mu^+\mu^-$ channel to the corresponding one's by KORALW. Spectra generated by PHOTOS are obtained from sample of $Z \to \mu^+\mu^-$ PYTHIA generated decays. Red (dark grey) error bars represent spectra by unmodified PHOTOS [11]. Black error bars represent spectra by improved PHOTOS with matrix element (14) installed into it. Green (light grey) error bars represent spectra by improved PHOTOS with kernel of extra pair emission given by the formula (42).

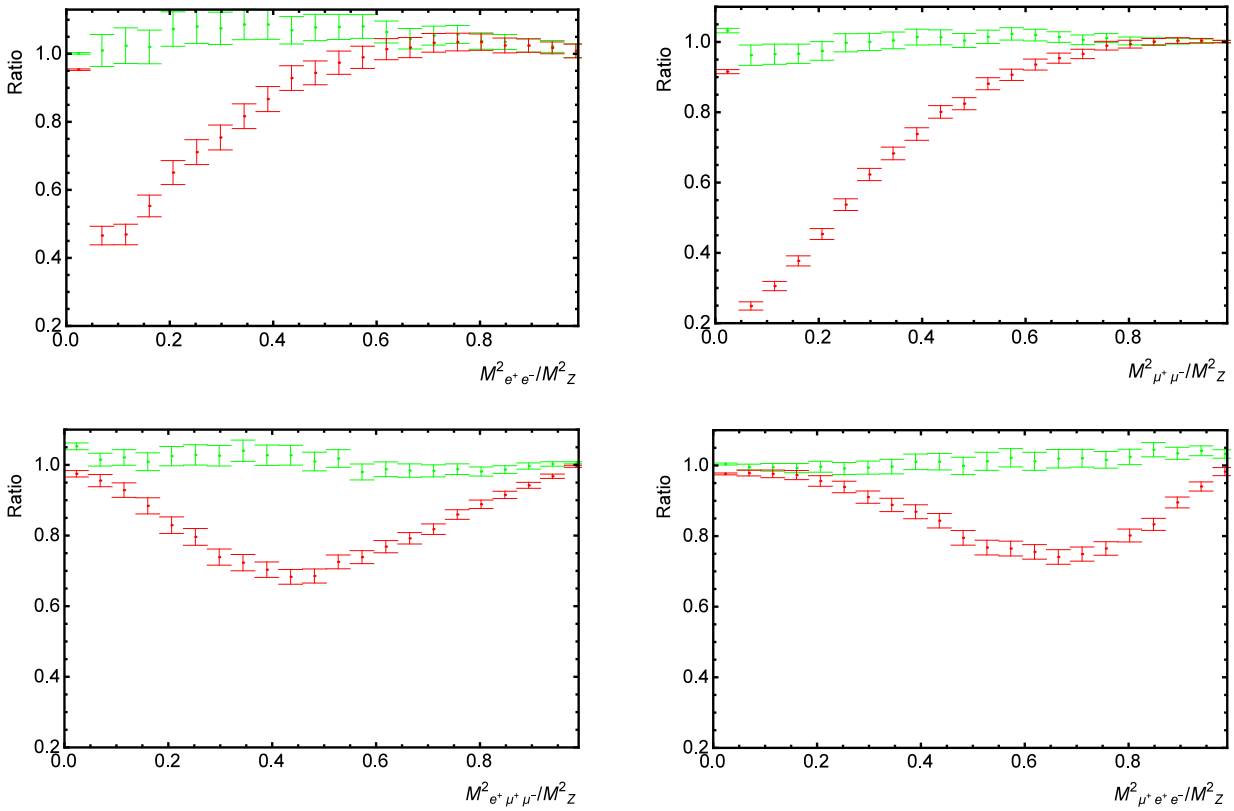

Figure B.23: Ratios of PHOTOS generated spectra (of squared mass of e^+e^- pair ($M^2_{e^+e^-}$), of $\mu^+\mu^-$ pair ($M^2_{\mu^+\mu^-}$), of squared mass of $\mu^+e^+e^-$ three ($M^2_{\mu^+e^+e^-}$) and of squared mass of $e^+\mu^+\mu^-$ three ($M^2_{e^+\mu^+\mu^-}$)) at CMS energy of $E_{CMS} = M_Z$ in $Z \to e^+e^-\mu^+\mu^-$ channel to the corresponding one's, that are generated by improved PHOTOS with matrix element (14) installed into it. Spectra generated by PHOTOS are obtained from samples of equal number of $Z \to e^+e^-$ and $Z \to \mu^+\mu^-$ PYTHIA generated decays. Red (dark grey) error bars represent spectra by unmodified PHOTOS [11]. Green (light grey) error bars represent spectra by improved PHOTOS with kernel of extra pair emission given by the formula (42).

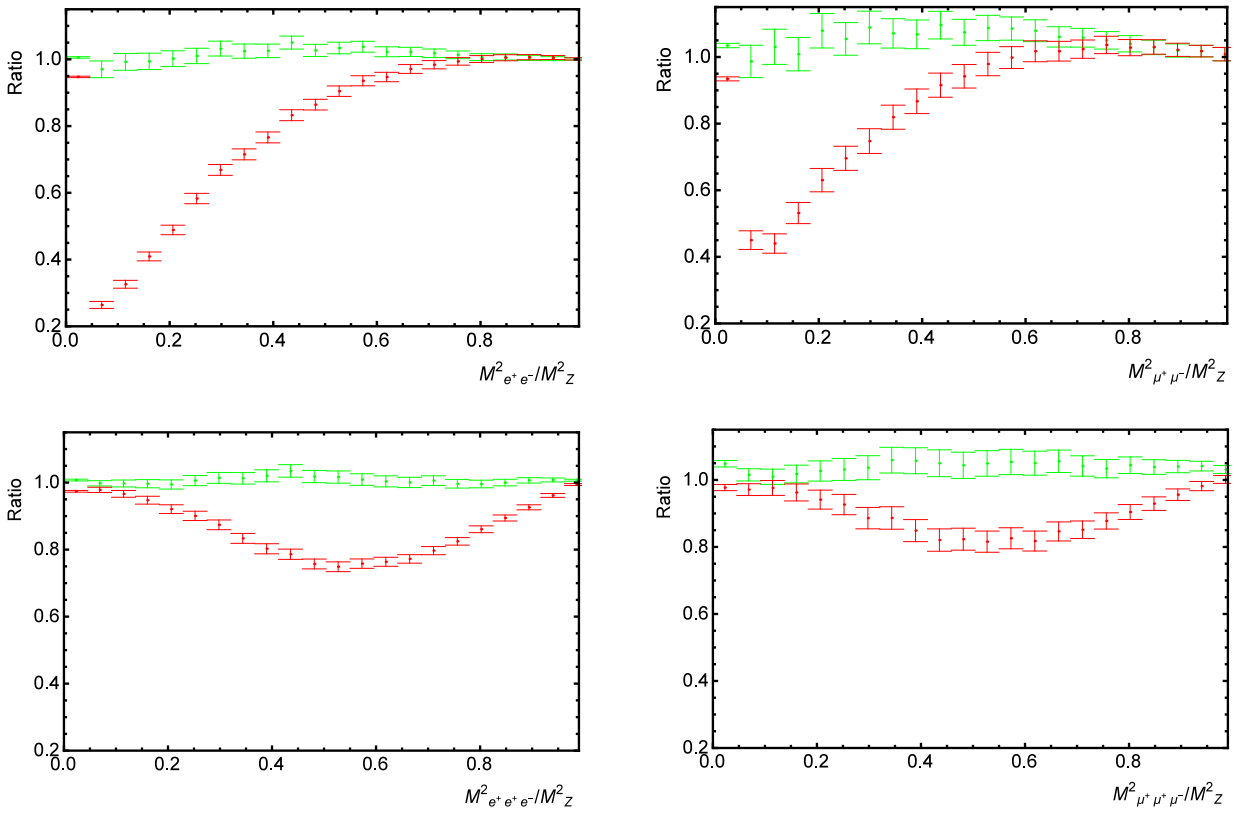

Figure B.24: Ratios of PHOTOS generated spectra (of squared mass of e^+e^- pair ($M^2_{e^+e^-}$), of $\mu^+\mu^-$ pair ($M^2_{\mu^+\mu^-}$), of squared mass of $e^+e^+e^-$ three ($M^2_{e^+e^+e^-}$) and of squared mass of $\mu^+\mu^+\mu^-$ three ($M^2_{\mu^+\mu^+\mu^-}$)) at CMS energy of $E_{CMS} = M_Z$ in $Z \to \mu^+\mu^-\mu^+\mu^-$ and $Z \to e^+e^-e^+e^-$ channels to the corresponding one's, that are generated by improved PHOTOS with matrix element (14) installed into it. Spectra generated by PHOTOS are obtained from samples of $Z \to e^+e^-$ and $Z \to \mu^+\mu^-$ PYTHIA generated decays. Red (dark grey) error bars represent spectra by unmodified PHOTOS [11]. Green (light grey) error bars represent spectra by improved PHOTOS with kernel of extra pair emission given by the formula (42).

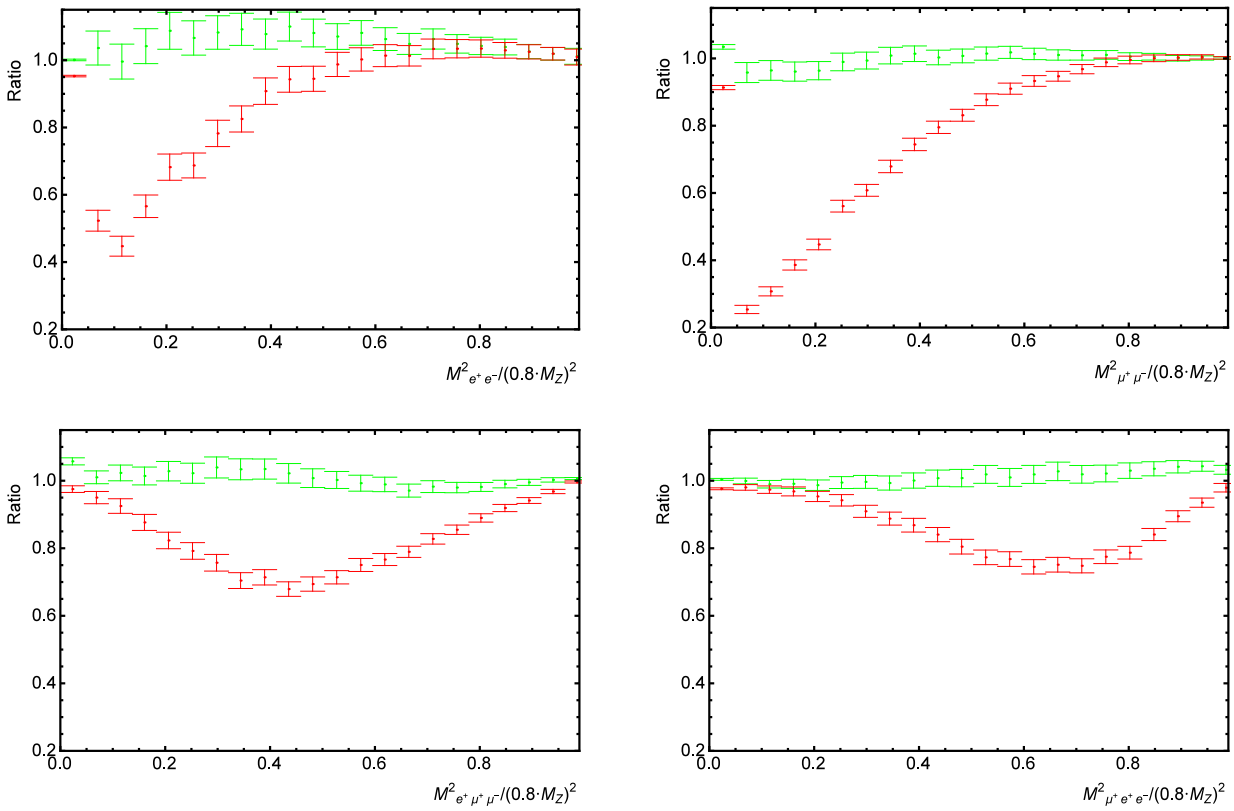

Figure B.25: Ratios of PHOTOS generated spectra (of squared mass of e^+e^- pair ($M^2_{e^+e^-}$), of $\mu^+\mu^-$ pair ($M^2_{\mu^+\mu^-}$), of squared mass of $\mu^+e^+e^-$ three ($M^2_{\mu^+e^+e^-}$) and of squared mass of $e^+\mu^+\mu^-$ three ($M^2_{e^+\mu^+\mu^-}$)) at CMS energy of $E_{CMS} = 0.8 \cdot M_Z$ in $Z \to e^+e^-\mu^+\mu^-$ channel to the corresponding one's, that are generated by improved PHOTOS with matrix element (14) installed into it. Spectra generated by PHOTOS are obtained from samples of equal number of $Z \to e^+e^-$ and $Z \to \mu^+\mu^-$ PYTHIA generated decays. Red (dark grey) error bars represent spectra by unmodified PHOTOS [11]. Green (light grey) error bars represent spectra by improved PHOTOS with kernel of extra pair emission given by the formula (42).

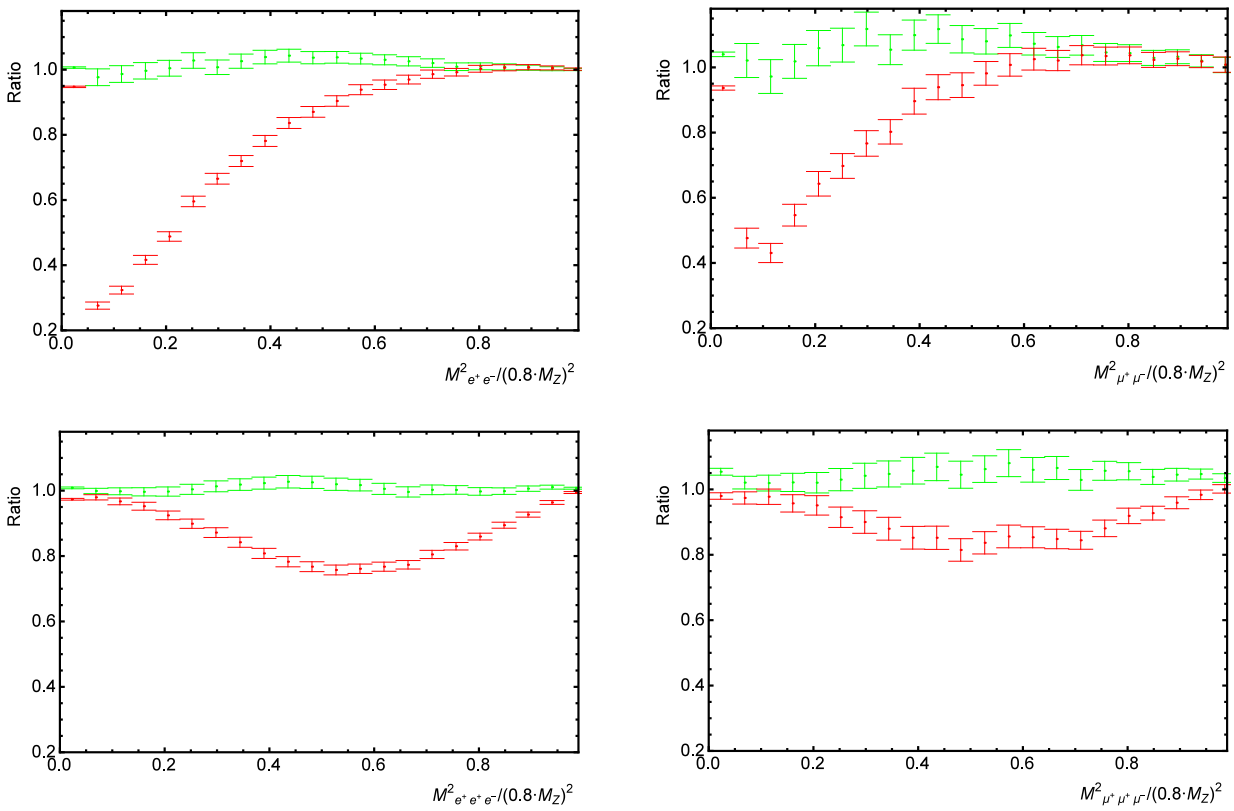

Figure B.26: Ratios of PHOTOS generated spectra (of squared mass of e^+e^- pair ($M^2_{e^+e^-}$), of $\mu^+\mu^-$ pair ($M^2_{\mu^+\mu^-}$), of squared mass of $e^+e^+e^-$ three ($M^2_{e^+e^+e^-}$) and of squared mass of $\mu^+\mu^+\mu^-$ three ($M^2_{\mu^+\mu^+\mu^-}$)) at CMS energy of $E_{CMS} = 0.8\cdot M_Z$ in $Z \to \mu^+\mu^-\mu^+\mu^-$ and $Z \to e^+e^-e^+e^-$ channels to the corresponding one's, that are generated by improved PHOTOS with matrix element (14) installed into it. Spectra generated by PHOTOS are obtained from samples of $Z \to e^+e^-$ and $Z \to \mu^+\mu^-$ PYTHIA generated decays. Red (dark grey) error bars represent spectra by unmodified PHOTOS [11]. Green (light grey) error bars represent spectra by improved PHOTOS with kernel of extra pair emission given by the formula (42).

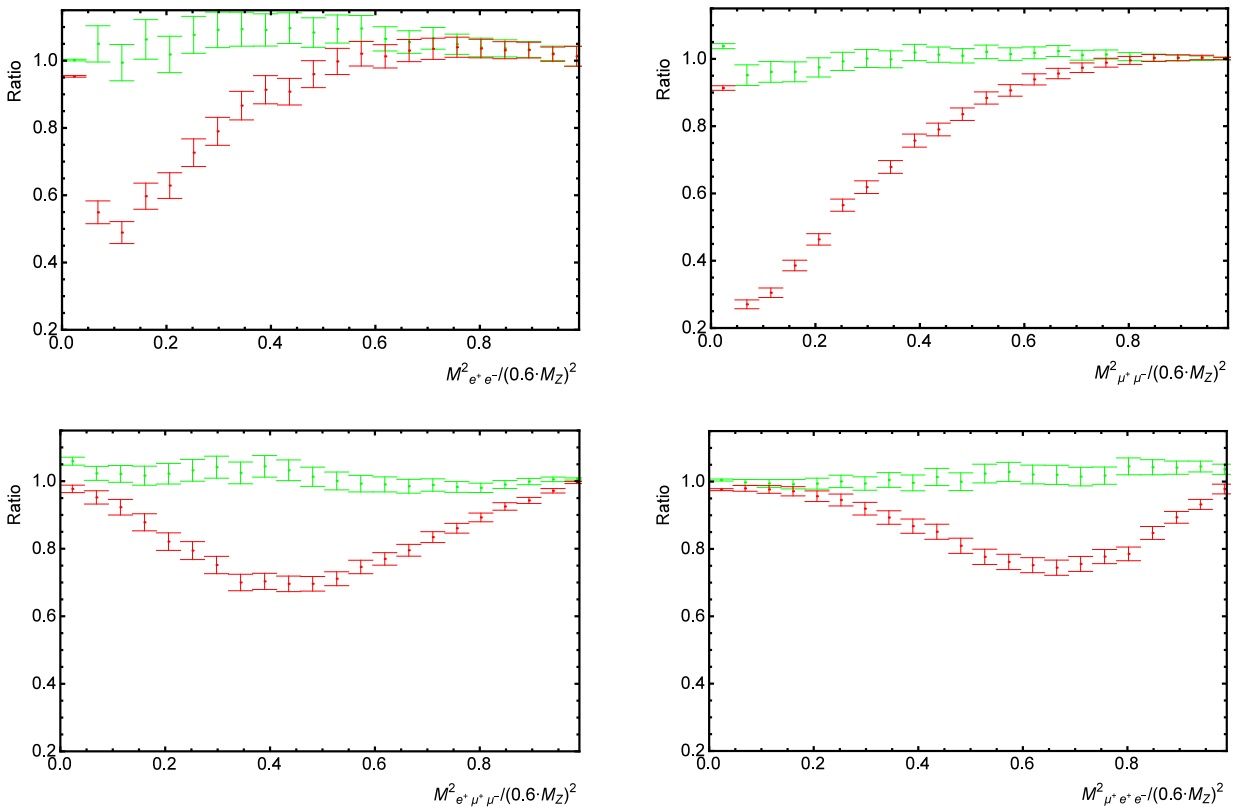

Figure B.27: Ratios of PHOTOS generated spectra (of squared mass of e^+e^- pair ($M^2_{e^+e^-}$), of $\mu^+\mu^-$ pair ($M^2_{\mu^+\mu^-}$), of squared mass of $\mu^+e^+e^-$ three ($M^2_{\mu^+e^+e^-}$) and of squared mass of $e^+\mu^+\mu^-$ three ($M^2_{e^+\mu^+\mu^-}$)) at CMS energy of $E_{CMS} = 0.6 \cdot M_Z$ in $Z \to e^+e^-\mu^+\mu^-$ channel to the corresponding one's, that are generated by improved PHOTOS with matrix element (14) installed into it. Spectra generated by PHOTOS are obtained from samples of equal number of $Z \to e^+e^-$ and $Z \to \mu^+\mu^-$ PYTHIA generated decays. Red (dark grey) error bars represent spectra by unmodified PHOTOS [11]. Green (light grey) error bars represent spectra by improved PHOTOS with kernel of extra pair emission given by the formula (42).

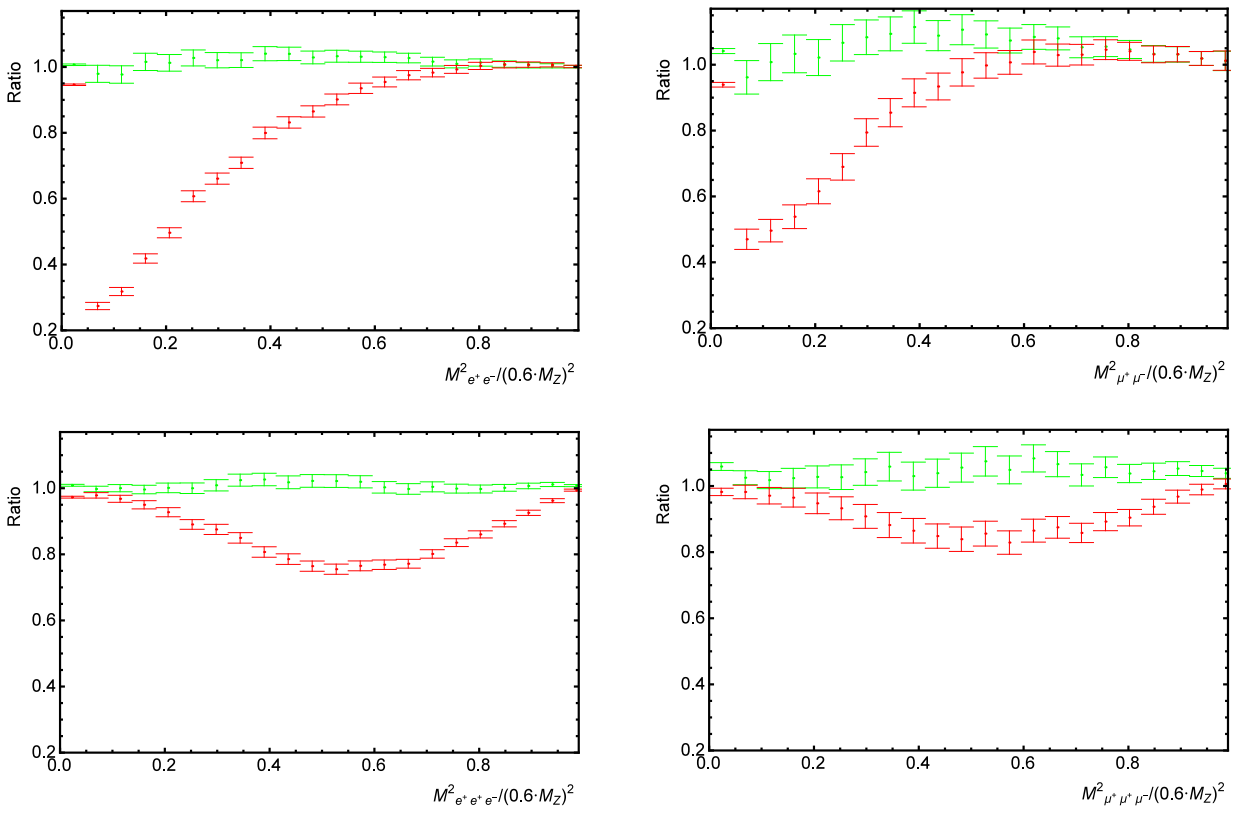

Figure B.28: Ratios of PHOTOS generated spectra (of squared mass of e^+e^- pair ($M^2_{e^+e^-}$), of $\mu^+\mu^-$ pair ($M^2_{\mu^+\mu^-}$), of squared mass of $e^+e^+e^-$ three ($M^2_{e^+e^+e^-}$) and of squared mass of $\mu^+\mu^+\mu^-$ three ($M^2_{\mu^+\mu^+\mu^-}$)) at CMS energy of $E_{CMS} = 0.6\cdot M_Z$ in $Z \to \mu^+\mu^-\mu^+\mu^-$ and $Z \to e^+e^-e^+e^-$ channels to the corresponding one's, that are generated by improved PHOTOS with matrix element (14) installed into it. Spectra generated by PHOTOS are obtained from samples of $Z \to e^+e^-$ and $Z \to \mu^+\mu^-$ PYTHIA generated decays. Red (dark grey) error bars represent spectra by unmodified PHOTOS [11]. Green (light grey) error bars represent spectra by improved PHOTOS with kernel of extra pair emission given by the formula (42).

B.4 Effective factorization of matrix element, plots

Spectra by PHOTOS with kernel F_{test6} (43) are presented in Figs. B.29-B.33.

Figs. B.29, B.31, B.20 present data in $Z \to e^+e^-e^+e^-$ and $Z \to \mu^+\mu^-\mu^+\mu^-$ channels for beam CMS energies of $E_{CMS} = M_Z$, $0.8 \cdot M_Z$, $0.6 \cdot M_Z$ correspondingly. Figs. B.29, B.31, B.33 present ratios of PHOTOS generated spectra of squared mass of e^+e^- pair ($M^2_{e^+e^-}$), of $\mu^+\mu^-$ pair ($M^2_{\mu^+\mu^-}$), of squared mass of $e^+e^+e^-$ three ($M^2_{e^+e^+e^-}$) and of squared mass of $\mu^+\mu^+\mu^-$ three ($M^2_{\mu^+\mu^+\mu^-}$) to the corresponding one's by PHOTOS with matrix element (14). Agreement between PHOTOS with kernel F_{test4} (41) and PHOTOS with matrix element (14) is good. Numbers of e^+e^- pairs never deviate more than 10% from corresponding numbers of etalon spectra. Numbers of $\mu^+\mu^-$ pairs never deviate more than 5% from corresponding numbers of etalon spectra. Numbers of e^+e^- and $\mu^+\mu^-$ pairs with invariant mass close to beam CMS energy coincide with corresponding numbers of etalon spectra.

Figs. B.30, B.32 present data in $Z \to e^+e^-\mu^+\mu^-$ channel for beam CMS energies of $0.8 \cdot M_Z$, $0.6 \cdot M_Z$ correspondingly. Figs. B.30, B.32 present ratios of PHOTOS generated spectra of squared mass of e^+e^- pair ($M^2_{e^+e^-}$), of $\mu^+\mu^-$ pair ($M^2_{\mu^+\mu^-}$), of squared mass of $\mu^+e^+e^-$ three ($M^2_{\mu^+e^+e^-}$) and of squared mass of $e^+\mu^+\mu^-$ three ($M^2_{e^+\mu^+\mu^-}$) to the corresponding one's by PHOTOS with matrix element (14).

Results of this test are unsatisfying. In each channel disagreement between e^+e^- (or $\mu^+\mu^-$) pair spectrum by PHOTOS with kernel F_{test6} (43) and by PHOTOS with matrix element (14) is up to 125% for some parts of the spectra. However, considered pair spectra ratios for each tested CMS beam energy ($E_{CMS} = 0.6 \cdot M_Z$, $0.8 \cdot M_Z$, M_Z) and in the each channel ($e^+e^-\mu^+\mu^-$, $\mu^+\mu^-\mu^+\mu^-$ and $e^+e^-e^+e^-$) have some remarkable similarities. First, presented in this test, pair spectra ratios fluctuate around 1 for most populated and most important bins of the spectra, that are $M_{pair} \sim E_{CMS}$. Second, derivative of presented pair spectra ratios seems to be constant. All these constants (one for each pair spectra ratio) are the same number for each kind of an extra pair.

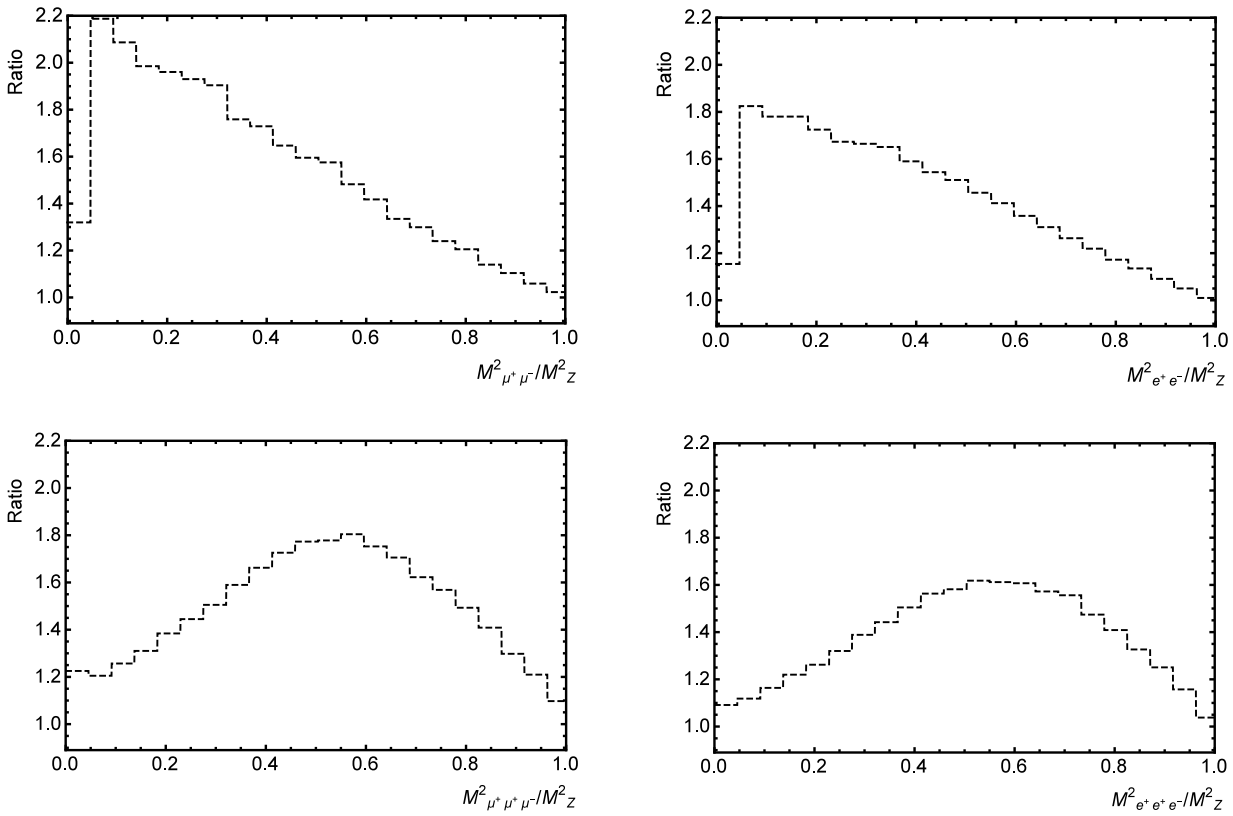

Figure B.29: Ratios of PHOTOS generated spectra (of squared mass of e^+e^- pair ($M^2_{e^+e^-}$), of $\mu^+\mu^-$ pair ($M^2_{\mu^+\mu^-}$), of squared mass of $e^+e^+e^-$ three ($M^2_{e^+e^+e^-}$) and of squared mass of $\mu^+\mu^+\mu^-$ three ($M^2_{\mu^+\mu^+\mu^-}$)) at CMS energy of $E_{CMS} = M_Z$ in $Z \to \mu^+\mu^-\mu^+\mu^-$ and $Z \to e^+e^-e^+e^-$ channels to the corresponding one's, that are generated by improved PHOTOS with matrix element (14) installed into it. Dark dashed line represents spectra by PHOTOS with kernel of extra pair emission given by the formula (43).

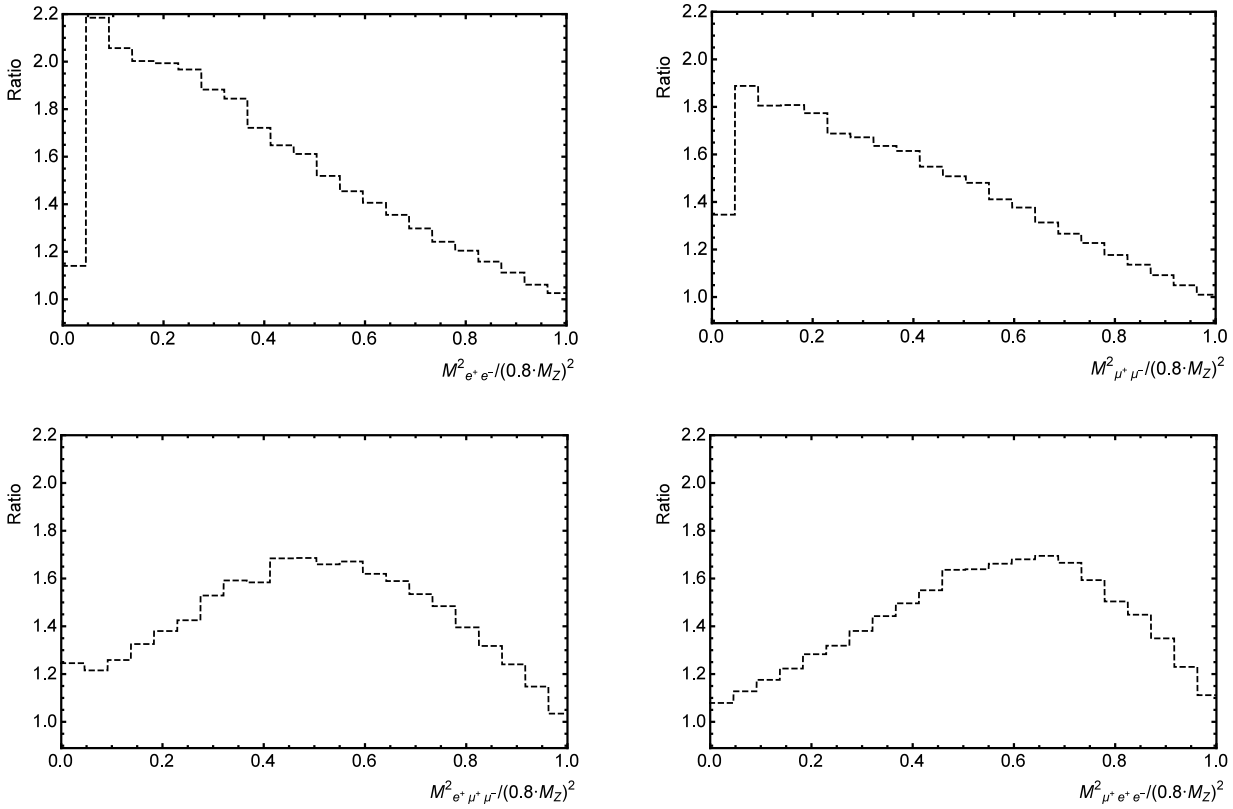

Figure B.30: Ratios of PHOTOS generated spectra (of squared mass of e^+e^- pair ($M^2_{e^+e^-}$), of $\mu^+\mu^-$ pair ($M^2_{\mu^+\mu^-}$), of squared mass of $\mu^+e^+e^-$ three ($M^2_{\mu^+e^+e^-}$) and of squared mass of $e^+\mu^+\mu^-$ three ($M^2_{e^+\mu^+\mu^-}$)) at CMS energy of $E_{CMS} = 0.8 \cdot M_Z$ in $Z \to e^+e^-\mu^+\mu^-$ channel to the corresponding one's, that are generated by improved PHOTOS with matrix element (14) installed into it. Dark dashed line represents spectra by PHOTOS with kernel of extra pair emission given by the formula (43).

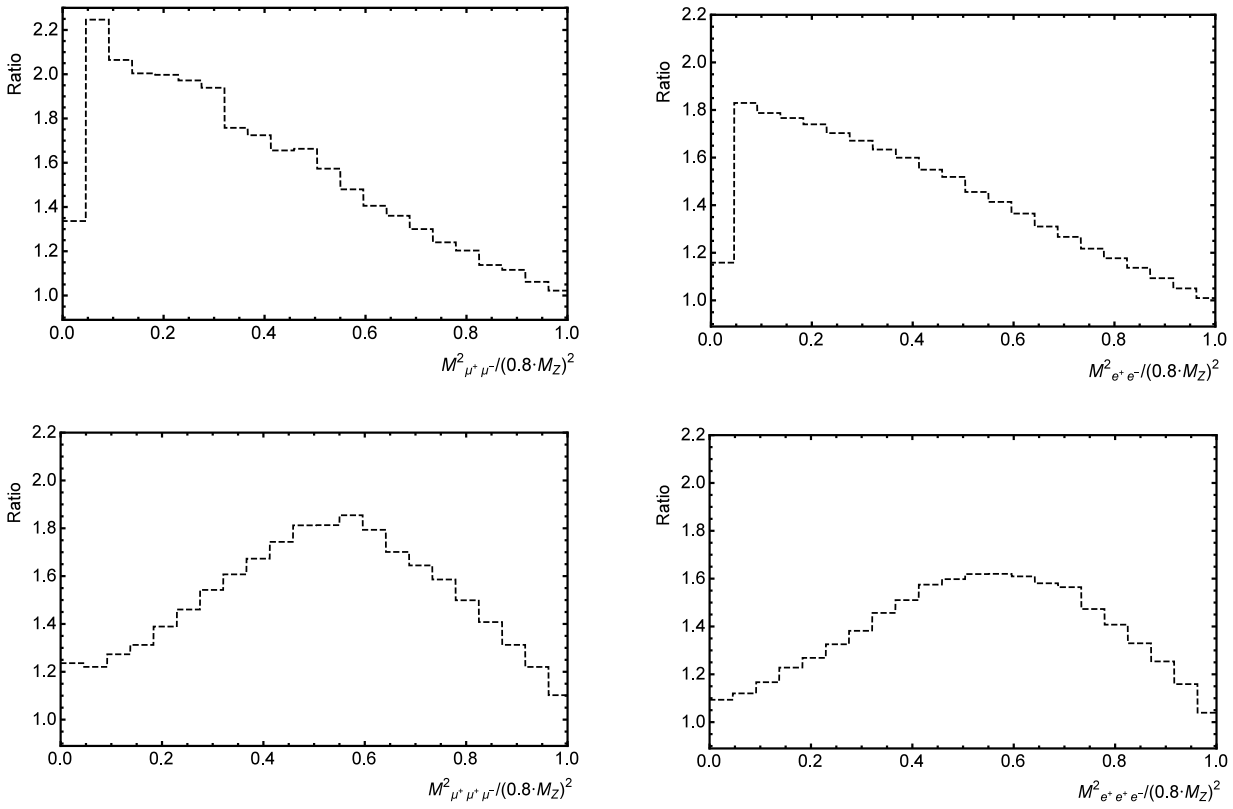

Figure B.31: Ratios of PHOTOS generated spectra (of squared mass of e^+e^- pair ($M^2_{e^+e^-}$), of $\mu^+\mu^-$ pair ($M^2_{\mu^+\mu^-}$), of squared mass of $e^+e^+e^-$ three ($M^2_{e^+e^+e^-}$) and of squared mass of $\mu^+\mu^+\mu^-$ three ($M^2_{\mu^+\mu^+\mu^-}$)) at CMS energy of $E_{CMS} = 0.8\cdot M_Z$ in $Z \to \mu^+\mu^-\mu^+\mu^-$ and $Z \to e^+e^-e^+e^-$ channels to the corresponding one's, that are generated by improved PHOTOS with matrix element (14) installed into it. Dark dashed line represents spectra by PHOTOS with kernel of extra pair emission given by the formula (43).

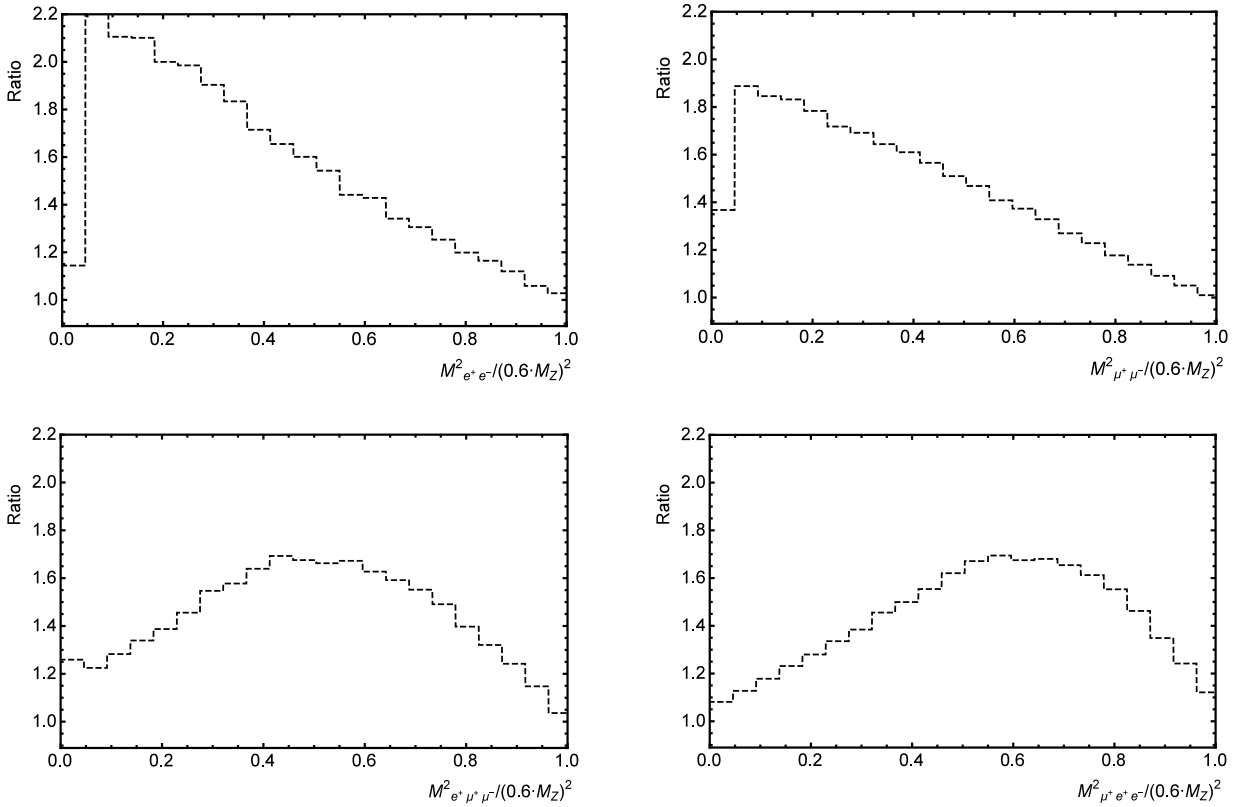

Figure B.32: Ratios of PHOTOS generated spectra (of squared mass of e^+e^- pair ($M^2_{e^+e^-}$), of $\mu^+\mu^-$ pair ($M^2_{\mu^+\mu^-}$), of squared mass of $\mu^+e^+e^-$ three ($M^2_{\mu^+e^+e^-}$) and of squared mass of $e^+\mu^+\mu^-$ three ($M^2_{e^+\mu^+\mu^-}$)) at CMS energy of $E_{CMS} = 0.6 \cdot M_Z$ in $Z \to e^+e^-\mu^+\mu^-$ channel to the corresponding one's, that are generated by improved PHOTOS with matrix element (14) installed into it. Dark dashed line represents spectra by PHOTOS with kernel of extra pair emission given by the formula (43).

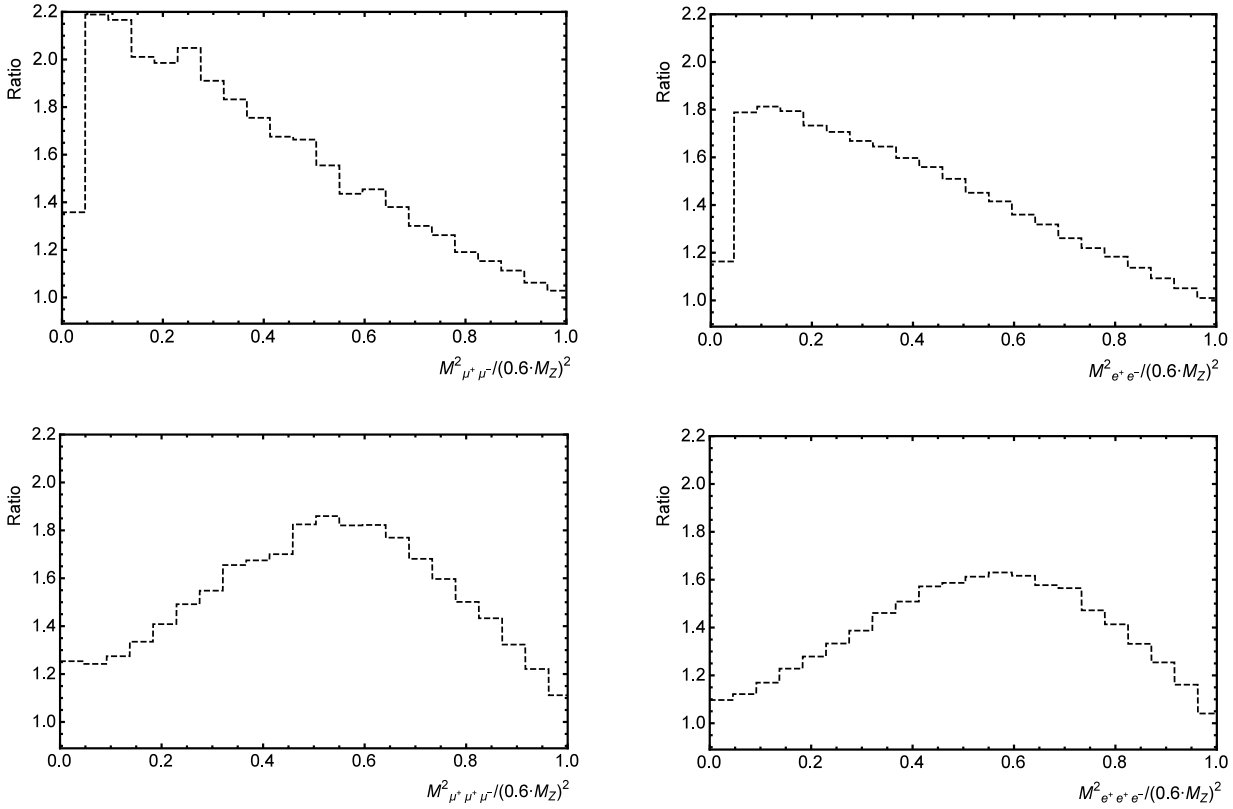

Figure B.33: Ratios of PHOTOS generated spectra (of squared mass of e^+e^- pair ($M^2_{e^+e^-}$), of $\mu^+\mu^-$ pair ($M^2_{\mu^+\mu^-}$), of squared mass of $e^+e^+e^-$ three ($M^2_{e^+e^+e^-}$) and of squared mass of $\mu^+\mu^+\mu^-$ three ($M^2_{\mu^+\mu^+\mu^-}$)) at CMS energy of $E_{CMS} = 0.6\cdot M_Z$ in $Z \to \mu^+\mu^-\mu^+\mu^-$ and $Z \to e^+e^-e^+e^-$ channels to the corresponding one's, that are generated by improved PHOTOS with matrix element (14) installed into it. Dark dashed line represents spectra by PHOTOS with kernel of extra pair emission given by the formula (43).

Spectra by PHOTOS with kernel F_{test7} (44) are presented in Figs. B.34-B.40.

Fig. B.34 present data in $Z \to \mu^+\mu^-\mu^+\mu^-$ channel. Fig. B.34 presents ratios of PHOTOS generated summated spectra of squared mass of $\mu^+\mu^-$ pair ($M^2_{\mu^+\mu^-}$) and of squared mass of $\mu^+\mu^+\mu^-$ three ($\mu^+\mu^+\mu^-$), spectra of squared mass of $\mu^+\mu^+$ pair ($M^2_{\mu^+\mu^+}$), and of $\mu^-\mu^-$ pair ($M^2_{\mu^-\mu^-}$) to the corresponding one's by KORALW. Agreement between PHOTOS with kernel F_{test7} (44) and KORALW is good.

Figs. B.35, B.37, B.39 present data in $Z \to e^+e^-\mu^+\mu^-$ channel for beam CMS energies of $E_{CMS} = M_Z$, $0.8 \cdot M_Z$, $0.6 \cdot M_Z$ correspondingly. Figs. B.35, B.37, B.39 present ratios of PHOTOS generated spectra of squared mass of e^+e^- pair ($M^2_{e^+e^-}$), of $\mu^+\mu^-$ pair ($M^2_{\mu^+\mu^-}$), of squared mass of $\mu^+e^+e^-$ three ($M^2_{\mu^+e^+e^-}$) and of squared mass of $e^+\mu^+\mu^-$ three ($M^2_{e^+\mu^+\mu^-}$) to the corresponding one's by PHOTOS with matrix element (14). Agreement between PHOTOS with kernel ρ_{test7} (44) and PHOTOS with matrix element (14) is good. The ratio of numbers of e^+e^- pairs never differs from 1. more than 10% for all (except one) of the bins, ratio error decreases for the most populated bins $M^2_{e^+e^-} > 0.6 \cdot M^2_Z$. The ratio of numbers of $\mu^+\mu^-$ pairs by PHOTOS and by KORALW never differs from 1. more than 6% for all of the bins, ratio error decreases for the most populated bins $M^2_{\mu^+\mu^-} > 0.6 \cdot M^2_Z$. Such differences rather vanish for most of the bins with statistics increase. It is distinct overproduction (up to 15%) of e^+e^- pairs of a small invariant mass and of the least populated parts of spectra. This overproduction can be neglected since it is for one bin only and such bins are near minimums of the spectra.

Figs. B.36, B.38, B.40 present data in $Z \to e^+e^-e^+e^-$ and $Z \to \mu^+\mu^-\mu^+\mu^-$ channels for beam CMS energies of $E_{CMS} = M_Z$, $0.8 \cdot M_Z$, $0.6 \cdot M_Z$ correspondingly. Figs. B.36, B.38, B.40 present ratios of PHOTOS generated spectra of squared mass of e^+e^- pair ($M^2_{e^+e^-}$), of $\mu^+\mu^-$ pair ($M^2_{\mu^+\mu^-}$), of squared mass of $e^+e^+e^-$ three ($M^2_{e^+e^+e^-}$) and of squared mass of $\mu^+\mu^+\mu^-$ three ($M^2_{\mu^+\mu^+\mu^-}$) to the corresponding one's by PHOTOS with matrix element (14). Agreement between PHOTOS kernel F_{test7} (44) and PHOTOS with matrix element (16) is good. The ratio of numbers of $\mu^+\mu^-$ pairs never differs from 1. more than 10% for all (except one) of the bins, ratio error decreases for the most populated bins $M^2_{\mu^+\mu^-} > 0.6 \cdot M^2_Z$. The ratio of numbers of e^+e^- pairs by PHOTOS and by KORALW never differs from 1. more than 6% for all of the bins, ratio error decreases for the most populated bins $M^2_{e^+e^-} > 0.6 \cdot M^2_Z$. Such differences rather vanish for most of the bins with statistics increase. It is distinct overproduction (up to 15%) of $\mu^+\mu^-$ pairs of a small invariant mass and of the least populated parts of spectra. This overproduction can be neglected since it is for one bin only and such bins are near minimums of the spectra.

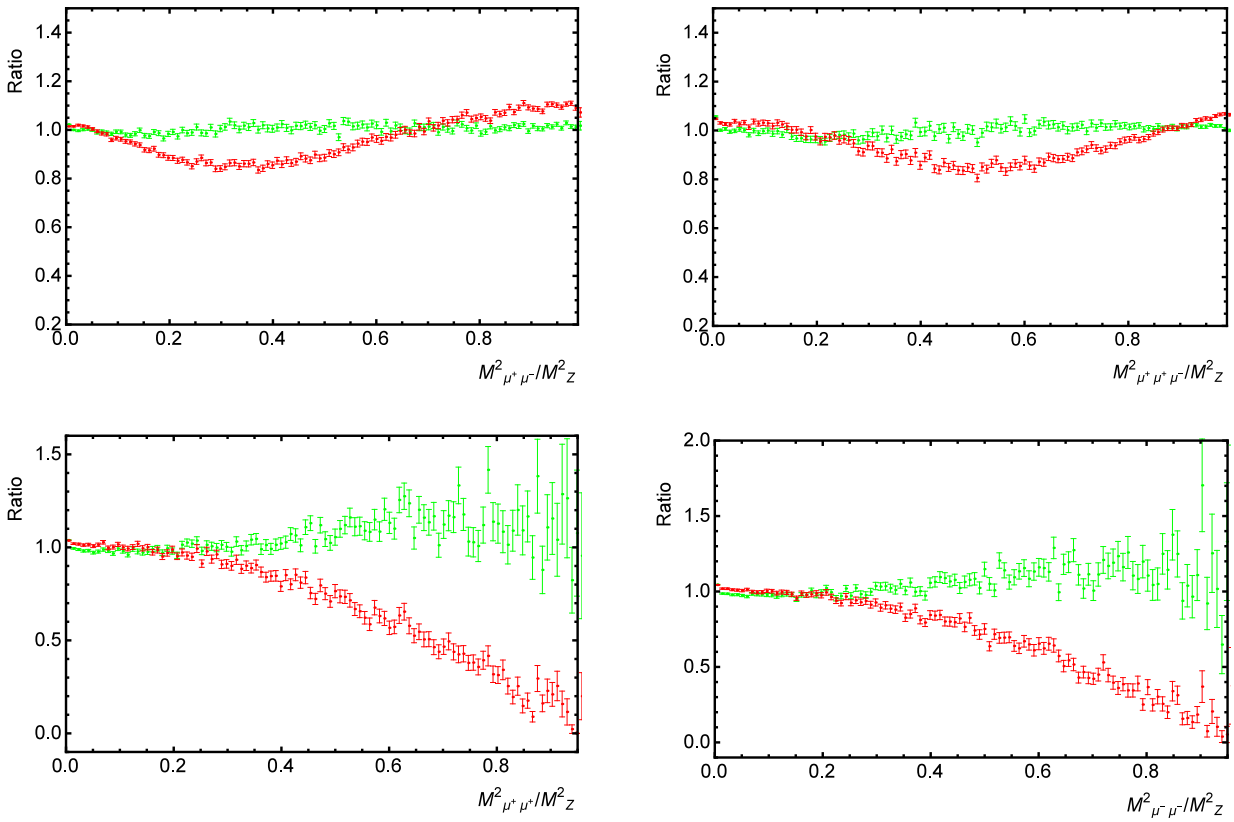

Figure B.34: Ratios of PHOTOS generated spectra (of squared mass of $\mu^+\mu^+\mu^-$ three ($M^2_{\mu^+\mu^+\mu^-}$), of $\mu^+\mu^+$ pair ($M^2_{\mu^+\mu^+}$), of $\mu^-\mu^-$ pair ($M^2_{\mu^-\mu^-}$) and sum of $\mu^+\mu^-$ pair ($M^2_{\mu^+\mu^-}$) spectra) at CMS energy of $E_{CMS} = M_Z$ in $Z \to \mu^+\mu^-\mu^+\mu^-$ channel to the corresponding one's by KORALW. Spectra generated by PHOTOS are obtained from sample of $Z \to \mu^+\mu^-$ PYTHIA generated decays. Red (dark grey) error bars represent spectra by unmodified PHOTOS [11]. Green (light grey) error bars represent spectra by improved PHOTOS with kernel of extra pair emission given by the formula (44).

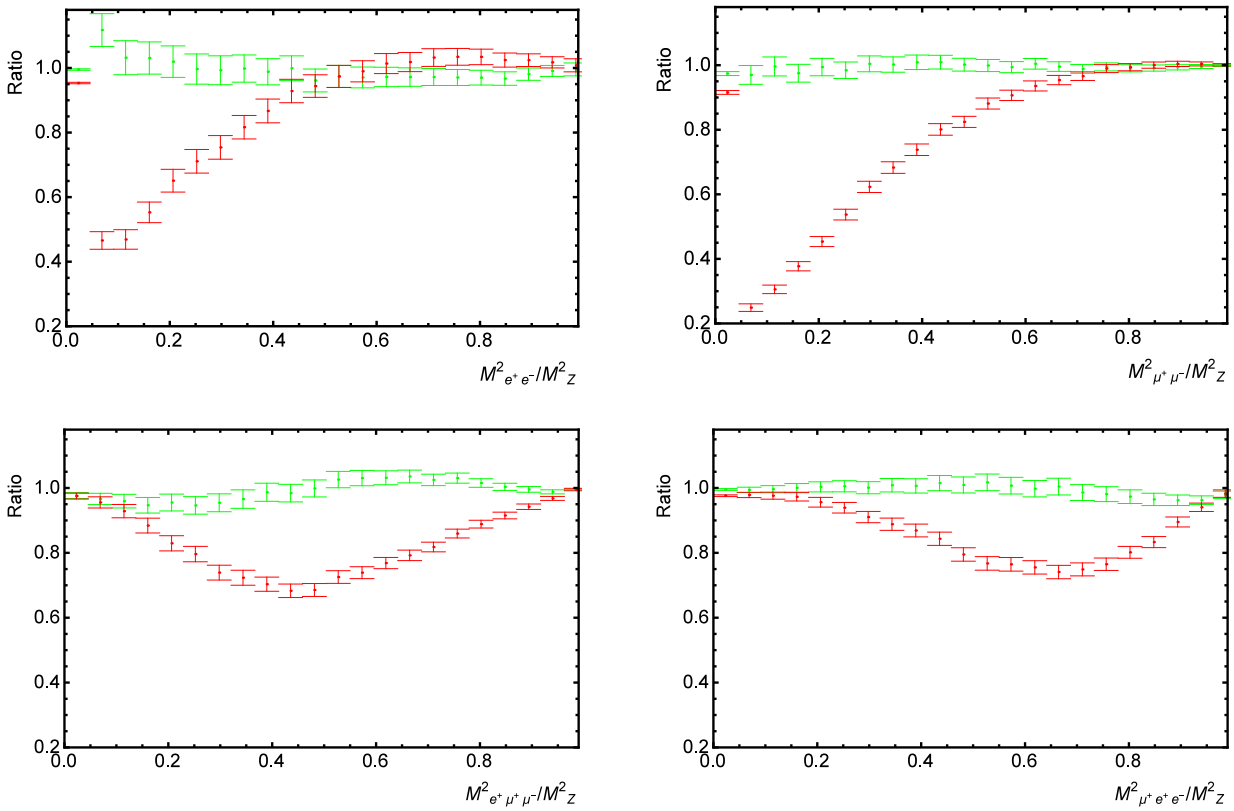

Figure B.35: Ratios of PHOTOS generated spectra (of squared mass of e^+e^- pair ($M^2_{e^+e^-}$), of $\mu^+\mu^-$ pair ($M^2_{\mu^+\mu^-}$), of squared mass of $\mu^+e^+e^-$ three ($M^2_{\mu^+e^+e^-}$) and of squared mass of $e^+\mu^+\mu^-$ three ($M^2_{e^+\mu^+\mu^-}$)) at CMS energy of $E_{CMS} = M_Z$ in the $Z \to \mu^+\mu^-e^+e^-$ channel to the corresponding one's, that are generated by improved PHOTOS with matrix element (14) installed into it. Spectra generated by PHOTOS are obtained from samples of equal number of $Z \to e^+e^-$ and $Z \to \mu^+\mu^-$ PYTHIA generated decays. Red (dark grey) error bars represent spectra by unmodified PHOTOS [11]. Green (light grey) error bars represent spectra by improved PHOTOS with kernel of extra pair emission given by the formula (44).

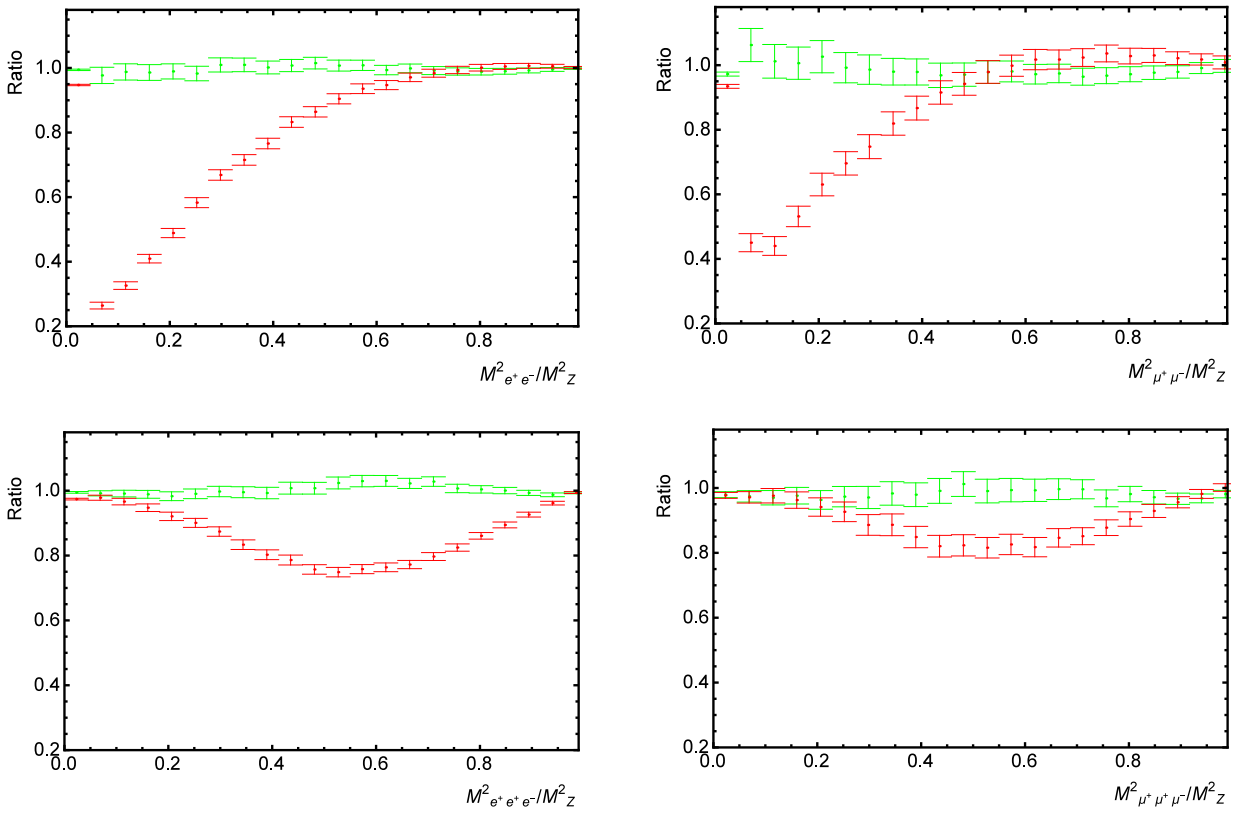

Figure B.36: Ratios of PHOTOS generated spectra (of squared mass of e^+e^- pair ($M^2_{e^+e^-}$), of $\mu^+\mu^-$ pair ($M^2_{\mu^+\mu^-}$), of squared mass of $e^+e^+e^-$ three ($M^2_{e^+e^+e^-}$) and of squared mass of $\mu^+\mu^+\mu^-$ three ($M^2_{\mu^+\mu^+\mu^-}$)) at CMS energy of $E_{CMS} = M_Z$ in $Z \to \mu^+\mu^-\mu^+\mu^-$ and $Z \to e^+e^-e^+e^-$ channels to the corresponding one's, that are generated by improved PHOTOS with matrix element (14) installed into it. Spectra generated by PHOTOS are obtained from samples of $Z \to e^+e^-$ and $Z \to \mu^+\mu^-$ PYTHIA generated decays. Red (dark grey) error bars represent spectra by unmodified PHOTOS [11]. Green (light grey) error bars represent spectra by improved PHOTOS with kernel of extra pair emission given by the formula (44).

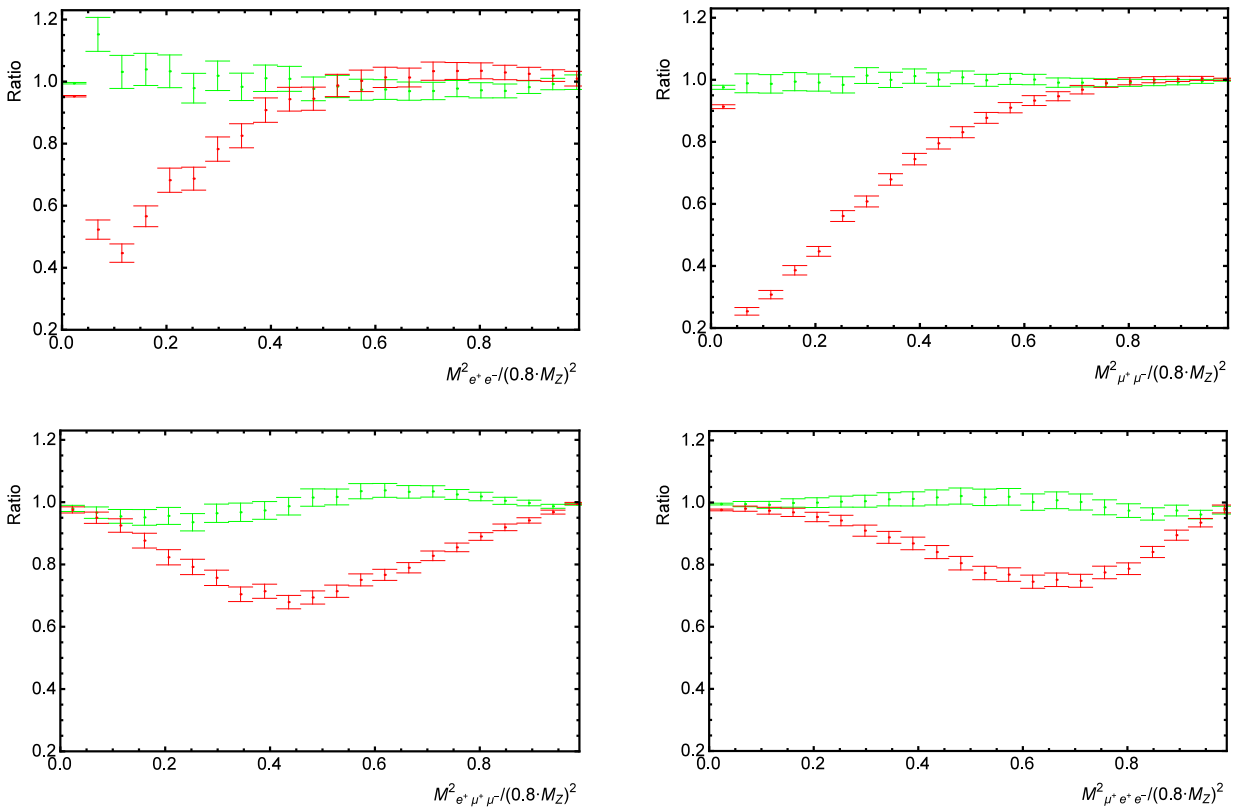

Figure B.37: Ratios of PHOTOS generated spectra (of squared mass of e^+e^- pair ($M^2_{e^+e^-}$), of $\mu^+\mu^-$ pair ($M^2_{\mu^+\mu^-}$), of squared mass of $\mu^+e^+e^-$ three ($M^2_{\mu^+e^+e^-}$) and of squared mass of $e^+\mu^+\mu^-$ three ($M^2_{e^+\mu^+\mu^-}$)) at CMS energy of $E_{CMS} = 0.8 \cdot M_Z$ in the $Z \to \mu^+\mu^-e^+e^-$ channel to the corresponding one's, that are generated by improved PHOTOS with matrix element (14) installed into it. Spectra generated by PHOTOS are obtained from samples of equal number of $Z \to e^+e^-$ and $Z \to \mu^+\mu^-$ PYTHIA generated decays. Red (dark grey) error bars represent spectra by unmodified PHOTOS [11]. Green (light grey) error bars represent spectra by improved PHOTOS with kernel of extra pair emission given by the formula (44).

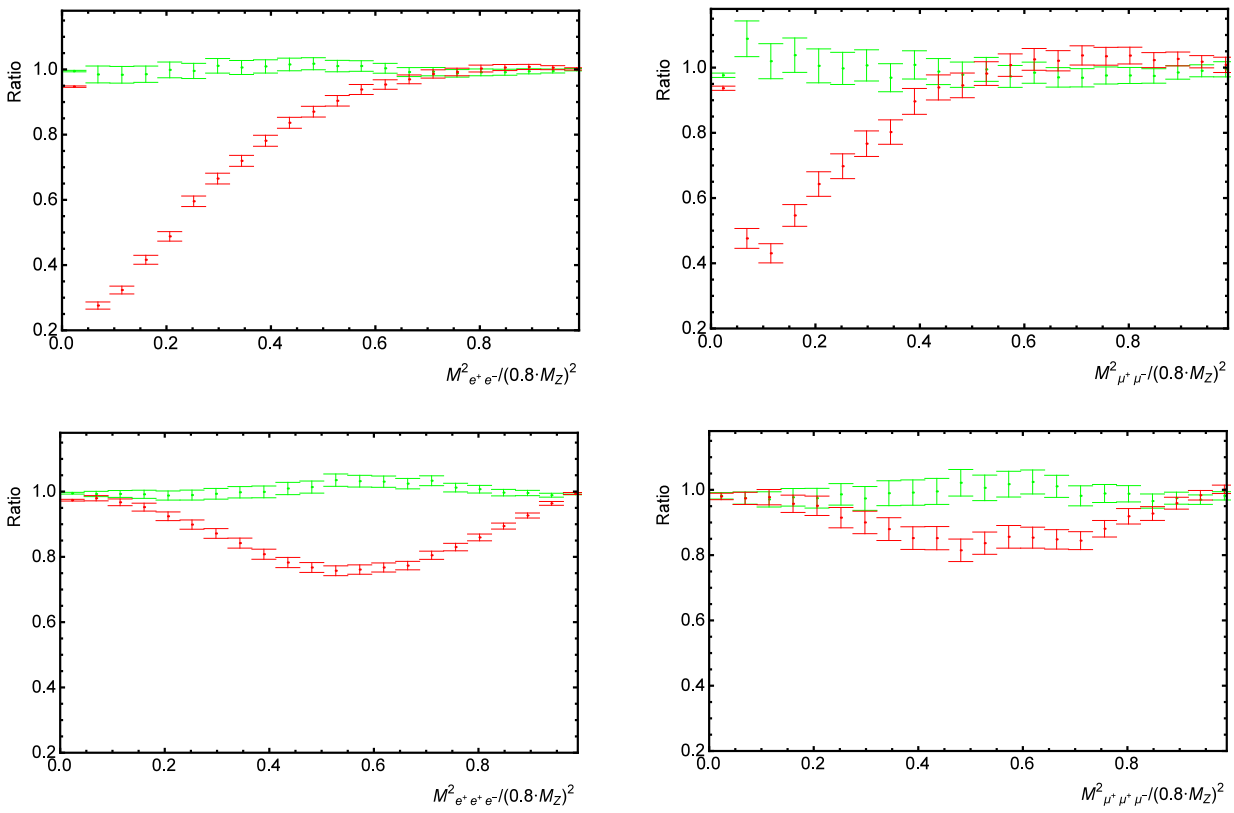

Figure B.38: Ratios of PHOTOS generated spectra (of squared mass of e^+e^- pair ($M^2_{e^+e^-}$), of $\mu^+\mu^-$ pair ($M^2_{\mu^+\mu^-}$), of squared mass of $e^+e^+e^-$ three ($M^2_{e^+e^+e^-}$) and of squared mass of $\mu^+\mu^+\mu^-$ three ($M^2_{\mu^+\mu^+\mu^-}$)) at CMS energy of $E_{CMS} = 0.8\cdot M_Z$ in $Z \to \mu^+\mu^-\mu^+\mu^-$ and $Z \to e^+e^-e^+e^-$ channels to the corresponding one's, that are generated by improved PHOTOS with matrix element (14) installed into it. Spectra generated by PHOTOS are obtained from samples of $Z \to e^+e^-$ and $Z \to \mu^+\mu^-$ PYTHIA generated decays. Red (dark grey) error bars represent spectra by unmodified PHOTOS [11]. Green (light grey) error bars represent spectra by improved PHOTOS with kernel of extra pair emission given by the formula (44).

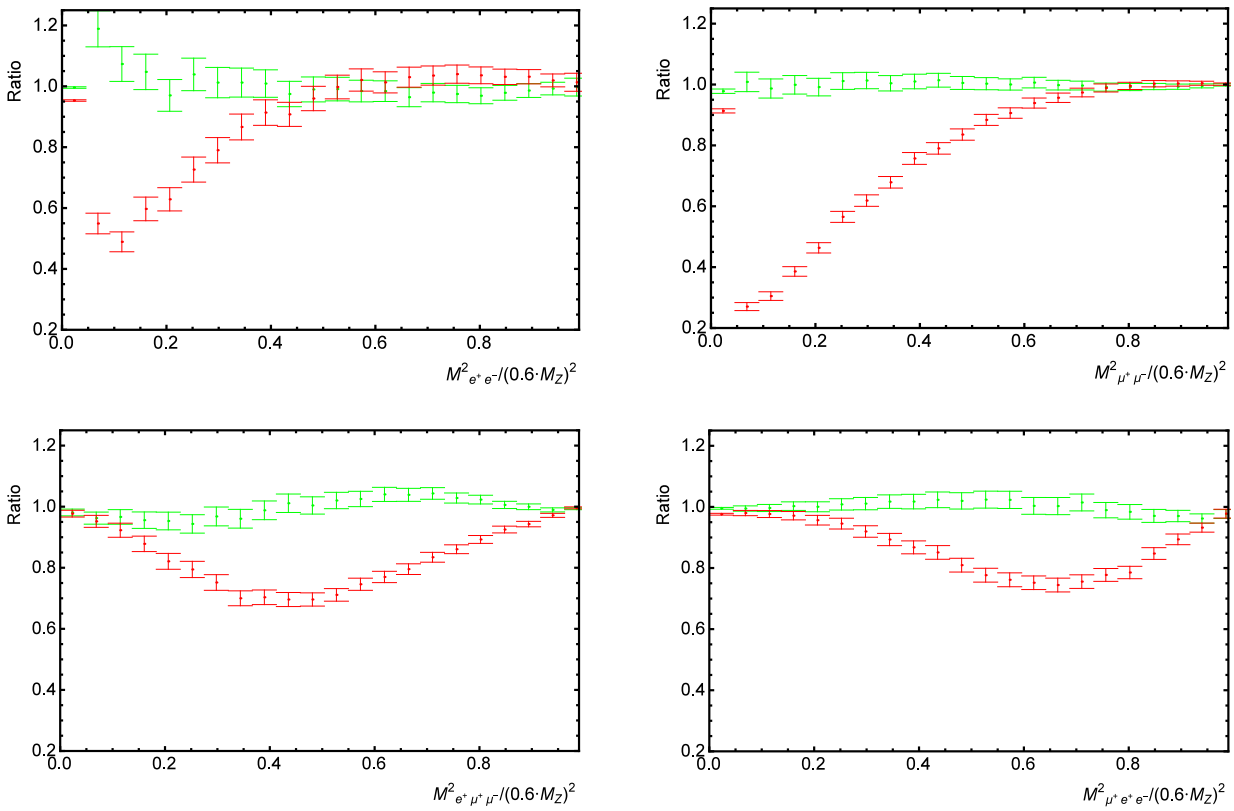

Figure B.39: Ratios of PHOTOS generated spectra (of squared mass of e^+e^- pair ($M^2_{e^+e^-}$), of $\mu^+\mu^-$ pair ($M^2_{\mu^+\mu^-}$), of squared mass of $\mu^+e^+e^-$ three ($M^2_{\mu^+e^+e^-}$) and of squared mass of $e^+\mu^+\mu^-$ three ($M^2_{e^+\mu^+\mu^-}$)) at CMS energy of $E_{CMS} = 0.6 \cdot M_Z$ in the $Z \to \mu^+\mu^-e^+e^-$ channel to the corresponding one's, that are generated by improved PHOTOS with matrix element (14) installed into it. Spectra generated by PHOTOS are obtained from samples of equal number of $Z \to e^+e^-$ and $Z \to \mu^+\mu^-$ PYTHIA generated decays. Red (dark grey) error bars represent spectra by unmodified PHOTOS [11]. Green (light grey) error bars represent spectra by improved PHOTOS with kernel of extra pair emission given by the formula (44).

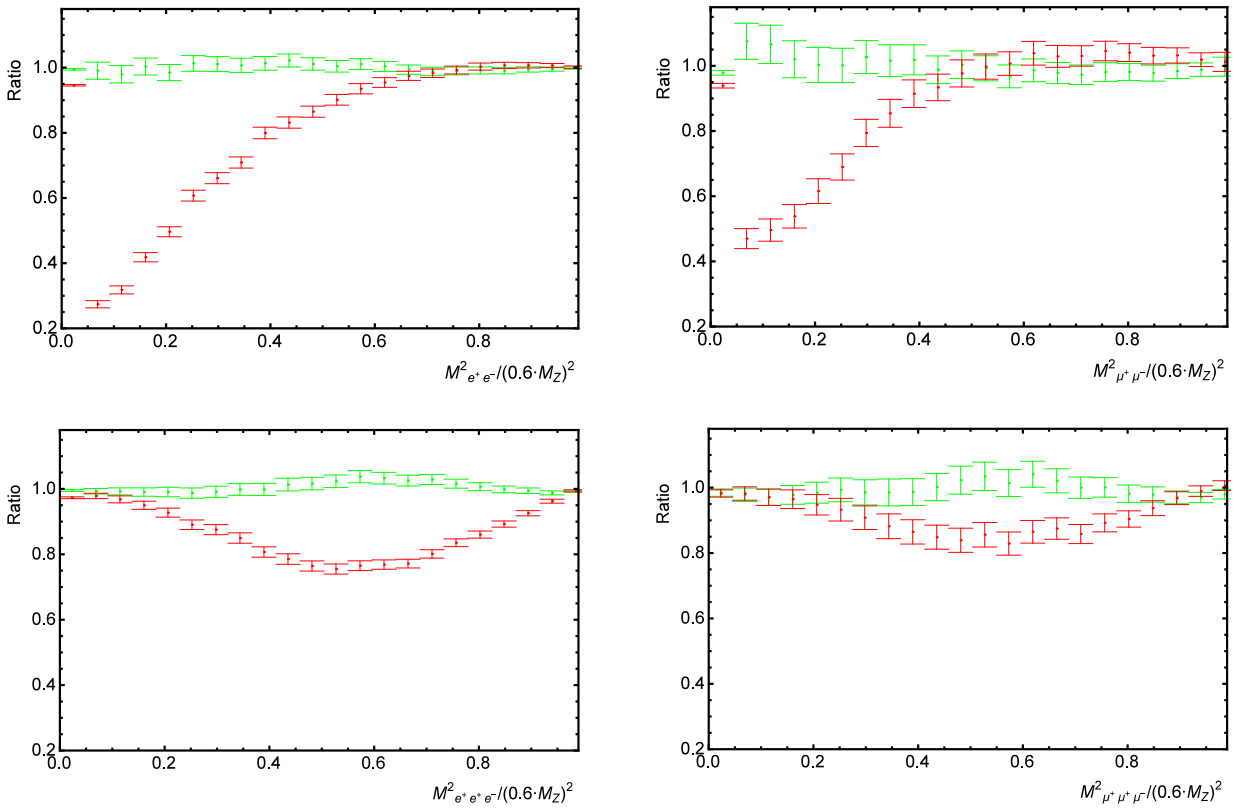

Figure B.40: Ratios of PHOTOS generated spectra (of squared mass of e^+e^- pair ($M^2_{e^+e^-}$), of $\mu^+\mu^-$ pair ($M^2_{\mu^+\mu^-}$), of squared mass of $e^+e^+e^-$ three ($M^2_{e^+e^+e^-}$) and of squared mass of $\mu^+\mu^+\mu^-$ three ($M^2_{\mu^+\mu^+\mu^-}$)) at CMS energy of $E_{CMS} = 0.6\cdot M_Z$ in $Z \to \mu^+\mu^-\mu^+\mu^-$ and $Z \to e^+e^-e^+e^-$ channels to the corresponding one's, that are generated by improved PHOTOS with matrix element (14) installed into it. Spectra generated by PHOTOS are obtained from samples of $Z \to e^+e^-$ and $Z \to \mu^+\mu^-$ PYTHIA generated decays. Red (dark grey) error bars represent spectra by unmodified PHOTOS [11]. Green (light grey) error bars represent spectra by improved PHOTOS with kernel of extra pair emission given by the formula (44).

C Formulae

C.1 Calculation of matrix element

In the following calculations in general I use notations of [46].

$$iM_1 = (-ie)\,\bar{v}\,(p_2)\,\gamma^\mu u\,(p_1)\,\frac{-i\left(g_{\mu\nu}+(1-\xi)\frac{k_\mu k_\nu}{k^2}\right)}{(p_1+p_2)^2}\,(-ie)\,\bar{u}\,(p_3)\,\gamma^\nu\frac{-i\,(\not{p}_4+\not{q}-m_2)}{(p_4+q)^2-m_2^2}\times$$
$$\times\,(-ie)\,\gamma^\alpha v\,(p_4)\,\frac{-i\left(g_{\mu\nu}+(1-\xi)\frac{k_\mu k_\nu}{k^2}\right)}{q^2}\,(-ie)\,\bar{u}\,(p_5)\,\gamma^\beta v\,(p_6)$$

$$iM_2 = (-ie)\,\bar{v}\,(p_2)\,\gamma^\mu u\,(p_1)\,\frac{-i\left(g_{\mu\nu}+(1-\xi)\frac{k_\mu k_\nu}{k^2}\right)}{(p_1+p_2)^2}\,(-ie)\,\bar{u}\,(p_3)\,\gamma^\alpha\frac{i\,(\not{p}_3+\not{q}+m_2)}{(p_3+q)^2-m_2^2}\times$$
$$\times\,(-ie)\,\gamma^\nu v\,(p_4)\,\frac{-i\left(g_{\mu\nu}+(1-\xi)\frac{k_\mu k_\nu}{k^2}\right)}{q^2}\,(-ie)\,\bar{u}\,(p_5)\,\gamma^\beta v\,(p_6)$$

$$iM_3 = (-ie)\,\bar{v}\,(p_2)\,\gamma^\mu u\,(p_1)\,\frac{-i\left(g_{\mu\nu}+(1-\xi)\frac{k_\mu k_\nu}{k^2}\right)}{(p_1+p_2)^2}\,(-ie)\,\bar{u}\,(p_5)\,\gamma^\nu\frac{-i\,(\not{p}_6+\not{q}_2-m_3)}{(p_6+q)^2-m_3^2}\times$$
$$\times\,(-ie)\,\gamma^\alpha v\,(p_6)\,\frac{-i\left(g_{\mu\nu}+(1-\xi)\frac{k_\mu k_\nu}{k^2}\right)}{q_2^2}\,(-ie)\,\bar{u}\,(p_3)\,\gamma^\beta v\,(p_4)$$

$$iM_4 = (-ie)\,\bar{v}\,(p_2)\,\gamma^\mu u\,(p_1)\,\frac{-i\left(g_{\mu\nu}+(1-\xi)\frac{k_\mu k_\nu}{k^2}\right)}{(p_1+p_2)^2}\,(-ie)\,\bar{u}\,(p_5)\,\gamma^\alpha\frac{i\,(\not{p}_5+\not{q}_2+m_3)}{(p_5+q_2)^2-m_3^2}\times$$
$$\times\,(-ie)\,\gamma^\nu v\,(p_4)\,\frac{-i\left(g_{\mu\nu}+(1-\xi)\frac{k_\mu k_\nu}{k^2}\right)}{q_2^2}\,(-ie)\,\bar{u}\,(p_3)\,\gamma^\beta v\,(p_4)$$

Here I switch to Feynman gauge, i.e. $\xi = 1$.

$$M_1+M_2+M_3+M_4 = \frac{-e^4}{(p_1+p_2)^2\,q^2}\,[\bar{v}\,(p_2)\,\gamma_\mu u\,(p_1)]\times$$
$$\times\left[\bar{u}\,(p_3)\left(\gamma^\alpha\frac{\not{p}_3+\not{q}+m_2}{(p_3+q)^2-m_2^2}\gamma^\mu-\gamma^\mu\frac{\not{p}_4+\not{q}-m_2}{(p_4+q)^2-m_2^2}\gamma^\alpha\right)v\,(p_4)\right][\bar{u}\,(p_5)\,\gamma_\alpha v\,(p_6)]+$$
$$+\,\frac{-e^4}{(p_1+p_2)^2\,q_2^2}\,[\bar{v}\,(p_2)\,\gamma_\mu u\,(p_1)]\times$$

$$\times\left[\bar{u}\left(p_5\right)\left(\gamma^{\alpha}\frac{\not{p}_5+\not{q}_2+m_3}{\left(p_5+q_2\right)^2-m_3^2}\gamma^{\mu}-\gamma^{\mu}\frac{\not{p}_6+\not{q}_2-m_3}{\left(p_6+q_2\right)^2-m_3^2}\gamma^{\alpha}\right)\upsilon\left(p_6\right)\right]\left[\bar{u}\left(p_3\right)\gamma_{\alpha}\upsilon\left(p_4\right)\right]$$

$$\left(M_1+M_2+M_3+M_4\right)^{\dagger}=\frac{-e^4}{\left(p_1+p_2\right)^2q^2}\left[\bar{\upsilon}\left(p_6\right)\gamma_{\alpha}u\left(p_5\right)\right]\times$$
$$\times\left[\bar{\upsilon}\left(p_4\right)\left(\gamma^{\mu}\frac{\not{p}_3+\not{q}+m_2}{\left(p_3+q\right)^2-m_2^2}\gamma^{\alpha}-\gamma^{\alpha}\frac{\not{p}_4+\not{q}-m_2}{\left(p_4+q\right)^2-m_2^2}\gamma^{\mu}\right)u\left(p_3\right)\right]\left[\bar{u}\left(p_1\right)\gamma_{\mu}\upsilon\left(p_2\right)\right]+$$
$$+\frac{-e^4}{\left(p_1+p_2\right)^2q_2^2}\left[\bar{\upsilon}\left(p_4\right)\gamma_{\alpha}u\left(p_3\right)\right]\times$$
$$\times\left[\bar{\upsilon}\left(p_6\right)\left(\gamma^{\mu}\frac{\not{p}_5+\not{q}_2+m_3}{\left(p_5+q_2\right)^2-m_3^2}\gamma^{\alpha}-\gamma^{\alpha}\frac{\not{p}_6+\not{q}_2-m_3}{\left(p_6+q_2\right)^2-m_3^2}\gamma^{\mu}\right)u\left(p_5\right)\right]\left[\bar{u}\left(p_1\right)\gamma_{\mu}\upsilon\left(p_2\right)\right]$$

$$\left|M_1+M_2+M_3+M_4\right|^2=\frac{e^8}{\left(p_1+p_2\right)^4}\times$$
$$\times\left\{\frac{1}{q^4}\left[\bar{\upsilon}\left(p_2\right)\gamma_{\mu}u\left(p_1\right)\right]\left[\bar{u}\left(p_3\right)\left(\gamma^{\alpha}\frac{\not{p}_3+\not{q}+m_2}{\left(p_3+q\right)^2-m_2^2}\gamma^{\mu}-\gamma^{\mu}\frac{\not{p}_4+\not{q}-m_2}{\left(p_4+q\right)^2-m_2^2}\gamma^{\alpha}\right)\upsilon\left(p_4\right)\right]\left[\bar{u}\left(p_5\right)\gamma_{\alpha}\upsilon\left(p_6\right)\right]\times\right.$$
$$\times\left[\bar{\upsilon}\left(p_6\right)\gamma_{\beta}u\left(p_5\right)\right]\left[\bar{\upsilon}\left(p_4\right)\left(\gamma^{\nu}\frac{\not{p}_3+\not{q}+m_2}{\left(p_3+q\right)^2-m_2^2}\gamma^{\beta}-\gamma^{\beta}\frac{\not{p}_4+\not{q}-m_2}{\left(p_4+q\right)^2-m_2^2}\gamma^{\nu}\right)u\left(p_3\right)\right]\left[\bar{u}\left(p_1\right)\gamma_{\nu}\upsilon\left(p_2\right)\right]+$$
$$+\frac{1}{q_2^4}\left[\bar{\upsilon}\left(p_2\right)\gamma_{\mu}u\left(p_1\right)\right]\left[\bar{u}\left(p_5\right)\left(\gamma^{\alpha}\frac{\not{p}_5+\not{q}_2+m_3}{\left(p_5+q_2\right)^2-m_3^2}\gamma^{\mu}-\gamma^{\mu}\frac{\not{p}_6+\not{q}_2-m_3}{\left(p_6+q_2\right)^2-m_3^2}\gamma^{\alpha}\right)\upsilon\left(p_6\right)\right]\left[\bar{u}\left(p_3\right)\gamma_{\alpha}\upsilon\left(p_4\right)\right]\times$$
$$\times\left[\bar{\upsilon}\left(p_4\right)\gamma_{\beta}u\left(p_3\right)\right]\left[\bar{\upsilon}\left(p_6\right)\left(\gamma^{\nu}\frac{\not{p}_5+\not{q}_2+m_3}{\left(p_5+q_2\right)^2-m_3^2}\gamma^{\beta}-\gamma^{\beta}\frac{\not{p}_6+\not{q}_2-m_3}{\left(p_6+q_2\right)^2-m_3^2}\gamma^{\nu}\right)u\left(p_5\right)\right]\left[\bar{u}\left(p_1\right)\gamma_{\nu}\upsilon\left(p_2\right)\right]+$$
$$\frac{1}{q^2q_2^2}\left[\bar{\upsilon}\left(p_2\right)\gamma_{\mu}u\left(p_1\right)\right]\left[\bar{u}\left(p_3\right)\left(\gamma^{\alpha}\frac{\not{p}_3+\not{q}+m_2}{\left(p_3+q\right)^2-m_2^2}\gamma^{\mu}-\gamma^{\mu}\frac{\not{p}_4+\not{q}-m_2}{\left(p_4+q\right)^2-m_2^2}\gamma^{\alpha}\right)\upsilon\left(p_4\right)\right]\left[\bar{u}\left(p_5\right)\gamma_{\alpha}\upsilon\left(p_6\right)\right]\times$$
$$\times\left[\bar{\upsilon}\left(p_6\right)\left(\gamma^{\nu}\frac{\not{p}_5+\not{q}_2+m_3}{\left(p_5+q_2\right)^2-m_3^2}\gamma^{\beta}-\gamma^{\beta}\frac{\not{p}_6+\not{q}_2-m_3}{\left(p_6+q_2\right)^2-m_3^2}\gamma^{\nu}\right)u\left(p_5\right)\right]\left[\bar{\upsilon}\left(p_4\right)\gamma_{\beta}u\left(p_3\right)\right]\left[\bar{u}\left(p_1\right)\gamma_{\nu}\upsilon\left(p_2\right)\right]+$$
$$\frac{1}{q^2q_2^2}\left[\bar{\upsilon}\left(p_2\right)\gamma_{\mu}u\left(p_1\right)\right]\left[\bar{u}\left(p_5\right)\left(\gamma^{\alpha}\frac{\not{p}_5+\not{q}_2+m_3}{\left(p_5+q_2\right)^2-m_3^2}\gamma^{\mu}-\gamma^{\mu}\frac{\not{p}_6+\not{q}_2-m_3}{\left(p_6+q_2\right)^2-m_3^2}\gamma^{\alpha}\right)\upsilon\left(p_6\right)\right]\left[\bar{u}\left(p_3\right)\gamma_{\alpha}\upsilon\left(p_4\right)\right]\times$$
$$\left.\times\left[\bar{\upsilon}\left(p_4\right)\left(\gamma^{\nu}\frac{\not{p}_3+\not{q}+m_2}{\left(p_3+q\right)^2-m_2^2}\gamma^{\beta}-\gamma^{\beta}\frac{\not{p}_4+\not{q}-m_2}{\left(p_4+q\right)^2-m_2^2}\gamma^{\nu}\right)u\left(p_3\right)\right]\left[\bar{\upsilon}\left(p_6\right)\gamma_{\beta}u\left(p_5\right)\right]\left[\bar{u}\left(p_1\right)\gamma_{\nu}\upsilon\left(p_2\right)\right]\right\}\quad\text{(C.1)}$$

Here I am using following gamma matrices property

$$\gamma^{\mu}\not{p}=-\not{p}\gamma^{\mu}+2p^{\mu}$$

$$\left|M_1+M_2+M_3+M_4\right|^2=\frac{e^8}{\left(p_1+p_2\right)^4}\left\{\frac{1}{q^4}\left[\bar{\upsilon}\left(p_2\right)\gamma_{\mu}u\left(p_1\right)\right]\times\right.$$

$$\times \left[\bar{u}\left(p_3\right)\left(\frac{-\left(\not{p}_3-m_2\right)\gamma^\alpha+2p_3^\alpha+\gamma^\alpha\not{q}}{\left(p_3+q\right)^2-m_2^2}\gamma^\mu-\gamma^\mu\frac{-\gamma^\alpha\left(\not{p}_4+m_2\right)+2p_4^\alpha+\not{q}\gamma^\alpha}{\left(p_4+q\right)^2-m_2^2}\right)\upsilon\left(p_4\right)\right]\times$$

$$\times\left[\bar{u}\left(p_5\right)\gamma_\alpha\upsilon\left(p_6\right)\right]\left[\bar{\upsilon}\left(p_6\right)\gamma_\beta u\left(p_5\right)\right]\left[\bar{\upsilon}\left(p_4\right)\left(\gamma^\nu\frac{-\gamma^\beta\left(\not{p}_3-m_2\right)+2p_3^\beta+\not{q}\gamma^\beta}{\left(p_3+q\right)^2-m_2^2}-\right.\right.$$

$$\left.\left.-\frac{-\left(\not{p}_4+m_2\right)\gamma^\beta+2p_4^\beta+\gamma^\beta\not{q}}{\left(p_4+q\right)^2-m_2^2}\gamma^\nu\right)u\left(p_3\right)\right]\left[\bar{u}\left(p_1\right)\gamma_\nu\upsilon\left(p_2\right)\right]+$$

$$+\frac{1}{q_2^4}\left[\bar{\upsilon}\left(p_2\right)\gamma_\mu u\left(p_1\right)\right]\left[\bar{u}\left(p_5\right)\left(\frac{-\left(\not{p}_5-m_3\right)\gamma^\alpha+2p_5^\alpha+\gamma^\alpha\not{q}_2}{\left(p_5+q_2\right)^2-m_3^2}\gamma^\mu-\right.\right.$$

$$\left.\left.-\gamma^\mu\frac{-\gamma^\alpha\left(\not{p}_6+m_3\right)+2p_6^\alpha+\not{q}_2\gamma^\alpha}{\left(p_6+q_2\right)^2-m_3^2}\right)\upsilon\left(p_6\right)\right]\left[\bar{u}\left(p_3\right)\gamma_\alpha\upsilon\left(p_4\right)\right]\times$$

$$\times\left[\bar{\upsilon}\left(p_4\right)\gamma_\beta u\left(p_3\right)\right]\left[\bar{\upsilon}\left(p_6\right)\left(\gamma^\nu\frac{-\gamma^\beta\left(\not{p}_5-m_3\right)+2p_5^\beta+\not{q}_2\gamma^\beta}{\left(p_5+q_2\right)^2-m_3^2}-\right.\right.$$

$$\left.\left.-\frac{-\left(\not{p}_6+m_3\right)\gamma^\beta+2p_6^\beta+\gamma^\beta\not{q}_2}{\left(p_6+q_2\right)^2-m_3^2}\gamma^\nu\right)u\left(p_5\right)\right]\left[\bar{u}\left(p_1\right)\gamma_\nu\upsilon\left(p_2\right)\right]+$$

$$+\frac{1}{q^2q_2^2}\left[\bar{\upsilon}\left(p_2\right)\gamma_\mu u\left(p_1\right)\right]\left[\bar{u}\left(p_3\right)\left(\frac{-\left(\not{p}_3-m_2\right)\gamma^\alpha+2p_3^\alpha+\gamma^\alpha\not{q}}{\left(p_3+q\right)^2-m_2^2}\gamma^\mu-\right.\right.$$

$$\left.\left.-\gamma^\mu\frac{-\gamma^\alpha\left(\not{p}_4+m_2\right)+2p_4^\alpha+\not{q}\gamma^\alpha}{\left(p_4+q\right)^2-m_2^2}\right)\upsilon\left(p_4\right)\right]\left[\bar{u}\left(p_5\right)\gamma_\alpha\upsilon\left(p_6\right)\right]\times$$

$$\times\left[\bar{\upsilon}\left(p_6\right)\left(\gamma^\nu\frac{-\gamma^\beta\left(\not{p}_5-m_3\right)+2p_5^\beta+\not{q}_2\gamma^\beta}{\left(p_5+q_2\right)^2-m_3^2}-\right.\right.$$

$$\left.\left.-\frac{-\left(\not{p}_6+m_3\right)\gamma^\beta+2p_6^\beta+\gamma^\beta\not{q}_2}{\left(p_6+q_2\right)^2-m_3^2}\gamma^\nu\right)u\left(p_5\right)\right]\left[\bar{\upsilon}\left(p_4\right)\gamma_\beta u\left(p_3\right)\right]\left[\bar{u}\left(p_1\right)\gamma_\nu\upsilon\left(p_2\right)\right]+$$

$$+\frac{1}{q^2q_2^2}\left[\bar{\upsilon}\left(p_2\right)\gamma_\mu u\left(p_1\right)\right]\left[\bar{u}\left(p_5\right)\left(\frac{-\left(\not{p}_5-m_3\right)\gamma^\alpha+2p_5^\alpha+\gamma^\alpha\not{q}_2}{\left(p_5+q_2\right)^2-m_3^2}\gamma^\mu-\right.\right.$$

$$\left.\left.-\gamma^\mu\frac{-\gamma^\alpha\left(\not{p}_6+m_3\right)+2p_6^\alpha+\not{q}_2\gamma^\alpha}{\left(p_6+q_2\right)^2-m_3^2}\right)\upsilon\left(p_6\right)\right]\left[\bar{u}\left(p_3\right)\gamma_\alpha\upsilon\left(p_4\right)\right]\times$$

$$\times\left[\bar{\upsilon}\left(p_4\right)\left(\gamma^\nu\frac{-\gamma^\beta\left(\not{p}_3-m_2\right)+2p_3^\beta+\not{q}\gamma^\beta}{\left(p_3+q\right)^2-m_2^2}-\right.\right.$$

$$\left.\left.-\frac{-\left(\not{p}_4+m_2\right)\gamma^\beta+2p_4^\beta+\gamma^\beta\not{q}}{\left(p_4+q\right)^2-m_2^2}\gamma^\nu\right)u\left(p_3\right)\right]\left[\bar{\upsilon}\left(p_6\right)\gamma_\beta u\left(p_5\right)\right]\left[\bar{u}\left(p_1\right)\gamma_\nu\upsilon\left(p_2\right)\right]\Bigg\} \quad \text{(C.2)}$$

In the above expression (C.2), I've separated terms that fulfill Dirac equation

$$\begin{aligned}(\not{p}-m)\,u\,(p)=0\\(\not{p}+m)\,\upsilon\,(p)=0\\\bar{u}\,(p)\,(\not{p}-m)=0\\\bar{\upsilon}\,(p)\,(\not{p}+m)=0\end{aligned}$$

so these terms immediately vanish

$$\begin{aligned}&|M_1+M_2+M_3+M_4|^2=\frac{e^8}{(p_1+p_2)^4}\times\\&\times\left\{\frac{1}{q^4}\left[\bar{\upsilon}\,(p_2)\,\gamma_\mu u\,(p_1)\right]\left[\bar{u}\,(p_3)\left(\frac{2p_3^\alpha\gamma^\mu+\gamma^\alpha\not{q}\gamma^\mu}{(p_3+q)^2-m_2^2}-\frac{2p_4^\alpha\gamma^\mu+\gamma^\mu\not{q}\gamma^\alpha}{(p_4+q)^2-m_2^2}\right)\upsilon\,(p_4)\right]\left[\bar{u}\,(p_5)\,\gamma_\alpha\upsilon\,(p_6)\right]\times\right.\\&\times\left[\bar{\upsilon}\,(p_6)\,\gamma_\beta u\,(p_5)\right]\left[\bar{\upsilon}\,(p_4)\left(\frac{2p_3^\beta\gamma^\nu+\gamma^\nu\not{q}\gamma^\beta}{(p_3+q)^2-m_2^2}-\frac{2p_4^\beta\gamma^\nu+\gamma^\beta\not{q}\gamma^\nu}{(p_4+q)^2-m_2^2}\right)u\,(p_3)\right]\left[\bar{u}\,(p_1)\,\gamma_\nu\upsilon\,(p_2)\right]+\\&+\frac{1}{q_2^4}\left[\bar{\upsilon}\,(p_2)\,\gamma_\mu u\,(p_1)\right]\left[\bar{u}\,(p_5)\left(\frac{2p_5^\alpha\gamma^\mu+\gamma^\alpha\not{q}_2\gamma^\mu}{(p_5+q_2)^2-m_3^2}-\frac{2p_6^\alpha\gamma^\mu+\gamma^\mu\not{q}_2\gamma^\alpha}{(p_6+q_2)^2-m_3^2}\right)\upsilon\,(p_6)\right]\left[\bar{u}\,(p_3)\,\gamma_\alpha\upsilon\,(p_4)\right]\times\\&\times\left[\bar{\upsilon}\,(p_4)\,\gamma_\beta u\,(p_3)\right]\left[\bar{\upsilon}\,(p_6)\left(\frac{2p_5^\beta\gamma^\nu+\gamma^\nu\not{q}_2\gamma^\beta}{(p_5+q_2)^2-m_3^2}-\frac{2p_6^\beta\gamma^\nu+\gamma^\beta\not{q}_2\gamma^\nu}{(p_6+q_2)^2-m_3^2}\right)u\,(p_5)\right]\left[\bar{u}\,(p_1)\,\gamma_\nu\upsilon\,(p_2)\right]+\\&\frac{1}{q^2q_2^2}\left[\bar{\upsilon}\,(p_2)\,\gamma_\mu u\,(p_1)\right]\left[\bar{u}\,(p_3)\left(\frac{2p_3^\alpha\gamma^\mu+\gamma^\alpha\not{q}\gamma^\mu}{(p_3+q)^2-m_2^2}-\frac{2p_4^\alpha\gamma^\mu+\gamma^\mu\not{q}\gamma^\alpha}{(p_4+q)^2-m_2^2}\right)\upsilon\,(p_4)\right]\left[\bar{u}\,(p_5)\,\gamma_\alpha\upsilon\,(p_6)\right]\times\\&\times\left[\bar{\upsilon}\,(p_6)\left(\frac{2p_5^\beta\gamma^\nu+\gamma^\nu\not{q}_2\gamma^\beta}{(p_5+q_2)^2-m_3^2}-\frac{2p_6^\beta\gamma^\nu+\gamma^\beta\not{q}_2\gamma^\nu}{(p_6+q_2)^2-m_3^2}\right)u\,(p_5)\right]\left[\bar{\upsilon}\,(p_4)\,\gamma_\beta u\,(p_3)\right]\left[\bar{u}\,(p_1)\,\gamma_\nu\upsilon\,(p_2)\right]+\\&\frac{1}{q^2q_2^2}\left[\bar{\upsilon}\,(p_2)\,\gamma_\mu u\,(p_1)\right]\left[\bar{u}\,(p_5)\left(\frac{2p_5^\alpha\gamma^\mu+\gamma^\alpha\not{q}_2\gamma^\mu}{(p_5+q_2)^2-m_3^2}-\frac{2p_6^\alpha\gamma^\mu+\gamma^\mu\not{q}_2\gamma^\alpha}{(p_6+q_2)^2-m_3^2}\right)\upsilon\,(p_6)\right]\left[\bar{u}\,(p_3)\,\gamma_\alpha\upsilon\,(p_4)\right]\times\\&\times\left.\left[\bar{\upsilon}\,(p_4)\left(\frac{2p_3^\beta\gamma^\nu+\gamma^\nu\not{q}\gamma^\beta}{(p_3+q)^2-m_2^2}-\frac{2p_4^\beta\gamma^\nu+\gamma^\beta\not{q}\gamma^\nu}{(p_4+q)^2-m_2^2}\right)u\,(p_3)\right]\left[\bar{\upsilon}\,(p_6)\,\gamma_\beta u\,(p_5)\right]\left[\bar{u}\,(p_1)\,\gamma_\nu\upsilon\,(p_2)\right]\right\}\end{aligned}$$

Next I am applying Casimir's trick. Here is an example of such a calculation for outgoing τ^+,τ^- particles:

$$\begin{aligned}\sum_{spin}u\,(p_5)\,\bar{u}\,(p_5)=\not{p}_5+m_3\\\sum_{spin}\upsilon\,(p_6)\,\bar{\upsilon}\,(p_6)=\not{p}_6-m_3\end{aligned}\tag{C.3}$$

Summation over spins for p_5 creates trace

$$\sum_{spins}\left[\bar{u}\,(p_5)\,\gamma_\alpha\upsilon\,(p_6)\right]\left[\bar{\upsilon}\,(p_6)\,\gamma_\beta u\,(p_5)\right]=\sum_{spins}\bar{u}\,(p_5)\,\gamma_\alpha\,(\not{p}_6-m_3)\,\gamma_\beta u\,(p_5)=Tr\left[(\not{p}_5+m_3)\,\gamma_\alpha\,(\not{p}_6-m_3)\,\gamma_\beta\right]\tag{C.4}$$

I perform step by step summation over spins of all incoming and outgoing particles similarly to (C.3-C.4):

$$\sum_{spins}\left|M_1+M_2+M_3+M_4\right|^2=\frac{\alpha^4\left(4\pi\right)^4}{\left(p_1+p_2\right)^4}\sum_{spins}\left\{\frac{1}{q^4}\left[\bar{\upsilon}\left(p_2\right)\gamma_\mu u\left(p_1\right)\right]\times\right.$$
$$\times\left[\bar{u}\left(p_3\right)\left(\frac{2p_3^\alpha\gamma^\mu+\gamma^\alpha\not{q}\gamma^\mu}{\left(p_3+q\right)^2-m_2^2}-\frac{2p_4^\alpha\gamma^\mu+\gamma^\mu\not{q}\gamma^\alpha}{\left(p_4+q\right)^2-m_2^2}\right)\upsilon\left(p_4\right)\right]\left[\bar{u}\left(p_5\right)\gamma_\alpha\left(\not{p}_6-m_3\right)\gamma_\beta u\left(p_5\right)\right]\times$$
$$\times\left[\bar{\upsilon}\left(p_4\right)\left(\frac{2p_3^\beta\gamma^\nu+\gamma^\nu\not{q}\gamma^\beta}{\left(p_3+q\right)^2-m_2^2}-\frac{2p_4^\beta\gamma^\nu+\gamma^\beta\not{q}\gamma^\nu}{\left(p_4+q\right)^2-m_2^2}\right)u\left(p_3\right)\right]\left[\bar{u}\left(p_1\right)\gamma_\nu\upsilon\left(p_2\right)\right]+$$
$$+\frac{1}{q_2^4}\left[\bar{\upsilon}\left(p_2\right)\gamma_\mu u\left(p_1\right)\right]\left[\bar{u}\left(p_5\right)\left(\frac{2p_5^\alpha\gamma^\mu+\gamma^\alpha\not{q}_2\gamma^\mu}{\left(p_5+q_2\right)^2-m_3^2}-\frac{2p_6^\alpha\gamma^\mu+\gamma^\mu\not{q}_2\gamma^\alpha}{\left(p_6+q_2\right)^2-m_3^2}\right)\upsilon\left(p_6\right)\right]\left[\bar{u}\left(p_3\right)\gamma_\alpha\left(\not{p}_4-m_2\right)\gamma_\beta u\left(p_3\right)\right]\times$$
$$\times\left[\bar{\upsilon}\left(p_6\right)\left(\frac{2p_5^\beta\gamma^\nu+\gamma^\nu\not{q}_2\gamma^\beta}{\left(p_5+q_2\right)^2-m_3^2}-\frac{2p_6^\beta\gamma^\nu+\gamma^\beta\not{q}_2\gamma^\nu}{\left(p_6+q_2\right)^2-m_3^2}\right)u\left(p_5\right)\right]\left[\bar{u}\left(p_1\right)\gamma_\nu\upsilon\left(p_2\right)\right]+$$
$$+\frac{1}{q^2q_2^2}\left[\bar{\upsilon}\left(p_2\right)\gamma_\mu u\left(p_1\right)\right]\left[\bar{u}\left(p_3\right)\left(\frac{2p_3^\alpha\gamma^\mu+\gamma^\alpha\not{q}\gamma^\mu}{\left(p_3+q\right)^2-m_2^2}-\frac{2p_4^\alpha\gamma^\mu+\gamma^\mu\not{q}\gamma^\alpha}{\left(p_4+q\right)^2-m_2^2}\right)\upsilon\left(p_4\right)\right]\times$$
$$\times\left[\bar{u}\left(p_5\right)\gamma_\alpha\left(\not{p}_6-m_3\right)\left(\frac{2p_5^\beta\gamma^\nu+\gamma^\nu\not{q}_2\gamma^\beta}{\left(p_5+q_2\right)^2-m_3^2}-\frac{2p_6^\beta\gamma^\nu+\gamma^\beta\not{q}_2\gamma^\nu}{\left(p_6+q_2\right)^2-m_3^2}\right)u\left(p_5\right)\right]\left[\bar{\upsilon}\left(p_4\right)\gamma_\beta u\left(p_3\right)\right]\left[\bar{u}\left(p_1\right)\gamma_\nu\upsilon\left(p_2\right)\right]+$$
$$+\frac{1}{q^2q_2^2}\left[\bar{\upsilon}\left(p_2\right)\gamma_\mu u\left(p_1\right)\right]\left[\bar{u}\left(p_5\right)\left(\frac{2p_5^\alpha\gamma^\mu+\gamma^\alpha\not{q}_2\gamma^\mu}{\left(p_5+q_2\right)^2-m_3^2}-\frac{2p_6^\alpha\gamma^\mu+\gamma^\mu\not{q}_2\gamma^\alpha}{\left(p_6+q_2\right)^2-m_3^2}\right)\upsilon\left(p_6\right)\right]\times$$
$$\left.\times\left[\bar{u}\left(p_3\right)\gamma_\alpha\left(\not{p}_4-m_2\right)\left(\frac{2p_3^\beta\gamma^\nu+\gamma^\nu\not{q}\gamma^\beta}{\left(p_3+q\right)^2-m_2^2}-\frac{2p_4^\beta\gamma^\nu+\gamma^\beta\not{q}\gamma^\nu}{\left(p_4+q\right)^2-m_2^2}\right)u\left(p_3\right)\right]\left[\bar{\upsilon}\left(p_6\right)\gamma_\beta u\left(p_5\right)\right]\left[\bar{u}\left(p_1\right)\gamma_\nu\upsilon\left(p_2\right)\right]\right\}=$$
$$=\frac{\alpha^4\left(4\pi\right)^4}{\left(p_1+p_2\right)^4}\sum_{spins}\left\{\frac{1}{q^4}\left[\bar{\upsilon}\left(p_2\right)\gamma_\mu u\left(p_1\right)\right]\left[\bar{u}\left(p_3\right)\left(\frac{2p_3^\alpha\gamma^\mu+\gamma^\alpha\not{q}\gamma^\mu}{\left(p_3+q\right)^2-m_2^2}-\frac{2p_4^\alpha\gamma^\mu+\gamma^\mu\not{q}\gamma^\alpha}{\left(p_4+q\right)^2-m_2^2}\right)\upsilon\left(p_4\right)\right]\times\right.$$
$$\times\left[\bar{\upsilon}\left(p_4\right)\left(\frac{2p_3^\beta\gamma^\nu+\gamma^\nu\not{q}\gamma^\beta}{\left(p_3+q\right)^2-m_2^2}-\frac{2p_4^\beta\gamma^\nu+\gamma^\beta\not{q}\gamma^\nu}{\left(p_4+q\right)^2-m_2^2}\right)u\left(p_3\right)\right]\left[\bar{u}\left(p_1\right)\gamma_\nu\upsilon\left(p_2\right)\right]Tr\left[\left(\not{p}_5+m_3\right)\gamma_\alpha\left(\not{p}_6-m_3\right)\gamma_\beta\right]+$$
$$+\frac{1}{q_2^4}Tr\left[\left(\not{p}_3+m_2\right)\gamma_\alpha\left(\not{p}_4-m_2\right)\gamma_\beta\right]\left[\bar{\upsilon}\left(p_2\right)\gamma_\mu u\left(p_1\right)\right]\left[\bar{u}\left(p_5\right)\left(\frac{2p_5^\alpha\gamma^\mu+\gamma^\alpha\not{q}_2\gamma^\mu}{\left(p_5+q_2\right)^2-m_3^2}-\frac{2p_6^\alpha\gamma^\mu+\gamma^\mu\not{q}_2\gamma^\alpha}{\left(p_6+q_2\right)^2-m_3^2}\right)\upsilon\left(p_6\right)\right]\times$$
$$\times\left[\bar{\upsilon}\left(p_6\right)\left(\frac{2p_5^\beta\gamma^\nu+\gamma^\nu\not{q}_2\gamma^\beta}{\left(p_5+q_2\right)^2-m_3^2}-\frac{2p_6^\beta\gamma^\nu+\gamma^\beta\not{q}_2\gamma^\nu}{\left(p_6+q_2\right)^2-m_3^2}\right)u\left(p_5\right)\right]\left[\bar{u}\left(p_1\right)\gamma_\nu\upsilon\left(p_2\right)\right]+$$
$$+\frac{1}{q^2q_2^2}Tr\left[\left(\not{p}_5+m_3\right)\gamma_\alpha\left(\not{p}_6-m_3\right)\left(\frac{2p_5^\beta\gamma^\nu+\gamma^\nu\not{q}_2\gamma^\beta}{\left(p_5+q_2\right)^2-m_3^2}-\frac{2p_6^\beta\gamma^\nu+\gamma^\beta\not{q}_2\gamma^\nu}{\left(p_6+q_2\right)^2-m_3^2}\right)\right]\times$$
$$\times\left[\bar{\upsilon}\left(p_2\right)\gamma_\mu u\left(p_1\right)\right]\left[\bar{u}\left(p_3\right)\left(\frac{2p_3^\alpha\gamma^\mu+\gamma^\alpha\not{q}\gamma^\mu}{\left(p_3+q\right)^2-m_2^2}-\frac{2p_4^\alpha\gamma^\mu+\gamma^\mu\not{q}\gamma^\alpha}{\left(p_4+q\right)^2-m_2^2}\right)\upsilon\left(p_4\right)\right]\left[\bar{\upsilon}\left(p_4\right)\gamma_\beta u\left(p_3\right)\right]\left[\bar{u}\left(p_1\right)\gamma_\nu\upsilon\left(p_2\right)\right]+$$
$$+\frac{1}{q^2q_2^2}Tr\left[\left(\not{p}_3+m_2\right)\gamma_\alpha\left(\not{p}_4-m_2\right)\left(\frac{2p_3^\beta\gamma^\nu+\gamma^\nu\not{q}\gamma^\beta}{\left(p_3+q\right)^2-m_2^2}-\frac{2p_4^\beta\gamma^\nu+\gamma^\beta\not{q}\gamma^\nu}{\left(p_4+q\right)^2-m_2^2}\right)\right]\times$$

$$\times \left[\bar{\upsilon}\left(p_2\right)\gamma_\mu u\left(p_1\right)\right]\left[\bar{u}\left(p_5\right)\left(\frac{2p_5^\alpha\gamma^\mu+\gamma^\alpha \not{q}_2\gamma^\mu}{\left(p_5+q_2\right)^2-m_3^2}-\frac{2p_6^\alpha\gamma^\mu+\gamma^\mu \not{q}_2\gamma^\alpha}{\left(p_6+q_2\right)^2-m_3^2}\right)\upsilon\left(p_6\right)\right]\left[\bar{\upsilon}\left(p_6\right)\gamma_\beta u\left(p_5\right)\right]\left[\bar{u}\left(p_1\right)\gamma_\nu\upsilon\left(p_2\right)\right]\Bigg\} =$$

$$=\frac{\alpha^4\left(4\pi\right)^4}{\left(p_1+p_2\right)^4}\sum_{spins}\Bigg\{\frac{1}{q^4}Tr\left[\left(\not{p}_5+m_3\right)\gamma_\alpha\left(\not{p}_6-m_3\right)\gamma_\beta\right]\left[\bar{\upsilon}\left(p_2\right)\gamma_\mu u\left(p_1\right)\right]\times$$

$$\times\left[\bar{u}\left(p_3\right)\left(\frac{2p_3^\alpha\gamma^\mu+\gamma^\alpha \not{q}\gamma^\mu}{\left(p_3+q\right)^2-m_2^2}-\frac{2p_4^\alpha\gamma^\mu+\gamma^\mu \not{q}\gamma^\alpha}{\left(p_4+q\right)^2-m_2^2}\right)\left(\not{p}_4-m_2\right)\left(\frac{2p_3^\beta\gamma^\nu+\gamma^\nu \not{q}\gamma^\beta}{\left(p_3+q\right)^2-m_2^2}-\frac{2p_4^\beta\gamma^\nu+\gamma^\beta \not{q}\gamma^\nu}{\left(p_4+q\right)^2-m_2^2}\right)u\left(p_3\right)\right]\left[\bar{u}\left(p_1\right)\gamma_\nu\upsilon\left(p_2\right)\right]+$$

$$+\frac{1}{q_2^4}Tr\left[\left(\not{p}_3+m_2\right)\gamma_\alpha\left(\not{p}_4-m_2\right)\gamma_\beta\right]\left[\bar{\upsilon}\left(p_2\right)\gamma_\mu u\left(p_1\right)\right]\times$$

$$\times\left[\bar{u}\left(p_5\right)\left(\frac{2p_5^\alpha\gamma^\mu+\gamma^\alpha \not{q}_2\gamma^\mu}{\left(p_5+q_2\right)^2-m_3^2}-\frac{2p_6^\alpha\gamma^\mu+\gamma^\mu \not{q}_2\gamma^\alpha}{\left(p_6+q_2\right)^2-m_3^2}\right)\left(\not{p}_6-m_3\right)\left(\frac{2p_5^\beta\gamma^\nu+\gamma^\nu \not{q}_2\gamma^\beta}{\left(p_5+q_2\right)^2-m_3^2}-\frac{2p_6^\beta\gamma^\nu+\gamma^\beta \not{q}_2\gamma^\nu}{\left(p_6+q_2\right)^2-m_3^2}\right)u\left(p_5\right)\right]\left[\bar{u}\left(p_1\right)\gamma_\nu\upsilon\left(p_2\right)\right]+$$

$$+\frac{1}{q^2q_2^2}Tr\left[\left(\not{p}_5+m_3\right)\gamma_\alpha\left(\not{p}_6-m_3\right)\left(\frac{2p_5^\beta\gamma^\nu+\gamma^\nu \not{q}_2\gamma^\beta}{\left(p_5+q_2\right)^2-m_3^2}-\frac{2p_6^\beta\gamma^\nu+\gamma^\beta \not{q}_2\gamma^\nu}{\left(p_6+q_2\right)^2-m_3^2}\right)\right]\left[\bar{\upsilon}\left(p_2\right)\gamma_\mu u\left(p_1\right)\right]\times$$

$$\times\left[\bar{u}\left(p_3\right)\left(\frac{2p_3^\alpha\gamma^\mu+\gamma^\alpha \not{q}\gamma^\mu}{\left(p_3+q\right)^2-m_2^2}-\frac{2p_4^\alpha\gamma^\mu+\gamma^\mu \not{q}\gamma^\alpha}{\left(p_4+q\right)^2-m_2^2}\right)\left(\not{p}_4-m_2\right)\gamma_\beta u\left(p_3\right)\right]\left[\bar{u}\left(p_1\right)\gamma_\nu\upsilon\left(p_2\right)\right]+$$

$$+\frac{1}{q^2q_2^2}Tr\left[\left(\not{p}_3+m_2\right)\gamma_\alpha\left(\not{p}_4-m_2\right)\left(\frac{2p_3^\beta\gamma^\nu+\gamma^\nu \not{q}\gamma^\beta}{\left(p_3+q\right)^2-m_2^2}-\frac{2p_4^\beta\gamma^\nu+\gamma^\beta \not{q}\gamma^\nu}{\left(p_4+q\right)^2-m_2^2}\right)\right]\left[\bar{\upsilon}\left(p_2\right)\gamma_\mu u\left(p_1\right)\right]\times$$

$$\times\left[\bar{u}\left(p_5\right)\left(\frac{2p_5^\alpha\gamma^\mu+\gamma^\alpha \not{q}_2\gamma^\mu}{\left(p_5+q_2\right)^2-m_3^2}-\frac{2p_6^\alpha\gamma^\mu+\gamma^\mu \not{q}_2\gamma^\alpha}{\left(p_6+q_2\right)^2-m_3^2}\right)\left(\not{p}_6-m_3\right)\gamma_\beta u\left(p_5\right)\right]\left[\bar{u}\left(p_1\right)\gamma_\nu\upsilon\left(p_2\right)\right]\Bigg\} =$$

$$=\frac{\alpha^4\left(4\pi\right)^4}{\left(p_1+p_2\right)^4}\sum_{spins}\Bigg\{\frac{1}{q^4}Tr\left[\left(\not{p}_5+m_3\right)\gamma_\alpha\left(\not{p}_6-m_3\right)\gamma_\beta\right]\left[\bar{\upsilon}\left(p_2\right)\gamma_\mu u\left(p_1\right)\right]\left[\bar{u}\left(p_1\right)\gamma_\nu\upsilon\left(p_2\right)\right]\times$$

$$\times Tr\left[\left(\not{p}_3+m_2\right)\left(\frac{2p_3^\alpha\gamma^\mu+\gamma^\alpha \not{q}\gamma^\mu}{\left(p_3+q\right)^2-m_2^2}-\frac{2p_4^\alpha\gamma^\mu+\gamma^\mu \not{q}\gamma^\alpha}{\left(p_4+q\right)^2-m_2^2}\right)\left(\not{p}_4-m_2\right)\left(\frac{2p_3^\beta\gamma^\nu+\gamma^\nu \not{q}\gamma^\beta}{\left(p_3+q\right)^2-m_2^2}-\frac{2p_4^\beta\gamma^\nu+\gamma^\beta \not{q}\gamma^\nu}{\left(p_4+q\right)^2-m_2^2}\right)\right]+$$

$$+\frac{1}{q_2^4}Tr\left[\left(\not{p}_3+m_2\right)\gamma_\alpha\left(\not{p}_4-m_2\right)\gamma_\beta\right]\left[\bar{\upsilon}\left(p_2\right)\gamma_\mu u\left(p_1\right)\right]\left[\bar{u}\left(p_1\right)\gamma_\nu\upsilon\left(p_2\right)\right]\times$$

$$\times Tr\left[\left(\not{p}_5+m_3\right)\left(\frac{2p_5^\alpha\gamma^\mu+\gamma^\alpha \not{q}_2\gamma^\mu}{\left(p_5+q_2\right)^2-m_3^2}-\frac{2p_6^\alpha\gamma^\mu+\gamma^\mu \not{q}_2\gamma^\alpha}{\left(p_6+q_2\right)^2-m_3^2}\right)\left(\not{p}_6-m_3\right)\left(\frac{2p_5^\beta\gamma^\nu+\gamma^\nu \not{q}_2\gamma^\beta}{\left(p_5+q_2\right)^2-m_3^2}-\frac{2p_6^\beta\gamma^\nu+\gamma^\beta \not{q}_2\gamma^\nu}{\left(p_6+q_2\right)^2-m_3^2}\right)\right]+$$

$$+\frac{1}{q^2q_2^2}Tr\left[\left(\not{p}_5+m_3\right)\gamma_\alpha\left(\not{p}_6-m_3\right)\left(\frac{2p_5^\beta\gamma^\nu+\gamma^\nu \not{q}_2\gamma^\beta}{\left(p_5+q_2\right)^2-m_3^2}-\frac{2p_6^\beta\gamma^\nu+\gamma^\beta \not{q}_2\gamma^\nu}{\left(p_6+q_2\right)^2-m_3^2}\right)\right]\times$$

$$\times Tr\left[\left(\not{p}_3+m_2\right)\left(\frac{2p_3^\alpha\gamma^\mu+\gamma^\alpha \not{q}\gamma^\mu}{\left(p_3+q\right)^2-m_2^2}-\frac{2p_4^\alpha\gamma^\mu+\gamma^\mu \not{q}\gamma^\alpha}{\left(p_4+q\right)^2-m_2^2}\right)\left(\not{p}_3-m_2\right)\gamma_\beta\right]\left[\bar{\upsilon}\left(p_2\right)\gamma_\mu u\left(p_1\right)\right]\left[\bar{u}\left(p_1\right)\gamma_\nu\upsilon\left(p_2\right)\right]+$$

$$+\frac{1}{q^2q_2^2}Tr\left[\left(\not{p}_3+m_2\right)\gamma_\alpha\left(\not{p}_4-m_2\right)\left(\frac{2p_3^\beta\gamma^\nu+\gamma^\nu \not{q}\gamma^\beta}{\left(p_3+q\right)^2-m_2^2}-\frac{2p_4^\beta\gamma^\nu+\gamma^\beta \not{q}\gamma^\nu}{\left(p_4+q\right)^2-m_2^2}\right)\right]\times$$

$$\times Tr\left[\left(\not{p}_5+m_3\right)\left(\frac{2p_5^\alpha\gamma^\mu+\gamma^\alpha \not{q}_2\gamma^\mu}{\left(p_5+q_2\right)^2-m_3^2}-\frac{2p_6^\alpha\gamma^\mu+\gamma^\mu \not{q}_2\gamma^\alpha}{\left(p_6+q_2\right)^2-m_3^2}\right)\left(\not{p}_6-m_3\right)\gamma_\beta\right]\left[\bar{\upsilon}\left(p_2\right)\gamma_\mu u\left(p_1\right)\right]\left[\bar{u}\left(p_1\right)\gamma_\nu\upsilon\left(p_2\right)\right]\Bigg\},$$

where lambda is lambda QED constant, and finally

$$\sum_{spins} |M_1 + M_2 + M_3 + M_4|^2 = \tag{C.5}$$

$$= \frac{\alpha^4 (4\pi)^4}{(p_1+p_2)^4} \frac{1}{q^4} Tr\left[(\not{p}_1 + m_1)\gamma_\mu (\not{p}_2 - m_1)\gamma_\nu\right] Tr\left[(\not{p}_5 + m_3)\gamma_\alpha (\not{p}_6 - m_3)\gamma_\beta\right] \times \tag{C.6}$$

$$\times Tr\left[(\not{p}_3 + m_2)\left(\frac{2p_3^\alpha\gamma^\mu + \gamma^\alpha \not{q}\gamma^\mu}{(p_3+q)^2 - m_2^2} - \frac{2p_4^\alpha\gamma^\mu + \gamma^\mu \not{q}\gamma^\alpha}{(p_4+q)^2 - m_2^2}\right) \times \right. \tag{C.7}$$

$$\left. \times (\not{p}_4 - m_2)\left(\frac{2p_3^\beta\gamma^\nu + \gamma^\nu \not{q}\gamma^\beta}{(p_3+q)^2 - m_2^2} - \frac{2p_4^\beta\gamma^\nu + \gamma^\beta \not{q}\gamma^\nu}{(p_4+q)^2 - m_2^2}\right)\right] + \tag{C.8}$$

$$+ \frac{\alpha^4 (4\pi)^4}{(p_1+p_2)^4} \frac{1}{q_2^4} Tr\left[(\not{p}_1 + m_1)\gamma_\mu (\not{p}_2 - m_1)\gamma_\nu\right] Tr\left[(\not{p}_3 + m_2)\gamma_\alpha (\not{p}_4 - m_2)\gamma_\beta\right] \times \tag{C.9}$$

$$\times Tr\left[(\not{p}_5 + m_3)\left(\frac{2p_5^\alpha\gamma^\mu + \gamma^\alpha \not{q}_2\gamma^\mu}{(p_5+q_2)^2 - m_3^2} - \frac{2p_6^\alpha\gamma^\mu + \gamma^\mu \not{q}_2\gamma^\alpha}{(p_6+q_2)^2 - m_3^2}\right) \times \right. \tag{C.10}$$

$$\left. \times (\not{p}_6 - m_3)\left(\frac{2p_5^\beta\gamma^\nu + \gamma^\nu \not{q}_2\gamma^\beta}{(p_5+q_2)^2 - m_3^2} - \frac{2p_6^\beta\gamma^\nu + \gamma^\beta \not{q}_2\gamma^\nu}{(p_6+q_2)^2 - m_3^2}\right)\right] + \tag{C.11}$$

$$+ \frac{\alpha^4 (4\pi)^4}{(p_1+p_2)^4} \frac{1}{q^2 q_2^2} Tr\left[(\not{p}_1 + m_1)\gamma_\mu (\not{p}_2 - m_1)\gamma_\nu\right] \times \tag{C.12}$$

$$\times Tr\left[(\not{p}_3 + m_2)\left(\frac{2p_3^\alpha\gamma^\mu + \gamma^\alpha \not{q}\gamma^\mu}{(p_3+q)^2 - m_2^2} - \frac{2p_4^\alpha\gamma^\mu + \gamma^\mu \not{q}\gamma^\alpha}{(p_4+q)^2 - m_2^2}\right)(\not{p}_4 - m_2)\gamma_\beta\right] \times \tag{C.13}$$

$$\times Tr\left[(\not{p}_5 + m_3)\gamma_\alpha (\not{p}_6 - m_3)\left(\frac{2p_5^\beta\gamma^\nu + \gamma^\nu \not{q}_2\gamma^\beta}{(p_5+q_2)^2 - m_3^2} - \frac{2p_6^\beta\gamma^\nu + \gamma^\beta \not{q}_2\gamma^\nu}{(p_6+q_2)^2 - m_3^2}\right)\right] + \tag{C.14}$$

$$+ \frac{\alpha^4 (4\pi)^4}{(p_1+p_2)^4} \frac{1}{q^2 q_2^2} Tr\left[(\not{p}_1 + m_1)\gamma_\mu (\not{p}_2 - m_1)\gamma_\nu\right] \times \tag{C.15}$$

$$\times Tr\left[(\not{p}_3 + m_2)\gamma_\alpha (\not{p}_4 - m_2)\left(\frac{2p_3^\beta\gamma^\nu + \gamma^\nu \not{q}\gamma^\beta}{(p_3+q)^2 - m_2^2} - \frac{2p_4^\beta\gamma^\nu + \gamma^\beta \not{q}\gamma^\nu}{(p_4+q)^2 - m_2^2}\right)\right] \times \tag{C.16}$$

$$\times Tr\left[(\not{p}_5 + m_3)\left(\frac{2p_5^\alpha\gamma^\mu + \gamma^\alpha \not{q}_2\gamma^\mu}{(p_5+q_2)^2 - m_3^2} - \frac{2p_6^\alpha\gamma^\mu + \gamma^\mu \not{q}_2\gamma^\alpha}{(p_6+q_2)^2 - m_3^2}\right)(\not{p}_6 - m_3)\gamma_\beta\right] \tag{C.17}$$

The line of calculations for spin summation of matrix element in the form (C.1) is similar:

$$\sum_{spins} |M_1 + M_2 + M_3 + M_4|^2 = \tag{C.18}$$

$$= \frac{\alpha^4 (4\pi)^4}{(p_1+p_2)^4}\frac{1}{q^4} Tr\left[(\not p_1 + m_1)\gamma_\mu(\not p_2 - m_1)\gamma_\nu\right] Tr\left[(\not p_5 + m_3)\gamma_\alpha(\not p_6 - m_3)\gamma_\beta\right] \times \tag{C.19}$$

$$\times Tr\left[(\not p_3 + m_2)\left(\gamma^\alpha \frac{\not p_3 + \not q + m_2}{(p_3+q)^2 - m_2^2}\gamma^\mu - \gamma^\mu \frac{\not p_4 + \not q - m_2}{(p_4+q)^2 - m_2^2}\gamma^\alpha\right)\times \right. \tag{C.20}$$

$$\left. \times (\not p_4 - m_2)\left(\gamma^\nu \frac{\not p_3 + \not q + m_2}{(p_3+q)^2 - m_2^2}\gamma^\beta - \gamma^\beta \frac{\not p_4 + \not q - m_2}{(p_4+q)^2 - m_2^2}\gamma^\nu\right)\right] + \tag{C.21}$$

$$+ \frac{\alpha^4 (4\pi)^4}{(p_1+p_2)^4}\frac{1}{q_2^4} Tr\left[(\not p_1 + m_1)\gamma_\mu(\not p_2 - m_1)\gamma_\nu\right] Tr\left[(\not p_3 + m_2)\gamma_\alpha(\not p_4 - m_2)\gamma_\beta\right] \times$$

$$\times Tr\left[(\not p_5 + m_3)\left(\gamma^\alpha \frac{\not p_5 + \not q_2 + m_3}{(p_5+q_2)^2 - m_3^2}\gamma^\mu - \gamma^\mu \frac{\not p_6 + \not q_2 - m_3}{(p_6+q_2)^2 - m_3^2}\gamma^\alpha\right)\times \right.$$

$$\left. \times (\not p_6 - m_3)\left(\gamma^\nu \frac{\not p_5 + \not q_2 + m_3}{(p_5+q_2)^2 - m_3^2}\gamma^\beta - \gamma^\beta \frac{\not p_6 + \not q_2 - m_3}{(p_6+q_2)^2 - m_3^2}\gamma^\nu\right)\right] +$$

$$+ \frac{\alpha^4 (4\pi)^4}{(p_1+p_2)^4}\frac{1}{q^2 q_2^2} Tr\left[(\not p_1 + m_1)\gamma_\mu(\not p_2 - m_1)\gamma_\nu\right] \times$$

$$\times Tr\left[(\not p_3 + m_2)\left(\gamma^\alpha \frac{\not p_3 + \not q + m_2}{(p_3+q)^2 - m_2^2}\gamma^\mu - \gamma^\mu \frac{\not p_4 + \not q - m_2}{(p_4+q)^2 - m_2^2}\gamma^\alpha\right)(\not p_4 - m_2)\gamma_\beta\right] \times$$

$$\times Tr\left[(\not p_5 + m_3)\gamma_\alpha(\not p_6 - m_3)\left(\gamma^\nu \frac{\not p_5 + \not q_2 + m_3}{(p_5+q_2)^2 - m_3^2}\gamma^\beta - \gamma^\beta \frac{\not p_6 + \not q_2 - m_3}{(p_6+q_2)^2 - m_3^2}\gamma^\nu\right)\right] +$$

$$+ \frac{\alpha^4 (4\pi)^4}{(p_1+p_2)^4}\frac{1}{q^2 q_2^2} Tr\left[(\not p_1 + m_1)\gamma_\mu(\not p_2 - m_1)\gamma_\nu\right] \times$$

$$\times Tr\left[(\not p_3 + m_2)\gamma_\alpha(\not p_4 - m_2)\left(\gamma^\nu \frac{\not p_3 + \not q + m_2}{(p_3+q)^2 - m_2^2}\gamma^\beta - \gamma^\beta \frac{\not p_4 + \not q - m_2}{(p_4+q)^2 - m_2^2}\gamma^\nu\right)\right] \times$$

$$\times Tr\left[(\not p_5 + m_3)\left(\gamma^\alpha \frac{\not p_5 + \not q_2 + m_3}{(p_5+q_2)^2 - m_3^2}\gamma^\mu - \gamma^\mu \frac{\not p_6 + \not q_2 - m_3}{(p_6+q_2)^2 - m_3^2}\gamma^\alpha\right)(\not p_6 - m_3)\gamma_\beta\right]$$

From the expression above for terms (C.19-C.21) it follows immediately that for the case of small q, i.e. $p_3 \gg q, p_4 \gg q$, we can easily neglect q in numerator. I keep this notice in mind.

C.2 $|M_1 + M_2|^2$

Here I continue calculation of term (C.6-C.8) of the expression (C.6-C.17), it corresponds to matrix element $M_1 + M_2$ defined by Fig. 2:

$$\sum_{spins} |M_1 + M_2|^2 = \frac{\alpha^4 (4\pi)^4}{(p_1+p_2)^4}\frac{1}{q^4} Tr\left[(\not p_1 + m_1)\gamma_\mu(\not p_2 - m_1)\gamma_\nu\right] Tr\left[(\not p_5 + m_3)\gamma_\alpha(\not p_6 - m_3)\gamma_\beta\right] \times$$

$$\times Tr\left[(\not{p}_3+m_2)\left(\frac{2p_3^\alpha\gamma^\mu+\gamma^\alpha\not{q}\gamma^\mu}{(p_3+q)^2-m_2^2}-\frac{2p_4^\alpha\gamma^\mu+\gamma^\mu\not{q}\gamma^\alpha}{(p_4+q)^2-m_2^2}\right)\times\right.$$
$$\left.\times(\not{p}_4-m_2)\left(\frac{2p_3^\beta\gamma^\nu+\gamma^\nu\not{q}\gamma^\beta}{(p_3+q)^2-m_2^2}-\frac{2p_4^\beta\gamma^\nu+\gamma^\beta\not{q}\gamma^\nu}{(p_4+q)^2-m_2^2}\right)\right].$$

I split above expression into four parts

$$\sum_{spins}|M_1+M_2|^2=\frac{\alpha^4(4\pi)^4}{(p_1+p_2)^4}\frac{1}{q^4}Tr\left[(\not{p}_1+m_1)\gamma_\mu(\not{p}_2-m_1)\gamma_\nu\right]\times \tag{C.22}$$
$$\times\left\{Tr\left[(\not{p}_3+m_2)\gamma^\mu(\not{p}_4-m_2)\gamma^\nu\right]Tr\left[(\not{p}_5+m_3)\gamma_\alpha(\not{p}_6-m_3)\gamma_\beta\right]\times\right. \tag{C.23}$$
$$\times\left(\frac{2p_3^\alpha}{(p_3+q)^2-m_2^2}-\frac{2p_4^\alpha}{(p_4+q)^2-m_2^2}\right)\left(\frac{2p_3^\beta}{(p_3+q)^2-m_2^2}-\frac{2p_4^\beta}{(p_4+q)^2-m_2^2}\right)+ \tag{C.24}$$
$$+Tr\left[(\not{p}_5+m_3)\gamma_\alpha(\not{p}_6-m_3)\gamma_\beta\right]\times \tag{C.25}$$
$$\times Tr\left[(\not{p}_3+m_2)\left(\frac{\gamma^\alpha\not{q}\gamma^\mu}{(p_3+q)^2-m_2^2}-\frac{\gamma^\mu\not{q}\gamma^\alpha}{(p_4+q)^2-m_2^2}\right)\times\right. \tag{C.26}$$
$$\left.\times(\not{p}_4-m_2)\left(\frac{\gamma^\nu\not{q}\gamma^\beta}{(p_3+q)^2-m_2^2}-\frac{\gamma^\beta\not{q}\gamma^\nu}{(p_4+q)^2-m_2^2}\right)\right]+ \tag{C.27}$$
$$+Tr\left[(\not{p}_5+m_3)\left(\frac{2\not{p}_3}{(p_3+q)^2-m_2^2}-\frac{2\not{p}_4}{(p_4+q)^2-m_2^2}\right)(\not{p}_6-m_3)\gamma_\beta\right]\times \tag{C.28}$$
$$\times Tr\left[(\not{p}_3+m_2)\gamma^\mu(\not{p}_4-m_2)\left(\frac{\gamma^\nu\not{q}\gamma^\beta}{(p_3+q)^2-m_2^2}-\frac{\gamma^\beta\not{q}\gamma^\nu}{(p_4+q)^2-m_2^2}\right)\right]+ \tag{C.29}$$
$$+Tr\left[(\not{p}_5+m_3)\gamma_\alpha(\not{p}_6-m_3)\left(\frac{2\not{p}_3}{(p_3+q)^2-m_2^2}-\frac{2\not{p}_4}{(p_4+q)^2-m_2^2}\right)\right]\times \tag{C.30}$$
$$\left.\times Tr\left[(\not{p}_3+m_2)\left(\frac{\gamma^\alpha\not{q}\gamma^\mu}{(p_3+q)^2-m_2^2}-\frac{\gamma^\mu\not{q}\gamma^\alpha}{(p_4+q)^2-m_2^2}\right)(\not{p}_4-m_2)\gamma^\nu\right]\right\} \tag{C.31}$$

PHOTOS feature matrix element for extra pair emission in soft approximation, i.e. for $q\to 0$ the whole expression above reduces to (C.22-C.24):

$$\sum_{spins}|M_1+M_2|^2_{soft}\equiv\frac{\alpha^4(4\pi)^4}{(p_1+p_2)^4}\frac{1}{q^4}Tr\left[(\not{p}_1+m_1)\gamma_\mu(\not{p}_2-m_1)\gamma_\nu\right]\times$$
$$\times Tr\left[(\not{p}_3+m_2)\gamma^\mu(\not{p}_4-m_2)\gamma^\nu\right]Tr\left[(\not{p}_5+m_3)\gamma_\alpha(\not{p}_6-m_3)\gamma_\beta\right]\times$$
$$\times\left(\frac{2p_3^\alpha}{(p_3+q)^2-m_2^2}-\frac{2p_4^\alpha}{(p_4+q)^2-m_2^2}\right)\left(\frac{2p_3^\beta}{(p_3+q)^2-m_2^2}-\frac{2p_4^\beta}{(p_4+q)^2-m_2^2}\right).$$

Writing last one of the above traces in straightforward manner I come to

$$\sum_{spins} |M_1 + M_2|^2_{soft} = \tag{C.32}$$

$$= \frac{\alpha^4 (4\pi)^4}{(p_1+p_2)^4} Tr\left[(\not{p}_1 + m_1)\gamma_\mu (\not{p}_2 - m_1)\gamma_\nu\right] Tr\left[(\not{p}_3 + m_2)\gamma^\mu (\not{p}_4 - m_2)\gamma^\nu\right] \times \tag{C.33}$$

$$\times \frac{4}{q^4}\left(p_5^\alpha p_6^\beta + p_6^\alpha p_5^\beta - (p_5 p_6 + m_3^2)\cdot g^{\alpha\beta}\right) \times \tag{C.34}$$

$$\times \left(\frac{2p_3^\alpha}{(p_3+q)^2 - m_2^2} - \frac{2p_4^\alpha}{(p_4+q)^2 - m_2^2}\right)\left(\frac{2p_3^\beta}{(p_3+q)^2 - m_2^2} - \frac{2p_4^\beta}{(p_4+q)^2 - m_2^2}\right) \tag{C.35}$$

One can notice that neglecting energy taken out by $f_3\overline{f}_3$ pair emission the term on the line (C.33) up to a constant factor coincides with Born-level unpolarized cross section for the process $f_1\overline{f}_1 \to \gamma \to f_2\overline{f}_2$, while expression at lines (C.34-C.35) is factorized part of matrix element has a meaning of probability density of extra $f_3\overline{f}_3$ pair emission. This probability density depends on four-momenta of outgoing particles only and can be simulated independently for lightest $f_3\overline{f}_3$ pairs. Harder $f_3\overline{f}_3$ pair emission is, larger discrepancy between the term on the line (C.33) and the Born-level unpolarized cross section for the process $f_1\overline{f}_1 \to \gamma \to f_2\overline{f}_2$ is. Probability density in a form of expression at lines (C.34-C.35) is not yet properly normalized.

Here follow relations that help performing transformation of expression at lines (C.34-C.35). Since tensor at line (C.35) is symmetric one, one can interchange α and β summation indexes:

$$\left(p_5^\alpha p_6^\beta + p_6^\alpha p_5^\beta\right)\left(\frac{2p_3^\alpha}{(p_3+q)^2 - m_2^2} - \frac{2p_4^\alpha}{(p_4+q)^2 - m_2^2}\right)\left(\frac{2p_3^\beta}{(p_3+q)^2 - m_2^2} - \frac{2p_4^\beta}{(p_4+q)^2 - m_2^2}\right) =$$

$$= 2p_5^\alpha p_6^\beta \left(\frac{2p_3^\alpha}{(p_3+q)^2 - m_2^2} - \frac{2p_4^\alpha}{(p_4+q)^2 - m_2^2}\right)\left(\frac{2p_3^\beta}{(p_3+q)^2 - m_2^2} - \frac{2p_4^\beta}{(p_4+q)^2 - m_2^2}\right)$$

All momenta p_1–p_6 correspond to on shell particles, thus $p_3^2 = p_4^2 = m_2^2$, $p_5^2 = p_6^2 = m_3^2$ and

$$4\left(p_5^\alpha p_6^\beta + p_6^\alpha p_5^\beta - (p_5 p_6 + m_3^2)\cdot g^{\alpha\beta}\right) = 4\left(2p_5^\alpha p_6^\beta - \left(p_5 p_6 + \frac{(p_5)^2 + (p_6)^2}{2}\right)\cdot g^{\alpha\beta}\right) =$$

$$= 4\left(2p_5^\alpha p_6^\beta - \frac{(p_5+p_6)^2}{2}\cdot g^{\alpha\beta}\right) = 2\left(4p_5^\alpha p_6^\beta - q^2\cdot g^{\alpha\beta}\right)$$

$$(p_3+q)^2 - m_2^2 = 2p_3 q + q^2 = \{p_3 \gg q\} = 2p_3 q$$

$$(p_4+q)^2-m_2^2=2p_4q+q^2=\{p_4\gg q\}=2p_4q$$

Finally I come to equation

$$\sum_{spins}|M_1+M_2|^2_{soft}=\frac{\alpha^2\left(4\pi\right)^2}{\left(p_1+p_2\right)^4}Tr\left[\left(\not{p}_1+m_1\right)\gamma_\mu\left(\not{p}_2-m_1\right)\gamma_\nu\right]Tr\left[\left(\not{p}_3+m_2\right)\gamma^\mu\left(\not{p}_4-m_2\right)\gamma^\nu\right]\times \tag{C.36}$$

$$\times\,2\left(4\pi\alpha\right)^2\frac{4p_5^\alpha p_6^\beta-q^2\cdot g^{\alpha\beta}}{q^4}\left(\frac{p_3^\alpha}{p_3q}-\frac{p_4^\alpha}{p_4q}\right)\left(\frac{p_3^\beta}{p_3q}-\frac{p_4^\beta}{p_4q}\right), \tag{C.37}$$

where (C.36-C.37) is factorized matrix element with probability density of extra pair emission (C.37), which coincides up to normalization coefficient with integrand from formula (1) from [13] for the $a=0$ case.

Since part (C.22-C.24) of the matrix element (C.22-C.31) is already covered by `PHOTOS`, I proceed with calculation of three remaining parts (C.25-C.31) of the matrix element. I am using gamma-matrices properties in order to proceed with calculation of traces

$$Tr\left[\gamma^{\nu_1}\gamma^{\nu_2}...\gamma^{\nu_N}\right]=0, \tag{C.38}$$

where N is odd number; for any even number N a recursive formula is valid:

$$Tr\left[\gamma^{\nu_1}\gamma^{\nu_2}...\gamma^{\nu_N}\right]=\sum_{i=2}^{N}\left(-1\right)^i g^{\nu_1\nu_i}Tr\left[\gamma^{\nu_1}\gamma^{\nu_2}...\gamma^{\nu_{i-1}}\gamma^{\nu_{i+1}}...\gamma^{\nu_N}\right], \tag{C.39}$$

and

$$Tr\left[I_4\right]=4,$$

since I_4 is identity matrix in four dimensions. Here recursion starts:

$$Tr\left[\gamma^\mu\gamma^\nu\right]=g^{\mu\nu}Tr\left[I_4\right]=4g^{\mu\nu}, \tag{C.40}$$

$$Tr\left[\gamma^\alpha\gamma^\beta\gamma^\mu\gamma^\nu\right]=g^{\alpha\beta}Tr\left[\gamma^\mu\gamma^\nu\right]-g^{\alpha\mu}Tr\left[\gamma^\beta\gamma^\nu\right]+g^{\alpha\nu}Tr\left[\gamma^\beta\gamma^\mu\right], \tag{C.41}$$

$$\begin{aligned}Tr\left[\gamma^\xi\gamma^\chi\gamma^\alpha\gamma^\beta\gamma^\mu\gamma^\nu\right]&=g^{\xi\chi}Tr\left[\gamma^\alpha\gamma^\beta\gamma^\mu\gamma^\nu\right]-g^{\xi\alpha}Tr\left[\gamma^\chi\gamma^\beta\gamma^\mu\gamma^\nu\right]+\\&+g^{\xi\beta}\left[\gamma^\chi\gamma^\alpha\gamma^\mu\gamma^\nu\right]-g^{\xi\mu}Tr\left[\gamma^\chi\gamma^\alpha\gamma^\beta\gamma^\nu\right]+g^{\xi\nu}Tr\left[\gamma^\chi\gamma^\alpha\gamma^\beta\gamma^\mu\right]=\\&=4\big(g^{\alpha\beta}g^{\mu\chi}g^{\nu\xi}-g^{\alpha\beta}g^{\mu\xi}g^{\nu\chi}+g^{\alpha\beta}g^{\mu\nu}g^{\xi\chi}-g^{\alpha\mu}g^{\beta\chi}g^{\nu\xi}+g^{\alpha\mu}g^{\beta\xi}g^{\nu\chi}-\\&-g^{\alpha\mu}g^{\beta\nu}g^{\xi\chi}+g^{\alpha\chi}g^{\beta\mu}g^{\nu\xi}+g^{\alpha\nu}g^{\beta\mu}g^{\xi\chi}+g^{\alpha\nu}g^{\beta\chi}g^{\mu\xi}-g^{\alpha\nu}g^{\beta\xi}g^{\mu\chi}+\\&+g^{\alpha\xi}g^{\beta\nu}g^{\mu\chi}+g^{\alpha\chi}g^{\beta\xi}g^{\mu\nu}-g^{\alpha\xi}g^{\beta\chi}g^{\mu\nu}-g^{\alpha\xi}g^{\beta\mu}g^{\nu\chi}-g^{\alpha\chi}g^{\beta\nu}g^{\mu\xi}\big),\end{aligned} \tag{C.42}$$

$$\begin{aligned}Tr\left[\gamma^\varphi\gamma^\omega\gamma^\xi\gamma^\chi\gamma^\alpha\gamma^\beta\gamma^\mu\gamma^\nu\right]&=g^{\varphi\omega}Tr\left[\gamma^\xi\gamma^\chi\gamma^\alpha\gamma^\beta\gamma^\mu\gamma^\nu\right]-g^{\varphi\xi}Tr\left[\gamma^\omega\gamma^\chi\gamma^\alpha\gamma^\beta\gamma^\mu\gamma^\nu\right]+\\&+g^{\varphi\chi}Tr\left[\gamma^\omega\gamma^\xi\gamma^\alpha\gamma^\beta\gamma^\mu\gamma^\nu\right]-g^{\varphi\alpha}Tr\left[\gamma^\omega\gamma^\xi\gamma^\chi\gamma^\beta\gamma^\mu\gamma^\nu\right]+g^{\varphi\beta}Tr\left[\gamma^\omega\gamma^\xi\gamma^\chi\gamma^\alpha\gamma^\mu\gamma^\nu\right]-\\&-g^{\varphi\mu}Tr\left[\gamma^\omega\gamma^\xi\gamma^\chi\gamma^\alpha\gamma^\beta\gamma^\nu\right]+g^{\varphi\nu}Tr\left[\gamma^\omega\gamma^\xi\gamma^\chi\gamma^\alpha\gamma^\beta\gamma^\mu\right].\end{aligned} \tag{C.43}$$

Identities (C.40-C.43) together with rule for trace of odd number of gamma matrices (C.38) are intensively used in below calculation of expressions (C.25-C.31). All four parts (C.22-C.31) of the matrix element include contraction with the same tensor $Tr\left[\left(\not{p}_1+m_1\right)\gamma_\mu\left(\not{p}_2-m_1\right)\gamma_\nu\right.$ This tensor comes from summation of spins of incoming particles. Calculation of contraction over indexes α and β in the tensor expression at the lines (C.25-C.27) of the matrix element (C.22-C.31) follows

$$N_1^{\mu\nu}=Tr\left[\left(\not{p}_5+m_3\right)\gamma_\alpha\left(\not{p}_6-m_3\right)\gamma_\beta\right]Tr\left[\left(\not{p}_3+m_2\right)\left(\frac{\gamma^\alpha\not{q}\gamma^\mu}{\left(p_3+q\right)^2-m_2^2}-\frac{\gamma^\mu\not{q}\gamma^\alpha}{\left(p_4+q\right)^2-m_2^2}\right)\times\right.$$

$$\left.\times\left(\not{p}_4-m_2\right)\left(\frac{\gamma^\nu\not{q}\gamma^\beta}{\left(p_3+q\right)^2-m_2^2}-\frac{\gamma^\beta\not{q}\gamma^\nu}{\left(p_4+q\right)^2-m_2^2}\right)\right]=Tr\left[\left(\not{p}_5+m_3\right)\gamma_\alpha\left(\not{p}_6-m_3\right)\gamma_\beta\right]\times$$

$$\times\left\{\frac{Tr\left[\left(\not{p}_3+m_2\right)\gamma^\alpha\not{q}\gamma^\mu\left(\not{p}_4-m_2\right)\gamma^\nu\not{q}\gamma^\beta\right]}{\left(2p_3q+q^2\right)^2}+\frac{Tr\left[\left(\not{p}_3+m_2\right)\gamma^\mu\not{q}\gamma^\alpha\left(\not{p}_4-m_2\right)\gamma^\beta\not{q}\gamma^\nu\right]}{\left(2p_4q+q^2\right)^2}-\right.$$

$$\left.-\frac{Tr\left[\left(\not{p}_3+m_2\right)\gamma^\alpha\not{q}\gamma^\mu\left(\not{p}_4-m_2\right)\gamma^\beta\not{q}\gamma^\nu\right]+Tr\left[\left(\not{p}_3+m_2\right)\gamma^\mu\not{q}\gamma^\alpha\left(\not{p}_4-m_2\right)\gamma^\nu\not{q}\gamma^\beta\right]}{\left(2p_3q+q^2\right)\left(2p_4q+q^2\right)}\right\}=$$

$$=4\left(\left(p_5\right)_\alpha\left(p_6\right)_\beta+\left(p_5\right)_\beta\left(p_6\right)_\alpha-\left(p_5p_6+m_3^2\right)\cdot g_{\alpha\beta}\right)\times$$

$$\times\left\{\frac{Tr\left[\not{p}_3\gamma^\alpha\not{q}\gamma^\mu\not{p}_4\gamma^\nu\not{q}\gamma^\beta\right]-m_2^2Tr\left[\gamma^\alpha\not{q}\gamma^\mu\gamma^\nu\not{q}\gamma^\beta\right]}{\left(2p_3q+q^2\right)^2}+\frac{Tr\left[\not{p}_3\gamma^\mu\not{q}\gamma^\alpha\not{p}_4\gamma^\beta\not{q}\gamma^\nu\right]-m_2^2Tr\left[\gamma^\mu\not{q}\gamma^\alpha\gamma^\beta\not{q}\gamma^\nu\right]}{\left(2p_4q+q^2\right)^2}-\right.$$

$$\left.-\frac{Tr\left[\not{p}_3\gamma^\alpha\not{q}\gamma^\mu\not{p}_4\gamma^\beta\not{q}\gamma^\nu\right]+Tr\left[\not{p}_3\gamma^\mu\not{q}\gamma^\alpha\not{p}_4\gamma^\nu\not{q}\gamma^\beta\right]-m_2^2\left(Tr\left[\gamma^\alpha\not{q}\gamma^\mu\gamma^\beta\not{q}\gamma^\nu\right]+Tr\left[\gamma^\mu\not{q}\gamma^\alpha\gamma^\nu\not{q}\gamma^\beta\right]\right)}{\left(2p_3q+q^2\right)\left(2p_4q+q^2\right)}\right\}=$$

$$=\left\{\frac{p_3^\varphi p_4^\omega q_\sigma q_\rho Tr\left[\gamma_\varphi\gamma^\alpha\gamma^\sigma\gamma^\mu\gamma_\omega\gamma^\nu\gamma^\rho\gamma^\beta\right]-m_2^2q_\sigma q_\rho Tr\left[\gamma^\alpha\gamma^\sigma\gamma^\mu\gamma^\nu\gamma^\rho\gamma^\beta\right]}{\left(2p_3q+q^2\right)^2}+\right.$$

$$+\frac{p_3^\varphi p_4^\omega q_\sigma q_\rho Tr\left[\gamma_\varphi\gamma^\mu\gamma^\sigma\gamma^\alpha\gamma_\omega\gamma^\beta\gamma^\rho\gamma^\nu\right]-m_2^2q_\sigma q_\rho Tr\left[\gamma^\mu\gamma^\sigma\gamma^\alpha\gamma^\beta\gamma^\rho\gamma^\nu\right]}{\left(2p_4q+q^2\right)^2}-$$

$$-\frac{p_3^\varphi p_4^\omega q_\sigma q_\rho\left(Tr\left[\gamma_\varphi\gamma^\alpha\gamma^\sigma\gamma^\mu\gamma_\omega\gamma^\beta\gamma^\rho\gamma^\nu\right]+Tr\left[\gamma_\varphi\gamma^\mu\gamma^\sigma\gamma^\alpha\gamma_\omega\gamma^\nu\gamma^\rho\gamma^\beta\right]\right)}{\left(2p_3q+q^2\right)\left(2p_4q+q^2\right)}+$$

$$\left.+\frac{m_2^2q_\sigma q_\rho\left(Tr\left[\gamma^\alpha\gamma^\sigma\gamma^\mu\gamma^\beta\gamma^\rho\gamma^\nu\right]+Tr\left[\gamma^\mu\gamma^\sigma\gamma^\alpha\gamma^\nu\gamma^\rho\gamma^\beta\right]\right)}{\left(2p_3q+q^2\right)\left(2p_4q+q^2\right)}\right\}\times$$

$$\times4\left(\left(p_5\right)_\alpha\left(p_6\right)_\beta+\left(p_5\right)_\beta\left(p_6\right)_\alpha-\left(p_5p_6+m_3^2\right)\cdot g_{\alpha\beta}\right)=$$

$$=\left\{\left(2q^\nu p_3^\mu p_4^\beta q^\alpha+2q^\nu p_3^\beta p_4^\mu q^\alpha-2g^{\mu\beta}\cdot p_3p_4\cdot q^\nu q^\alpha-2p_4^\beta q^\mu p_3^\nu q^\alpha+2q^\mu p_3^\beta p_4^\nu q^\alpha-\right.\right.$$

$$-2g^{\nu\beta}p_3^\mu\cdot qp_4\cdot q^\alpha+2g^{\mu\beta}p_3^\nu\cdot qp_4\cdot q^\alpha-2p_3^\beta g^{\mu\nu}\cdot qp_4\cdot q^\alpha+2g^{\nu\beta}q^\mu\cdot p_3p_4\cdot q^\alpha-2q^\nu p_3^\mu p_4^\alpha q^\beta+$$

$$+2q^\mu p_3^\nu p_4^\alpha q^\beta+2q^\nu p_3^\alpha p_4^\mu q^\beta+2q^\mu p_3^\alpha p_4^\nu q^\beta+2g^{\nu\alpha}p_3^\mu\cdot qp_4\cdot q^\beta-2g^{\mu\alpha}p_3^\nu\cdot qp_4\cdot q^\beta-$$

$$-2p_3^\alpha g^{\mu\nu}\cdot qp_4\cdot q^\beta-2g^{\nu\alpha}q^\mu\cdot p_3p_4\cdot q^\beta+2g^{\mu\alpha}q^\nu\cdot p_3p_4\cdot q^\beta+2g^{\nu\alpha}\cdot qp_3\cdot p_4^\beta q^\mu-$$

$$
\begin{aligned}
&- 2g^{\alpha\beta}p_4^{\nu}\cdot qp_3\cdot q^{\mu} - 2p_4^{\alpha}g^{\nu\beta}\cdot qp_3\cdot q^{\mu} + 2g^{\mu\beta}\cdot qp_3\cdot p_4^{\alpha}q^{\nu} - 2g^{\mu\alpha}p_4^{\beta}\cdot qp_3\cdot q^{\nu} - \\
&- 2g^{\alpha\beta}p_4^{\mu}\cdot qp_3\cdot q^{\nu} + g^{\mu\nu}p_3^{\beta}p_4^{\alpha}q^2 + g^{\nu\beta}p_3^{\mu}p_4^{\alpha}q^2 + g^{\mu\nu}p_3^{\alpha}p_4^{\beta}q^2 + g^{\mu\alpha}p_3^{\nu}p_4^{\beta}q^2 - g^{\nu\alpha}p_4^{\beta}p_3^{\mu}q^2 - \\
&- g^{\nu\alpha}p_3^{\beta}p_4^{\mu}q^2 + g^{\alpha\beta}p_3^{\nu}p_4^{\mu}q^2 - p_3^{\alpha}g^{\nu\beta}p_4^{\mu}q^2 - p_4^{\alpha}g^{\mu\beta}p_3^{\nu}q^2 - g^{\mu\alpha}p_3^{\beta}p_4^{\nu}q^2 + g^{\alpha\beta}p_3^{\mu}p_4^{\nu}q^2 - p_3^{\alpha}g^{\mu\beta}p_4^{\nu}q^2 + \\
&+ g^{\mu\beta}g^{\nu\alpha}\cdot p_3p_4\cdot q^2 - g^{\mu\alpha}g^{\nu\beta}\cdot p_3p_4\cdot q^2 - g^{\alpha\beta}g^{\mu\nu}\cdot p_3p_4\cdot q^2 - 2g^{\nu\alpha}g^{\mu\beta}\cdot qp_3\cdot qp_4 + \\
&+ 2g^{\mu\alpha}g^{\nu\beta}\cdot qp_3\cdot qp_4 + 2g^{\alpha\beta}g^{\mu\nu}\cdot qp_3\cdot qp_4\Bigg)\times\frac{4}{\left(2p_3q+q^2\right)^2} - \frac{4m_2^2}{\left(2p_3q+q^2\right)^2}\Bigg(2q^{\alpha}q^{\nu}g^{\beta\mu} - \\
&- 2q^{\alpha}q^{\mu}g^{\beta\nu} + 2q^{\beta}q^{\mu}g^{\alpha\nu} - 2q^{\beta}q^{\nu}g^{\alpha\mu} - q^2g^{\alpha\nu}g^{\beta\mu} + q^2g^{\alpha\mu}g^{\beta\nu} + q^2g^{\alpha\beta}g^{\mu\nu}\Bigg) + \Bigg(2q^{\nu}p_3^{\mu}p_4^{\beta}q^{\alpha} + \\
&+ 2q^{\mu}p_3^{\nu}p_4^{\beta}q^{\alpha} + 2q^{\nu}p_3^{\beta}p_4^{\mu}q^{\alpha} - 2g^{\beta\mu}\cdot p_3p_4\cdot q^{\nu}q^{\alpha} - 2p_3^{\beta}q^{\mu}p_4^{\nu}q^{\alpha} + 2g^{\beta\mu}\cdot qp_3\cdot p_4^{\nu}q^{\alpha} - \\
&- 2g^{\beta\nu}p_4^{\mu}\cdot qp_3\cdot q^{\alpha} - 2p_4^{\beta}g^{\mu\nu}\cdot qp_3\cdot q^{\alpha} + 2g^{\beta\nu}q^{\mu}\cdot p_3p_4\cdot q^{\alpha} + 2q^{\nu}p_3^{\mu}p_4^{\alpha}q^{\beta} + 2q^{\mu}p_3^{\nu}p_4^{\alpha}q^{\beta} + \\
&+ 2g^{\alpha\nu}\cdot qp_3\cdot p_4^{\mu}q^{\beta} - 2p_3^{\alpha}p_4^{\mu}q^{\nu}q^{\beta} + 2q^{\mu}p_3^{\alpha}p_4^{\nu}q^{\beta} - 2g^{\alpha\mu}p_4^{\nu}\cdot qp_3\cdot q^{\beta} - 2p_4^{\alpha}g^{\mu\nu}\cdot qp_3\cdot q^{\beta} - \\
&- 2g^{\alpha\nu}q^{\mu}\cdot p_3p_4\cdot q^{\beta} + 2g^{\alpha\mu}q^{\nu}\cdot p_3p_4\cdot q^{\beta} + 2g^{\alpha\nu}p_3^{\beta}\cdot qp_4\cdot q^{\mu} - 2g^{\alpha\beta}p_3^{\nu}\cdot qp_4\cdot q^{\mu} - \\
&- 2p_3^{\alpha}g^{\beta\nu}\cdot qp_4\cdot q^{\mu} + 2g^{\beta\mu}p_3^{\alpha}\cdot qp_4\cdot q^{\nu} - 2g^{\alpha\mu}p_3^{\beta}\cdot qp_4\cdot q^{\nu} - 2g^{\alpha\beta}p_3^{\mu}\cdot qp_4\cdot q^{\nu} + g^{\mu\nu}p_3^{\beta}p_4^{\alpha}q^2 + \\
&+ g^{\mu\nu}p_3^{\alpha}p_4^{\beta}q^2 - g^{\alpha\nu}p_4^{\beta}p_3^{\mu}q^2 - p_4^{\alpha}g^{\beta\nu}p_3^{\mu}q^2 + g^{\beta\nu}p_3^{\alpha}p_4^{\mu}q^2 - g^{\alpha\nu}p_3^{\beta}p_4^{\mu}q^2 + g^{\alpha\beta}p_3^{\nu}p_4^{\mu}q^2 - g^{\alpha\mu}p_4^{\beta}p_3^{\nu}q^2 - \\
&- p_4^{\alpha}g^{\beta\mu}p_3^{\nu}q^2 + g^{\alpha\mu}p_3^{\beta}p_4^{\nu}q^2 + g^{\alpha\beta}p_3^{\mu}p_4^{\nu}q^2 - p_3^{\alpha}g^{\beta\mu}p_4^{\nu}q^2 + g^{\beta\mu}g^{\alpha\nu}\cdot p_3p_4\cdot q^2 - g^{\alpha\mu}g^{\beta\nu}\cdot p_3p_4\cdot q^2 - \\
&- g^{\alpha\beta}g^{\mu\nu}\cdot p_3p_4\cdot q^2 - 2g^{\alpha\nu}g^{\beta\mu}\cdot qp_3\cdot qp_4\cdot + 2g^{\alpha\mu}g^{\beta\nu}\cdot qp_3\cdot qp_4 + 2g^{\alpha\beta}g^{\mu\nu}\cdot qp_3\cdot qp_4\Bigg)\times \\
&\times\frac{4}{\left(2p_4q+q^2\right)^2} - \frac{4m_2^2}{\left(2p_4q+q^2\right)^2}\Bigg(2q^{\alpha}q^{\nu}g^{\beta\mu} - 2q^{\alpha}q^{\mu}g^{\beta\nu} + 2q^{\beta}q^{\mu}g^{\alpha\nu} - 2q^{\beta}q^{\nu}g^{\alpha\mu} - q^2g^{\alpha\nu}g^{\beta\mu} + \\
&+ q^2g^{\alpha\mu}g^{\beta\nu} + q^2g^{\alpha\beta}g^{\mu\nu}\Bigg) - \Bigg(2g^{\mu\nu}\cdot qp_3\cdot p_4^{\beta}q^{\alpha} + 4q^{\beta}p_3^{\nu}p_4^{\mu}q^{\alpha} + 4q^{\beta}p_3^{\mu}p_4^{\nu}q^{\alpha} - 2g^{\beta\nu}p_4^{\mu}\cdot qp_3\cdot q^{\alpha} - \\
&- 2g^{\beta\mu}p_4^{\nu}\cdot qp_3\cdot q^{\alpha} + 2g^{\mu\nu}p_3^{\beta}\cdot qp_4\cdot q^{\alpha} - 2g^{\beta\nu}p_3^{\mu}\cdot qp_4\cdot q^{\alpha} - 2g^{\beta\mu}p_3^{\nu}\cdot qp_4\cdot q^{\alpha} + \\
&+ 4g^{\beta\nu}q^{\mu}\cdot p_3p_4\cdot q^{\alpha} - 4q^{\beta}g^{\mu\nu}\cdot p_3p_4\cdot q^{\alpha} + 2g^{\mu\nu}\cdot qp_3\cdot p_4^{\alpha}q^{\beta} - 2g^{\alpha\nu}p_4^{\mu}\cdot qp_3\cdot q^{\beta} \\
&- 2g^{\alpha\mu}p_4^{\nu}\cdot qp_3\cdot q^{\beta} + 2g^{\mu\nu}p_3^{\alpha}\cdot qp_4\cdot q^{\beta} - 2g^{\alpha\nu}p_3^{\mu}\cdot qp_4\cdot q^{\beta} - 2g^{\alpha\mu}p_3^{\nu}\cdot qp_4\cdot q^{\beta} + 4g^{\alpha\mu}q^{\nu}\cdot p_3p_4\cdot q^{\beta} + \\
&+ 4q^{\nu}p_3^{\beta}p_4^{\alpha}q^{\mu} + 4q^{\nu}p_3^{\alpha}p_4^{\beta}q^{\mu} - 4g^{\alpha\beta}\cdot p_3p_4\cdot q^{\nu}q^{\mu} + 2g^{\alpha\beta}\cdot qp_3\cdot p_4^{\nu}q^{\mu} - 2g^{\alpha\nu}p_4^{\beta}\cdot qp_3\cdot q^{\mu} - \\
&- 2p_4^{\alpha}g^{\beta\nu}\cdot qp_3\cdot q^{\mu} - 2g^{\alpha\nu}p_3^{\beta}\cdot qp_4\cdot q^{\mu} + 2g^{\alpha\beta}p_3^{\nu}\cdot qp_4\cdot q^{\mu} - 2p_3^{\alpha}g^{\beta\nu}\cdot qp_4\cdot q^{\mu} + 2g^{\alpha\beta}\cdot qp_3\cdot p_4^{\mu}q^{\nu} - \\
&- 2g^{\alpha\mu}p_4^{\beta}\cdot qp_3\cdot q^{\nu} - 2p_4^{\alpha}g^{\beta\mu}\cdot qp_3\cdot q^{\nu} - 2g^{\alpha\mu}p_3^{\beta}\cdot qp_4\cdot q^{\nu} + 2g^{\alpha\beta}p_3^{\mu}\cdot qp_4\cdot q^{\nu} - 2p_3^{\alpha}g^{\beta\mu}\cdot qp_4\cdot q^{\nu} + \\
&+ 2g^{\beta\mu}p_3^{\nu}p_4^{\alpha}q^2 + 2g^{\alpha\nu}p_3^{\mu}p_4^{\beta}q^2 + 2g^{\alpha\nu}p_3^{\beta}p_4^{\mu}q^2 - 2g^{\alpha\beta}p_4^{\mu}p_3^{\nu}q^2 + 2g^{\beta\mu}p_3^{\alpha}p_4^{\nu}q^2 - 2g^{\alpha\beta}p_3^{\mu}p_4^{\nu}q^2 - \\
&- 2p_4^{\alpha}p_3^{\beta}g^{\mu\nu}q^2 - 2p_3^{\alpha}p_4^{\beta}g^{\mu\nu}q^2 - 2g^{\alpha\nu}g^{\beta\mu}\cdot p_3p_4\cdot q^2 - 2g^{\alpha\mu}g^{\beta\nu}\cdot p_3p_4\cdot q^2 + 2g^{\alpha\beta}g^{\mu\nu}\cdot p_3p_4\cdot q^2 + \\
&+ 4g^{\beta\mu}g^{\alpha\nu}\cdot qp_3\cdot qp_4 + 4g^{\alpha\mu}g^{\beta\nu}\cdot qp_3\cdot qp_4 - 4g^{\alpha\beta}g^{\mu\nu}\cdot qp_3\cdot qp_4\Bigg)\times\frac{4}{\left(2p_3q+q^2\right)\left(2p_4q+q^2\right)} +
\end{aligned}
$$

$$+\frac{4m_2^2}{(2p_3q+q^2)(2p_4q+q^2)}\Bigg(4q^\alpha q^\beta g^{\mu\nu}-4q^\alpha q^\mu g^{\beta\nu}-4q^\beta q^\nu g^{\alpha\mu}+4q^\mu q^\nu g^{\alpha\beta}+2q^2 g^{\alpha\nu}g^{\beta\mu}+$$

$$+2q^2 g^{\alpha\mu}g^{\beta\nu}-2q^2 g^{\alpha\beta}g^{\mu\nu}\Bigg)\Bigg\}4\Big((p_5)_\alpha (p_6)_\beta+(p_5)_\beta (p_6)_\alpha-(p_5p_6+m_3^2)\cdot g_{\alpha\beta}\Big)$$

and

$$N_1^{\mu\nu}=\frac{32}{(2p_3q+q^2)^2}\Bigg(g^{\mu\nu}\Bigg(q^2m_2^2\cdot p_5p_6+q^2m_3^2\cdot p_3p_4-2m_3^2\cdot qp_3\cdot qp_4+2q^2m_2^2m_3^2+$$

$$+q^2\cdot p_4p_5\cdot p_3p_6+q^2\cdot p_3p_5\cdot p_4p_6-2\cdot p_3p_6\cdot qp_4\cdot qp_5-2\cdot p_3p_5\cdot qp_4\cdot qp_6\Big)+$$

$$+p_4^\mu\left(-m_3^2p_3^\nu q^2+2m_3^2q^\nu\cdot qp_3+2q^\nu\cdot p_3p_5\cdot qp_6+2q^\nu\cdot p_3p_6\cdot qp_5-p_6^\nu q^2\cdot p_3p_5-p_5^\nu q^2\cdot p_3p_6\right)+$$

$$+p_4^\nu\left(-m_3^2p_3^\mu q^2+2m_3^2q^\mu\cdot qp_3+2q^\mu\cdot p_3p_5\cdot qp_6+2q^\mu\cdot p_3p_6\cdot qp_5-p_6^\mu q^2\cdot p_3p_5-p_5^\mu q^2\cdot p_3p_6\right)\Bigg)+$$

$$+\frac{32}{(2p_4q+q^2)^2}\Bigg(g^{\mu\nu}\Bigg(m_2^2q^2\cdot p_5p_6+m_3^2q^2\cdot p_3p_4-2m_3^2\cdot qp_3\cdot qp_4+2m_2^2m_3^2q^2+q^2\cdot p_4p_5\cdot p_3p_6+$$

$$+q^2\cdot p_3p_5\cdot p_4p_6-2\cdot p_4p_6\cdot qp_3\cdot qp_5-2\cdot p_4p_5\cdot qp_3\cdot qp_6\Big)+$$

$$+p_3^\mu\left(-p_4^\nu m_3^2q^2+2m_3^2q^\nu\cdot qp_4+2q^\nu\cdot p_4p_5\cdot qp_6+2q^\nu\cdot p_4p_6\cdot qp_5-p_6^\nu\cdot q^2\cdot p_4p_5-p_5^\nu\cdot q^2\cdot p_4p_6\right)+$$

$$+p_3^\nu\left(-p_4^\mu m_3^2q^2+2m_3^2q^\mu\cdot qp_4+2q^\mu\cdot p_4p_5\cdot qp_6+2q^\mu\cdot p_4p_6\cdot qp_5-p_6^\mu\cdot q^2\cdot p_4p_5-p_5^\mu\cdot q^2p_4p_6\right)\Bigg)+$$

$$+\frac{32}{(2p_3q+q^2)(2p_4q+q^2)}\Bigg(-2p_4^\nu q^\mu\cdot qp_3\cdot p_5p_6-2p_4^\mu q^\nu\cdot qp_3\cdot p_5p_6+$$

$$+q^\nu q^\mu\left(-4m_2^2m_3^2-4\cdot p_3p_6\cdot p_4p_5-4\cdot p_3p_5\cdot p_4p_6+4\cdot p_3p_4\cdot p_5p_6\right)+$$

$$+p_6^\mu\Bigg[q^\nu\left(-2\cdot qp_5\cdot m_2^2-2\cdot qp_5\cdot p_3p_4+2\cdot qp_4\cdot p_3p_5+2\cdot qp_3\cdot p_4p_5\right)+$$

$$+p_4^\nu\left(2\cdot qp_3\cdot qp_5-q^2\cdot p_3p_5\right)+p_3^\nu\left(2\cdot qp_4\cdot qp_5-q^2\cdot p_4p_5\right)\Bigg]+$$

$$+p_6^\nu\Bigg[q^\mu\left(-2\cdot qp_5\cdot m_2^2-2\cdot qp_5\cdot p_3p_4+2\cdot qp_4\cdot p_3p_5+2\cdot qp_3\cdot p_4p_5\right)$$

$$+p_4^\mu\left(2\cdot qp_3\cdot qp_5-q^2\cdot p_3p_5\right)+p_3^\mu\left(2\cdot qp_4\cdot qp_5-q^2\cdot p_4p_5\right)\Bigg]+$$

$$+p_3^\nu\left(p_4^\mu\left(2q^2\cdot p_5p_6-4\cdot qp_5\cdot qp_6\right)-2q^\mu\cdot qp_4\cdot p_5p_6\right)+$$

$$+p_3^\mu\left(p_4^\nu\left(2q^2\cdot p_5p_6-4\cdot qp_5\cdot qp_6\right)-2q^\nu\cdot qp_4\cdot p_5p_6\right)+$$

$$+p_5^\nu\Bigg[q^\mu\left(-2\cdot qp_6\cdot m_2^2-2\cdot qp_6\cdot p_3p_4+2\cdot qp_4\cdot p_3p_6+2\cdot qp_3\cdot p_4p_6\right)+$$

$$+p_6^{\mu}\left(2m_2^2q^2+2\cdot p_3p_4\cdot q^2-4\cdot qp_3\cdot qp_4\right)+p_4^{\mu}\left(2\cdot qp_3\cdot qp_6-q^2\cdot p_3p_6\right)+p_3^{\mu}\left(2\cdot qp_4\cdot qp_6-q^2\cdot p_4p_6\right)\Big]+$$

$$+p_5^{\mu}\Big[q^{\nu}\left(-2\cdot qp_6\cdot m_2^2-2\cdot qp_6\cdot p_3p_4+2\cdot qp_4\cdot p_3p_6+2\cdot qp_3\cdot p_4p_6\right)+$$

$$+p_6^{\nu}\left(2m_2^2q^2+2\cdot p_3p_4\cdot q^2-4\cdot qp_3\cdot qp_4\right)+p_4^{\nu}\left(2\cdot qp_3\cdot qp_6-q^2\cdot p_3p_6\right)+p_3^{\nu}\left(2\cdot qp_4\cdot qp_6-q^2\cdot p_4p_6\right)\Big]+$$

$$+g^{\mu\nu}\Big(-2\cdot p_5p_6\cdot m_2^2q^2-2\cdot p_3p_4\cdot m_3^2q^2+2\cdot p_4p_5\cdot p_3p_6\cdot q^2+2\cdot p_3p_5\cdot p_4p_6\cdot q^2-4\cdot p_3p_4\cdot p_5p_6\cdot q^2-$$

$$-2\cdot qp_4\cdot qp_6\cdot p_3p_5-2\cdot qp_3\cdot qp_6\cdot p_4p_5+4m_2^2\cdot qp_5\cdot qp_6+4\cdot p_3p_4\cdot qp_5\cdot qp_6-2\cdot qp_4\cdot qp_5\cdot p_3p_6-$$

$$-2\cdot qp_3\cdot qp_5\cdot p_4p_6+4\cdot qp_3\cdot qp_4\cdot p_5p_6\Big)\Big). \tag{C.44}$$

Calculation of contraction over indexes α and β in the tensor expression at the lines (C.28-C.29) of the matrix element (C.22-C.31) follows

$$N_2^{\mu\nu}=Tr\left[\left(\not p_5+m_3\right)\left(\frac{2\not p_3}{\left(p_3+q\right)^2-m_2^2}-\frac{2\not p_4}{\left(p_4+q\right)^2-m_2^2}\right)\left(\not p_6-m_3\right)\gamma_\beta\right]\times$$

$$\times Tr\left[\left(\not p_3+m_2\right)\gamma^\mu\left(\not p_4-m_2\right)\left(\frac{\gamma^\nu\not q\gamma^\beta}{\left(p_3+q\right)^2-m_2^2}-\frac{\gamma^\beta\not q\gamma^\nu}{\left(p_4+q\right)^2-m_2^2}\right)\right]=$$

$$=\left(\left(\frac{2Tr\left[\not p_5\not p_3\not p_6\gamma_\beta\right]}{2p_3q+q^2}-\frac{2Tr\left[\not p_5\not p_4\not p_6\gamma_\beta\right]}{2p_4q+q^2}\right)-m_3^2\cdot\left(\frac{2Tr\left[\not p_3\gamma_\beta\right]}{2p_3q+q^2}-\frac{2Tr\left[\not p_4\gamma_\beta\right]}{2p_4q+q^2}\right)\right)\times$$

$$\times\left(\left(\frac{Tr\left[\not p_3\gamma^\mu\not p_4\gamma^\nu\not q\gamma^\beta\right]}{2p_3q+q^2}-\frac{Tr\left[\not p_3\gamma^\mu\not p_4\gamma^\beta\not q\gamma^\nu\right]}{2p_4q+q^2}\right)-m_2^2\cdot\left(\frac{Tr\left[\gamma^\mu\gamma^\nu\not q\gamma^\beta\right]}{2p_3q+q^2}-\frac{Tr\left[\gamma^\mu\gamma^\beta\not q\gamma^\nu\right]}{2p_4q+q^2}\right)\right)=$$

$$=32\Bigg(\frac{-\left(p_3\right)_\beta m_3^2-\left(p_3\right)_\beta\cdot p_5p_6+\left(p_6\right)_\beta\cdot p_3p_5+\left(p_5\right)_\beta\cdot p_3p_6}{2p_3q+q^2}-$$

$$-\frac{-\left(p_4\right)_\beta m_3^2-\left(p_4\right)_\beta\cdot p_5p_6+\left(p_6\right)_\beta\cdot p_4p_5+\left(p_5\right)_\beta\cdot p_4p_6}{2p_4q+q^2}\Bigg)\times\Bigg[\Big(m_2^2q^\mu g^{\beta\nu}-m_2^2q^\nu g^{\beta\mu}-$$

$$-q^\beta m_2^2g^{\mu\nu}-q^\beta g^{\mu\nu}\cdot p_3p_4+q^\mu g^{\beta\nu}\cdot p_3p_4-q^\nu g^{\beta\mu}\cdot p_3p_4+p_4^\beta g^{\mu\nu}\cdot p_3q-p_4^\nu g^{\beta\mu}\cdot p_3q-$$

$$-p_4^\mu g^{\beta\nu}\cdot p_3q+p_3^\nu g^{\beta\mu}\cdot p_4q-p_3^\mu g^{\beta\nu}\cdot p_4q-p_3^\beta g^{\mu\nu}\cdot p_4q+p_4^\mu p_3^\nu q^\beta+p_3^\mu p_4^\nu q^\beta-p_4^\beta p_3^\nu q^\mu+$$

$$+p_3^\beta p_4^\nu q^\mu+p_4^\beta p_3^\mu q^\nu+p_3^\beta p_4^\mu q^\nu\Big)/\left(2p_3q+q^2\right)-\Big(m_2^2q^\mu g^{\beta\nu}-m_2^2q^\nu g^{\beta\mu}-q^\beta m_2^2g^{\mu\nu}-$$

$$-q^\beta g^{\mu\nu}\cdot p_3p_4+q^\mu g^{\beta\nu}\cdot p_3p_4-q^\nu g^{\beta\mu}\cdot p_3p_4+p_4^\nu g^{\beta\mu}\cdot p_3q-p_4^\mu g^{\beta\nu}\cdot p_3q-p_4^\beta g^{\mu\nu}\cdot p_3q+$$

$$+p_3^\beta g^{\mu\nu}\cdot p_4q-p_3^\nu g^{\beta\mu}\cdot p_4q-p_3^\mu g^{\beta\nu}\cdot p_4q+p_4^\mu p_3^\nu q^\beta+p_3^\mu p_4^\nu q^\beta+p_4^\beta p_3^\nu q^\mu-p_3^\beta p_4^\nu q^\mu+p_4^\beta p_3^\mu q^\nu+$$

$$+p_3^\beta p_4^\mu q^\nu\Big)/\left(2p_4q+q^2\right)\Bigg]$$

and

$$
\begin{aligned}
N_2^{\mu\nu} = \frac{32}{(2p_3q+q^2)^2}\Bigg(& g^{\mu\nu}\Big(m_3^2\cdot qp_3\cdot m_2^2 - qp_6\cdot p_3p_5\cdot m_2^2 - qp_5\cdot p_3p_6\cdot m_2^2 + qp_3\cdot p_5p_6\cdot m_2^2 + \\
& + m_3^2p_3^2\cdot qp_4 - qp_6\cdot p_3p_4\cdot p_3p_5 - qp_5\cdot p_3p_4\cdot p_3p_6 - 2\cdot qp_4\cdot p_3p_5\cdot p_3p_6 + qp_3\cdot p_4p_5\cdot p_3p_6 + \\
& + qp_3\cdot p_3p_5\cdot p_4p_6 + p_3^2\cdot qp_4\cdot p_5p_6\Big) + \\
& + p_4^\nu\left(2\cdot p_3p_5\cdot p_3p_6\cdot q^\mu - p_3^2\cdot p_5p_6\cdot q^\mu - q^\mu m_3^2p_3^2 + p_3^\mu\left(p_3p_5\cdot qp_6 + qp_5\cdot p_3p_6\right)\right) + \\
& + p_4^\mu\left(2\cdot p_3p_5\cdot p_3p_6\cdot q^\nu - p_3^2\cdot p_5p_6\cdot q^\nu - q^\nu m_3^2p_3^2 + p_3^\nu\left(p_3p_5\cdot qp_6 + qp_5\cdot p_3p_6\right)\right) + \\
& + p_3^\mu\left(m_2^2m_3^2q^\nu + p_4p_5\cdot p_3p_6\cdot q^\nu + p_3p_5\cdot p_4p_6\cdot q^\nu + m_2^2\cdot p_5p_6\cdot q^\nu\right) + \\
& + p_3^\nu\left(-p_5p_6\cdot m_2^2q^\mu - p_3p_6\cdot p_4p_5\cdot q^\mu - p_3p_5\cdot p_4p_6\cdot q^\mu - q^\mu m_2^2m_3^2\right) + \\
& + p_6^\mu\left(-p_3p_4\cdot p_3p_5\cdot q^\nu - q^\nu m_2^2\cdot p_3p_5 - p_4^\nu\cdot qp_3\cdot p_3p_5 + p_3^\nu\cdot qp_4\cdot p_3p_5\right) + \\
& + p_6^\nu\left(m_2^2\cdot p_3p_5\cdot q^\mu + p_3p_4\cdot p_3p_5\cdot q^\mu - p_4^\mu\cdot qp_3\cdot p_3p_5 - p_3^\mu\cdot qp_4\cdot p_3p_5\right) + \\
& + p_5^\nu\left(m_2^2\cdot p_3p_6\cdot q^\mu + p_3p_4\cdot p_3p_6\cdot q^\mu - p_4^\mu\cdot qp_3\cdot p_3p_6 - p_3^\mu\cdot qp_4\cdot p_3p_6\right) + \\
& + p_5^\mu\left(-p_3p_4\cdot p_3p_6\cdot q^\nu - q^\nu m_2^2\cdot p_3p_6 - p_4^\nu\cdot qp_3\cdot p_3p_6 + p_3^\nu\cdot qp_4\cdot p_3p_6\right)\Bigg) + \\
& + \frac{32}{(2p_4q+q^2)^2}\Bigg(p_6^\mu\left(-p_3p_4\cdot p_4p_5\cdot q^\nu - q^\nu m_2^2\cdot p_4p_5\right) + p_6^\nu\left(m_2^2\cdot p_4p_5\cdot q^\mu + p_3p_4\cdot p_4p_5\cdot q^\mu\right) + \\
& + p_5^\nu\left(m_2^2\cdot p_4p_6\cdot q^\mu + p_3p_4\cdot p_4p_6\cdot q^\mu\right) + p_5^\mu\left(-p_3p_4\cdot p_4p_6\cdot q^\nu - q^\nu m_2^2\cdot p_4p_6\right) \\
& + p_4^\nu\Big[p_3^\mu\left(p_4p_5\cdot qp_6 + qp_5\cdot p_4p_6\right) - q^\mu m_2^2m_3^2 - p_3p_6\cdot p_4p_5\cdot q^\mu - p_3p_5\cdot p_4p_6\cdot q^\mu - q^\mu m_2^2\cdot p_5p_6 + \\
& + p_6^\mu\cdot qp_3\cdot p_4p_5 + p_5^\mu\cdot qp_3\cdot p_4p_6\Big] + \\
& + p_4^\mu\Big[p_3^\nu\left(p_4p_5\cdot qp_6 + qp_5\cdot p_4p_6\right) + q^\nu m_2^2m_3^2 + p_4p_5\cdot p_3p_6\cdot q^\nu + p_3p_5\cdot p_4p_6\cdot q^\nu + q^\nu m_2^2\cdot p_5p_6 - \\
& - p_6^\nu\cdot qp_3\cdot p_4p_5 - p_5^\nu\cdot qp_3\cdot p_4p_6\Big] + \\
& + p_3^\mu\left(2\cdot p_4p_5\cdot p_4p_6\cdot q^\nu - p_4^2\cdot p_5p_6\cdot q^\nu - q^\nu m_3^2p_4^2 - p_6^\nu\cdot qp_4\cdot p_4p_5 - p_5^\nu\cdot qp_4\cdot p_4p_6\right) + \\
& + p_3^\nu\left(2\cdot p_4p_5\cdot p_4p_6\cdot q^\mu - p_4^2\cdot p_5p_6\cdot q^\mu - q^\mu m_3^2p_4^2 - p_6^\mu\cdot qp_4\cdot p_4p_5 - p_5^\mu\cdot qp_4\cdot p_4p_6\right) + \\
& + g^{\mu\nu}\Big[m_3^2\cdot qp_4\cdot m_2^2 - qp_6\cdot p_4p_5\cdot m_2^2 - qp_5\cdot p_4p_6\cdot m_2^2 + qp_4\cdot p_5p_6\cdot m_2^2 + m_3^2\cdot qp_3\cdot p_4^2 - \\
& - qp_6\cdot p_3p_4\cdot p_4p_5 + qp_4\cdot p_4p_5\cdot p_3p_6 - qp_5\cdot p_3p_4\cdot p_4p_6 + qp_4\cdot p_3p_5\cdot p_4p_6 - \\
& - 2\cdot qp_3\cdot p_4p_5\cdot p_4p_6 + qp_3\cdot p_4^2\cdot p_5p_6\Big]\Bigg) +
\end{aligned}
$$

$$+\frac{32}{(2p_3q+q^2)(2p_4q+q^2)}\Bigg(g^{\mu\nu}\Big(m_3^2\cdot qp_3\cdot m_2^2-qp_6\cdot p_3p_5\cdot m_2^2-qp_5\cdot p_3p_6\cdot m_2^2+$$
$$+qp_3\cdot p_5p_6\cdot m_2^2+m_3^2p_3^2\cdot qp_4-qp_6\cdot p_3p_4\cdot p_3p_5-qp_5\cdot p_3p_4\cdot p_3p_6-2\cdot qp_4\cdot p_3p_5\cdot p_3p_6+$$
$$+qp_3\cdot p_4p_5\cdot p_3p_6+qp_3\cdot p_3p_5\cdot p_4p_6+p_3^2\cdot qp_4\cdot p_5p_6\Big)+$$
$$+p_3^\mu\left(+m_2^2\cdot p_5p_6\cdot q^\nu+p_4p_5\cdot p_3p_6\cdot q^\nu+\cdot p_3p_5\cdot p_4p_6\cdot q^\nu+q^\nu m_2^2m_3^2\right)+$$
$$+p_3^\nu\left(-p_5p_6\cdot m_2^2q^\mu-p_3p_6\cdot p_4p_5\cdot q^\mu-p_3p_5\cdot p_4p_6\cdot q^\mu-q^\mu m_2^2m_3^2\right)+$$
$$+p_6^\mu\left(-q^\nu m_2^2\cdot p_3p_5-q^\nu\cdot p_3p_4\cdot p_3p_5-p_4^\nu\cdot qp_3\cdot p_3p_5+p_3^\nu\cdot qp_4\cdot p_3p_5\right)+$$
$$+p_6^\nu\left(+q^\mu m_2^2\cdot p_3p_5+q^\mu\cdot p_3p_4\cdot p_3p_5-p_4^\mu\cdot qp_3\cdot p_3p_5-p_3^\mu\cdot qp_4\cdot p_3p_5\right)+$$
$$+p_5^\nu\left(m_2^2\cdot p_3p_6\cdot q^\mu+p_3p_4\cdot p_3p_6\cdot q^\mu-p_4^\mu\cdot qp_3\cdot p_3p_6-p_3^\mu\cdot qp_4\cdot p_3p_6\right)+$$
$$+p_5^\mu\left(-p_3p_4\cdot p_3p_6\cdot q^\nu-q^\nu m_2^2\cdot p_3p_6-p_4^\nu\cdot qp_3\cdot p_3p_6+p_3^\nu\cdot qp_4\cdot p_3p_6\right)+$$
$$+p_4^\nu\left(2\cdot p_3p_5\cdot p_3p_6\cdot q^\mu-p_3^2\cdot p_5p_6\cdot q^\mu-q^\mu m_3^2p_3^2+p_3^\mu\left(p_3p_5\cdot qp_6+qp_5\cdot p_3p_6\right)\right)+$$
$$+p_4^\mu\left(2\cdot p_3p_5\cdot p_3p_6\cdot q^\nu-p_3^2\cdot p_5p_6\cdot q^\nu-q^\nu m_3^2p_3^2+p_3^\nu\left(p_3p_5\cdot qp_6+qp_5\cdot p_3p_6\right)\right)\Bigg).\quad\text{(C.45)}$$

Calculation of contraction over indexes α and β in the tensor expression at the lines (C.30-C.31) of matrix element (C.22-C.31)

$$N_3^{\mu\nu}=Tr\left[\left(\not p_5+m_3\right)\gamma_\alpha\left(\not p_6-m_3\right)\left(\frac{2\not p_3}{\left(p_3+q\right)^2-m_2^2}-\frac{2\not p_4}{\left(p_4+q\right)^2-m_2^2}\right)\right]\times$$
$$\times Tr\left[\left(\not p_3+m_2\right)\left(\frac{\gamma^\alpha\not q\gamma^\mu}{\left(p_3+q\right)^2-m_2^2}-\frac{\gamma^\mu\not q\gamma^\alpha}{\left(p_4+q\right)^2-m_2^2}\right)\left(\not p_4-m_2\right)\gamma^\nu\right]\Bigg\}=$$
$$=\left(\left(\frac{2Tr\left[\not p_5\gamma_\alpha\not p_6\not p_3\right]}{2p_3q+q^2}-\frac{2Tr\left[\not p_5\gamma_\alpha\not p_6\not p_4\right]}{2p_4q+q^2}\right)-m_3^2\cdot\left(\frac{2Tr\left[\gamma_\alpha\not p_3\right]}{2p_3q+q^2}-\frac{2Tr\left[\gamma_\alpha\not p_4\right]}{2p_4q+q^2}\right)\right)\times$$
$$\times\left(\left(\frac{Tr\left[\not p_3\gamma^\alpha\not q\gamma^\mu\not p_4\gamma^\nu\right]}{2p_3q+q^2}-\frac{Tr\left[\not p_3\gamma^\mu\not q\gamma^\alpha\not p_4\gamma^\nu\right]}{2p_4q+q^2}\right)-m_2^2\cdot\left(\frac{Tr\left[\gamma^\alpha\not q\gamma^\mu\gamma^\nu\right]}{2p_3q+q^2}-\frac{Tr\left[\gamma^\mu\not q\gamma^\alpha\gamma^\nu\right]}{2p_4q+q^2}\right)\right)=$$
$$=32\Bigg(\frac{-\left(p_3\right)_\alpha m_3^2-\left(p_3\right)_\alpha\left(p_5p_6\right)+\left(p_6\right)_\alpha\left(p_3p_5\right)+\left(p_5\right)_\alpha\left(p_3p_6\right)}{2p_3q+q^2}-$$
$$-\frac{-\left(p_4\right)_\alpha m_3^2-\left(p_4\right)_\alpha\cdot p_5p_6+\left(p_6\right)_\alpha\cdot p_4p_5+\left(p_5\right)_\alpha\cdot p_4p_6}{2p_4q+q^2}\Bigg)\times\Bigg[\Bigg(-m_2^2q^\mu g^{\alpha\nu}+m_2^2q^\nu g^{\alpha\mu}-$$
$$-q^\alpha m_2^2g^{\mu\nu}-q^\alpha g^{\mu\nu}\cdot p_3p_4-q^\mu g^{\alpha\nu}\cdot p_3p_4+q^\nu g^{\alpha\mu}\cdot p_3p_4+p_4^\alpha g^{\mu\nu}\cdot p_3q-p_4^\nu g^{\alpha\mu}\cdot p_3q-$$
$$-p_4^\mu g^{\alpha\nu}\cdot p_3q+p_3^\mu g^{\alpha\nu}\cdot p_4q-p_3^\nu g^{\alpha\mu}\cdot p_4q-p_3^\alpha g^{\mu\nu}\cdot p_4q+p_4^\mu p_3^\nu q^\alpha+p_3^\mu p_4^\nu q^\alpha+p_4^\alpha p_3^\nu q^\mu+$$
$$+p_3^\alpha p_4^\nu q^\mu-p_4^\alpha p_3^\mu q^\nu+p_3^\alpha p_4^\mu q^\nu\Bigg)/\left(2p_3q+q^2\right)-\Bigg(-m_2^2q^\mu g^{\alpha\nu}+m_2^2q^\nu g^{\alpha\mu}-q^\alpha m_2^2g^{\mu\nu}-$$
$$-q^\alpha g^{\mu\nu}\cdot p_3p_4-q^\mu g^{\alpha\nu}\cdot p_3p_4+q^\nu g^{\alpha\mu}\cdot p_3p_4+p_4^\mu g^{\alpha\nu}\cdot p_3q-p_4^\nu g^{\alpha\mu}\cdot p_3q-p_4^\alpha g^{\mu\nu}\cdot p_3q+$$
$$+p_3^\alpha g^{\mu\nu}\cdot p_4q-p_3^\nu g^{\alpha\mu}\cdot p_4q-p_3^\mu g^{\alpha\nu}\cdot p_4q+p_4^\mu p_3^\nu q^\alpha+p_3^\mu p_4^\nu q^\alpha+p_4^\alpha p_3^\nu q^\mu+p_3^\alpha p_4^\mu q^\nu+p_4^\alpha p_3^\mu q^\nu-$$

$$- p_3^\alpha p_4^\mu q^\nu \Big) / \left(2p_4 q + q^2\right) \Big] =$$

and

$$N_3^{\mu\nu} = \frac{32}{\left(2p_3 q + q^2\right)^2} \Bigg(g^{\mu\nu} \Big(m_3^2 \cdot qp_3 \cdot m_2^2 - qp_6 \cdot p_3 p_5 \cdot m_2^2 - qp_5 \cdot p_3 p_6 \cdot m_2^2 + qp_3 \cdot p_5 p_6 \cdot m_2^2 +$$
$$+ m_3^2 p_3^2 \cdot qp_4 - qp_6 \cdot p_3 p_4 \cdot p_3 p_5 - qp_5 \cdot p_3 p_4 \cdot p_3 p_6 - 2 \cdot qp_4 \cdot p_3 p_5 \cdot p_3 p_6 + qp_3 \cdot p_4 p_5 \cdot p_3 p_6 +$$
$$+ qp_3 \cdot p_3 p_5 \cdot p_4 p_6 + p_3^2 \cdot qp_4 \cdot p_5 p_6 \Big)$$
$$+ p_4^\nu \left(2 \cdot p_3 p_5 \cdot p_3 p_6 \cdot q^\mu - p_3^2 \cdot p_5 p_6 \cdot q^\mu - q^\mu m_3^2 p_3^2 + p_3^\mu \left(p_3 p_5 \cdot qp_6 + qp_5 \cdot p_3 p_6\right)\right) +$$
$$+ p_4^\mu \left(2 \cdot p_3 p_5 \cdot p_3 p_6 \cdot q^\nu - p_3^2 \cdot p_5 p_6 \cdot q^\nu - q^\nu m_3^2 p_3^2 + p_3^\nu \left(p_3 p_5 \cdot qp_6 + qp_5 \cdot p_3 p_6\right)\right) +$$
$$+ p_3^\mu \left(-p_5 p_6 \cdot m_2^2 q^\nu - p_3 p_6 \cdot p_4 p_5 \cdot q^\nu - p_3 p_5 \cdot p_4 p_6 \cdot q^\nu - q^\nu m_2^2 m_3^2\right) +$$
$$+ p_3^\nu \left(m_2^2 m_3^2 q^\mu + p_4 p_5 \cdot p_3 p_6 \cdot q^\mu + p_3 p_5 \cdot p_4 p_6 \cdot q^\mu + m_2^2 \cdot p_5 p_6 \cdot q^\mu\right) +$$
$$+ p_6^\mu \left(m_2^2 \cdot p_3 p_5 \cdot q^\nu + p_3 p_4 \cdot p_3 p_5 \cdot q^\nu - p_4^\nu \cdot qp_3 \cdot p_3 p_5 - p_3^\nu \cdot qp_4 \cdot p_3 p_5\right) +$$
$$+ p_6^\nu \left(-p_3 p_4 \cdot p_3 p_5 \cdot q^\mu - q^\mu m_2^2 \cdot p_3 p_5 - p_4^\mu \cdot qp_3 \cdot p_3 p_5 + p_3^\mu \cdot qp_4 \cdot p_3 p_5\right) +$$
$$+ p_5^\mu \left(m_2^2 \cdot p_3 p_6 \cdot q^\nu + p_3 p_4 \cdot p_3 p_6 \cdot q^\nu - p_4^\nu \cdot qp_3 \cdot p_3 p_6 - p_3^\nu \cdot qp_4 \cdot p_3 p_6\right) +$$
$$+ p_5^\nu \left(-p_3 p_4 \cdot p_3 p_6 \cdot q^\mu - q^\mu m_2^2 \cdot p_3 p_6 - p_4^\mu \cdot qp_3 \cdot p_3 p_6 + p_3^\mu \cdot qp_4 \cdot p_3 p_6\right) \Bigg) +$$
$$+ \frac{32}{\left(2p_4 q + q^2\right)^2} \Bigg(p_6^\mu \left(m_2^2 \cdot p_4 p_5 \cdot q^\nu + p_3 p_4 \cdot p_4 p_5 \cdot q^\nu\right) + p_6^\nu \left(-p_3 p_4 \cdot p_4 p_5 \cdot q^\mu - q^\mu m_2^2 \cdot p_4 p_5\right) +$$
$$+ p_5^\mu \left(m_2^2 \cdot p_4 p_6 \cdot q^\nu + p_3 p_4 \cdot p_4 p_6 \cdot q^\nu\right) + p_5^\nu \left(-p_3 p_4 \cdot p_4 p_6 \cdot q^\mu - q^\mu m_2^2 \cdot p_4 p_6\right) +$$
$$+ g^{\mu\nu} \Big[m_3^2 \cdot qp_4 \cdot m_2^2 - qp_6 \cdot p_4 p_5 \cdot m_2^2 - qp_5 \cdot p_4 p_6 \cdot m_2^2 + qp_4 \cdot p_5 p_6 \cdot m_2^2 + m_3^2 \cdot qp_3 \cdot p_4^2 -$$
$$- qp_6 \cdot p_3 p_4 \cdot p_4 p_5 + qp_4 \cdot p_4 p_5 \cdot p_3 p_6 - qp_5 \cdot p_3 p_4 \cdot p_4 p_6 + qp_4 \cdot p_3 p_5 \cdot p_4 p_6 -$$
$$- 2 \cdot qp_3 \cdot p_4 p_5 \cdot p_4 p_6 + qp_3 \cdot p_4^2 \cdot p_5 p_6 \Big] +$$
$$+ p_4^\nu \Big[m_2^2 m_3^2 q^\mu + p_4 p_5 \cdot p_3 p_6 \cdot q^\mu + p_3 p_5 \cdot p_4 p_6 \cdot q^\mu + m_2^2 \cdot p_5 p_6 \cdot q^\mu - p_6^\mu \cdot qp_3 \cdot p_4 p_5 -$$
$$- p_5^\mu \cdot qp_3 \cdot p_4 p_6 + p_3^\mu \left(p_4 p_5 \cdot qp_6 + qp_5 \cdot p_4 p_6\right) \Big] +$$
$$+ p_4^\mu \Big[- p_5 p_6 \cdot m_2^2 q^\nu - p_3 p_6 \cdot p_4 p_5 \cdot q^\nu - p_3 p_5 \cdot p_4 p_6 \cdot q^\nu + qp_3 \cdot p_4 p_5 \cdot p_6^\nu - q^\nu m_2^2 m_3^2 +$$
$$+ qp_3 \cdot p_5^\nu \cdot p_4 p_6 + p_3^\nu \left(p_4 p_5 \cdot qp_6 + qp_5 \cdot p_4 p_6\right) \Big] +$$
$$+ p_3^\mu \left(2 \cdot p_4 p_5 \cdot p_4 p_6 \cdot q^\nu - p_4^2 \cdot p_5 p_6 \cdot q^\nu - q^\nu m_3^2 p_4^2 - p_6^\nu \cdot qp_4 \cdot p_4 p_5 - p_5^\nu \cdot qp_4 \cdot p_4 p_6\right) +$$

$$+ p_3^{\nu}\left(2\cdot p_4p_5\cdot p_4p_6\cdot q^{\mu} - p_4^2\cdot p_5p_6\cdot q^{\mu} - q^{\mu}m_3^2p_4^2 - p_6^{\mu}\cdot qp_4\cdot p_4p_5 - p_5^{\mu}\cdot qp_4\cdot p_4p_6\right)\Bigg)+$$

$$+\frac{32}{\left(2p_3q+q^2\right)\left(2p_4q+q^2\right)}\Bigg(g^{\mu\nu}\Big[- qp_4\cdot m_3^2m_2^2 - qp_3\cdot m_3^2m_2^2 + p_3p_5\cdot qp_6\cdot m_2^2 + p_4p_5\cdot qp_6\cdot m_2^2+$$
$$+ qp_5\cdot p_3p_6\cdot m_2^2 + qp_5\cdot p_4p_6\cdot m_2^2 - qp_3\cdot p_5p_6\cdot m_2^2 - qp_4\cdot p_5p_6\cdot m_2^2 - 2\cdot qp_3\cdot p_3p_4\cdot m_3^2-$$
$$- 2\cdot qp_4\cdot p_3p_4\cdot m_3^2 + m_3^2\cdot qp_3\cdot p_4^2 + m_3^2p_3^2\cdot qp_4 + p_3p_4\cdot p_3p_5\cdot qp_6 + p_3p_4\cdot p_4p_5\cdot qp_6+$$
$$+ p_3p_4\cdot qp_5\cdot p_3p_6 - 2\cdot qp_4\cdot p_3p_5\cdot p_3p_6 + qp_3\cdot p_4p_5\cdot p_3p_6 + qp_4\cdot p_4p_5\cdot p_3p_6+$$
$$+ p_3p_4\cdot qp_5\cdot p_4p_6 + qp_3\cdot p_3p_5\cdot p_4p_6 + qp_4\cdot p_3p_5\cdot p_4p_6 - 2\cdot qp_3\cdot p_4p_5\cdot p_4p_6+$$
$$+ qp_3\cdot p_4^2\cdot p_5p_6 + p_3^2\cdot qp_4\cdot p_5p_6 - 2\cdot qp_3\cdot p_3p_4\cdot p_5p_6 - 2\cdot qp_4\cdot p_3p_4\cdot p_5p_6\Big]+$$
$$+ p_3^{\mu}\Big[m_2^2m_3^2q^{\nu} - p_4^2m_3^2q^{\nu} + 2m_3^2\cdot p_3p_4\cdot q^{\nu} - p_3p_6\cdot p_4p_5\cdot q^{\nu} - p_3p_5\cdot p_4p_6\cdot q^{\nu}+$$
$$+ 2\cdot p_4p_5\cdot p_4p_6\cdot q^{\nu} - p_4^2\cdot p_5p_6\cdot q^{\nu} + m_2^2\cdot p_5p_6\cdot q^{\nu} + 2\cdot p_3p_4\cdot p_5p_6\cdot q^{\nu}+$$
$$+ p_6^{\nu}\left(qp_4\cdot p_3p_5 - qp_4\cdot p_4p_5\right) + p_5^{\nu}\left(qp_4\cdot p_3p_6 - qp_4\cdot p_4p_6\right)+$$
$$+ p_4^{\nu}\left(2\cdot qp_4\cdot m_3^2 - qp_6\cdot p_3p_5 - qp_6\cdot p_4p_5 - qp_5\cdot p_3p_6 - qp_5\cdot p_4p_6 + 2\cdot qp_4\cdot p_5p_6\right)\Big]+$$
$$+ p_3^{\nu}\Big[m_3^2p_4^2q^{\mu} - p_5p_6\cdot m_2^2q^{\mu} - p_3p_6\cdot p_4p_5\cdot q^{\mu} - p_3p_5\cdot p_4p_6\cdot q^{\mu} - 2\cdot p_4p_5\cdot p_4p_6\cdot q^{\mu}+$$
$$+ p_4^2\cdot p_5p_6\cdot q^{\mu} - q^{\mu}m_2^2m_3^2 + p_6^{\mu}\left(qp_4\cdot p_3p_5 + qp_4\cdot p_4p_5\right) + p_5^{\mu}\left(qp_4\cdot p_3p_6 + qp_4\cdot p_4p_6\right)+$$
$$+ p_3^{\mu}\left(-2\cdot qp_4\cdot m_3^2 - 2\cdot qp_4\cdot p_5p_6\right)+$$
$$+ p_4^{\mu}\left(2\cdot qp_3\cdot m_3^2 - qp_6\cdot p_3p_5 - qp_6\cdot p_4p_5 - qp_5\cdot p_3p_6 - qp_5\cdot p_4p_6 + 2\cdot qp_3\cdot p_5p_6\right)\Big]+$$
$$+ p_6^{\mu}\left(-p_4p_5\cdot m_2^2q^{\nu} - p_3p_4\cdot p_3p_5\cdot q^{\nu} - p_3p_4\cdot p_4p_5\cdot q^{\nu} - q^{\nu}m_2^2\cdot p_3p_5\right)+$$
$$+ p_6^{\nu}\left(m_2^2\cdot p_3p_5\cdot q^{\mu} + p_3p_4\cdot p_3p_5\cdot q^{\mu} + m_2^2\cdot p_4p_5\cdot q^{\mu} + p_3p_4\cdot p_4p_5\cdot q^{\mu}\right)+$$
$$+ p_5^{\nu}\left(m_2^2\cdot p_3p_6\cdot q^{\mu} + p_3p_4\cdot p_3p_6\cdot q^{\mu} + m_2^2\cdot p_4p_6\cdot q^{\mu} + p_3p_4\cdot p_4p_6\cdot q^{\mu}\right)+$$
$$+ p_5^{\mu}\left(-p_4p_6\cdot m_2^2q^{\nu} - p_3p_4\cdot p_3p_6\cdot q^{\nu} - p_3p_4\cdot p_4p_6\cdot q^{\nu} - q^{\nu}m_2^2\cdot p_3p_6\right)+$$
$$+ p_4^{\mu}\Big[m_2^2m_3^2q^{\nu} - p_3^2m_3^2q^{\nu} + 2m_3^2\cdot p_3p_4\cdot q^{\nu} - p_3p_6\cdot p_4p_5\cdot q^{\nu} + 2\cdot p_3p_5\cdot p_3p_6\cdot q^{\nu}-$$
$$- p_3p_5\cdot p_4p_6\cdot q^{\nu} + m_2^2\cdot p_5p_6\cdot q^{\nu} - p_3^2\cdot p_5p_6\cdot q^{\nu} + 2\cdot p_3p_4\cdot p_5p_6\cdot q^{\nu}+$$
$$+ p_6^{\nu}\left(qp_3\cdot p_4p_5 - qp_3\cdot p_3p_5\right) + p_5^{\nu}\left(qp_3\cdot p_4p_6 - qp_3\cdot p_3p_6\right)\Big]+$$
$$+ p_4^{\nu}\Big[- p_5p_6\cdot m_2^2q^{\mu} + m_3^2p_3^2q^{\mu} - p_3p_6\cdot p_4p_5\cdot q^{\mu} - 2\cdot p_3p_5\cdot p_3p_6\cdot q^{\mu} - p_3p_5\cdot p_4p_6\cdot q^{\mu}+$$
$$+ p_3^2\cdot p_5p_6\cdot q^{\mu} - q^{\mu}m_2^2m_3^2 + p_6^{\mu}\left(qp_3\cdot p_3p_5 + qp_3\cdot p_4p_5\right) + p_5^{\mu}\left(qp_3\cdot p_3p_6 + qp_3\cdot p_4p_6\right)+$$

$$+ p_4^{\mu}\left(-2\cdot qp_3\cdot m_3^2 - 2\cdot qp_3\cdot p_5p_6\right)\Big]\Bigg). \tag{C.46}$$

Expressions (C.44-C.46) are result of step by step calculation and contain terms that should not be present in the final result. End state particles are on mass shell, so $p_3^2 = p_4^2 = m_2^2$, $p_5^2 = p_6^2 = m_3^2$. I keep using short note of q^2 for invariant mass squared of extra pair $q^2 = (p_5 + p_6)^2$ and short note of q_2^2 for invariant mass squared of pair $q_2^2 = (p_3 + p_4)^2$, I keep using notation of q as part of scalar products, but four vector q^{μ} is presented as $p_5^{\mu} + p_6^{\mu}$. Born level spin summarized matrix element (C.33) contain two contractions of indexes. I present matrix element $\sum_{spins}|M_1 + M_2|^2$ for diagrams of Fig. 2 as contractions between tensor corresponding to incoming particles and tensors (C.44-C.46), I attempt to present these end state tensors as traces. Calculation of the matrix element (C.22-C.31) follows

$$\sum_{spins}|M_1 + M_2|^2 = \sum_{spins}|M_1 + M_2|^2_{soft} + \frac{\alpha^4(4\pi)^4}{(p1+p2)^4}\frac{1}{q^4}Tr\left[(\not{p}_1 + m_1)\gamma^{\mu}(\not{p}_2 - m_1)\gamma^{\nu}\right]\times$$
$$\times\Bigg\{\frac{16}{\left(2(p_3q)+q^2\right)^2}\Bigg[4g^{\mu\nu}m_2^2\frac{q^2}{2}\left(\frac{q^2}{2}+m_3^2\right) + Tr\left[\not{p}_3\gamma^{\mu}\not{p}_4\gamma^{\nu}\right]\frac{q^2}{2}\left(p_3q - m_3^2\right) +$$
$$+ Tr\left[\not{p}_4\gamma^{\mu}\not{p}_6\gamma^{\nu}\right]\left(-(p_3p_5)^2 - m_2^2\frac{q^2}{2} + p_3p_6\frac{q^2}{2} + m_3^2\cdot p_3q + p_3p_5\cdot p_3p_6\right) +$$
$$+ Tr\left[\not{p}_4\gamma^{\mu}\not{p}_5\gamma^{\nu}\right]\left(-(p_3p_6)^2 - m_2^2\frac{q^2}{2} + p_3p_3\frac{q^2}{2} + m_3^2\cdot p_3q + p_3p_5\cdot p_3p_6\right)\Bigg] +$$
$$+\frac{16}{\left(2(p_4q)+q^2\right)^2}\Bigg[4g^{\mu\nu}m_2^2\frac{q^2}{2}\left(\frac{q^2}{2}+m_3^2\right) + Tr\left[\not{p}_3\gamma^{\mu}\not{p}_4\gamma^{\nu}\right]\frac{q^2}{2}\left(p_4q - m_3^2\right) +$$
$$+ Tr\left[\not{p}_3\gamma^{\mu}\not{p}_6\gamma^{\nu}\right]\left(-(p_4p_5)^2 - m_2^2\frac{q^2}{2} + p_4p_6\frac{q^2}{2} + m_3^2\cdot p_4q + p_4p_5\cdot p_4p_6\right) +$$
$$+ Tr\left[\not{p}_3\gamma^{\mu}\not{p}_5\gamma^{\nu}\right]\left(-(p_4p_6)^2 - m_2^2\frac{q^2}{2} + p_4p_5\frac{q^2}{2} + m_3^2\cdot p_4q + p_4p_5\cdot p_4p_6\right)\Bigg] +$$
$$+\frac{16}{\left(2(p_3q)+q^2\right)\left(2(p_4q)+q^2\right)}\Bigg[-\left(Tr\left[\not{p}_5\gamma^{\mu}\not{p}_5\gamma^{\nu}\right] + Tr\left[\not{p}_6\gamma^{\mu}\not{p}_6\gamma^{\nu}\right]\right)\left(m_2^2\frac{q^2}{2} + m_3^2\frac{q_2^2}{2}\right) -$$
$$- 2Tr\left[\not{p}_5\gamma^{\mu}\not{p}_6\gamma^{\nu}\right]\left(m_2^2m_3^2 + p_3p_6\cdot p_4p_5 + p_3p_5\cdot p_4p_6 - p_3p_4\cdot p_5p_6\right) +$$
$$+ 2Tr\left[\not{p}_5\gamma^{\mu}\not{p}_5\gamma^{\nu}\right]p_3p_6\cdot p_4p_6 + 2Tr\left[\not{p}_6\gamma^{\mu}\not{p}_6\gamma^{\nu}\right]p_3p_5\cdot p_4p_5 -$$
$$- 2Tr\left[\not{p}_3\gamma^{\mu}\not{p}_4\gamma^{\nu}\right]m_3^2\frac{q^2}{2} - Tr\left[\not{p}_3\gamma^{\mu}\not{p}_3\gamma^{\nu}\right]p_4q\frac{q^2}{2} - Tr\left[\not{p}_4\gamma^{\mu}\not{p}_4\gamma^{\nu}\right]p_3q\frac{q^2}{2} +$$
$$+ Tr\left[\not{p}_3\gamma^{\mu}\not{p}_6\gamma^{\nu}\right]\left(m_3^2\cdot p_4p_6 + p_4p_5\left(p_3(p_5-p_6) - p_5p_6\right) + p_3p_4\frac{q^2}{2}\right) +$$
$$+ Tr\left[\not{p}_3\gamma^{\mu}\not{p}_5\gamma^{\nu}\right]\left(m_3^2\cdot p_4p_5 - p_4p_6\left(p_3(p_5-p_6) + p_5p_6\right) + p_3p_4\frac{q^2}{2}\right) +$$

$$+ Tr\left[\not p_4\gamma^\mu \not p_6\gamma^\nu\right]\left(m_3^2\cdot p_3p_6 + p_3p_5\left(p_4\left(p_5-p_6\right)-p_5p_6\right)+p_3p_4\frac{q^2}{2}\right)+$$

$$+ Tr\left[\not p_4\gamma^\mu \not p_5\gamma^\nu\right]\left(m_3^2\cdot p_3p_5 - p_3p_6\left(p_4\left(p_5-p_6\right)+p_5p_6\right)+p_3p_4\frac{q^2}{2}\right)+$$

$$+ 4g^{\mu\nu}\left(2m_3^2\left(p_3p_5\cdot p_4p_5+p_3p_6\cdot p_4p_6\right)-2p_5p_6\left(p_3p_6\cdot p_4p_5+p_3p_5\cdot p_4p_6\right)-\right.$$

$$\left.-2m_2^2m_3^2\frac{q^2}{2}-4m_3^2\cdot p_3p_4\cdot\frac{q^2}{2}\right)\Bigg]\Bigg\}=$$

$$=\sum_{spins}\left|M_1+M_2\right|^2_{soft}+\frac{\alpha^4\left(4\pi\right)^4}{\left(p1+p2\right)^4}\frac{1}{q^4}Tr\left[\left(\not p_1+m_1\right)\gamma^\mu\left(\not p_2-m_1\right)\gamma^\nu\right]\times$$

$$\times\left\{\frac{16}{\left(2\left(p_3q\right)+q^2\right)^2}\left[4g^{\mu\nu}m_2^2\frac{q^2}{2}\left(\frac{q^2}{2}+m_3^2\right)+Tr\left[\not p_3\gamma^\mu\not p_4\gamma^\nu\right]\frac{q^2}{2}\left(p_3q-m_3^2\right)-\right.\right.$$

$$\left.-Tr\left[\not p_4\gamma^\mu\not q\gamma^\nu\right]\left(\left(p_3p_5\right)^2+\left(p_3p_6\right)^2+m_2^2\frac{q^2}{2}-m_3^2\cdot p_3q\right)\right]+$$

$$+\frac{8}{\left(2\left(p_3q\right)+q^2\right)}\left[Tr\left[\not p_4\gamma^\mu\not p_6\gamma^\nu\right]p_3p_6+Tr\left[\not p_4\gamma^\mu\not p_5\gamma^\nu\right]p_3p_5\right]+$$

$$+\frac{16}{\left(2\left(p_4q\right)+q^2\right)^2}\left[4g^{\mu\nu}m_2^2\frac{q^2}{2}\left(\frac{q^2}{2}+m_3^2\right)+Tr\left[\not p_3\gamma^\mu\not p_4\gamma^\nu\right]\frac{q^2}{2}\left(p_4q-m_3^2\right)-\right.$$

$$\left.-Tr\left[\not p_3\gamma^\mu\not q\gamma^\nu\right]\left(\left(p_4p_5\right)^2+\left(p_4p_6\right)^2+m_2^2\frac{q^2}{2}-m_3^2\cdot p_4q\right)\right]+$$

$$+\frac{8}{\left(2\left(p_4q\right)+q^2\right)}\left[Tr\left[\not p_3\gamma^\mu\not p_5\gamma^\nu\right]p_4p_5+Tr\left[\not p_3\gamma^\mu\not p_6\gamma^\nu\right]p_4p_6\right]+$$

$$+\frac{16}{\left(2\left(p_3q\right)+q^2\right)\left(2\left(p_4q\right)+q^2\right)}\left[-\left(Tr\left[\not p_5\gamma^\mu\not p_5\gamma^\nu\right]+Tr\left[\not p_6\gamma^\mu\not p_6\gamma^\nu\right]\right)\left(m_2^2\frac{q^2}{2}+m_3^2\frac{q_2^2}{2}\right)-\right.$$

$$-2Tr\left[\not p_5\gamma^\mu\not p_6\gamma^\nu\right]\left(m_2^2m_3^2+p_3p_6\cdot p_4p_5+p_3p_5\cdot p_4p_6-p_3p_4\cdot p_5p_6\right)+$$

$$+2Tr\left[\not p_5\gamma^\mu\not p_5\gamma^\nu\right]p_3p_6\cdot p_4p_6+2Tr\left[\not p_6\gamma^\mu\not p_6\gamma^\nu\right]p_3p_5\cdot p_4p_5-$$

$$-2Tr\left[\not p_3\gamma^\mu\not p_4\gamma^\nu\right]m_3^2\frac{q^2}{2}-Tr\left[\not p_3\gamma^\mu\not p_3\gamma^\nu\right]p_4q\frac{q^2}{2}-Tr\left[\not p_4\gamma^\mu\not p_4\gamma^\nu\right]p_3q\frac{q^2}{2}+$$

$$+Tr\left[\not p_3\gamma^\mu\not p_6\gamma^\nu\right]\left(-p_4p_5\left(p_3q+\frac{q^2}{2}\right)+m_3^2\cdot p_4q+2p_4p_5\cdot p_3p_5+p_3p_4\frac{q^2}{2}\right)+$$

$$+Tr\left[\not p_3\gamma^\mu\not p_5\gamma^\nu\right]\left(-p_4p_6\left(p_3q+\frac{q^2}{2}\right)+m_3^2\cdot p_4q+2p_4p_6\cdot p_3p_6+p_3p_4\frac{q^2}{2}\right)+$$

$$+Tr\left[\not p_4\gamma^\mu\not p_6\gamma^\nu\right]\left(-p_3p_5\left(p_4q+\frac{q^2}{2}\right)+m_3^2\cdot p_3q+2p_3p_5\cdot p_4p_5+p_3p_4\frac{q^2}{2}\right)+$$

$$+ Tr\left[\not p_4\gamma^\mu \not p_5\gamma^\nu\right]\left(-p_3p_6\left(p_4q+\frac{q^2}{2}\right)+m_3^2\cdot p_3q+2p_3p_6\cdot p_4p_6+p_3p_4\frac{q^2}{2}\right)+$$

$$+4g^{\mu\nu}\left(2m_3^2\left(p_3p_5\cdot p_4p_5+p_3p_6\cdot p_4p_6\right)-2p_5p_6\left(p_3p_6\cdot p_4p_5+p_3p_5\cdot p_4p_6\right)-\right.$$

$$\left.-2m_2^2m_3^2\frac{q^2}{2}-4m_3^2\cdot p_3p_4\cdot\frac{q^2}{2}\right)\Bigg]\Bigg\}=$$

$$=\sum_{spins}\left|M_1+M_2\right|^2_{soft}+\frac{\alpha^4\left(4\pi\right)^4}{\left(p1+p2\right)^4}\frac{1}{q^4}Tr\left[\left(\not p_1+m_1\right)\gamma^\mu\left(\not p_2-m_1\right)\gamma^\nu\right]\times$$

$$\times\left\{\frac{16}{\left(2\left(p_3q\right)+q^2\right)^2}\left[4g^{\mu\nu}m_2^2\frac{q^2}{2}\left(\frac{q^2}{2}+m_3^2\right)+Tr\left[\not p_3\gamma^\mu\not p_4\gamma^\nu\right]\frac{q^2}{2}\left(p_3q-m_3^2\right)-\right.\right.$$

$$\left.-Tr\left[\not p_4\gamma^\mu\not q\gamma^\nu\right]\left(\left(p_3p_5\right)^2+\left(p_3p_6\right)^2+m_2^2\frac{q^2}{2}\right)\right]+$$

$$+\frac{8}{\left(2\left(p_3q\right)+q^2\right)}\left[Tr\left[\not p_4\gamma^\mu\left(\not p_5-\not p_6\right)\gamma^\nu\right]p_3\left(p_5-p_6\right)\right]+$$

$$+\frac{16}{\left(2\left(p_4q\right)+q^2\right)^2}\left[4g^{\mu\nu}m_2^2\frac{q^2}{2}\left(\frac{q^2}{2}+m_3^2\right)+Tr\left[\not p_3\gamma^\mu\not p_4\gamma^\nu\right]\frac{q^2}{2}\left(p_4q-m_3^2\right)-\right.$$

$$\left.-Tr\left[\not p_3\gamma^\mu\not q\gamma^\nu\right]\left(\left(p_4p_5\right)^2+\left(p_4p_6\right)^2+m_2^2\frac{q^2}{2}\right)\right]+$$

$$+\frac{8}{\left(2\left(p_4q\right)+q^2\right)}\left[Tr\left[\not p_3\gamma^\mu\left(\not p_5-\not p_6\right)\gamma^\nu\right]p_4\left(p_5-p_6\right)\right]+$$

$$+\frac{16}{\left(2\left(p_3q\right)+q^2\right)\left(2\left(p_4q\right)+q^2\right)}\left[-\left(Tr\left[\not p_5\gamma^\mu\not p_5\gamma^\nu\right]+Tr\left[\not p_6\gamma^\mu\not p_6\gamma^\nu\right]\right)\left(m_2^2\frac{q^2}{2}+m_3^2\frac{q_2^2}{2}\right)-\right.$$

$$-2Tr\left[\not p_5\gamma^\mu\not p_6\gamma^\nu\right]\left(m_2^2m_3^2+p_3p_6\cdot p_4p_5+p_3p_5\cdot p_4p_6-p_3p_4\cdot p_5p_6\right)+Tr\left[\not q_2\gamma^\mu\not q\gamma^\nu\right]\left(p_3p_4\frac{q^2}{2}\right)-$$

$$-2Tr\left[\not p_3\gamma^\mu\not p_4\gamma^\nu\right]m_3^2\frac{q^2}{2}-Tr\left[\not p_3\gamma^\mu\not p_3\gamma^\nu\right]p_4q\frac{q^2}{2}-Tr\left[\not p_4\gamma^\mu\not p_4\gamma^\nu\right]p_3q\frac{q^2}{2}+$$

$$+2Tr\left[\left(\not p_3+\not p_4+\not p_6\right)\gamma^\mu\not p_6\gamma^\nu\right]\left(p_3p_5\cdot p_4p_5\right)+2Tr\left[\left(\not p_3+\not p_4+\not p_5\right)\gamma^\mu\not p_5\gamma^\nu\right]\left(p_3p_6\cdot p_4p_6\right)+$$

$$+4g^{\mu\nu}\left(2m_3^2\left(p_3p_5\cdot p_4p_5+p_3p_6\cdot p_4p_6\right)-2p_5p_6\left(p_3p_6\cdot p_4p_5+p_3p_5\cdot p_4p_6\right)-\right.$$

$$\left.-2m_2^2m_3^2\frac{q^2}{2}-4m_3^2\cdot p_3p_4\cdot\frac{q^2}{2}\right)\Bigg]+$$

$$+\left(\frac{1}{\left(2\left(p_3q\right)+q^2\right)}+\frac{1}{\left(2\left(p_4q\right)+q^2\right)}\right)8m_3^2\left(\frac{2p_4q\cdot Tr\left[\not p_3\gamma^\mu\not q\gamma^\nu\right]}{2p_4q+q^2}+\frac{2p_3q\cdot Tr\left[\not p_4\gamma^\mu\not q\gamma^\nu\right]}{2p_3q+q^2}\right)\Bigg\}=$$

$$=\sum_{spins}\left|M_1+M_2\right|^2_{soft}+\frac{\alpha^4\left(4\pi\right)^4}{\left(p1+p2\right)^4}\frac{1}{q^4}Tr\left[\left(\not p_1+m_1\right)\gamma^\mu\left(\not p_2-m_1\right)\gamma^\nu\right]\times$$

$$\times\Bigg\{\frac{16}{\left(2\left(p_3q\right)+q^2\right)^2}\Bigg[4g^{\mu\nu}m_2^2\frac{q^2}{2}\left(\frac{q^2}{2}+m_3^2\right)+Tr\left[\not p_3\gamma^\mu\not p_4\gamma^\nu\right]\frac{q^2}{2}\cdot p_3q-$$

$$-Tr\left[\not p_4\gamma^\mu\not q\gamma^\nu\right]\left(\left(p_3p_5\right)^2+\left(p_3p_6\right)^2+m_2^2\frac{q^2}{2}\right)\Bigg]+$$

$$+\frac{8}{\left(2\left(p_3q\right)+q^2\right)}\Bigg[Tr\left[\not p_4\gamma^\mu\left(\not p_5-\not p_6\right)\gamma^\nu\right]p_3\left(p_5-p_6\right)\Bigg]+$$

$$+\frac{16}{\left(2\left(p_4q\right)+q^2\right)^2}\Bigg[4g^{\mu\nu}m_2^2\frac{q^2}{2}\left(\frac{q^2}{2}+m_3^2\right)+Tr\left[\not p_3\gamma^\mu\not p_4\gamma^\nu\right]\frac{q^2}{2}\cdot p_4q-$$

$$-Tr\left[\not p_3\gamma^\mu\not q\gamma^\nu\right]\left(\left(p_4p_5\right)^2+\left(p_4p_6\right)^2+m_2^2\frac{q^2}{2}\right)\Bigg]+$$

$$+\frac{8}{\left(2\left(p_4q\right)+q^2\right)}\Bigg[Tr\left[\not p_3\gamma^\mu\left(\not p_5-\not p_6\right)\gamma^\nu\right]p_4\left(p_5-p_6\right)\Bigg]+$$

$$+\frac{16}{\left(2\left(p_3q\right)+q^2\right)\left(2\left(p_4q\right)+q^2\right)}\Bigg[-\left(Tr\left[\not p_5\gamma^\mu\not p_5\gamma^\nu\right]+Tr\left[\not p_6\gamma^\mu\not p_6\gamma^\nu\right]\right)\left(m_2^2\frac{q^2}{2}+m_3^2\frac{q_2^2}{2}\right)-$$

$$-2Tr\left[\not p_5\gamma^\mu\not p_6\gamma^\nu\right]\left(m_2^2m_3^2+p_3p_6\cdot p_4p_5+p_3p_5\cdot p_4p_6-p_3p_4\cdot p_5p_6\right)+$$

$$+Tr\left[\not q_2\gamma^\mu\not q\gamma^\nu\right]\left(p_3p_4\frac{q^2}{2}\right)-Tr\left[\not p_3\gamma^\mu\not p_3\gamma^\nu\right]p_4q\frac{q^2}{2}-Tr\left[\not p_4\gamma^\mu\not p_4\gamma^\nu\right]p_3q\frac{q^2}{2}+$$

$$+2Tr\left[\left(\not p_3+\not p_4+\not p_6\right)\gamma^\mu\not p_6\gamma^\nu\right]\left(p_3p_5\cdot p_4p_5\right)+2Tr\left[\left(\not p_3+\not p_4+\not p_5\right)\gamma^\mu\not p_5\gamma^\nu\right]\left(p_3p_6\cdot p_4p_6\right)+$$

$$+4g^{\mu\nu}\Bigg(2m_3^2\left(p_3p_5\cdot p_4p_5+p_3p_6\cdot p_4p_6\right)-2p_5p_6\left(p_3p_6\cdot p_4p_5+p_3p_5\cdot p_4p_6\right)-$$

$$-2m_3^2\frac{q^2}{2}(\frac{q_2^2}{2}+p_3p_4)\Bigg)\Bigg]+16m_3^2\left(\frac{1}{\left(2\left(p_3q\right)+q^2\right)}+\frac{1}{\left(2\left(p_4q\right)+q^2\right)}\right)\times$$

$$\times\left(\frac{Tr\left[\not p_3\gamma^\mu\not q\gamma^\nu\right]p_4q}{2p_4q+q^2}+\frac{Tr\left[\not p_4\gamma^\mu\not q\gamma^\nu\right]p_3q}{2p_3q+q^2}-\frac{Tr\left[\not p_3\gamma^\mu\not p_4\gamma^\nu\right]\frac{q^2}{2}}{2\left(p_3q\right)+q^2}-\frac{Tr\left[\not p_3\gamma^\mu\not p_4\gamma^\nu\right]\frac{q^2}{2}}{2\left(p_4q\right)+q^2}\right)\Bigg\}$$

and

$$\sum_{spins}\left|M_1+M_2\right|^2=\sum_{spins}\left|M_1+M_2\right|^2_{soft}+\frac{\alpha^4\left(4\pi\right)^4}{\left(p_1+p_2\right)^4}\frac{1}{q^4}Tr\left[\left(\not p_1+m_1\right)\gamma_\mu\left(\not p_2-m_1\right)\gamma_\nu\right]\times$$

$$\times\left\{\frac{16}{\left(2\left(p_3q\right)+q^2\right)^2}\left[4g^{\mu\nu}m_2^2\frac{q^2}{2}\left(\frac{q^2}{2}+m_3^2\right)+Tr\left[\not p_3\gamma^\mu\not p_4\gamma^\nu\right]\frac{q^2}{2}\cdot p_3q+\right.\right.$$
$$+Tr\left[\not p_4\gamma^\mu\left(\not p_5-\not p_6\right)\gamma^\nu\right]\frac{q^2}{2}\cdot p_3\left(p_5-p_6\right)-$$
$$-Tr\left[\not p_4\gamma^\mu\not p_5\gamma^\nu\right]\left(2\left(p_3p_6\right)^2+m_2^2\frac{q^2}{2}\right)-Tr\left[\not p_4\gamma^\mu\not p_6\gamma^\nu\right]\left(2\left(p_3p_5\right)^2+m_2^2\frac{q^2}{2}\right)\Bigg]+$$
$$+\frac{16}{\left(2\left(p_4q\right)+q^2\right)^2}\left[4g^{\mu\nu}m_2^2\frac{q^2}{2}\left(\frac{q^2}{2}+m_3^2\right)+Tr\left[\not p_3\gamma^\mu\not p_4\gamma^\nu\right]\frac{q^2}{2}\cdot p_4q+\right.$$
$$+Tr\left[\not p_3\gamma^\mu\left(\not p_5-\not p_6\right)\gamma^\nu\right]\frac{q^2}{2}\cdot p_4\left(p_5-p_6\right)-$$
$$-Tr\left[\not p_3\gamma^\mu\not p_5\gamma^\nu\right]\left(2\left(p_4p_6\right)^2+m_2^2\frac{q^2}{2}\right)-Tr\left[\not p_3\gamma^\mu\not p_6\gamma^\nu\right]\left(2\left(p_4p_5\right)^2+m_2^2\frac{q^2}{2}\right)\Bigg]+$$
$$+\frac{16}{\left(2\left(p_3q\right)+q^2\right)\left(2\left(p_4q\right)+q^2\right)}\Bigg[-\left(Tr\left[\not p_5\gamma^\mu\not p_5\gamma^\nu\right]+Tr\left[\not p_6\gamma^\mu\not p_6\gamma^\nu\right]\right)\left(m_2^2\frac{q^2}{2}+m_3^2\frac{q_2^2}{2}\right)-$$
$$-2Tr\left[\not p_5\gamma^\mu\not p_6\gamma^\nu\right]\left(m_2^2m_3^2+p_3p_6\cdot p_4p_5+p_3p_5\cdot p_4p_6-p_3p_4\cdot p_5p_6\right)+$$
$$+Tr\left[\not q_2\gamma^\mu\not q\gamma^\nu\right]\left(p_3p_4\frac{q^2}{2}\right)-Tr\left[\not p_3\gamma^\mu\not p_3\gamma^\nu\right]p_4q\frac{q^2}{2}-Tr\left[\not p_4\gamma^\mu\not p_4\gamma^\nu\right]p_3q\frac{q^2}{2}+$$
$$+2Tr\left[\left(\not p_3+\not p_4+\not p_6\right)\gamma^\mu\not p_6\gamma^\nu\right]\left(p_3p_5\cdot p_4p_5\right)+2Tr\left[\left(\not p_3+\not p_4+\not p_5\right)\gamma^\mu\not p_5\gamma^\nu\right]\left(p_3p_6\cdot p_4p_6\right)+$$
$$+4g^{\mu\nu}\Bigg(2m_3^2\left(p_3p_5\cdot p_4p_5+p_3p_6\cdot p_4p_6\right)-2p_5p_6\left(p_3p_6\cdot p_4p_5+p_3p_5\cdot p_4p_6\right)-$$
$$-2m_3^2\frac{q^2}{2}(\frac{q_2^2}{2}+p_3p_4)\Bigg)\Bigg]+16m_3^2\left(\frac{1}{\left(2\left(p_3q\right)+q^2\right)}+\frac{1}{\left(2\left(p_4q\right)+q^2\right)}\right)\times$$
$$\times\left(\frac{Tr\left[\not p_3\gamma^\mu\not q\gamma^\nu\right]p_4q}{2p_4q+q^2}+\frac{Tr\left[\not p_4\gamma^\mu\not q\gamma^\nu\right]p_3q}{2p_3q+q^2}-\frac{Tr\left[\not p_3\gamma^\mu\not p_4\gamma^\nu\right]\frac{q^2}{2}}{2\left(p_3q\right)+q^2}-\frac{Tr\left[\not p_3\gamma^\mu\not p_4\gamma^\nu\right]\frac{q^2}{2}}{2\left(p_4q\right)+q^2}\right)\Bigg\},\qquad\text{(C.47)}$$

where $\sum_{spins}\left|M_1+M_2\right|^2_{soft}$ is defined by formula (C.32-C.35). Formula for $\sum_{spins}\left|M_3+M_4\right|$ defined by expression (C.9-C.11) obtains from formula (C.47) through formal replacement $p_3\leftrightarrow p_5$, $p_4\leftrightarrow p_6$, $m_2\leftrightarrow m_3$.

C.3 Four fermions matrix element

Here I complete calculation of matrix element $\sum_{spins}\left|M_1+M_2+M_3+M_4\right|^2$ with interference terms coming from expression (C.12-C.17):

$$\sum_{spins}\left|M_1+M_2+M_3+M_4\right|^2-\sum_{spins}\left|M_1+M_2\right|^2-\sum_{spins}\left|M_3+M_4\right|^2=$$

$$= \frac{\alpha^4 (4\pi)^4}{(p_1+p_2)^4} \frac{1}{q^2 q_2^2} Tr\left[(\not{p}_1 + m_1)\gamma_\mu (\not{p}_2 - m_1)\gamma_\nu\right] \Bigg\{ \frac{8}{(2p_3q+q^2)(2p_5q_2+q_2^2)}$$

$$\Bigg[Tr\left[\not{p}_6\gamma^\mu \not{p}_6\gamma^\nu\right]\left(m_2^2\cdot p_3p_5 + m_2^2\cdot p_4p_5 - m_3^2\cdot p_3p_4 + 2\cdot p_3p_5\cdot p_4p_5 - m_2^2m_3^2\right)$$

$$+Tr\left[\not{p}_5\gamma^\mu \not{p}_5\gamma^\nu\right]\left(-3m_2^2\cdot p_3p_6 - m_2^2\cdot p_4p_6 + m_3^2\cdot p_3p_4 + 2\cdot p_3p_5\cdot p_4p_6 - 2\cdot p_3p_4\cdot p_3p_6 + m_2^2m_3^2\right)$$

$$+ Tr\left[\not{p}_4\gamma^\mu \not{p}_4\gamma^\nu\right]\left(-m_2^2\cdot p_5p_6 + m_3^2\cdot p_3p_5 + m_3^2\cdot p_3p_6 + 2\cdot p_3p_5\cdot p_3p_6 - m_2^2m_3^2\right)$$

$$+ Tr\left[\not{p}_5\gamma^\mu \not{p}_6\gamma^\nu\right]\Bigg(- m_2^2\cdot p_3p_5 - m_2^2\cdot p_3p_6 + m_2^2\cdot p_4p_5 - m_2^2\cdot p_4p_6 + 2m_2^2\cdot p_5p_6$$

$$+ 2m_3^2\cdot p_3p_4 - 2\cdot p_3p_5\cdot p_4p_6 + 2\cdot p_3p_4\cdot p_5p_6 - 2\cdot p_3p_4\cdot p_3p_5 - 2\cdot p_3p_5\cdot p_4p_5 + 2m_2^2m_3^2\Bigg)$$

$$+ Tr\left[\not{p}_4\gamma^\mu \not{p}_6\gamma^\nu\right]\Bigg(4\left(p_3p_5\right)^2 - m_2^2\cdot p_3p_5 - m_2^2\cdot p_4p_5 + 3m_2^2\cdot p_5p_6 + 3m_3^2\cdot p_3p_4$$

$$- m_3^2\cdot p_3p_5 - m_3^2\cdot p_3p_6 + 2\cdot p_3p_6\cdot p_4p_5 - 2\cdot p_3p_5\cdot p_4p_6 + 2\cdot p_3p_4\cdot p_5p_6 + 4m_2^2m_3^2\Bigg)$$

$$+ Tr\left[\not{p}_3\gamma^\mu \not{p}_5\gamma^\nu\right]\Bigg(- m_2^2\cdot p_3p_6 - m_2^2\cdot p_4p_6 + 3m_2^2\cdot p_5p_6 + 3m_3^2\cdot p_3p_4 - m_3^2\cdot p_4p_5$$

$$- m_3^2\cdot p_4p_6 + 2\cdot p_3p_6\cdot p_4p_5 + 2\cdot p_3p_5\cdot p_4p_6 + 2\cdot p_3p_4\cdot p_5p_6 + 4m_2^2m_3^2\Bigg)$$

$$+ Tr\left[\not{p}_4\gamma^\mu \not{p}_5\gamma^\nu\right]\Bigg(- m_2^2\cdot p_3p_6 + m_2^2\cdot p_4p_6 + m_2^2\cdot p_5p_6 + m_3^2\cdot p_3p_4 - m_3^2\cdot p_3p_5$$

$$+ m_3^2\cdot p_3p_6 - 2\cdot p_3p_4\cdot p_3p_6 - 2\cdot p_3p_5\cdot p_5p_6 + 2m_2^2m_3^2\Bigg)$$

$$+ Tr\left[\not{p}_3\gamma^\mu \not{p}_4\gamma^\nu\right]\Bigg(2m_2^2\cdot p_5p_6 + 2m_3^2\cdot p_3p_4 - m_3^2\cdot p_3p_5 + m_3^2\cdot p_3p_6 - m_3^2\cdot p_4p_5$$

$$- m_3^2\cdot p_4p_6 - 2\cdot p_3p_5\cdot p_4p_6 + 2\cdot p_3p_4\cdot p_5p_6 - 2\cdot p_3p_5\cdot p_3p_6 - 2\cdot p_3p_5\cdot p_5p_6 + 2m_2^2m_3^2\Bigg)$$

$$+Tr\left[\not{p}_3\gamma^\mu \not{p}_3\gamma^\nu\right]\left(m_2^2\cdot p_5p_6 - 3m_3^2\cdot p_4p_5 - m_3^2\cdot p_4p_6 + 2\cdot p_3p_5\cdot p_4p_6 - 2\cdot p_4p_5\cdot p_5p_6 + m_2^2m_3^2\right)$$

$$+ Tr\left[\not{p}_3\gamma^\mu \not{p}_6\gamma^\nu\right]\Bigg(- m_2^2\cdot p_3p_5 + m_2^2\cdot p_4p_5 + m_2^2\cdot p_5p_6 + m_3^2\cdot p_3p_4 - m_3^2\cdot p_4p_5$$

$$+ m_3^2\cdot p_4p_6 - 2\cdot p_3p_4\cdot p_3p_5 - 2\cdot p_4p_5\cdot p_5p_6 + 2m_2^2m_3^2\Bigg)$$

$$+ 4g^{\mu\nu}\Bigg(4\cdot p_4p_6\left(p_3p_5\right)^2 - 2m_2^4\cdot p_5p_6 + m_3^4\left(-2\cdot p_3p_4 - 2m_2^2\right)$$

$$+ m_2^2\left(2\cdot p_3p_6\cdot p_4p_5 + 2\cdot p_3p_5\cdot p_4p_6 - 2\cdot p_3p_4\cdot p_5p_6 + 4\cdot p_3p_5\cdot p_3p_6 + 4\cdot p_3p_5\cdot p_5p_6\right)$$

$$+ m_3^2\Bigg(m_2^2\left(-2\cdot p_3p_4 + 8\cdot p_3p_5 - 2\cdot p_5p_6\right) + 2\cdot p_3p_6\cdot p_4p_5 + 2\cdot p_3p_5\cdot p_4p_6$$

$$- 2 \cdot p_3p_4 \cdot p_5p_6 + 4 \cdot p_3p_4 \cdot p_3p_5 + 4 \cdot p_3p_5 \cdot p_4p_5 - 2m_2^4\Big) + 4 \cdot p_3p_5 \cdot p_3p_6 \cdot p_4p_5\Big)\Big]$$

$$+ \frac{8}{(2p_3q + q^2)\,(2p_6q_2 + q_2^2)}$$

$$\Big[Tr\left[\not{p}_6\gamma^\mu\not{p}_6\gamma^\nu\right]\left(3m_2^2 \cdot p_3p_5 + m_2^2 \cdot p_4p_5 - m_3^2 \cdot p_3p_4 - 2 \cdot p_3p_6 \cdot p_4p_5 + 2 \cdot p_3p_4 \cdot p_3p_5 - m_2^2m_3^2\right)$$

$$+ Tr\left[\not{p}_5\gamma^\mu\not{p}_5\gamma^\nu\right]\left(-m_2^2 \cdot p_3p_6 - m_2^2 \cdot p_4p_6 + m_3^2 \cdot p_3p_4 - 2 \cdot p_3p_6 \cdot p_4p_6 + m_2^2m_3^2\right) +$$

$$+ Tr\left[\not{p}_4\gamma^\mu\not{p}_4\gamma^\nu\right]\left(m_2^2 \cdot p_5p_6 - m_3^2 \cdot p_3p_5 - m_3^2 \cdot p_3p_6 - 2 \cdot p_3p_5 \cdot p_3p_6 + m_2^2m_3^2\right) +$$

$$+ Tr\left[\not{p}_4\gamma^\mu\not{p}_5\gamma^\nu\right]\Big(- 4\left(p_3p_6\right)^2 + m_2^2 \cdot p_3p_6 + m_2^2 \cdot p_4p_6 - 3m_2^2 \cdot p_5p_6 - 3m_3^2 \cdot p_3p_4$$

$$+ m_3^2 \cdot p_3p_5 + m_3^2 \cdot p_3p_6 + 2 \cdot p_3p_6 \cdot p_4p_5 - 2 \cdot p_3p_5 \cdot p_4p_6 - 2 \cdot p_3p_4 \cdot p_5p_6 - 4m_2^2m_3^2\Big)$$

$$+ Tr\left[\not{p}_3\gamma^\mu\not{p}_6\gamma^\nu\right]\Big(m_2^2 \cdot p_3p_5 + m_2^2 \cdot p_4p_5 - 3m_2^2 \cdot p_5p_6 - 3m_3^2 \cdot p_3p_4 + m_3^2 \cdot p_4p_5$$

$$+ m_3^2 \cdot p_4p_6 - 2 \cdot p_3p_6 \cdot p_4p_5 - 2 \cdot p_3p_5 \cdot p_4p_6 - 2 \cdot p_3p_4 \cdot p_5p_6 - 4m_2^2m_3^2\Big)$$

$$+ Tr\left[\not{p}_5\gamma^\mu\not{p}_6\gamma^\nu\right]\Big(m_2^2 \cdot p_3p_5 + m_2^2 \cdot p_3p_6 + m_2^2 \cdot p_4p_5 - m_2^2 \cdot p_4p_6 - 2m_2^2 \cdot p_5p_6$$

$$- 2m_3^2 \cdot p_3p_4 + 2 \cdot p_3p_6 \cdot p_4p_5 - 2 \cdot p_3p_4 \cdot p_5p_6 + 2 \cdot p_3p_4 \cdot p_3p_6 + 2 \cdot p_3p_6 \cdot p_4p_6 - 2m_2^2m_3^2\Big)$$

$$+ Tr\left[\not{p}_4\gamma^\mu\not{p}_6\gamma^\nu\right]\Big(m_2^2 \cdot p_3p_5 - m_2^2 \cdot p_4p_5 - m_2^2 \cdot p_5p_6 - m_3^2 \cdot p_3p_4 - m_3^2 \cdot p_3p_5$$

$$+ m_3^2 \cdot p_3p_6 + 2 \cdot p_3p_4 \cdot p_3p_5 + 2 \cdot p_3p_6 \cdot p_5p_6 - 2m_2^2m_3^2\Big)$$

$$+ Tr\left[\not{p}_3\gamma^\mu\not{p}_4\gamma^\nu\right]\Big(- 2m_2^2 \cdot p_5p_6 - 2m_3^2 \cdot p_3p_4 - m_3^2 \cdot p_3p_5 + m_3^2 \cdot p_3p_6 + m_3^2 \cdot p_4p_5$$

$$+ m_3^2 \cdot p_4p_6 + 2 \cdot p_3p_6 \cdot p_4p_5 - 2 \cdot p_3p_4 \cdot p_5p_6 + 2 \cdot p_3p_5 \cdot p_3p_6 + 2 \cdot p_3p_6 \cdot p_5p_6 - 2m_2^2m_3^2\Big)$$

$$+ Tr\left[\not{p}_3\gamma^\mu\not{p}_5\gamma^\nu\right]\Big(m_2^2 \cdot p_3p_6 - m_2^2 \cdot p_4p_6 - m_2^2 \cdot p_5p_6 - m_3^2 \cdot p_3p_4 - m_3^2 \cdot p_4p_5$$

$$+ m_3^2 \cdot p_4p_6 + 2 \cdot p_3p_4 \cdot p_3p_6 + 2 \cdot p_4p_6 \cdot p_5p_6 - 2m_2^2m_3^2\Big)$$

$$+ Tr\left[\not{p}_3\gamma^\mu\not{p}_3\gamma^\nu\right]\Big(- m_2^2 \cdot p_5p_6 + m_3^2 \cdot p_4p_5 + 3m_3^2 \cdot p_4p_6 - 2 \cdot p_3p_6 \cdot p_4p_5$$

$$+ 2 \cdot p_4p_6 \cdot p_5p_6 - m_2^2m_3^2\Big)$$

$$
\begin{aligned}
&+4g^{\mu\nu}\Bigg(-4\cdot p_4p_5\left(p_3p_6\right)^2+2m_2^4\cdot p_5p_6+m_3^4\left(2\cdot p_3p_4+2m_2^2\right)\\
&+m_2^2\left(-2\cdot p_3p_6\cdot p_4p_5-2\cdot p_3p_5\cdot p_4p_6+2\cdot p_3p_4\cdot p_5p_6-4\cdot p_3p_5\cdot p_3p_6-4\cdot p_3p_6\cdot p_5p_6\right)\\
&+m_3^2\Bigg(m_2^2\left(2\cdot p_3p_4-8\cdot p_3p_6+2\cdot p_5p_6\right)-2\cdot p_3p_6\cdot p_4p_5-2\cdot p_3p_5\cdot p_4p_6\\
&+2\cdot p_3p_4\cdot p_5p_6-4\cdot p_3p_4\cdot p_3p_6-4\cdot p_3p_6\cdot p_4p_6+2m_2^4\Bigg)-4\cdot p_3p_5\cdot p_3p_6\cdot p_4p_6\Bigg)\Bigg]\\
&+\frac{8}{\left(2p_4q+q^2\right)\left(2p_5q_2+q_2^2\right)}\\
&\Bigg[Tr\left[\not{p}_6\gamma^\mu\not{p}_6\gamma^\nu\right]\left(-m_2^2\cdot p_3p_5-m_2^2\cdot p_4p_5+m_3^2\cdot p_3p_4-2\cdot p_3p_5\cdot p_4p_5+m_2^2m_3^2\right)\\
&+Tr\left[\not{p}_5\gamma^\mu\not{p}_5\gamma^\nu\right]\left(m_2^2\cdot p_3p_6+3m_2^2\cdot p_4p_6-m_3^2\cdot p_3p_4-2\cdot p_3p_6\cdot p_4p_5+2\cdot p_3p_4\cdot p_4p_6-m_2^2m_3^2\right)\\
&+Tr\left[\not{p}_3\gamma^\mu\not{p}_3\gamma^\nu\right]\left(m_2^2\cdot p_5p_6-m_3^2\cdot p_4p_5-m_3^2\cdot p_4p_6-2\cdot p_4p_5\cdot p_4p_6+m_2^2m_3^2\right)+\\
&+Tr\left[\not{p}_4\gamma^\mu\not{p}_5\gamma^\nu\right]\Bigg(m_2^2\cdot p_3p_6+m_2^2\cdot p_4p_6-3m_2^2\cdot p_5p_6-3m_3^2\cdot p_3p_4+m_3^2\cdot p_3p_5\\
&+m_3^2\cdot p_3p_6-2\cdot p_3p_6\cdot p_4p_5-2\cdot p_3p_5\cdot p_4p_6-2\cdot p_3p_4\cdot p_5p_6-4m_2^2m_3^2\Bigg)\\
&+Tr\left[\not{p}_3\gamma^\mu\not{p}_6\gamma^\nu\right]\Bigg(-4\left(p_4p_5\right)^2+m_2^2\cdot p_3p_5+m_2^2\cdot p_4p_5-3m_2^2\cdot p_5p_6-3m_3^2\cdot p_3p_4\\
&+m_3^2\cdot p_4p_5+m_3^2\cdot p_4p_6+2\cdot p_3p_6\cdot p_4p_5-2\cdot p_3p_5\cdot p_4p_6-2\cdot p_3p_4\cdot p_5p_6-4m_2^2m_3^2\Bigg)\\
&+Tr\left[\not{p}_5\gamma^\mu\not{p}_6\gamma^\nu\right]\Bigg(-m_2^2\cdot p_3p_5+m_2^2\cdot p_3p_6+m_2^2\cdot p_4p_5+m_2^2\cdot p_4p_6-2m_2^2\cdot p_5p_6\\
&-2m_3^2\cdot p_3p_4+2\cdot p_3p_6\cdot p_4p_5-2\cdot p_3p_4\cdot p_5p_6+2\cdot p_3p_4\cdot p_4p_5+2\cdot p_3p_5\cdot p_4p_5-2m_2^2m_3^2\Bigg)\\
&+Tr\left[\not{p}_4\gamma^\mu\not{p}_6\gamma^\nu\right]\Bigg(-m_2^2\cdot p_3p_5+m_2^2\cdot p_4p_5-m_2^2\cdot p_5p_6-m_3^2\cdot p_3p_4+m_3^2\cdot p_3p_5\\
&-m_3^2\cdot p_3p_6+2\cdot p_3p_4\cdot p_4p_5+2\cdot p_3p_5\cdot p_5p_6-2m_2^2m_3^2\Bigg)\\
&+Tr\left[\not{p}_4\gamma^\mu\not{p}_4\gamma^\nu\right]\Bigg(-m_2^2\cdot p_5p_6+3m_3^2\cdot p_3p_5+m_3^2\cdot p_3p_6-2\cdot p_3p_6\cdot p_4p_5\\
&+2\cdot p_3p_5\cdot p_5p_6-m_2^2m_3^2\Bigg)\\
&+Tr\left[\not{p}_3\gamma^\mu\not{p}_5\gamma^\nu\right]\Bigg(-m_2^2\cdot p_3p_6+m_2^2\cdot p_4p_6-m_2^2\cdot p_5p_6-m_3^2\cdot p_3p_4+m_3^2\cdot p_4p_5
\end{aligned}
$$

$$
\begin{aligned}
&- m_3^2 \cdot p_4p_6 + 2 \cdot p_3p_4 \cdot p_4p_6 + 2 \cdot p_4p_5 \cdot p_5p_6 - 2m_2^2m_3^2\Big) \\
&+ Tr\left[\not{p}_3\gamma^\mu\not{p}_4\gamma^\nu\right]\Big(- 2m_2^2 \cdot p_5p_6 - 2m_3^2 \cdot p_3p_4 + m_3^2 \cdot p_3p_5 + m_3^2 \cdot p_3p_6 + m_3^2 \cdot p_4p_5 \\
&- m_3^2 \cdot p_4p_6 + 2 \cdot p_3p_6 \cdot p_4p_5 - 2 \cdot p_3p_4 \cdot p_5p_6 + 2 \cdot p_4p_5 \cdot p_4p_6 + 2 \cdot p_4p_5 \cdot p_5p_6 - 2m_2^2m_3^2\Big) \\
&+ 4g^{\mu\nu}\Big(- 4 \cdot p_3p_6 \left(p_4p_5\right)^2 + m_2^4 \left(2 \cdot p_5p_6 + 2m_3^2\right) + 2m_3^4 \cdot p_3p_4 - 4 \cdot p_3p_5 \cdot p_4p_5 \cdot p_4p_6 \\
&+ m_2^2\Big(m_3^2 \left(2 \cdot p_3p_4 - 8 \cdot p_4p_5 + 2 \cdot p_5p_6\right) - 2 \cdot p_3p_6 \cdot p_4p_5 - 2 \cdot p_3p_5 \cdot p_4p_6 \\
&+ 2 \cdot p_3p_4 \cdot p_5p_6 - 4 \cdot p_4p_5 \cdot p_4p_6 - 4 \cdot p_4p_5 \cdot p_5p_6 + 2m_3^4\Big) \\
&+m_3^2 \left(-2 \cdot p_3p_6 \cdot p_4p_5 - 2 \cdot p_3p_5 \cdot p_4p_6 + 2 \cdot p_3p_4 \cdot p_5p_6 - 4 \cdot p_3p_4 \cdot p_4p_5 - 4 \cdot p_3p_5 \cdot p_4p_5\right)\Big)\Big] \\
&+ \frac{8}{\left(2p_4q + q^2\right)\left(2p_6q_2 + q_2^2\right)} \\
&\Big[Tr\left[\not{p}_6\gamma^\mu\not{p}_6\gamma^\nu\right]\left(-m_2^2 \cdot p_3p_5 - 3m_2^2 \cdot p_4p_5 + m_3^2 \cdot p_3p_4 + 2 \cdot p_3p_5 \cdot p_4p_6 - 2 \cdot p_3p_4 \cdot p_4p_5 + m_2^2m_3^2\right) \\
&+ Tr\left[\not{p}_5\gamma^\mu\not{p}_5\gamma^\nu\right]\left(m_2^2 \cdot p_3p_6 + m_2^2 \cdot p_4p_6 - m_3^2 \cdot p_3p_4 + 2 \cdot p_3p_6 \cdot p_4p_6 - m_2^2m_3^2\right) \\
&+ Tr\left[\not{p}_3\gamma^\mu\not{p}_3\gamma^\nu\right]\left(-m_2^2 \cdot p_5p_6 + m_3^2 \cdot p_4p_5 + m_3^2 \cdot p_4p_6 + 2 \cdot p_4p_5 \cdot p_4p_6 - m_2^2m_3^2\right) \\
&+ Tr\left[\not{p}_5\gamma^\mu\not{p}_6\gamma^\nu\right]\Big(- m_2^2 \cdot p_3p_5 + m_2^2 \cdot p_3p_6 - m_2^2 \cdot p_4p_5 - m_2^2 \cdot p_4p_6 + 2m_2^2 \cdot p_5p_6 \\
&+ 2m_3^2 \cdot p_3p_4 - 2 \cdot p_3p_5 \cdot p_4p_6 + 2 \cdot p_3p_4 \cdot p_5p_6 - 2 \cdot p_3p_4 \cdot p_4p_6 - 2 \cdot p_3p_6 \cdot p_4p_6 + 2m_2^2m_3^2\Big) \\
&+ Tr\left[\not{p}_4\gamma^\mu\not{p}_6\gamma^\nu\right]\Big(- m_2^2 \cdot p_3p_5 - m_2^2 \cdot p_4p_5 + 3m_2^2 \cdot p_5p_6 + 3m_3^2 \cdot p_3p_4 - m_3^2 \cdot p_3p_5 \\
&- m_3^2 \cdot p_3p_6 + 2 \cdot p_3p_6 \cdot p_4p_5 + 2 \cdot p_3p_5 \cdot p_4p_6 + 2 \cdot p_3p_4 \cdot p_5p_6 + 4m_2^2m_3^2\Big) \\
&+ Tr\left[\not{p}_3\gamma^\mu\not{p}_5\gamma^\nu\right]\Big(4 \left(p_4p_6\right)^2 - m_2^2 \cdot p_3p_6 - m_2^2 \cdot p_4p_6 + 3m_2^2 \cdot p_5p_6 + 3m_3^2 \cdot p_3p_4 \\
&- m_3^2 \cdot p_4p_5 - m_3^2 \cdot p_4p_6 + 2 \cdot p_3p_6 \cdot p_4p_5 - 2 \cdot p_3p_5 \cdot p_4p_6 + 2 \cdot p_3p_4 \cdot p_5p_6 + 4m_2^2m_3^2\Big) \\
&+ Tr\left[\not{p}_4\gamma^\mu\not{p}_4\gamma^\nu\right]\left(m_2^2 \cdot p_5p_6 - m_3^2 \cdot p_3p_5 - 3m_3^2 \cdot p_3p_6 + 2 \cdot p_3p_5 \cdot p_4p_6 - 2 \cdot p_3p_6 \cdot p_5p_6 + m_2^2m_3^2\right) \\
&+ Tr\left[\not{p}_4\gamma^\mu\not{p}_5\gamma^\nu\right]\Big(m_2^2 \cdot p_3p_6 - m_2^2 \cdot p_4p_6 + m_2^2 \cdot p_5p_6 + m_3^2 \cdot p_3p_4 + m_3^2 \cdot p_3p_5 \\
&- m_3^2 \cdot p_3p_6 - 2 \cdot p_3p_4 \cdot p_4p_6 - 2 \cdot p_3p_6 \cdot p_5p_6 + 2m_2^2m_3^2\Big)
\end{aligned}
$$

$$
\begin{aligned}
&+ Tr\left[\not{p}_3\gamma^\mu\not{p}_6\gamma^\nu\right]\Big(m_2^2\cdot p_3p_5 - m_2^2\cdot p_4p_5 + m_2^2\cdot p_5p_6 + m_3^2\cdot p_3p_4 + m_3^2\cdot p_4p_5\\
&- m_3^2\cdot p_4p_6 - 2\cdot p_3p_4\cdot p_4p_5 - 2\cdot p_4p_6\cdot p_5p_6 + 2m_2^2m_3^2\Big)\\
&+ Tr\left[\not{p}_3\gamma^\mu\not{p}_4\gamma^\nu\right]\Big(2m_2^2\cdot p_5p_6 + 2m_3^2\cdot p_3p_4 - m_3^2\cdot p_3p_5 - m_3^2\cdot p_3p_6 + m_3^2\cdot p_4p_5\\
&-m_3^2\cdot p_4p_6 - 2\cdot p_3p_5\cdot p_4p_6 + 2\cdot p_3p_4\cdot p_5p_6 - 2\cdot p_4p_5\cdot p_4p_6 - 2\cdot p_4p_6\cdot p_5p_6 + 2m_2^2m_3^2\Big)\\
&+ 4g^{\mu\nu}\Big(4\cdot p_3p_5\left(p_4p_6\right)^2 - 2m_2^4\cdot p_5p_6 + m_3^4\left(-2\cdot p_3p_4 - 2m_2^2\right) + 4\cdot p_3p_6\cdot p_4p_5\cdot p_4p_6\\
&+ m_2^2\left(2\cdot p_3p_6\cdot p_4p_5 + 2\cdot p_3p_5\cdot p_4p_6 - 2\cdot p_3p_4\cdot p_5p_6 + 4\cdot p_4p_5\cdot p_4p_6 + 4\cdot p_4p_6\cdot p_5p_6\right)\\
&+ m_3^2\Big(m_2^2\left(-2\cdot p_3p_4 + 8\cdot p_4p_6 - 2\cdot p_5p_6\right) + 2\cdot p_3p_6\cdot p_4p_5 + 2\cdot p_3p_5\cdot p_4p_6\\
&- 2\cdot p_3p_4\cdot p_5p_6 + 4\cdot p_3p_4\cdot p_4p_6 + 4\cdot p_3p_6\cdot p_4p_6 - 2m_2^4\Big)\Big)\Big]\Big\}
\end{aligned}
\tag{C.48}
$$